Folding and stability of β-barrel membrane proteins from Gram-negative bacteria

Dissertation zur Erlangung des akademischen Grades des Doktors der Naturwissenschaften

an der Universität Konstanz
Mathematisch -Naturwissenschaftliche Sektion
Fachbereich Biologie

Vorgelegt von
Dipl. Ing. Cosmin L. Pocanschi

Tag der mündlichen Prüfung: 15.11.2005

Referent 1: PD Dr. Jörg H. Kleinschmidt
Referent 2: Prof. Dr. Hans-Jürgen Apell

Table of contents

Abbreviations

ATR-FTIR	polarized attenuated total internal reflection-Fourier transform infrared spectroscopy
A8-35	anionic amphipathic polymer (MW = 8 kDa; fraction of free carboxylic groups = 35%)
borate	sodium tetraborate-10-hydrate
BR	bacteriorhodopsin
bromphenol blue	3',3",5',5"-tetrabromophenolsulfonephthalein
CD	circular dichroism
CMC	critical micelle concentration
di$C_{10:0}$PC	1,2-dicapryl-*sn*-glycero-3-phosphocholine
di$C_{18:1}$PC (DOPC)	1,2-dioleoyl-*sn*-glycero-3-phosphocholine
*di*phPC	1,2-diphytanoyl-*sn*-glycero-3-phosphocholine
DMPC	1,2-dimyristoyl-*sn*-glycero-3-phosphocholine
DMPG	1,2-dimyristoyl-*sn*-glycero-3-phosphoglycerol
DOPG	1,2-dioleoyl-*sn*-glycero-3-phosphoglycerol
DSC	differential scanning calorimetry
EDTA	ethylenediaminetetraacetic acid
Eq.	equation
E. coli	*Escherichia coli*
ESR	electron spin resonance
FhuA	ferric hydroxamate uptake protein A from *Escherichia coli*
FomA	major outer membrane protein A from *Fusobacterium nucleatum*
HEPES	4-(2-hydroxyethyl) piperazine-1-ethanesulfonic acid
hVDAC1	human voltage-dependent anion-selective channel protein isoform 1
IMPs	integral membrane proteins
IR	infrared
kDa	kilo Dalton
KTSE	kinetics of tertiary structure formation detected by electrophoresis
λ	wave length
LDAO	*N*-lauroyl-*N*,*N*-dimethylammonium-*N*-oxide
LPS	lipopolysaccharide
LUVs	large unilamellar vesicles
lyso$C_{10:0}$PC	1-capryl-2-hydroxy-*sn*-glycero-3-phosphocholine
Mcps	million counts per second
mdeg	millidegrees
MES	2-Morpholinoethanesulfonic acid
Ni-NTA	nickel-loaded chromatography material
OmpA	outer membrane protein A from *Escherichia coli*
OMPs	outer membrane proteins
SDS	sodium dodecyl sulfate
SDS-PAGE	SDS-polyacrylamide gel electrophoresis
SUVs	small unilamellar vesicles
Tris	tris(hydroxymethyl)aminomethane
TM	transmembrane
14-DGSL	1-acyl-2-[14-(4,4-dimethyloxazolidinyl-*N*-oxy)stearoyl]-*sn*-glycerol

14-PASL	1-acyl-2-(14-(4,4-dimethyl-oxazolidine-*N*-oxy))stearoyl-*sn*-glycero-3-phosphoric acid
14-PCSL	1-acyl-2-(14-(4,4-dimethyl-oxazolidine-*N*-oxy))stearoyl-*sn*-glycero-3-phosphocholine
14-PESL	1-acyl-2-(14-(4,4-dimethyl-oxazolidine-*N*-oxy))stearoyl-*sn*-glycero-3-phosphoethanolamine
14-PGSL	1-acyl-2-(14-(4,4-dimethyl-oxazolidine-*N*-oxy))stearoyl-*sn*-glycero-3-phosphoglycerol
14-PISL	1-acyl-2-(14-(4,4-dimethyl-oxazolidine-*N*-oxy))stearoyl-*sn*-glycero-3-phosphoinositol
14-PSSL	1-acyl-2-(14-(4,4-dimethyl-oxazolidine-*N*-oxy))stearoyl-*sn*-glycero-3-phosphoserine
14-SASL	14-(4,4-dimethyl-oxazolidine-*N*-oxy)stearic acid
wt	wild type

Konstanz, den 23.08.2005

Hiermit erkläre ich, Cosmin Lorin Pocanschi, dass alle Experimente von mir durchgeführt wurden, ausser folgenden:
Amphipole A8-35 wurde groszügigerweise von Prof. Dr. J.-L. Popot zur Verfügung gestellt.
Prof. Dr. H. B. Jensen hat freundlicherweise FomA in Form von Einschlusskörpern zur Verfügung gestellt.
Kapitel 6 und 7: Meine Anteile an diesen Studien waren die Isolation und Aufreinigung von wt-FhuA, FhuAΔ5-160 und wt-OmpA, die Rekonstitution in Membrandoppel-schichten sowie Mitwirkung bei der Publikation der Ergebnisse.

Cosmin L. Pocanschi

1 Scientific background and introduction

1.1 Biological membranes

Biomembranes are crucial components in the genesis of life and the structuring elements of the organisation of living cells. They preserve the functional integrity of cell organelles and regulate the exchange of solutes and signals between the different functional areas of the cell. All biological membranes, including plasma membranes and all organelle membranes, contain lipids and proteins.

The cell wall (Figure 1.1) of a bacterium is an essential structure that protects the delicate cell protoplast from osmotic lysis. The Gram-negative cell envelope is constituted of an outer membrane, a periplasmic space and a cytoplasmic membrane.

The **cytoplasmic membrane** consists of phospholipids (PL) and several protein components. The cytoplasmic membrane is the site of active transport, respiratory chain components, energy-transducing systems, the H^+-ATPase of the proton pump and membrane stages in the biosynthesis of phospholipids, peptidoglycan, LPS, and capsular polysaccharides. The peptidoglycan layer (PG) situated in the **periplasmic space** (PPS) is further anchored to the OM by lipoproteins (lp) and other proteins (p). Peptidoglycan consists of a glycan (polysaccharide) backbone consisting of N-acetyl muramic acid and N-acetyl glucosamine with peptide side chains. The side-chains are cross-linked by peptide bridges. The **outer membrane** (OM) is an asymmetric bilayer containing lipopolisaccharide (LPS) in the outer leaflet and phospholipids (PL) in the inner leaflet, as well as some unique proteins. The lipopolysaccharide is important to the bacterial cell since it helps to provide a permeability barrier, including hydrophobic substances. The outer LPS moiety is constituted by lipid A (LA), the core and the O-antigen region (O-Ag). The lipid A contains β-hydroxyfatty acids, the core contains several sugars (heptoses and ketodeoxyoctonic acid) and the O-Ag hydrophilic region contains polysaccharide. The LPS molecule displays endotoxin activity. The lipid A region is thought to be essential for OM assembly while the proximal end of the core is responsible for maintaining the barrier property of the OM. The proximal part of the core keeps out hydrophobic compounds including antibodies, mutagens, and detergents. The O-antigen region appears to help

virulence, escaping phagocytosis, and sticks out into the surrounding medium (Figure 1.1). The phospholipid composition of the OM is similar to that of cytoplasmic membrane except it has a slight augmentation in phosphatidylethanolamine. The porins are located in the OM together with other integral membrane proteins (I). Porins in the outer membrane form channels which allow passage of small hydrophilic nutrients (such as sugars) through the outer membrane.

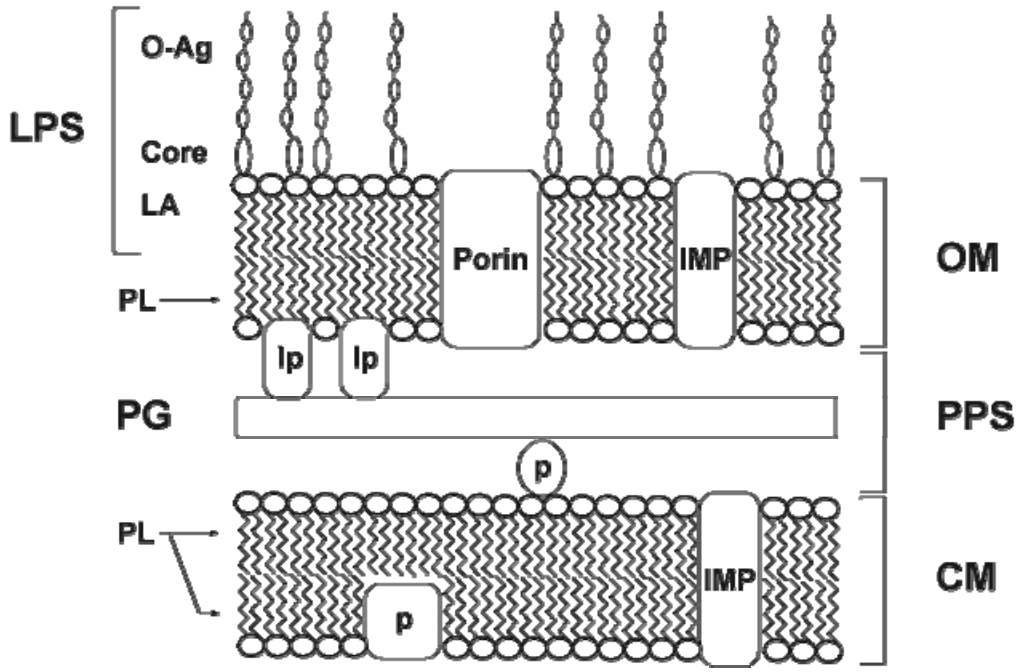

Figure 1.1 The cell envelope of Gram-negative bacteria The Gram-negative cell envelope is constituted of an outer membrane (OM), a periplasmic space (PPS) and a cytoplasmic membrane (CM) (see text for details). Figure modified from Lugtenberg and Van Alphen (Lugtenberg and Van Alphen 1983).

1.2 Membrane lipids

Lipids are essential components of all living organisms. They are often defined as water-insoluble (or sparingly soluble) organic compounds found in biological systems. They are either hydrophobic (nonpolar) or amphipathic (containing both polar and nonpolar regions). The lipids have a polar hydrophilic head and a non-polar hydrophobic tail. They form a bilayer with the hydrophobic tails facing each other and the hydrophilic heads facing the outside world or the inside of the cell. This bilayer is actually fluid and the

proteins are floating in it. This is called the fluid mosaic model (Singer and Nicolson 1972). Biological membranes mostly contain phospholipids like phosphatidylcholine (PC) and phosphatidylethanolamine (PE). Aside from these zwitterionic glycerophospholipids there are also charged phospholipids: phosphatidylglycerol (PG), phosphatidylserine (PS), phosphatidic acid (PA) and cardiolipin (CL) as well as sphingomyelin (Sph) and cholesterol (Cho). Other membrane components can be phosphatidylinositol (PI), glycolipids (GlyL), sulphatides, prostaglandins, diglycerids and fatty acids.

Lipids have diverse structures and also diverse biological functions. In addition to forming a building block in biological membranes they function in energy storage, thermal insulation, surface protection in some organisms etc. Some lipids also have highly specialized functions as regulators of metabolic activities (steroid hormones), blood pressure, body temperature etc.

1.3 Protein structure

The sequence of amino acids in each protein is determined by the gene that encodes it. The gene is transcribed into a messenger RNA (mRNA) and the mRNA is translated into a protein by the ribosome. **Primary structure** refers to the linear sequence of amino acids. There are 20 amino acids that represent the building blocks of proteins. Proteins are large polypeptides of defined amino acid sequence. **Secondary structure** refers to the ordered structure as a result of hydrogen bonding mainly within the peptide backbone. The most common secondary structures of proteins are the α-helix and the β-pleated sheet conformation.

The **α-helix** is like a bore tube (Figure 1.2A) which is right-handed, i. e. it twists in a clockwise direction. The peptide link plates form the wall of the tube with the C_α atoms projecting a little from the surface. The side chain groups, attached to the C_α atoms, project outwards from the wall of the tube. The α-helix makes a complete turn (0.54 nm) every 3.5 amino acids. The α-helix conformation has a particular stability for two main reasons. Firstly, the side chain groups are quite well separated. Secondly, and most importantly, each peptide link is involved in two hydrogen bonds. The C=O is hydrogen bonded to the N-H of the peptide link four units ahead in the primary structure. The atoms involved are arranged linearly so that the hydrogen bonds are nearly at their maximum strength. The

hydrogen bonds run down the length of the α-helix tube and lock the conformation in place.

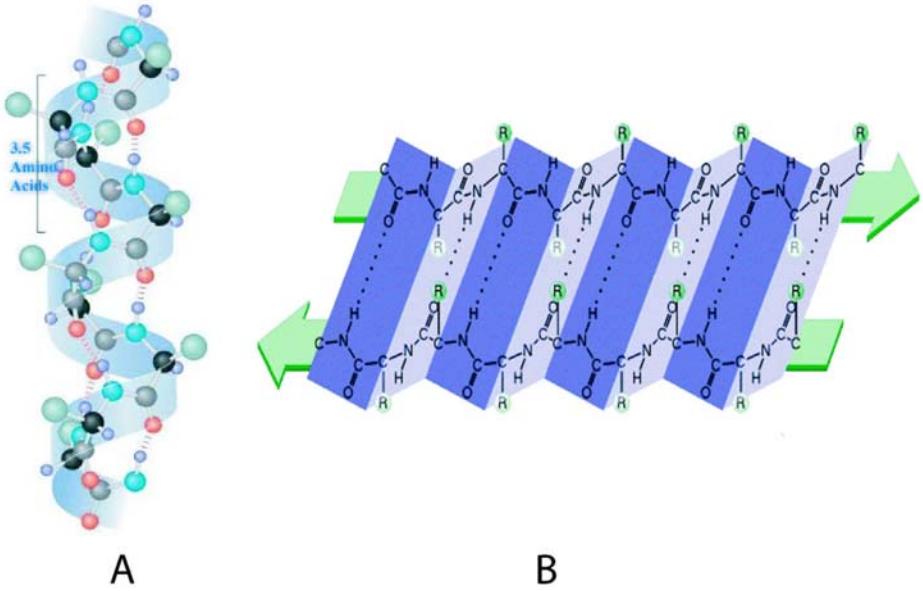

Figure 1.2 Protein secondary structures A: α-helix The helix has a specific hydrogen bonding pattern, where the backbone C=O group of residue n bonds with the N-H group of residue n+4. The atomic distance between the N and O measures 0.28nm. The H-bonds are almost parallel to the helix axis and the total dipole moment gives the helix a dipole moment that points from the N-term (+) to the C-term (-). **B: β-pleated sheet** In a β-sheet two or more polypeptide chains run alongside each other and are linked in a regular manner by hydrogen bonds between the main chain C=O and N-H groups. Therefore all hydrogen bonds in a beta-sheet are between different segments of polypeptide. The side chains of neighbouring residues in a β-strand point in opposite directions. β-strands are not stable structures but occur in association with neighboring strands. The α-C atoms of adjacent strands stand 0.35 nm apart (Figure from Lodish 2000).

In the **β-pleated sheet** structures (Figure 1.2B) the polypeptide backbone is nearly fully stretched. This allows the peptide N-H and C=O to point out at right angles to the line of the backbone. N-H and C=O groups alternate along each edge. When two or more of these extended chains (called β-strands) are side by side hydrogen bonds form between them to give an almost two dimensional sheet that is pleated like the bellows of an accordion. Alternate β-strands can run in the same direction to give a parallel β-pleated sheet or in opposite directions to give an antiparallel β-pleated sheet. The pleating in each case allows for the best alignment of the hydrogen bonded groups.

Tertiary structure refers to the complete three-dimensional structure of the polypeptide units of a given protein. The interactions of different domains are governed by hydrogen bonding, hydrophobic interactions, electrostatic interactions and van der Waals

forces. The structure formed by monomer-monomer interaction in an oligomeric protein resulting in an active unit is known as **quaternary structure**.

1.4 Membrane proteins

Two classes of membrane proteins are currently known that are characterized by the structure of their transmembrane domain.

The first class covers proteins that form very hydrophobic transmembrane **α-helices**. A prominent example is bacteriorhodopsin (BR), a 7 α-helix bundle membrane protein (see *e.g.* refs. Pebay-Peyroula et al. 1997; Luecke et al. 1999; Subramaniam and Henderson 2000). In α-helix bundle proteins, multiple helices are aligned in form of bundles and may contain polar residues at the interfaces between the helices that are not exposed to the lipid chains (Figure 1.3A). Monomeric and oligomeric α-helix bundle membrane proteins are known.

The second class covers **β-barrel** proteins in which antiparallel β-strands span the membrane and form a barrel like structure (Figure 1.3B). The H-bonding pattern is not regularly spaced with respect to the amino acid sequence. H-bonds span between amino acids on separate β-strands, which may be quite distant from each other in the sequence. In transmembrane β-strands, only every second amino acid faces the apolar lipid phase and must be a hydrophobic residue, while the others face the interior of the β-barrel and are mostly polar. Therefore, the average hydrophobicity of transmembrane β-barrels is low (–0.5 to –0.6 on the Kyte-Doolittle scale vs. > + 0.5 for α-helix bundle transmembrane proteins).

The geometry of the β-strands excludes that individual β-strands can exist in a lipid bilayer and all known integral membrane proteins with transmembrane β-strands form barrel structures in which at least 8 neighboring β-strands are connected by hydrogen bonds. The outer membrane proteins (OMPs) of bacteria form transmembrane β-barrels with even numbers of β-strands ranging from 8 to 22 (Schulz 2002; Kleinschmidt 2005). The strands are tilted by 36° to 44° relative to the barrel axis (Marsh and Páli 2001; Schulz 2002).

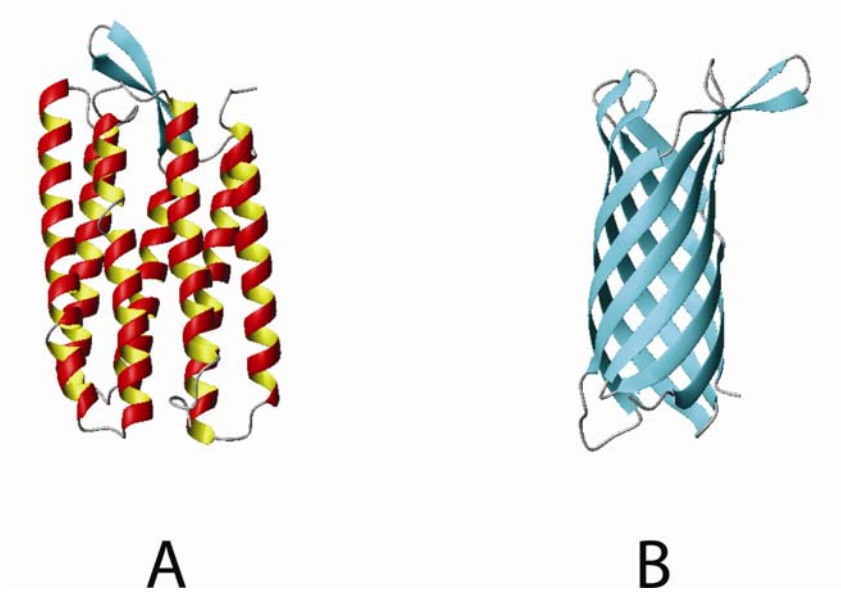

Figure 1.3 Examples of the two classes of membrane proteins A: α-helical Bacteriorhodopsin from *Halobacterium salinarum* (Faham et al. 2005). **B: β-barrel** - neisserial surface protein A (NspA) from *Neisseria meningitidis* (Vandeputte-Rutten et al. 2003). The membrane protein structures were generated with MolMol (Koradi et al. 1996).

Examples are OmpA (Pautsch and Schulz 2000; Arora et al. 2001), OmpX (Vogt and Schulz 1999; Fernandez et al. 2001; Hilty et al. 2004), NspA (Vandeputte-Rutten et al. 2003), and PagP (Hwang et al. 2002; Ahn et al. 2004) (8 β-strands); OmpT (Vandeputte-Rutten et al. 2001) (10 β-strands); NalP (Oomen et al. 2004) and OmPlA (Snijder et al. 1999) (12 β-strands); OmpG (Conlan and Bayley 2003) and FadL (van den Berg et al. 2004) (14 β-strands); Omp32 (Zeth et al. 2000), matrix porin (Weiss et al. 1991), OmpF (Cowan et al. 1995), and PhoE (Cowan et al. 1992) (16 β-strands); maltoporin (LamB) (Schirmer et al. 1995) and sucrose porin (ScrY) (Forst et al. 1998) (18 β-strands); FepA (Buchanan et al. 1999), BtuB (Chimento et al. 2003; Kurisu et al. 2003), and FhuA (Ferguson et al. 1998; Locher et al. 1998) (22 β-strands). Monomers (OmpA, FhuA, OmpG (Conlan et al. 2000)), dimers (OmPlA) and trimers (OmpF, PhoE) are known. Some examples of β-barrel membrane proteins of known structure are shown (Figure 1.4).

β-barrel membrane proteins serve a wide range of different functions: OmpA is a small ion channel (Arora et al. 2000), OmpT is a protease, NalP is an autotransporter, FadL is a long chain fatty acid transporter, PhoE is a diffusion pore, ScrY is a sucrose specific porin, OmPlA is a phospholipase. FhuA and BtuB are active transporters for ferrichrom iron and vitamin B_{12} uptake, respectively. TolC is involved in solute efflux (Koronakis et al. 2000).

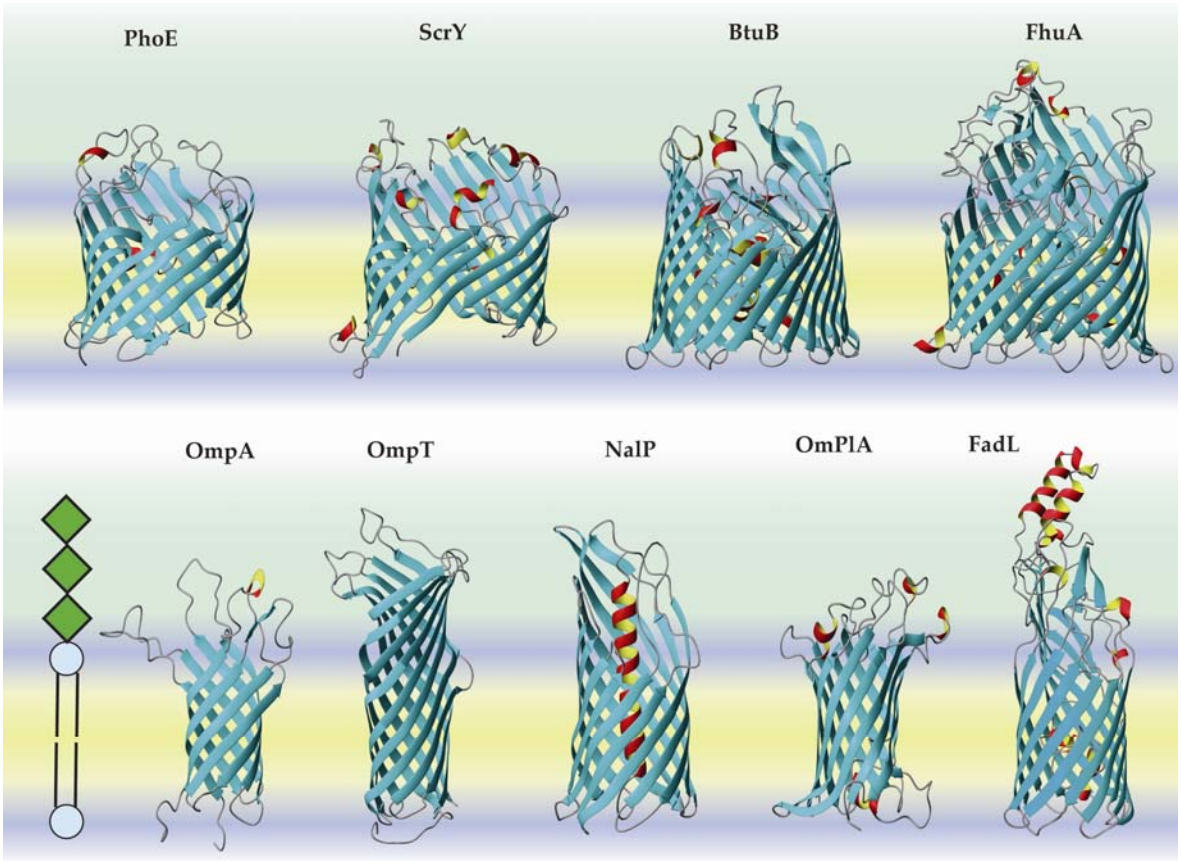

Figure 1.4 Known structures of β-barrel membrane proteins Integral membrane proteins with β-barrel structures are known from outer membranes of bacteria, mitochondria, and chloroplasts. The β-barrel is characterized by the number of antiparallel β-strands and by the shear number, which is a measure for the inclination angle of the β-strands against the barrel axis (Figure taken from Kleinschmidt 2005).

OMPs of mitochondria are predicted to form similar TM β-barrels. Examples are the VDAC channels, out of which more than a dozen have been sequenced (Heins et al. 1994).

The following outer membrane proteins have been studied for this thesis:

1.4.1 Outer membrane protein A (OmpA)

OmpA is an abundant structural protein of the outer membrane of Gram-negative bacteria (Sonntag et al. 1978). It is composed of a 171 residue 8-stranded β-barrel transmembrane domain and a 154 residue periplasmic domain (Figure 1.4). It is believed to connect the outer membrane structurally to the periplasmic peptidoglycan layer via its soluble periplasmic domain (Tamm et al. 2003), which consists of residues ~177-325 and adopts a βαβαββ-fold in aqueous solution (Grizot and Buchanan 2004). OmpA forms an ion channel with small (50-80 pS) and large (260-320 pS) conductivities (Arora et al.

2000; Saint et al. 2000), is involved in bacterial conjugation (Ried and Henning 1987) and acts as receptor for various bacteriophages (Morona et al. 1985) and some colicins (Foulds and Chai 1978).

1.4.2 Ferric hydroxamate uptake protein A (FhuA)

FhuA is a monomeric protein found in the outer membrane of *Escherichia coli*. It acts as an energy dependent channel protein whose primary function is to transport ferrichrome-iron across the outer membrane of *E. coli*. It derives energy from a Ton based protein complex (consisting of TonB, ExbB, and ExbD) located in the cytoplasmic membrane of *E. coli* (Ferguson et al. 1998). In addition to acting as a ferrichrome-iron receptor, FhuA also acts as a primary receptor for the antibiotic albomycin, four bacteriphages (T1, T5, UC-1, and f80), the peptide antibiotic microcin 25, and the bacterial toxin colicin M (Braun 1998). Since FhuA is a bacterial outer membrane protein, it does not have any true orthologs in any eukaryotic organisms; however, there is one predicted ortholog to FhuA found in the mitochondria of the common mosquito.

FhuA of *E. coli* consists of 714 residues (Coulton et al. 1986). It forms a 22-stranded β-barrel (residues 160-715) filled by a cork domain composed of the N-terminal 160 residues (Ferguson et al. 1998) (Figure 1.4).

1.4.3 Fusobacterial non-specific porin (FomA)

FomA, the major non-specific porin of *Fusobacterium nucleatum*, is predicted to form a 14-stranded β-barrel (Figure 1.5) (Puntervoll et al. 2002) and has been shown to function as a non-specific porin in lipid bilayer membranes (Kleivdal et al. 1995), or *in vivo*, when expressed in *E.coli* (Kleivdal et al. 1999). FomA forms water-filled channels in lipid bilayer membranes with conductances of one pore-forming unit in the range 0.66-1.3 nS (Kleivdal et al. 1995). FomA is assumed to be directly involved in the binding between fusobacteria and *Streptococus sanguis* on the tooth-surface, and to *Porphyromonas gingivalis* in the periodontal pockets (Kinder and Holt 1993).

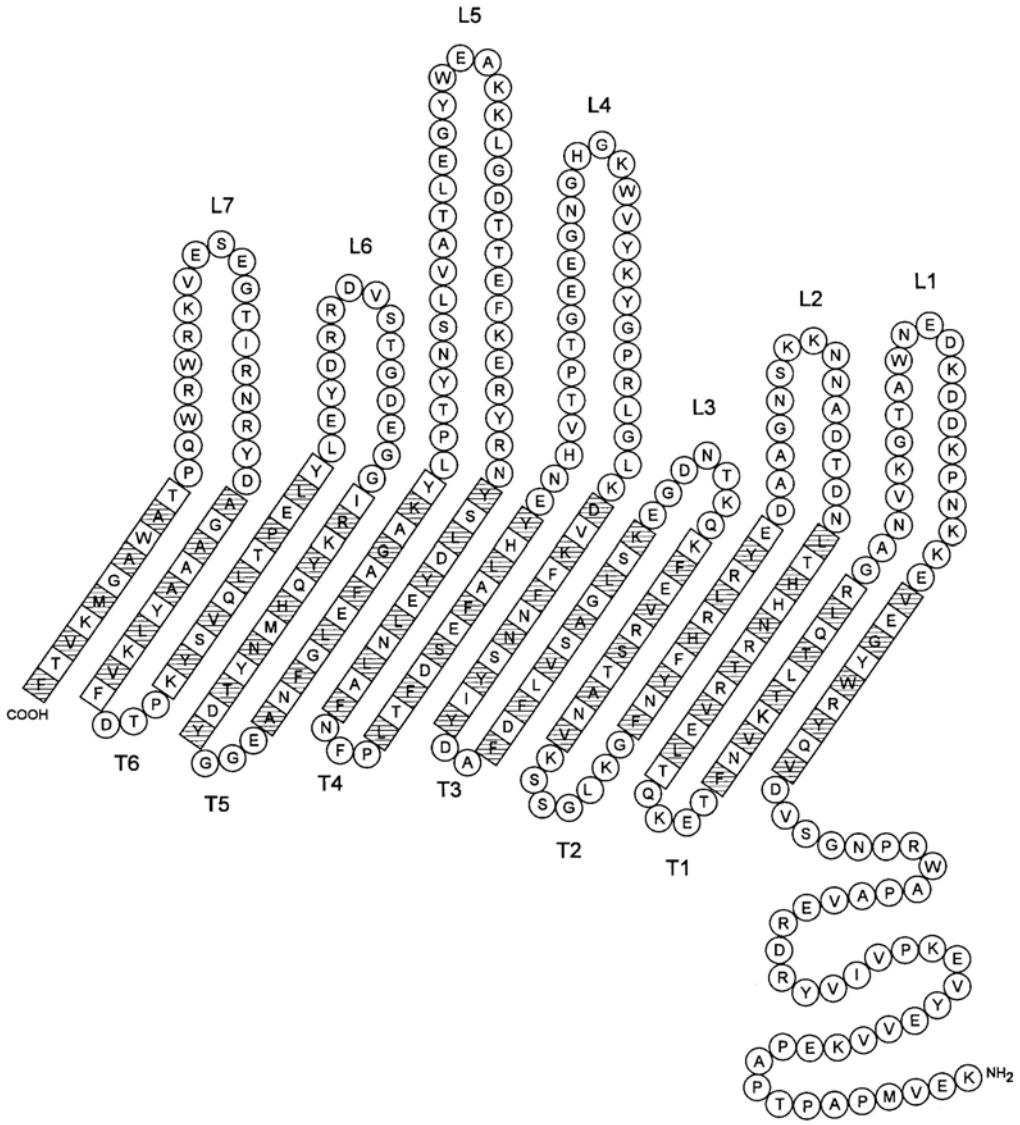

Figure 1.5 The 14-stranded topology model of the FomA protein of *F. nucleatum* The top of the model shows the putative surface-exposed loops and the central part represents the presumed transmembrane segments. Amino acid residues, shown in one-letter code, are indicated by boxes when they are supposed to form β-strands (shaded box if proposed to face the lipids or the subunit interface) and circles for turns (T), loops (L) and the putative periplasmic N-terminal domain. Figure modified from Puntervoll *et al*. (Puntervoll et al. 2002)

1.4.4 Human Voltage-Dependent Anion-selective Channel protein 1 (HVDAC1)

The voltage-dependent anion channel HVDAC1 (also known as mitochondrial porin) forms a channel through the mitochondrial outer membrane and also through the

plasma membrane from cells of all eukaryotic kingdoms (Colombini 1989; Sorgato and Moran 1993; Benz 1994). There is currently no crystal structure of VDAC but two structure models have been proposed. According to the first model VDAC consists of one α-helix and a 13 stranded β-barrel (Song et al. 1998). VDAC is also predicted to form a 16-stranded transmembrane β-barrel with a 20-residue, N-terminal domain (Casadio et al. 2002). The channel allows diffusion of small hydrophilic molecules. It adopts an open conformation at low or zero membrane potential and a closed conformation at potentials above 30-40 mV. The open state has a conductance of 4.2 nS and a weak anion selectivity whereas the closed state is cation-selective (Colombini et al. 1996). Physiologically, VDAC is thought to function as the primary pathway for the movement of adenine nucleotides and other metabolites through the mitochondrial outer membrane, thus controlling the traffic of these essential compounds to and from this organelle as well as the entry of other substrates into a variety of metabolic pathways. VDAC has also been shown to be the site for binding of hexokinase and glycerol kinase to the mitochondrial outer membrane. The binding of these enzymes to the mitochondrion is dynamic, varying between different tissues, during development, and depending on the metabolic state of the cell (Adams et al. 1991; McCabe 1994).

1.5 Membrane protein folding

A decisive step in the biosynthesis of many secretory and plasma membrane proteins is their transport across the endoplasmic reticulum (ER) membrane in eukaryotes or across the cytoplasmic membrane in prokaryotes. In co-translational translocation, the major partner is the ribosome. The elongating polypeptide chain moves directly from the ribosome into the associated membrane channel formed by the Sec61p complex in eukaryotes and SecY complex in eubacteria and archaea. In post-translational translocation, polypeptides are completed in the cytosol and then transported across the membrane. How do membrane proteins insert and fold into the outer membrane of bacteria after translocation is largely unknown.

The fatty core of a phospholipid bilayer requires hydrophobic amino acid residues at the interface of the integral membrane protein to the fatty acyl chains of the phospholipids. Amide hydrogens of transmembrane (TM) proteins that are located in the fatty region of the membrane must form hydrogen bonds with a carbonyl oxygene of a

peptide bond in close vicinity to allow the stable assembly of a protein segment in the hydrophobic region of the lipid bilayer.

In vitro, both classes of integral membrane proteins (IMPs) require either detergent micelles or lipid bilayers for folding.

The folding of IMPs into detergent micelles was mostly studied with the 7 α-helical bundle protein bacteriorhodopsin (BR) of *Halobium salinarium* (Engelman and Steitz 1981; Huang et al. 1981; Popot et al. 1987; Kahn and Engelman 1992; Booth and Curran 1999), OmpA (Dornmair et al. 1990; Kleinschmidt et al. 1999), OmpF (Surrey et al. 1996), OmpG (Conlan and Bayley 2003), PhoE (Van Gelder et al. 1994; de Cock and Tommassen 1996; de Cock et al. 1999) and AIDA (Mogensen et al. 2005). Huang et al. showed for the first time that α-helical integral membrane proteins can be refolded *in vitro* from a completely denatured state into their native, functionally state on the example of BR (Huang et al. 1981). BR can be delipidated and completely denatured in 88% formic acid or anhydrous trifluoroacetic acid. It regains its α-helix secondary structure upon addition of ethanol. Neutralization of the acid with ammonia followed by dialysis against a solution of sodium dodecyl sulfate and subsequent addition of the chromophore, phospholipids, and cholate lead to complete recovery of BR activity. Schweizer et al. (Schweizer et al. 1978) showed for the first time that the 8-stranded β-barrel OmpA partially regains native structure in presence of lipopolysaccharide and Triton-X-100 after dilution of the denaturants SDS or urea. Similarly, Dornmair et al. (Dornmair et al. 1990) demonstrated that after heat-denaturation in sodium dodecyl sulfate (SDS) micelles, the 8-stranded β-barrel OmpA can refold into micelles of the detergent octylglucoside in absence of LPS. These studies suggest that the information for the formation of native structure in integral membrane proteins is contained in their amino acid sequence, as previously described by the Anfinsen paradigm for soluble proteins (Anfinsen 1973).

Surrey and Jähnig (Surrey and Jähnig 1992) showed first that OmpA spontaneously inserts and folds into phospholipid bilayers. Completely unfolded and solubilized OmpA in 8 M urea was refolded upon strong dilution of the denaturant in presence of small unilamellar vesicles (SUVs) of dimyristoylphosphatidylcholine (*di*C_{14}PC). The SUVs were obtained by sonication and had a diameter of approximetely 20 nm. These bilayers have to be in the lamellar-disordered (liquid-crystalline) phase (Surrey and Jähnig 1992; Surrey and Jähnig 1995). In contrast, insertion and folding do not complete when the lipid bilayers are in the lamellar ordered (gel) phase or when refolding attempts are made into DMPC bilayers of large unilamellar vesicles (LUVs) that are prepared by extrusion. It has been

shown that folding and trimerization of OmpF (Surrey et al. 1996) take place after interaction of urea-unfolded OmpF with preformed lipid bilayers in absence of detergent. Membrane inserted dimers of OmpF are observed transiently. *In vitro*, the folding yields of OmpF are relatively modest (< ~30 %) under optimized conditions (Surrey et al. 1996). In comparison, folding yields of OmpA approach 100 % at pH 10, but are only ~70 % at neutral pH (Surrey and Jähnig 1995), which is very likely a consequence of an increased negative surface charge of OmpA (pI = 5.9) at pH 10 that increases the solubility of OmpA, i.e. suppresses the aggregation side reaction.

To explore constraints for the folding and membrane insertion of outer membrane proteins (OMPs), Kleinschmidt et al. (Kleinschmidt et al. 1999) investigated the folding of OmpA into a wide range of different phospholipids and detergents at different concentrations. They reported the successful folding of OmpA into 64 different detergents and phospholipids that had very different compositions of the polar headgroup, did not carry a net charge, and had a hydrophobic carbon chain length ranging from 7 to 14 carbon atoms.

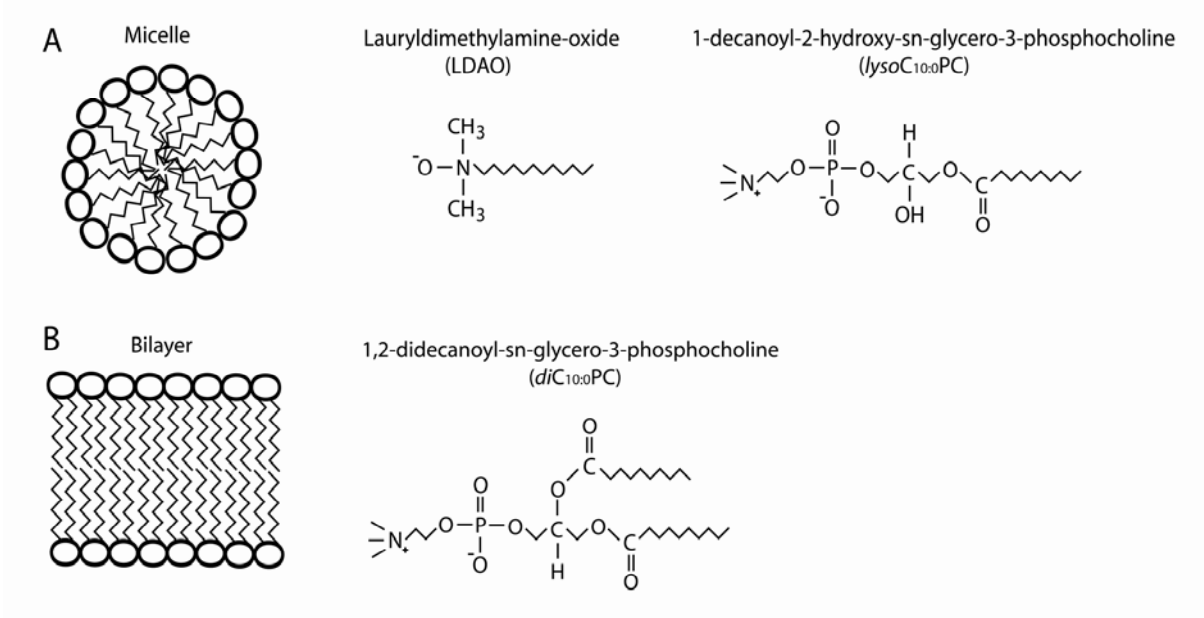

Figure 1.6 Micelle (A) and bilayer (B) forming lipids Amphiphiles with a single hydrocarbon chain, such as LDAO, must pack a number of head groups around a relatively small volume of hydrocarbon. This large surface area to volume ratio is achieved by forming a spherical micelle structure (A). In contrast, amphiphiles with two hydrocarbon chains, such as phospholipids, must pack the same number of headgroups around twice as large a volume of hydrocarbon. This smaller surface area to volume ratio is achieved by forming the bilayer structure (B).

The concentrations of these detergents or phospholipids had to be above their CMCs for successful OmpA folding, demonstrating that a supramolecular assembly, either a micelle or a lipid bilayer is a minimal requirement for native structure formation in β-barrel integral membrane proteins (Kleinschmidt et al. 1999). Examples of micelle and bilayer forming lipids are shown (Figure 1.6).

Folding of OmpA was detected by circular dichroism (CD) spectroscopy and by electrophoretic mobility measurements. Both methods indicated that after exposure to amphiphiles with short hydrophobic chains (with 14 or fewer carbons), OmpA assumes either both, secondary and tertiary structure (i.e. the native state) or no structure at all, dependent on the presence of supramolecular assemblies (micelles, bilayers). OmpA folding into micelles appeared to be a thermodynamically controlled two state process. These results indicated that protein secondary and tertiary structure does not form upon adsorption of detergent or lipid monomers to a newly formed hydrophobic surface of the protein. Instead the hydrophobic core of the micelle or bilayer must first be present to allow folding of OmpA.

SDS-polyacrylamide gel electrophoresis (SDS-PAGE) has been a very valuable tool to monitor folding of OmpA. The electrophoretic mobilities of folded and denatured outer membrane proteins are different, if the samples are not boiled prior to electrophoresis. This property was first described by Henning and coworkers for OmpA (Schweizer et al. 1978) and has also been observed for other β-barrels, such as FhuA (Locher and Rosenbusch 1997) or OmpG (Behlau et al. 2001). For example, folded OmpA migrates at 30 kDa, whereas unfolded OmpA migrates at 35 kDa (Schweizer et al. 1978). The 30 kDa form has been shown by Raman, FT-IR, and CD spectroscopy (Vogel and Jähnig 1986; Dornmair et al. 1990; Surrey and Jähnig 1992; Rodionova et al. 1995; Surrey and Jähnig 1995; Kleinschmidt et al. 1999), by phage inactivation assays (Schweizer et al. 1978), and by single channel conductivity measurements (Arora et al. 2000) to correspond to completely folded and functionally active OmpA.

The different electrophoretic mobilities of folded and unfolded OmpA have also been used to determine the kinetics of tertiary structure formation by electrophoresis (KTSE) with a simple kinetic gel-shift assay, taking advantage of the inhibition of OmpA folding by SDS (Surrey and Jähnig 1995; Kleinschmidt and Tamm 1996; Kleinschmidt and Tamm 2002). In this kinetic assay, SDS is added to small volumes of the reaction mixture that are taken out at defined times after initiation of folding. Negatively charged SDS binds quickly to folded and unfolded OmpA and stops OmpA folding. At the end of the kinetic

experiment, the fractions of folded OmpA in each sample are determined by cold SDS-PAGE (i. e. without heat-denaturing the samples) and subsequent densitometry of the bands of folded and of unfolded OmpA. In contrast to a quantitative refolding into a wide range of neutral detergents, completely denatured OmpA does not refold into SDS-micelles, as determined by electrophoretic mobility measurements and by CD spectroscopy (cf. ref. (Dornmair et al. 1990)). However, the negative charge of SDS only contributes to this effect of the SDS headgroup and cannot be the only cause of the inhibition of OmpA folding in presence of SDS, since OmpA can fold partially into micelles of negatively charged LPS (Bulieris et al. 2003) and also into bilayers containing negatively charged phosphatidylglycerol, which are both components of the bacterial outer membrane (Freudl et al. 1986; Bulieris et al. 2003). A range of detergents have also been used for refolding of other β-barrel membrane proteins for the subsequent membrane protein crystallization (for an overview, see e.g. ref. Buchanan 1999). While the presence of an aggregated state of detergents or lipids seems to be a minimal requirement for the *in vitro* folding of β-barrel membrane proteins such as OmpA, *in vivo* likely there are proteinaceous and other cofactors that promote efficient folding.

1.6 Methods

1.6.1 Fluorescence spectroscopy

Absorption of electromagnetic radiation in the ultraviolet and visible region leads to an electronically excited state of a molecule. In most cases, particularly for large molecules in solids and liquids, the energy of excitation is dissipated into the disordered thermal motion of its surroundings. However, a molecule may also lose energy by radiative decay, with the emission of a photon as the electron transfers back into its lower energy orbital. There are two modes of radiative decay namely fluorescence and phosphorescence. Fluorescence and phosphorescence are often observed when aromatic molecules are excited by ultraviolet or visible radiation. Fluorescence is the emission of radiation directly following absorption of excitation radiation. Phosphorescence is the emission of radiation over much longer timescales (seconds or even hours) following absorption of the excitation radiation. The delay in phosphorescence is a consequence of energy storage in an intermediate, temporary reservoir. The Jablonski diagram (Figure 1.7) illustrates the

fluorescence and phosphorescence and a typical arrangement of molecular electronic and vibrational energy levels. The absorption of radiation promotes the molecule from the ground electronic state (S_0) to vibrationally excited levels in an upper electronic state (S_1). The S nomenclature stands for singlet state and refers to the fact that the ground states of most molecules contain paired electron spins (↑↓), which can adopt only one orientation with respect to an external magnetic field.

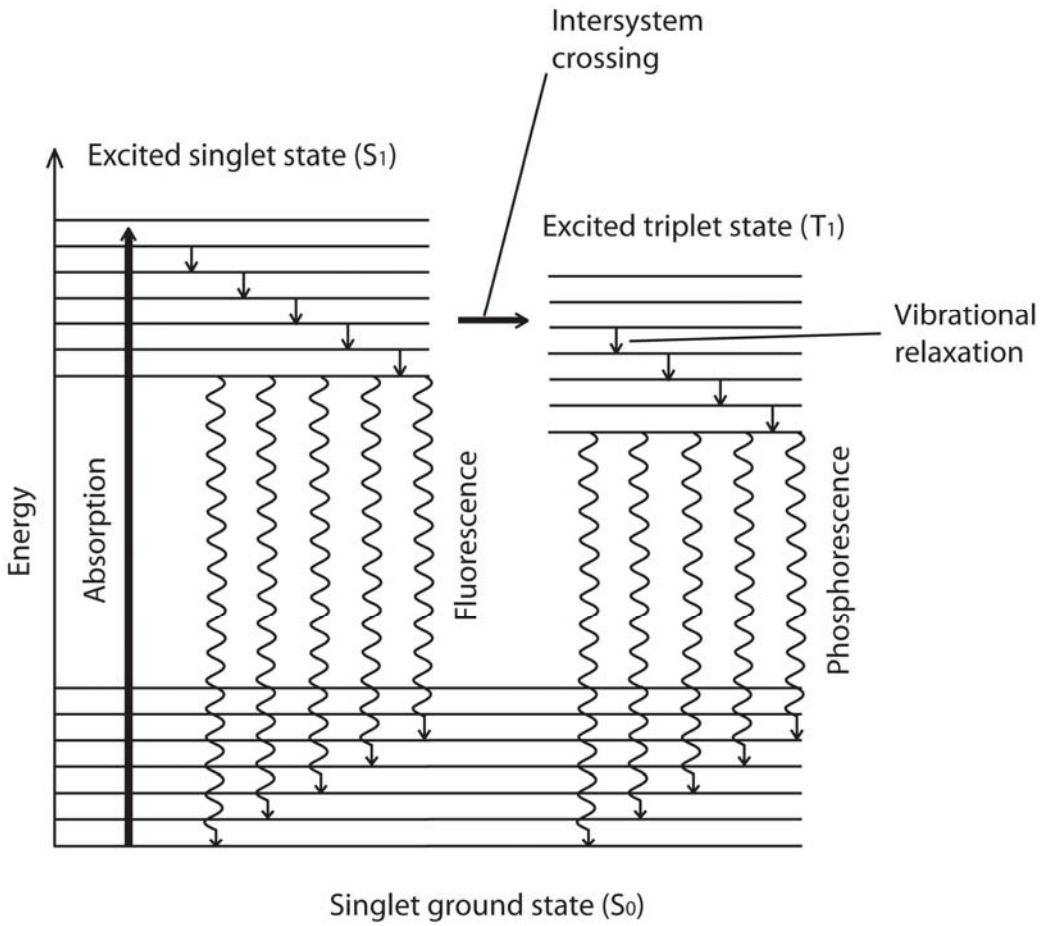

Figure 1.7 A Jablonski diagram illustrating energy levels participating in electronic absorption, fluorescence and phosphorescence (Figure from Whittaker et al. 2000)

Intersystem crossing is a spin-exchange mechanism by which singlet states can be converted into triplet states and triplet states can be converted into singlet states. In fluorescence quenching the excitation energy is transferred to special quencher molecules. The absorption process remains unaffected but the energy of the excited state is dissipated to the quencher molecules. Collisions of the excited molecule with surrounding molecules allow the excited state to lose its vibrational energy and sequentially step down the ladder of vibrational levels. The energy that the excited molecule needs to lose to return to the

electronic ground state is usually too large for the surrounding molecules to accept, but if this energy is lost in a radiative transition, a fluorescence spectrum is produced. The observed fluorescence spectrum is shifted towards longer wavelength corresponding to smaller frequencies and therefore to smaller energy. The fluorescence spectrum therefore shows structure characteristic of the vibrations of the lower state (Whittaker et al. 2000).

The contribution of fluorescence to the various deactivation processes of the excited state is termed the quantum yield. The quantum yield is defined by the quotient of the number of photons that are emitted and the number of photons that are absorbed. The fluorescence lifetime is the time the molecule remains on average in the excited state, before the emission takes place.

Some of the applications of fluorescence spectroscopy are the study of: protein structure and dynamics; protein-protein, protein-ligand and protein drug interactions; protein folding and stability.

1.6.1.1 Determination of $\Delta G°$ by fluorescence spectroscopy

The unfolding of a protein is a function of the urea concentration, or alternatively a function of temperature. Fluorescence emission spectra of a protein (f_f) depend on the degree of unfolding and are characterized by the spectral parameter $\langle\lambda_f\rangle$

$$\langle\lambda_F\rangle = \frac{\sum f_\lambda \cdot \lambda}{\sum f_\lambda} \qquad \text{(Eq. 1.1)}$$

f_λ are the fluorescence intensities at a given wavelength λ. $\langle\lambda_f\rangle$ depends on the entire spectrum and therefore better describes the contributions of the folded and unfolded states of the protein than the intensity at a selected individual wavelength. For an equilibrium unfolding transition between two conformational states ($S_1 \rightarrow S_2$) of a protein, the mole fraction of state S_1 can be expressed using $\langle\lambda_f\rangle$ of the spectrum of the mixture (i.e. $\langle\lambda_m\rangle$) and $\langle\lambda_f\rangle$ of the spectra of the states S_1 and S_2 (i.e. $\langle\lambda_1\rangle$ and $\langle\lambda_2\rangle$, respectively (cf. Mann and Matthews 1993; Roumestand et al. 2001). The spectrum F_λ at a selected urea concentration is a linear combination of the spectra of the states S_1 and S_2:

$$F_\lambda(S_1 + S_2)\cdot c = \left[X \cdot f_\lambda(S_1) + (1 - X)\cdot f_\lambda(S_2)\right]\cdot c \qquad \text{(Eq. 1.2)}$$

$f_\lambda(S_1)$ and $f_\lambda(S_2)$ are the fluorescence spectra of the states S_1 and S_2, respectively, X is the mole fraction of S_1, and c the concentration of the protein. With the parameters $\langle\lambda_M\rangle$, $\langle\lambda_1\rangle$, and $\langle\lambda_2\rangle$ for the fluorescence spectra of the mixture and the individual states S_1 and S_2, $\langle\lambda_M\rangle$ can be expressed as

$$\langle\lambda_M\rangle = \frac{\sum_\lambda \lambda \cdot F_\lambda(S_1+S_2)}{\sum_\lambda F_\lambda(S_1+S_2)} = \frac{X\cdot\sum_\lambda \lambda\cdot f_\lambda(S_1)+(1-X)\cdot\sum_\lambda \lambda\cdot f_\lambda(S_2)}{X\cdot\sum_\lambda f_\lambda(S_1)+(1-X)\cdot\sum_\lambda f_\lambda(S_2)} \qquad \text{(Eq. 1.3)}$$

This equation can be rewritten to obtain the mole fraction of the folded protein, X_1 and therefore the equilibrium constant K of the unfolding reaction:

$$X_1 = \left(\frac{\langle\lambda_M\rangle-\langle\lambda_1\rangle}{\langle\lambda_2\rangle-\langle\lambda_M\rangle}\cdot\frac{\sum_\lambda f_\lambda(S_1)}{\sum_\lambda f_\lambda(S_2)}+1\right)^{-1} \qquad K = \frac{\langle\lambda_1\rangle-\langle\lambda_M\rangle}{\langle\lambda_M\rangle-\langle\lambda_2\rangle}\cdot\frac{\sum_\lambda f_\lambda(S_1)}{\sum_\lambda f_\lambda(S_2)} \qquad \text{(Eq. 1.4)}$$

$\langle\lambda_M\rangle$ is therefore used to describe the fluorescence of a mixture of folded and unfolded protein as a function of the equilibrium constant K

$$\langle\lambda_M\rangle = \frac{\langle\lambda_1\rangle+\frac{1}{Q_R}K\langle\lambda_2\rangle}{\left(1+\frac{1}{Q_R}K\right)} \quad \text{with} \quad Q_R = \frac{\sum_\lambda f_\lambda(S_1)}{\sum_\lambda f_\lambda(S_2)} \qquad \text{(Eq. 1.5)}$$

Q_R is the ratio of the total fluorescence intensities of the folded over the unfolded state, respectively. The equilibrium constant and the free energy of the unfolding transition are given by:

$$\Delta G^\circ_{1\to2} = -RT\ln(K) = -RT\ln\left(\frac{1-X_1}{X_1}\right) \qquad \text{(Eq. 1.6)}$$

The free energy of unfolding depends linearly on the concentration of the denaturant urea in the transition region and can be obtained by extrapolation to 0 M urea (see e.g. Pace 1990; Pace et al. 1998):

$$\Delta G^{\circ}_{1\rightarrow 2} = \Delta G^{\circ}_{1\rightarrow 2}\left(\mathrm{H_2O}\right) - m \cdot c\left(\mathrm{urea}\right) \qquad \text{(Eq. 1.7)}$$

$\langle\lambda_1\rangle$ and $\langle\lambda_2\rangle$ were found to depend linearly on the denaturant concentration. Therefore we obtain:

$$\left\langle \lambda_M \right\rangle = \frac{\left(\left\langle \lambda_{1,0} \right\rangle + m_1 \cdot c_D\right) + \left(\left\langle \lambda_{2,0} \right\rangle + m_2 \cdot c_D\right)\frac{1}{Q_R}K}{\left(1 + \frac{1}{Q_R}K\right)} \qquad \text{(Eq. 1.8)}$$

Using relations (1.6), (1.7) and (1.8) leads to

$$\left\langle \lambda_M \right\rangle = \frac{\left(\left\langle \lambda_{1,0} \right\rangle + m_1 \cdot c_D\right) + \left(\left\langle \lambda_{2,0} \right\rangle + m_2 \cdot c_D\right)\frac{1}{Q_R}e^{-\frac{\Delta G^{\circ}(\mathrm{H_2O})}{RT} - m\frac{c_D}{RT}}}{\left(1 + \frac{1}{Q_R}e^{-\frac{\Delta G^{\circ}(\mathrm{H_2O})}{RT} - m\frac{c_D}{RT}}\right)} \qquad \text{(Eq. 1.9)}$$

Equation 1.9 was used here to fit all unfolding titrations monitored by fluorescence spectroscopy. The linear extrapolations from the pre- and post transition regions of the folded and unfolded states are therefore included in a direct fit of the unfolding titration obtained from the spectroscopic signal $\langle\lambda_F\rangle$ as a function of the denaturant concentration (c_D), where $\langle\lambda_{1,0}\rangle$, $\langle\lambda_{2,0}\rangle$, m_1, and m_2 are the intercepts ($\langle\lambda_{i,0}\rangle$) and slopes ($m_i$) of the pre- (index 1) and post- (index 2) transitional baselines, respectively. These parameters, the free energy of the unfolding transition in absence of the denaturant, $\Delta G^{o}(H_2O)$ and the slope m that describes the change in the free energy as a function of the denaturant concentration (c_D), are fit parameters. The ratio of the total fluorescence intensities is determined from the fluorescence spectra of the folded and unfolded form of the protein and used as a fixed fit parameter.

1.6.1.2 Temperature dependence of $\Delta G°$ and enthalpy of unfolding

The temperature dependence of $\Delta G°$ is described by a modified form of the Gibbs-Helmholtz equation (c.f. Pace et al. 1998). $\Delta G°(T) = \Delta H° - T\Delta S°$ can be obtained from the unfolding transition at the protein melting temperature (i.e. at the midpoint of the thermal unfolding transition):

$$\Delta G^{\circ}(T) = \Delta H^{\circ}{}_{M} - T \cdot \Delta S^{\circ}{}_{M} + \int_{G_M}^{G(T)} dG = \left(1 - \frac{T}{T_M}\right)\Delta H^{\circ}{}_{M} + \int_{T_M}^{T} dH - \int_{T_M}^{T} TdS - \int_{T_M}^{T} SdT$$

This leads to:

$$\Delta G^{\circ}(T) = \Delta H^{\circ}{}_{M} \cdot \left(1 - \frac{T}{T_M}\right) - \Delta c_P \left[T_M - T + T \cdot \ln\left(\frac{T}{T_M}\right)\right] \qquad \text{(Eq. 1.10)}$$

In Eq. 1.10, $\Delta G^{\circ}(T)$ is ΔG° at a temperature T and Δc_p is the change in heat capacity for the unfolding reaction. T_m is the melting temperature and $\Delta H^{\circ}{}_{M}$ the enthalpy change at the melting temperature. The enthalpy change was calculated from the temperature dependence of the equilibrium constant using the van't Hoff equation:

$$\frac{d\ln(K)}{d\,1/T} = -\frac{\Delta H^{\circ}}{R} \qquad \text{(Eq. 1.11)}$$

Here, R is the universal gas constant, K the equilibrium constant, T the temperature and ΔH° the change in enthalpy.

1.6.2 Single-channel recordings

The aim of channel reconstitution is to incorporate the channel into an artificial membrane in which its function can be investigated. For practical purposes this means a membrane system in which ion flow through the channel can be studied under voltage-clamp conditions, ideally with good enough resolution to permit the measurement of single-channel open and closed lifetimes. The starting point for such studies is the formation of an artificial planar phospholipid bilayer. A bilayer is formed across a small hole (0.1 mm^2) connecting two compartments in a teflon chamber filled with buffered salt solutions and containing electrodes which are used to detect any movement across the bilayer (Figure 1.8).

This method was named black lipid membrane method (Benz et al. 1978) because the lipid becomes optically black as soon as it forms a bilayer. The lipid bilayer is formed

using a solution of 1% diphythanoyl-glycerophosphocholine in *n*-decane. Detergent-solubilized membrane proteins are then added to the aqueous phase to a final concentration of 1-100 ng/ml. Functional membrane proteins are incorporated into the bilayer minutes thereafter. Each inserted membrane protein is able to transport a certain amount of ions per time unit between the two compartments of the teflon cell, detected by the electrodes as a stepwise increase of membrane conductance (i.e. current divided by voltage).

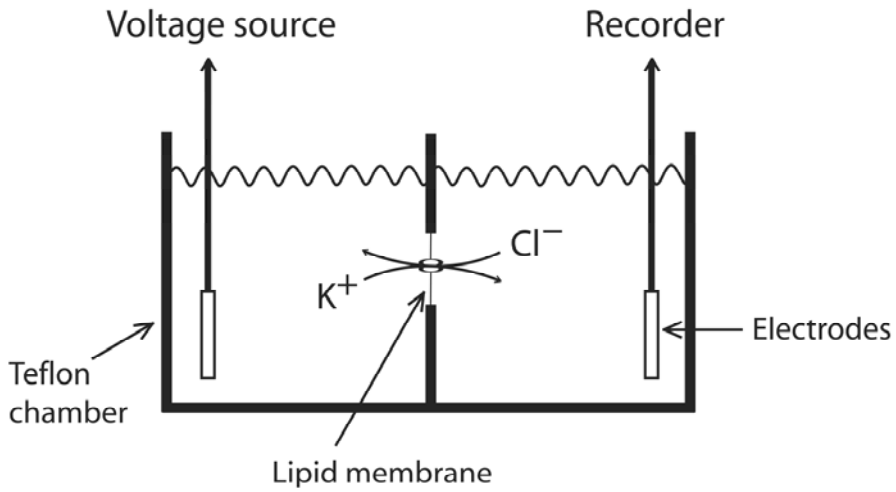

Figure 1.8 The setup of the black lipid film assay A teflon chamber is separated into two compartments by a wall which contains a small hole where a planar lipid bilayer is formed. Both compartments are filled with buffer containing salt. Two silver electrodes are connected to a voltage source and a recorder, respectively. The circuit is completed through earth. Reconstitution of porins into the lipid bilayer can be followed by current increase due to the movement of ions through the porins. Figure modified from Hancock et al. (Hancock et al 1987).

The lipid bilayer method allows the resolution of molecular events, as each increment is the conductance of one single pore-forming protein. The interpretation of single channel measurements requires a statistically significant number of recordings, in order to calculate the average value from the observed conductance distribution. The single channel conductance is given in nanoSiemens (nS), an excellent functional size-estimation when comparing different non-specific diffusion porins (Benz and Bauer 1988).

2 Amphipathic polymers: Tools to fold integral membrane proteins to their active form

2.1 Abstract

The structure of membrane proteins is specifically tailored for their integration into biological membranes, which are of very different and complex composition. Consequently, it is often difficult to isolate sufficient amounts of active membrane proteins using classical approaches. In view of their biotechnological importance and of relatively few available structures, novel strategies have been explored to isolate large amounts of functionally active membrane proteins. Here we demonstrate a completely new technology to refold overexpressed, but functionally inactive membrane proteins into a synthetic non-detergent surfactant, an amphipathic polymer. Neither natural biological compounds nor detergents are required for folding.

2.2 Introduction

Integral membrane proteins (IMPs) are essential components of all organisms. Some 20–30 % of the open reading frames in the sequenced genomes code for IMPs, at which more than 50% of today's drugs are targeted. Yet, IMPs represent only ~0.2% of all solved structures (Boyd et al. 1998; Wallin and von Heijne 1998) and the molecular bases of drug action on IMPs are not well understood. It is therefore necessary to develop novel technologies to solve bottlenecks that limit the acquisition of high-resolution IMP structures and the exploration of structure-function relationships. For such studies, IMPs must be available in sufficient quantity. Natural sources require large efforts for protein isolation and generally yield too low amounts. IMPs can be overexpressed, but most often under inactive forms that require refolding, a difficult task with established methods.

Here we report, that refolding of several membrane proteins to a functionally active state is successful with innovative non-biological, chemically synthesized amphipathic polymers (amphipols) that have properties of surfactants but unlike classical detergents, do

not solubilize biological membranes. In these refolding experiments, representative membrane proteins of both known structural types were used, namely the β-barrel membrane proteins OmpA from *E. coli* and FomA from *Fusobacterium nucleatum*. Amphipols are a new class of non-detergent surfactants to handle membrane proteins in aqueous solutions in absence of detergents. For the synthesis of amphipols, aliphatic amines, for example octylamine or dodecylamine, are covalently linked to a strongly hydrophilic polymer such as polyacrylate to confer amphipathy (Figure 2.1A). Amphipols have been shown to stabilize several integral membrane proteins in their native form in aqueous solution and to preserve their activity (Tribet et al. 1996; Champeil et al. 2000; Popot et al. 2003). In these studies, several membrane proteins were transferred from their detergent-micelle environment into amphipols and shown to remain functionally active. In the present work, we demonstrate that these novel tools in membrane protein research may be instrumental for the large-scale functional refolding of integral membrane proteins.

2.3 Materials and methods

2.3.1 Amphipol synthesis and purification

Amphipols were synthesized and purified as described previously (Tribet et al. 1996; Popot et al. 2003).

2.3.2 Refolding of outer membrane proteins

Refolding of OmpA was initiated by rapid 20-fold dilution of denatured OmpA in Borate/NaOH buffer (10 mM, pH 10.0 with 2 mM EDTA) that contained 8 M urea into the urea-free buffer containing a 35-fold molar excess of A8-35. The final concentrations were 15 μM OmpA and 520 μM A8-35, respectively. Similarly, refolding of FomA was performed with FomA in 10 M urea and borate buffer containing a 43-fold molar excess of FomA. The final concentrations were 11 μM FomA and 470 μM A8-35, respectively. Samples were incubated at 40 °C for 24 hours.

2.3.3 Protease digestion

Protection of the transmembrane domains of amphipol-refolded IMPs OmpA and FomA against proteolysis was tested by trypsin digestion as described previously (Surrey and Jähnig 1992). Samples containing the IMPs at 0.4 mg/ml were incubated with trypsin at 0.04 mg/ml at 37 °C for 2 hours. Digestion was stopped by addition of 0.04 mg/ml soybean trypsin inhibitor (type I-S, Sigma-Aldrich, Taufkirchen, Germany). For sodium dodecyl sulfate - polyacrylamide gel electrophoresis (SDS-PAGE), an equal volume of 0.125 M Tris buffer, pH 6.8, containing 4% SDS, 20% glycerol, 10% 2-mercaptoethanol and 0.01% bromphenol blue was added and 4 µg of IMP were applied to each lane of a 12% polyacrylamide gel.

2.3.4 Single-channel conductance experiments

The activities of OmpA and FomA, respectively, were tested by recording their single channel conductivities after refolding into A8-35 and reconstitution into black lipid membranes. The bilayer membrane was formed from a 1% solution of diphytanoyl-glycerophosphocholine (Avanti Polar Lipids, Alabaster, AL) in n-decane. The lipid solution was painted on a 500-µm hole in a Teflon partition separating two 6-ml compartments, which were filled with KCl/Tris buffer (1 M KCl, 10 mM Tris, pH 7.2) (Benz et al. 1978). The compartments were connected to the recording system through two silver electrodes coated with silver chloride, one of which (the front, *cis* side) was grounded, whereas the other (the rear, *trans* side) was connected to a custom designed trans-impedance amplifier. The painted *di*phPC/n-decane bilayer membranes were tested for integrity by checking the reflectance optically and also by their resistance and capacitance. For reconstitution, IMP/A8-35 complexes were simply added to the *cis*-compartment of the Teflon chamber. A voltage of 100 mV (OmpA) and 10 mV (FomA) was applied at a frequency bandwidth was 100 Hz (Kleivdal et al. 1995; Arora et al. 2000). Current signals were recorded at 22 °C.

2.4 Results

We initially performed folding studies with the β-barrel membrane proteins OmpA from *E. coli* and FomA from *Fusobacterium nucleatum* into amphipol A8-35. The first 171 residues of OmpA form an 8-stranded β-barrel domain (Pautsch and Schulz 1998) in the *E. coli* outer membrane, while the last 154 residues form a soluble periplasmic domain. OmpA functions as a small ion channel (Arora et al. 2000) and as a structural protein. FomA forms voltage-dependent general diffusion channels (Kleivdal et al. 1995; Kleivdal et al. 1999; Puntervoll et al. 2002) and is assumed to be directly involved in the binding between fusobacteria and *Streptococcus sanguis* on the tooth-surface.

When the denaturant urea of concentrated solutions of OmpA or FomA was diluted in presence of amphipol A8-35, the previously unfolded forms of OmpA and FomA remained in solution and did not precipitate. Circular dichroism (CD) spectra (Figure 2.1C and 2.1D) of OmpA and FomA indicated high content of β-sheet secondary structure of the A8-35- solubilized IMPs. The spectra had the typical line-shape expected for integral β-barrel membrane proteins. They were nearly identical to the CD spectra of correctly folded OmpA and FomA in LDAO detergent micelles that are shown for comparison.

The folding of outer membrane proteins can often be investigated by SDS-polyacrylamide gel electrophoresis (Kleinschmidt 2003). The electrophoretic mobilities of the folded and unfolded forms can be distinguished, if the samples are not boiled prior to electrophoresis. For OmpA, apparent molecular weights of 35 kDa (unfolded) and 30 kDa (native membrane protein) were determined previously (Schweizer et al. 1978; Surrey and Jähnig 1992), while FomA migrates at 40 kDa (unfolded form) and at 37 kDa (native membrane protein) (Bakken et al. 1989). In addition, the insertion of the transmembrane domains of integral membrane proteins has also been determined by protease digestion, since these domains are protected by the lipid bilayer (Schweizer et al. 1978; Surrey and Jähnig 1992). We were interested, whether A8-35 would provide a similar protection to OmpA and FomA after incubation with the unfolded forms. The migrations of the denatured and A8-35 reacted OmpA before and after limited proteolysis are shown in SDS-polyacrylamide gels (Figure 2.1D).

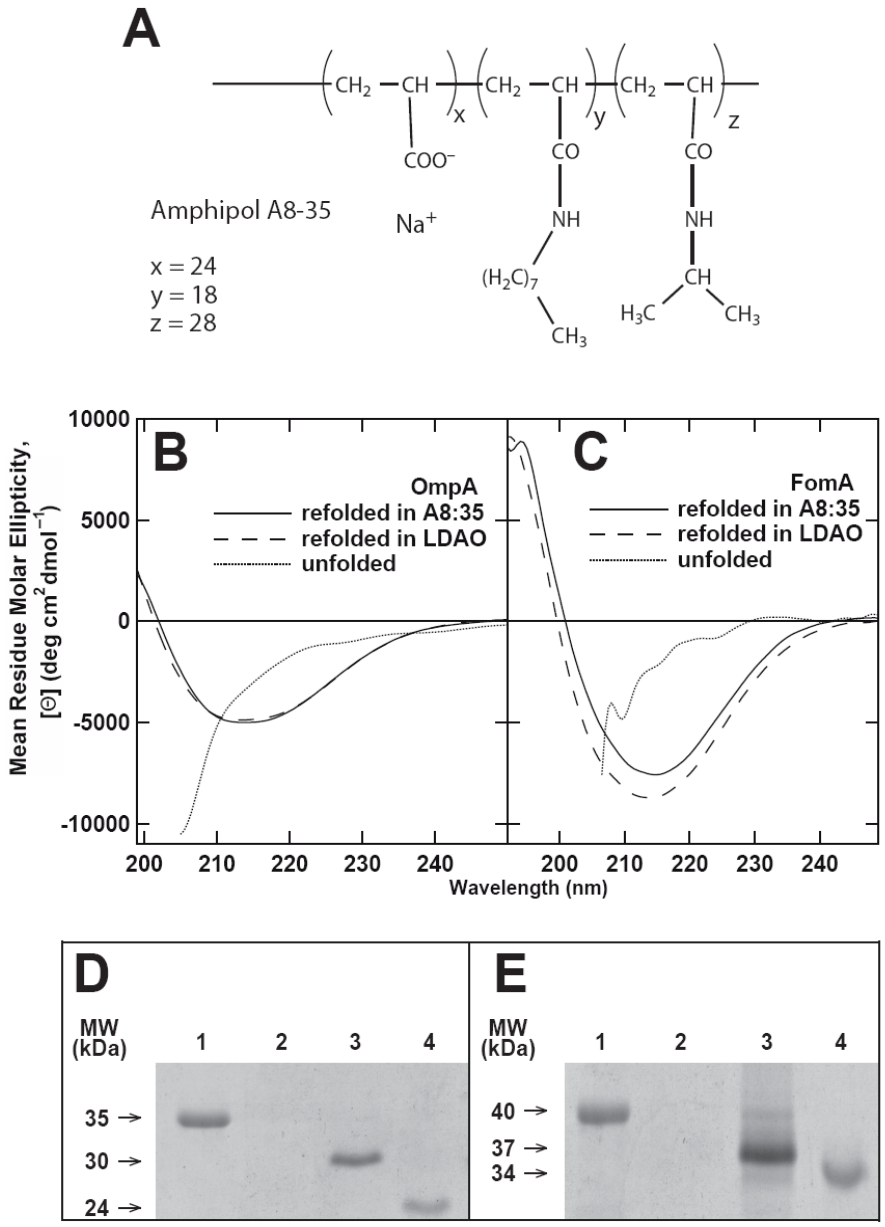

Figure 2.1 Chemical structure of amphipol A8-35 (**A**). Circular dichroism spectra of OmpA (**B**), and FomA (**C**) recorded before and after folding into amphipol A8-35. The spectra of folded OmpA and FomA in N- lauryl- N, N -dimethyl ammonium- N- oxide are shown for comparison. The migration of OmpA (**D**) and FomA (**E**) in SDS-PAGE indicates folding and protection against protease digestion with amphipol A8-35. In both, **D** and **E,** the lanes are: 1. Denatured in 8 M urea, 2. Denatured and then incubated (2 hrs) with trypsin, 3. Refolded in amphipol A8-35, and 4. Refolded in A8-35 and incubated (2 hrs) with trypsin.

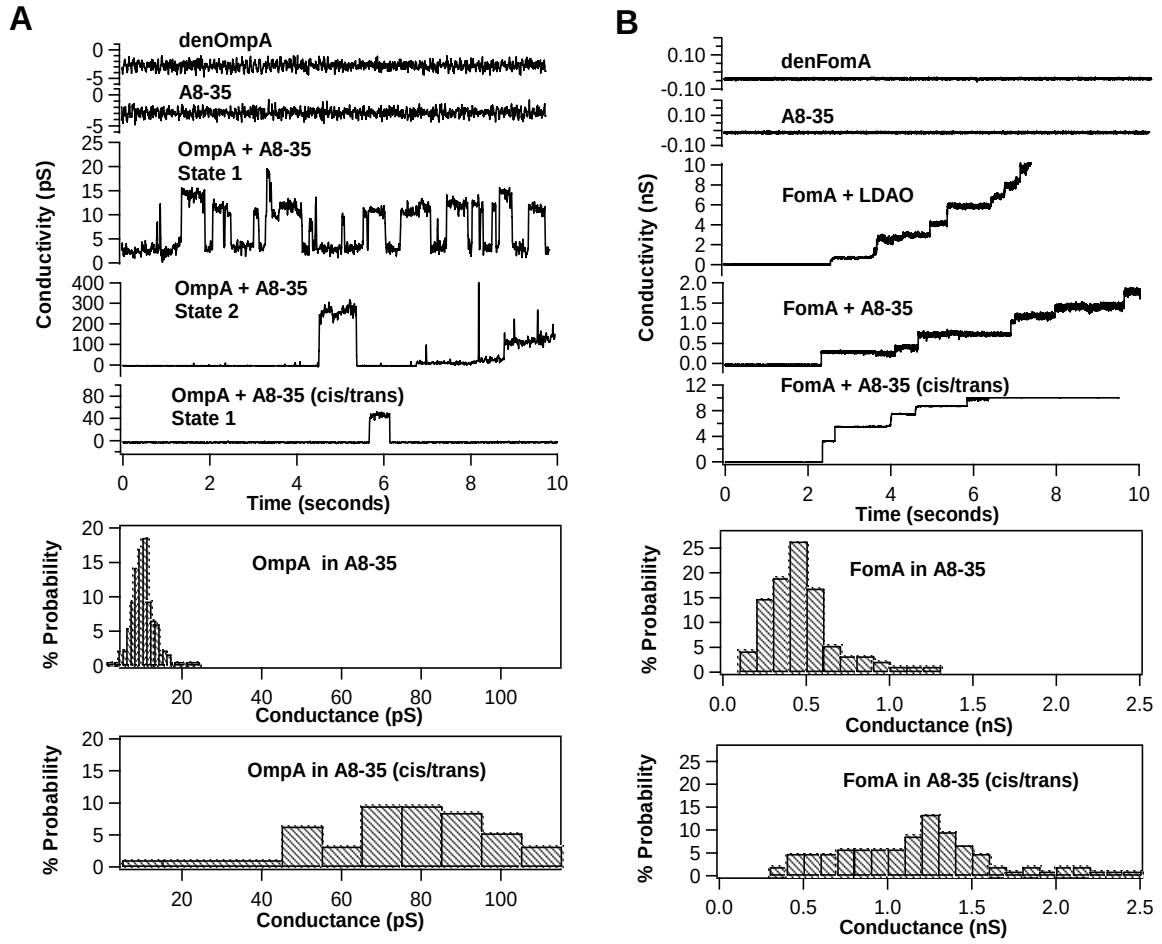

Figure 2.2 Single-channel recordings due to incorporation of OmpA (A) and FomA (B) **A** Amphipol folded OmpA formed small 4-16 pS channels (3rd panel). OmpA folded in C_8E_4 was previously found to form small (40-60 pS) and large (260-320 pS) channels. The smaller channels were associated with the N-terminal transmembrane domain, whereas both domains are required to form larger channels (Arora et al. 2000). The traces of a control experiment with denatured OmpA and A8-35 alone are also shown. The lower panels show histograms of the distribution of small channel openings and closings with A8-35/protein complexes added to the *cis* compartment of the chamber. The histogram at the bottom was obtained by additional presence of the A8-35 alone in the *trans* compartment of the Teflon chamber. The average single-channel conductance for refolded OmpA in A8-35 was 9.73 pS for 183 events and 70-80 pS when A8-35 was present in both compartments. **B** Single channel measurements of folded FomA in amphipol A8-35 (3rd panel). The conductance of one pore-forming unit was in the range 0.3 - 1.3 nS. Recordings of the denatured FomA and A8-35 are presented for comparison. Lower panel: Histogram of the probability of conductivity. A total of 95 events were analyzed and an average conductance of 0.42 nS was obtained (1.2 nS with A8-35 also present in the *trans*-compartment of the Teflon chamber).

As expected, denatured OmpA migrated at 35 kDa. The A8-35-refolded OmpA migrated at 30 kDa, indicating the formation of the folded, native form. A8-35 also protected the transmembrane domain of OmpA against proteolysis with trypsin, leading to the 24 kDa fragment that was observed previously for the proteolysis of lipid bilayer

inserted OmpA (Surrey and Jähnig 1992). FomA (Figure 2.1E) folded in presence of A8-35 and migrated at 37 kDa. After trypsin digestion, a proteolytic fragment of an apparent molecular weight of 34 kDa was obtained. These results provide strong evidence that A8-35 is a novel tool for successful folding of β-barrel membrane proteins.

To confirm complete folding, it was necessary to determine the functional activity of OmpA and FomA by performing single channel recordings. For these experiments, the A8-35 refolded outer membrane proteins OmpA and FomA were reconstituted into black lipid films of diphytanoyl phosphatidylcholine (*di*phPC). Confirmation of A8-35 induced folding and reactivation is possible, because neither OmpA nor FomA can be directly refolded into bilayers of *di*phPC (Figure 2.2). After reconstitution, OmpA formed small 4-16 pS channels as well as channels of larger, 250-320 pS conductance (Figure 2.2A). The small channel openings of detergent refolded OmpA had a conductance of 50 pS (Arora et al. 2000). We were able to obtain the same conductance for amphipol refolded OmpA after reconstitution into *di*phPC bilayers, when we added the same concentration of A8-35 (but without OmpA) to the *trans* compartment of the Teflon chamber used in the single channel recordings. We concluded that the initially observed reduced conductance was due to the sole presence of amphipol on the *cis* compartment, but not caused by alterations of the OmpA channel structure (Figure 2.2A).

We also performed single channel recordings on FomA in *di*phPC after refolding and subsequent reconstitution into *di*phPC black lipid bilayers. The conductance of one pore-forming unit of FomA was in the range 0.4 nS, in contrast to a conductance of 1.1 nS for FomA refolded into LDAO detergent prior to reconstitution into the black lipid bilayers (Figure 2.2B). Again, addition of A8-35 to the *trans* compartment of the Teflon chamber restored the full FomA conductance as observed for the detergent refolding FomA.

The human voltage-dependent anion-selective channel protein isoform 1 (hVDAC1) can also refold into amphipol A8-35. Upon folding, hVDAC1 develops β-sheet secondary structure as determined by CD spectroscopy (Figure 2.3A). Refolded hVDAC1 is functional active as determined by single-channel conductivity measurements (Figure 2.3B), with similar conductances as previously reported for the native purified protein (Colombini et al. 1996).

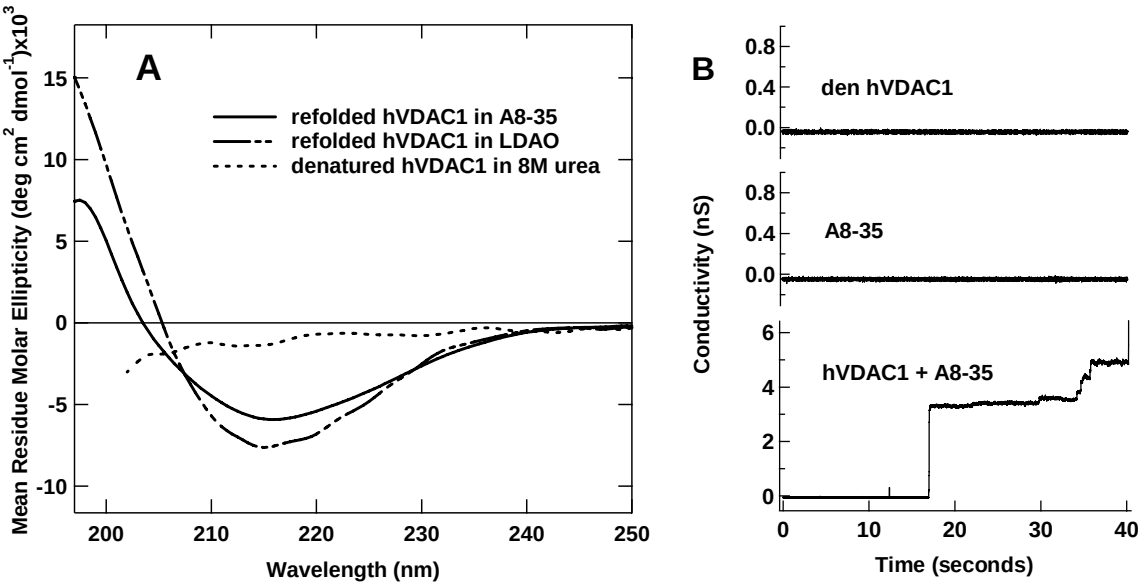

Figure 2.3 CD spectra (A) and single-channel recordings of hVDAC1 (B) **A** hVDAC1 was refolded in amphipol A8-35 at A8-35/hVDAC1 ratio = 32 mol/mol (solid line) and in LDAO micelles (solid-dotted line). Samples in 10 mM Borax/NaOH; 2 mM EDTA; pH 10 were incubated at 40°C for 6 hrs followed by dialysis over night at 10°C before spectra were recorded. Both spectra had their minima localized at 216 nm indicating β-sheet structure development after refolding. In contrast, the spectrum of the denatured hVDAC1 (dotted line) indicated random-coil structure. **B** Single-channel recordings indicated functional activity of refolded hVDAC1 in amphipol A8-35 with conductances of 0.5-3.5 nS. hVDAC1 was added to the *cis* compartment of the Teflon chamber to a final concentration of 50 ng/ml in 10 mM Tris; 1M KCl; pH 7.2. Amphipols were added to both compartments of the Teflon cell. The applied voltage was 10 mV and the frequency bandwidth was 100 Hz.

2.5 Discussion

The present observations are of both basic and practical interest. From a theoretical point of view it is remarkable that several structurally highly different IMPs could be refolded in a medium so unlike their native membrane environment. When solutions of denatured IMPs are depleted of denaturant – in our case urea- in the presence of amphipols, refolding proteins must find themselves entangled with an amphipathic polymer whose physico-chemical properties bear little similarity with those of a membrane environment. Nevertheless, they do manage to find their native fold quickly and with high efficiency, and this even in the complete absence of lipids. This strongly suggests that at least for the particular set of IMPs studied here, the detailed chemical composition and physical properties of the environment have little influence on the free energy minimum conformation of the polypeptide chain: the availability of a non-denaturing amphipathic

screen that shields the transmembrane region from water suffices, the rest of the physico-chemical information needed to achieve the native three-dimensional structure being provided by the amino acid sequence.

The rationale behind the success of A8-35 in promoting refolding is, very likely, that it has enough affinity for IMPs to prevent or slow down intermolecular associations between refolding proteins, while being unable to block the (re)formation of the intramolecular interactions that determine and stabilize their 3D structure.

Given the basic and biomedical importance of obtaining large amounts of properly folded IMPs for structural and pharmacological studies and the problems presented by large-scale expression of most IMPs under their native form, amphipols may represent an attractive alternative tool to try and refold them from inclusion bodies.

3 Folding kinetics of the outer membrane protein OmpA of *E. coli* into the amphipathic polymer A8-35

3.1 Abstract

Amphipathic polymers (amphipols) are a new class of non-detergent surfactants to handle membrane proteins in aqueous solutions in absence of detergents. We recently demonstrated that amphipols like A8-35 can be used to refold denatured integral membrane proteins such as the major outer membrane proteins OmpA from *E. coli* and FomA from *F. nucleatum* upon dilution of the denaturant urea. Folding can be monitored by circular dichroism and fluorescence spectroscopy, and formation of folded OmpA can be determined by electrophoretic mobility measurements, by protease digestion, and by single channel conductivity experiments.

In the present work, we investigated the folding kinetics of OmpA into amphipol A8-35 as functions of temperature and amphipol concentration. The temperature dependence of OmpA folding into amphipols revealed a multi-step refolding mechanism, similar to previous work on the folding of OmpA into lipid bilayers. At 40 °C, folding kinetics could be fitted to a first order rate law. Below 40 °C, folding kinetics were more complex and two folding phases were observed. The folding kinetics were fitted to double-exponential functions and the two rate constants were calculated at each temperature. Activation energies were ~ 5-6 kJ/mol for the fast step and ~27-35 kJ/mol for the slower step, independent of the experimental method. Equilibrium unfolding reveals that OmpA folding/unfolding into A8-35 is fully reversible and that amphipol-refolded OmpA is thermodynamically stable at room temperature.

3.2 Introduction

The biophysical principles of membrane protein folding have been studied with only relatively few integral membrane proteins (IMPs). While bacteriorhodopsin of *Halobium salinarium* has served as a model for IMPS with an α-helix bundle transmembrane domain (Popot and Engelman 2000; Booth and High 2004), outer membrane protein A (OmpA) of *E. coli* has been a popular model in investigating the folding of IMPs with a β-barrel structure of the transmembrane domain (Tamm et al. 2004; Kleinschmidt 2005). All currently known outer membrane proteins (OMPs) of Gram-negative bacteria form transmembrane β-barrels, while integral proteins of the cytoplasmic membrane have α-helical transmembrane domains. In previous work on the folding of IMPs, experiments were performed either with detergent micelles or with preformed lipid bilayers to investigate mechanisms of insertion and folding of IMPs. Detergent micelles have been used in folding studies for example on bacteriorhodopsin or on several OMPs, such as the monomeric OmpA (Dornmair et al. 1990; Kleinschmidt et al. 1999) and OmpG (Fajardo et al. 1998; Conlan et al. 2000; Conlan and Bayley 2003), and the trimeric PhoE (Van Gelder et al. 1994; de Cock et al. 1996; De Cock et al. 1999). In comparison, folding of OMPs into lipid bilayers has been studied using the monomeric OmpA (Surrey and Jähnig 1992; Surrey and Jähnig 1995; Kleinschmidt and Tamm 1996; Kleinschmidt and Tamm 1999; Kleinschmidt et al. 1999; Kleinschmidt and Tamm 2002; Bulieris et al. 2003), for recent reviews, see (Kleinschmidt 2003; Tamm et al. 2004; Kleinschmidt 2005) and FomA (Pocanschi et al. 2005) and the trimeric OmpF (Surrey et al. 1996). OmpA has been a preferred model in studies on the folding of OMPs, because it is relatively small and present as a monomer. The first 171 residues of OmpA form an 8-stranded β-barrel domain (Vogel and Jähnig 1986; Pautsch and Schulz 1998) in the *E. coli* outer membrane, while the last 154 residues form a soluble periplasmic domain. OmpA functions as a small ion channel in the outer membrane of *E. coli* (Arora et al. 2000; Zakharian and Reusch 2003; Zakharian and Reusch 2005) and as a structural protein (Wang 2002).

Amphipathic polymers (amphipols) are short amphipathic polymers comprised of a hydrophilic backbone grafted with alkyl chains, which can substitute for detergents to provide a milder, stabilizing environment to solubilized IMPs (Tribet et al. 1996; Zoonens et al. 2005). Amphipols are classified by their molecular weight, by their charge and by the

number of free carboxylic groups. For example, amphipol A8-35 (Tribet et al. 1996; Gohon et al. 2005) is anionic, has an average M_r of 8 kDa and the fraction of free carboxylic groups is 35%. Unlike detergent micelles, which are small and consist of relatively few amphiphiles that are in permanent exchange with monomers in solution, the non-polar side chains of the amphipols bind to the hydrophobic transmembrane surface of a membrane protein in a non-covalent, quasi-irreversible manner. In comparison to classical detergents, amphipols do not dissociate and therefore stabilize native IMPs in aqueous solution and preserve their activity (Tribet et al. 1996; Champeil et al. 2000; Popot et al. 2003; Zoonens et al. 2005). We have recently demonstrated that amphipol A8-35 can be used to quantitatively refold the outer membrane proteins OmpA of *E.coli* and FomA of *F. nucleatum* and also the α-helical bacteriorhodopsin to their active conformation from a completely denatured state in absence of detergent micelles or lipid bilayers (Pocanschi et al. 2005). These observations are of both practical and basic interest. They are remarkable since the chemical structure of amphipols is so different from the structures of the natural lipid environment of IMPs, suggesting that the presence of a non-denaturing amphipathic environment — shielding the transmembrane region from water — suffices to allow IMPs to fold to their native structure. The detailed chemical and physical properties of the direct vicinity of the IMPs have apparently very little impact on the free energy minimum of the conformational space of the polypeptide chain, which is defined by the amino acid sequence.

In the present study, we examined the thermodynamic stability of OmpA in A8-35 and the time course of formation of native OmpA structure in this amphipol to better understand the folding of this membrane protein. We determined the approximate A8-35/OmpA stoichiometries required for complete refolding of OmpA. From the temperature dependence of the OmpA folding kinetics into A8-35, we estimated the corresponding activation energies for folding. We compare our results are to the stability and folding of OmpA in lipid bilayers and detergent micelles.

3.3 Materials and methods

3.3.1 Materials

Diphytanoyl-glycerophosphocholine was from Avanti Polar Lipids (Alabaster, AL, USA). Coomassie Brilliant Blue was from BIO-RAD (Hercules, CA, USA), LDAO and n-decane were from Fluka (Buchs, Switzerland), 2-mercaptoethanol and glycerol were from Merck (Darmstadt, Germany), acrylamide, bis-acrylamide and urea were from Serva (Heidelberg, Germany), IPTG was from BioVectra (Oxford, CT, USA), SDS and TEMED were from Roth (Karlsruhe, Germany), Borate, Bromphenol Blue, EDTA, MES, Tris, trypsin, trypsin inhibitor and all other chemicals were purchased from standard sources such as Sigma (Steinheim, Germany) and were of analytical grade.

Amphipol A8-35 was synthesized and purified as described previously (Tribet et al. 1996; Popot et al. 2003). OmpA was purified from *E. coli* as described previously (Surrey and Jähnig 1992). OmpA concentrations of stock solutions were determined using the method of Lowry *et al* (Lowry et al. 1951).

3.3.2 Determination of OmpA folding by SDS-PAGE

The assay is based on the different electrophoretic mobilities of folded (apparent molecular mass 30 kDa) and unfolded OmpA (apparent molecular mass 35 kDa) in sodium dodecyl sulfate polyacrylamide gel electrophoresis (SDS-PAGE), when samples are not heat-denatured before electrophoresis. The 30 kDa form has been shown by Raman, FT-IR, and CD spectroscopy (Vogel and Jähnig 1986; Dornmair et al. 1990; Surrey and Jähnig 1992; Rodionova et al. 1995; Surrey and Jähnig 1995; Sugawara et al. 1996; Kleinschmidt et al. 1999), by phage inactivation assays (Schweizer et al. 1978), and by single channel conductivity measurements (Arora et al. 2000) to correspond to the native structure of OmpA. SDS-PAGE was performed as described previously (Bulieris et al. 2003) using the method of Laemmli (Laemmli 1970) with the modifications described by Weber and Osborne (Weber and Osborne 1964), but without heat denaturation of the samples, if not otherwise specified. The fraction of folded OmpA is determined by densitometry of the

stained polyacrylamide gels as described previously (Kleinschmidt and Tamm 1996; Kleinschmidt and Tamm 2002; Bulieris et al. 2003; Kleinschmidt 2003).

3.3.3 Kinetics of tertiary structure formation by electrophoresis (KTSE)

The kinetics of tertiary structure formation (KTSE) were determined as described (Kleinschmidt 2003). In short: To determine the kinetics of folding of OmpA (Schweizer et al. 1978; Surrey and Jähnig 1992; Kleinschmidt and Tamm 1996; Kleinschmidt 2003), folding reactions were initiated by rapidly diluting 10 µl urea-denatured OmpA into 180 µl of Borax/NaOH buffer (10 mM, pH 10.0, with 2 mM EDTA) containing A8-35. The final OmpA concentrations were 7.2 µM in experiments to determine the kinetics of folding as a function of A8-35 concentration and 15 µM in experiments to determine the kinetics of folding as a function of temperature, respectively. Samples of the reaction mixture were taken at different times after the initiation of folding, and an equal volume of 0.125 M Tris buffer, pH 6.8, containing 4% SDS, 20% glycerol, 10% 2-mercaptoethanol and 0.01% bromphenol blue was added. SDS binds to both folded and unfolded OmpA and inhibits further folding (Surrey and Jähnig 1995; Kleinschmidt and Tamm 1996 #5; Kleinschmidt 2003). Samples were subsequently analyzed by SDS-PAGE.

3.3.4 Trypsin digestion experiments

Since membrane-inserted OmpA is digested only partially, leaving the transmembrane β-barrel domain and a small part of the periplasmic domain intact, inaccessibility of the OmpA transmembrane domain to trypsin digestion was tested also after OmpA folding into A8-35, using protocols described previously (Surrey and Jähnig 1992). In short: samples containing protein at 0.4 mg/ml OmpA were incubated with trypsin at 0.04 mg/ml at 37°C for 2 hours. Digestion was stopped by addition of 0.04 mg/ml soybean trypsin inhibitor. An equal volume of 0.125 M Tris buffer, pH 6.8, containing 4% SDS, 20% glycerol, 10% 2-mercaptoethanol and 0.01% bromphenol blue was added. The samples were analyzed by SDS-PAGE (12% acrylamide). 4 µg OmpA was loaded per lane.

3.3.5 Folding monitored by circular dichroism spectroscopy

Far UV CD spectra of 45 μM OmpA were recorded on a Jasco 715 CD spectropolarimeter using a 0.1 mm cuvette. Samples were incubated for 24 h at 40°C before spectra were recorded. Eight scans were accumulated from 190 to 260 nm (205–260 nm in presence of 8 M urea) with a response time of 16 s, a bandwidth of 1 nm, and a scan speed of 20 nm/min. Background spectra without OmpA were subtracted. The recorded CD spectra were normalized to obtain the mean residue molar ellipticity according to

$$[\Theta](\lambda) = 100\frac{\Theta(\lambda)}{c \cdot n \cdot l} \qquad \text{(Eq. 3.1)}$$

where l is the path length of the cuvette, $\Theta(\lambda)$ is the recorded ellipticity at wavelength λ, c is the concentration and n the number of amino acid residues of FomA. Far UV circular dichroism (CD) spectra of 45 μM OmpA were recorded on a Jasco 715 CD spectropolarimeter using a 0.1 mm cuvette. OmpA samples with LDAO detergent or A8-35 detergent/OmpA ratio = 1000 mol/mol and A8-35/OmpA ratio = 8.8 mol/mol, respectively and simultaneous 30X urea dilution were incubated for 24 h at 40 °C to allow for OmpA refolding. All samples were then dialyzed at 10°C for 12 hrs against two liters of buffer (10 mM borate, 2 mM EDTA, pH 10). Dialysis buffer was exchanged 3 times. Dialysis was performed to remove urea, which causes high noise levels in the CD spectral region below 205 nm. Twelve scans, from 200 to 250 nm (205–250 nm in presence of 8 M urea) with a response time of 16 s, a bandwidth of 1 nm, and a scan speed of 20 nm/min were accumulated and averaged. Background spectra without OmpA were subtracted for all samples.

3.3.6 Single-channel conductance experiments

Single channel recordings were performed after reconstituting OmpA-amphipol complexes into planar lipid bilayers. Planar lipid bilayers were formed from a solution of 1% diphytanoyl phosphatidylcholine (*di*phPC) in *n*-decane using the method of Mueller *et al*. (Mueller et al. 1962), with modifications by Busath et al. (Busath and Szabo 1981). The lipid solution was painted on a 500-µm hole in a Teflon partition separating two 6-ml compartments, which were filled with KCl/Tris buffer (1 M KCl, 10 mM Tris, pH 7.2) (Benz et al. 1978). The compartments were connected to the recording system through two silver electrodes coated with silver chloride, one of which (the front, cis side) was grounded, whereas the other (the rear, trans side) was connected to a custom designed trans-impedance amplifier. The painted *di*phPC /n-decane bilayer membranes were tested for integrity by checking the reflectance optically and also by their resistance and capacitance. After the bilayers were formed, 3.4 µl of 1.4 mg/ml of OmpA in LDAO micelles and 3.1 µl of 1.6 mg/ml of OmpA in A8-35 at A8-35/OmpA ratio of 8/1 (mg/mg), respectively were added to the cis compartment. A potential of 100-mV was applied to the trans compartment (Arora et al. 2000). The frequency bandwith was 100 Hz. Current signals were recorded at 22 °C and single channel conductance events were analyzed using the software IGOR (Wavemetrics, Portland, OR) with the IGOR NIDAQ Tools extensions for data acquisition.

3.3.7 Folding kinetics monitored by fluorescence spectroscopy

Fluorescence kinetics were started by rapidly mixing 14 µl denatured OmpA with 986 µl of borate buffer (10 mM, pH 10, with 2 mM EDTA) containing A8-35 at a molar OmpA/A8-35 ratio of 35. The final OmpA concentration was 1.3 µM. To monitor OmpA folding, spectra were recorded immediately after addition of OmpA and then every 20 minutes up to a total of 480 minutes. Samples were slightly stirred between measurements.

3.3.8 Analysis of folding kinetics

To examine the kinetics of OmpA folding into amphipol A8-35, kinetics were fit to different models, composed of first-order (1.ord) or second-order (2.ord) rate laws (Kleinschmidt and Tamm 2002) assuming either one kinetic phase or two parallel kinetic phases. In the fits, the concentrations of the unfolded protein $[P_u]_0$, and of amphipol $[A]_0$ that were used in the experiment were known parameters and invariable. The rate constants of the first (k_1) and the second kinetic phase (k_2), the relative contributions *f* and 1-*f* of each of the kinetic phases, and the fraction of folded OmpA obtained at the end of the folding reaction (i.e. the folding yield, *R*) were the four fit parameters. For example, in two parallel folding phases, described by first and second order kinetics, the concentration of folded OmpA at time *t*, $[P_F](t)$, is:

(Eq. 3.2)

$$[P_F](t) = f[P_U]_0\{1-\exp(k_{1.ord}\cdot t)\} + [(1-f)-(1-R)]\frac{[P_U]_0[A]_0\cdot\left(\exp\{([P_U]_0-[A]_0)\cdot k_{2.ord}\cdot t\}-1\right)}{[P_U]_0\cdot\exp\{([P_U]_0-[A]_0)\cdot k_{2.ord}\cdot t\}-[A]_0}$$

We assumed for all kinetic models that either at low amphipol concentrations or at lower temperatures, the slow folding phase of OmpA would not complete and a fraction 1–*R* of OmpA would not be available for folding in the slow folding pathway.

3.3.9 Equilibrium unfolding monitored by fluorescence spectroscopy

To estimate and compare the thermodynamic stabilities ($\Delta G°$) of OmpA in either LDAO micelles or in A8-35, we performed equilibrium unfolding experiments and recorded fluorescence spectra of OmpA at different concentrations of the denaturant. For equilibrium unfolding/folding experiments, equilibration was monitored starting from either unfolded or folded forms in two different sets of experiments. In each of these sets, equilibration was monitored at selected urea concentrations until no further changes in fluorescence spectra were observed.

To monitor equilibration starting from the unfolded form, 1.4 µl of unfolded OmpA (31.4 mg/ml) in 10 M urea were mixed with 998.6 µl of an A8-35 solution (0.35 mg/ml) in borate buffer (10 mM pH 10, 2 mM EDTA) containing urea at different concentrations, ranging from 0 to 10 M. The molar A8-35/OmpA ratio was 35 and the final OmpA concentration was 1.3 µM in a total volume of 1 ml.

To monitor equilibration starting from the folded state, 26 µl folded OmpA (1.6 mg/ml) in A8-35 at a molar ratio A8-35/OmpA of 35 were mixed with 974 µl borate buffer (10 mM pH 10, 2 mM EDTA) containing different urea concentrations from 0 to 10 M urea.

All samples were incubated at 40°C until equilibration was reached. Similarly these procedures were applied for folding-unfolding reactions of OmpA in LDAO micelles at a molar LDAO/OmpA ratio of 800.

Fluorescence spectra were recorded as described previously (Bulieris et al. 2003) on a Spex Fluorolog-3 spectrofluorometer with double monochromators in the excitation and emission pathways. The excitation wavelength was 290 nm, and the bandwidths of the excitation monochromators were 2 nm. The bandwidths of the emission monochromators were 3.7 nm. The integration time was 0.05 s, and an increment of 0.5 nm was used to scan spectra in the range of 300–380 nm. Three scans were averaged for each sample.

3.3.10 Determination of the free energy of unfolding

The equilibrium unfolding titrations of OmpA with urea were fit to Eq. 1.9.

3.4 Results

3.4.1 OmpA folds quantitatively into the amphipathic polymer A8-35

OmpA is known to refold quantitatively into detergent micelles of neutral and zwitterionic detergents (Surrey and Jähnig 1992; Kleinschmidt et al. 1999) and into lipid bilayers of a range of phosphatidylcholines with different length of the fatty acyl chains (Kleinschmidt and Tamm 2002) at basic pH. We discovered that OmpA also folds in presence of the amphipathic polymer A8-35, when the denaturant urea is strongly diluted

in presence of amphipol A8-35. Evidence for folding was obtained with a range of different methods. We first examined the secondary structure of OmpA under different conditions and recorded circular dichroism spectra of OmpA in unfolded form in 8 M urea, after dilution of urea in presence of amphipol A8-35, and for reference purposes, after dilution of the denaturant urea in presence of LDAO detergent micelles (Figure 3.1A). OmpA is known to refold in LDAO detergent micelles at pH 10 (Kleinschmidt et al. 1999).

Fluorescence spectra of unfolded OmpA in urea and of OmpA in amphipol A8-35 were recorded at different temperatures (Figure 3.1B). Fluorescence spectra of OmpA in A8-35 had an intensity maximum at 328 nm, while the spectra of urea-unfolded OmpA had a maximum at 347 nm.

The CD spectrum of denatured OmpA in 8 M urea was typical for a random coil structure. The CD spectrum of the aqueous form of OmpA indicated a mixture of α-helix, β-sheet, and random coil secondary structure in OmpA after urea-dilution. After reacting unfolded OmpA either with LDAO or with A8-35, the CD spectra of OmpA indicated a high content of β-sheet secondary structure and had the typical line-shape expected for β-barrel integral membrane proteins. These spectra were nearly identical and they were very similar to those of the native protein reported before (Surrey and Jähnig 1992; Sugawara et al. 1996; Kleinschmidt et al. 1999).

OmpA folding into A8-35 was investigated by SDS-polyacrylamide gel electrophoresis (Schweizer et al. 1978; Kleinschmidt 2003) (Figure 3.1C), without heat-denaturing the samples prior to electrophoresis. Denatured OmpA migrated at 35 kDa (Lane 3) and OmpA incubated with LDAO micelles migrated at 30 kDa, indicating folding. Formation of the folded 30 kDa form of OmpA was also observed upon denaturant-dilution in presence of a 35-fold molar excess of A8-35 (Figure 3.1C lane 7) demonstrating that OmpA also folds into this novel non-detergent surfactant. In previous folding experiments with lipid bilayers, the protection of the transmembrane domain of OmpA by its environment, for example a lipid bilayer or a detergent micelle could be determined by trypsin digestion (Schweizer et al. 1978; Surrey and Jähnig 1992).

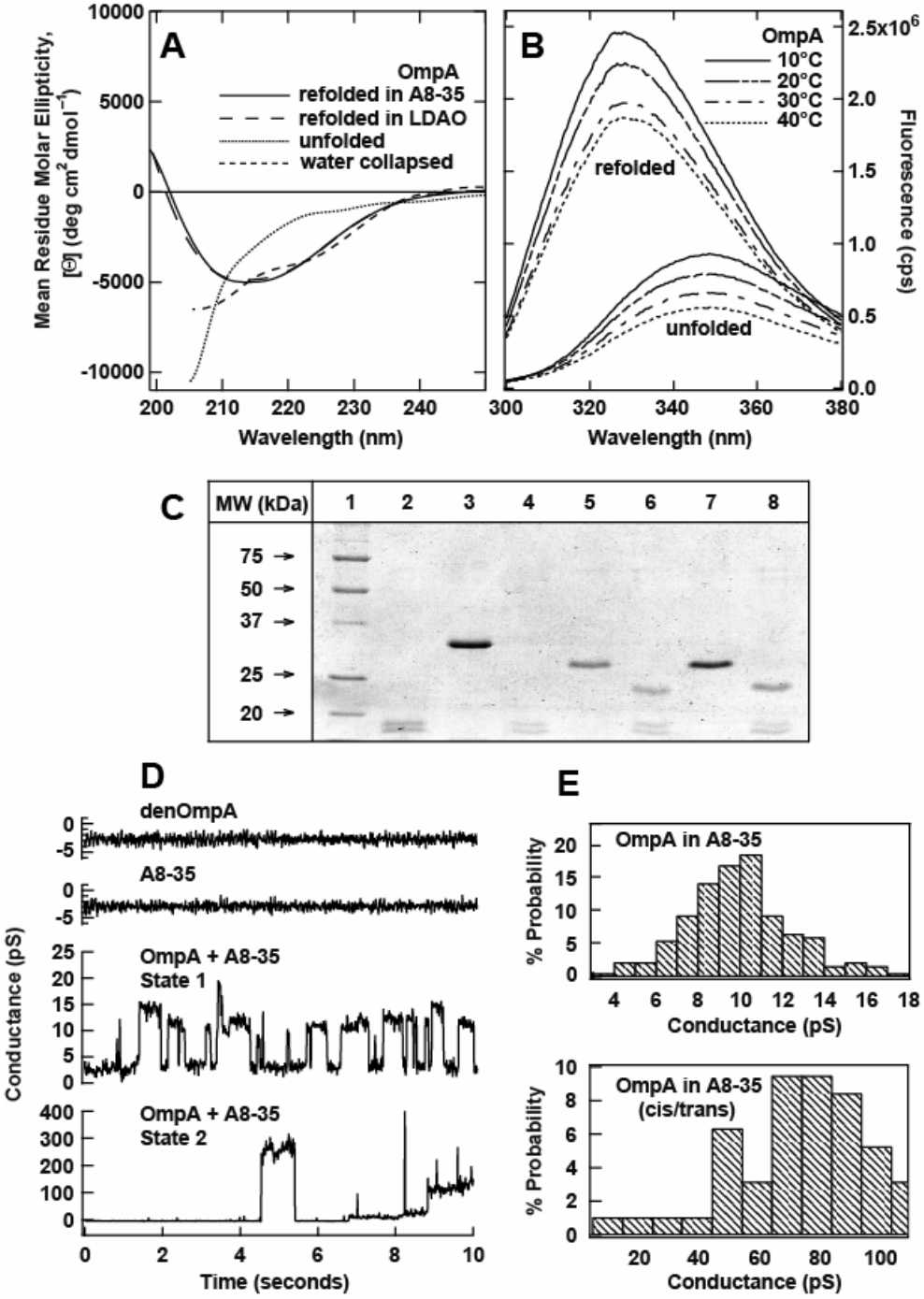

Figure 3.1 **A** Circular dichroism spectra of denatured OmpA in urea (dotted line), refolded OmpA after urea dilution in presence of LDAO micelles (dashed line) and after urea dilution presence of amphipol A8-35 (solid line). **B** Fluorescence spectra of unfolded OmpA in urea and of OmpA in amphipol A8-35 at different temperatures. **C** OmpA reacted with A8-35 is partially protected against proteolysis with trypsin. Lanes: 1. Molecular weight markers; 2. Trypsin inhibitor; 3. Unfolded OmpA; 4. Trypsin digested unfolded OmpA; 5. Refolded OmpA in LDAO micelles; 6. refolded OmpA in LDAO micelles after proteolysis with trypsin; 7. Refolded OmpA in A8-35; 8. refolded OmpA in A8-35 after proteolysis with trypsin. **D** Single-channel conductivity recordings across black lipid films after adding different samples to the *cis*-compartment of the Teflon chamber. Recorded traces are (from top to bottom): **1** addition of denatured OmpA; **2** addition of

A8-35; **3** OmpA state of small conductance 6-14 pS (state 1); and **4** OmpA state of large conductance large 250-350 pS (state 2) after refolding of OmpA into A8-35. **E** Histogram of the probability of conductance after adding A8-35/OmpA complexes to the *cis*-compartment (upper panel) and the same amount of A8-35 (but without OmpA) to the *trans*-compartment of the Teflon chamber (lower panel).

We were interested, whether A8-35 would provide a similar protection to OmpA after incubation with the unfolded forms. The migration of refolded OmpA after trypsin digestion is shown in Figure 3.1C for OmpA refolded the LDAO (lane 6) and for OmpA refolded in A8-35 (lane 8). A8-35 protected the transmembrane domain of OmpA against proteolysis with trypsin, leading to the 24 kDa fragment that was observed previously for the proteolysis of lipid bilayer inserted OmpA (Surrey and Jähnig 1992).

Functional activity of OmpA was confirmed with single channel recordings (Figure 3.1D and 3.1E). For these experiments, the A8-35 refolded OmpA was reconstituted into black lipid films of diphytanoyl phosphatidylcholine (*di*phPC). Confirmation of A8-35 induced folding and reactivation is possible, because OmpA cannot be directly refolded into bilayers of *di*phPC (Figure 3.1D, trace 1). After reconstitution, OmpA formed small 4-16 pS channels (Figure 3.1D, state 1) as well as channels of larger, 250-320 pS conductance (Figure 3.1D, state 2). The small channel openings of detergent refolded OmpA had a conductance of 50 pS (Arora et al. 2000), larger than the conductance that we observed for OmpA reconstituted from OmpA/A8-35 complexes. However, we were able to obtain the same conductance for A8-35 refolded OmpA after reconstitution into *di*phPC bilayers, when we added the same concentration of A8-35 (but without OmpA) to the *trans*-compartment of the Teflon chamber prior to performing single channel recordings (Figure 3.1E, lower panel). We concluded that the initially observed reduced conductance was due to the sole presence of A8-35 in the *cis*-compartment, but not caused by alterations of the OmpA channel structure.

3.4.2 Concentration-dependence of the folding kinetics of OmpA into A8-35

To investigate the stoichiometry of OmpA interactions with A8-35 and the basic mechanism of OmpA folding into A8-35, we performed kinetic studies as a function of the concentration of amphipol A8-35 (Figure 3.2). In a set of different experiments, OmpA was reacted with A8-35 at selected ratios of 0.5, 1, 2, 6, 8, 10, 16 mg/mg. Since synthesis

of A8-35 polymers results in different degrees of polymerization with an average M_r of 8 kDa, this corresponds to averaged molar A8-35/OmpA ratios of 2.2, 4.4, 8.8, 26.3, 35, 43.8 and 70. The time courses of folding were determined by SDS-PAGE as described in Materials and Methods.

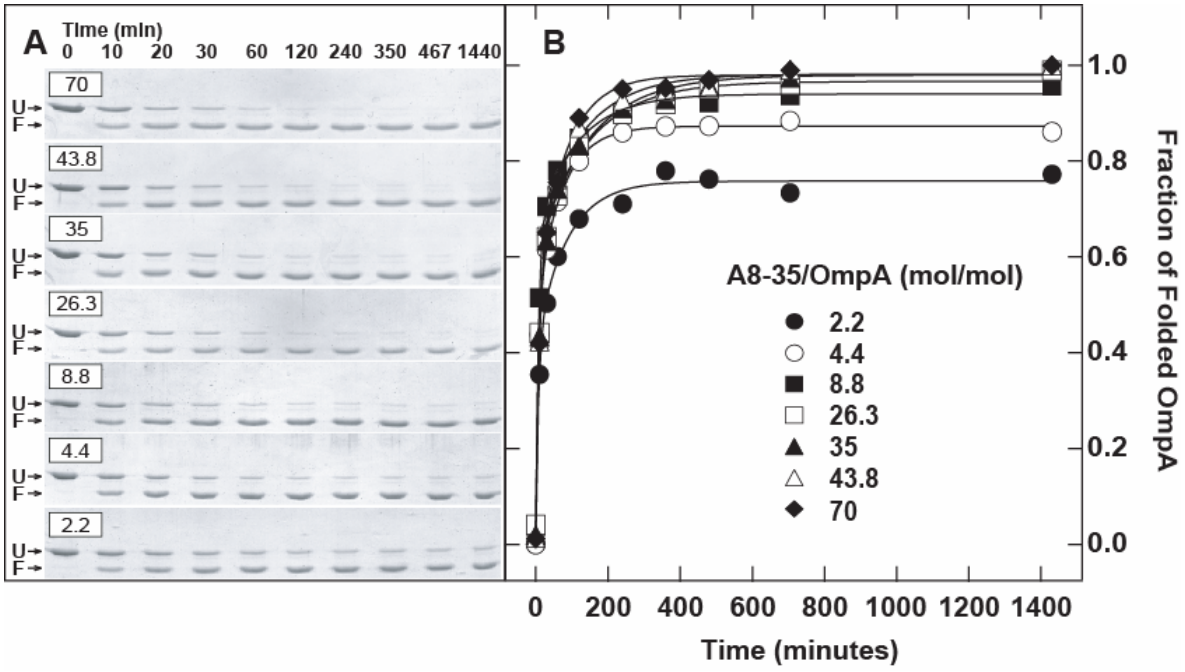

Figure 3.2 Kinetics of insertion and folding of OmpA into amphipol A8-35 determined at different concentrations of A8-35. A Each SDS-Polyacrylamide gels shows the formation of increasing amounts of the folded OmpA with increased incubation time after initiation of folding by denaurant-dilution of unfolded OmpA in urea with A8-35 solutions. Unfolded OmpA (U) migrated at 35 kDa, folded OmpA at 30 kDa (F). The OmpA concentration was 7.2 µM in all gels and the molar ratios amphipol/OmpA were 2.2, 4.4, 8.8, 26.3, 35, 43.8, and 70 (from the gel on the bottom to the gel on the top of panel A). **B** The fraction of folded OmpA was determined from the gels shown in panel **A** by densitometry and plotted as a function of time. All folding reactions were performed at 40°C in 10 mM Borax; 2 mM EDTA; pH 10.0.

Figure 3.2A shows the SDS-polyacrylamide gels obtained at the selected A8-35/OmpA ratios. Even at relatively low ratios, high refolding yields of OmpA were obtained within one hour. For analysis, the fraction of folded OmpA migrating at 30 kDa was determined relative to the total amount of OmpA migrating at 30 (F) and at 35 kDa (U) by densitometric analysis of the bands in each lane and then plotted as a function of time (Figure 3.2B) for each of the selected A8-35/OmpA ratios.

The time course of OmpA folding could not be well fitted by simple single-step kinetics, but in electrophoretic mobility analyses on the folding kinetics of OmpA, we observed only two bands at 35 and at 30 kDa representing the unfolded and folded forms

of OmpA, respectively. Intermediate forms of OmpA upon folding into A8-35 were not detected by SDS-PAGE. Since folding was measured by the relative increase of the 30 kDa form as a fraction of the total OmpA present and clearly a fast and a slow phase of formation of the 30 kDa form were observed (Figure 3.2B), our data indicate the presence of parallel pathways of OmpA folding into A8-35. To analyze the time course of OmpA folding into A8-35, we performed fits to three different kinetic models, assuming two parallel single folding steps. In these fits, we either assumed two parallel first-order steps, two parallel second-order steps or a first-order step parallel to a second-order step. A single-step second-order folding phase was observed previously for the folding of OmpA into lipid vesicles (Kleinschmidt and Tamm 2002) and we expected that it also would be observed in the present experiments, because the rates of interaction of OmpA with A8-35 should be faster with increasing A8-35 concentration.

The two rate constants, the relative contributions of the faster kinetic phase, and the fractions of OmpA folded at the end of the reaction were the fit parameters in all models and are shown in Table 3.1. In all 3 models, the relative contribution of the faster phase was independent of the concentration of A8-35 and also did not depend on the order of the fast and slow folding steps. On average, the faster process contributed 55 ± 9% to OmpA folding.

When two parallel first-order phases were fitted to the data, the rate constants k_1 and k_2 of the two folding processes did not depend on the A8-35 concentration. In contrast, the fits to the two models containing second-order folding steps indicated that the second order rate constants always decreased with increasing A8-35 concentration. This was unexpected and indicated that both folding pathways observed here must be of first order, since rate constants should be concentration independent. We therefore concluded that both the fast and the slow folding processes are of first order. The average first-order rate constants were 0.126 ± 0.020 min^{-1} for the fast process and 0.0100 ± 0.0026 for the slow process, corresponding two half-times, $\tau_{1/2} = \ln(2)/k_F$, of 5.5 min and 70 min, respectively.

Table 3.1 Rate constants of OmpA folding into A8-35 at different concentrations

A. Fits to kinetics composed of two first-order phases

T[a] (°C)	[P][b] (μM)	[A][c] (μM)	$[A]/[P]$ (mol/mol)	k_1[d] (min^{-1})	k_2[e] (min^{-1})	f[f]	R[g]
40	7.2	15.8	2.2	0.142 ± 0.038	0.012 ± 0.003	0.41 ± 0.05	0.76 ± 0.01
40	7.2	31.7	4.4	0.156 ± 0.014	0.014 ± 0.001	0.48 ± 0.02	0.87 ± 0.004
40	7.2	63.3	8.8	0.137 ± 0.018	0.009 ± 0.002	0.65 ± 0.04	0.94 ± 0.01
40	7.2	189.4	26.3	0.119 ± 0.020	0.008 ± 0.002	0.59 ± 0.05	0.97 ± 0.01
40	7.2	252	35	0.111 ± 0.014	0.007 ± 0.001	0.60 ± 0.04	0.98 ± 0.01
40	7.2	315.4	43.8	0.097 ± 0.012	0.008 ± 0.002	0.63 ± 0.04	0.98 ± 0.01
40	7.2	504	70	0.123 ± 0.021	0.012 ± 0.002	0.52 ± 0.05	0.98 ± 0.01

B. Fits to kinetics composed of two second-order phases

T[a] (°C)	[P][b] (μM)	[A][c] (μM)	$[A]/[P]$ (mol/mol)	k_1[d] ($l\ mol^{-1}min^{-1}$)	k_2[e] ($l\ mol^{-1}min^{-1}$)	f[f]	R[g]
40	7.2	15.8	2.2	12817 ± 5890	1043 ± 334	0.38 ± 0.08	0.76 ± 0.01
40	7.2	31.7	4.4	5771 ± 657	524 ± 49	0.47 ± 0.03	0.87 ± 0.004
40	7.2	63.3	8.8	2279 ± 324	150 ± 39	0.65 ± 0.04	0.94 ± 0.01
40	7.2	189.4	26.3	635 ± 110	40 ± 10	0.59 ± 0.05	0.97 ± 0.01
40	7.2	252	35	444 ± 57	29 ± 5	0.60 ± 0.04	0.98 ± 0.01
40	7.2	315.4	43.8	309 ± 39	26 ± 6	0.63 ± 0.04	0.98 ± 0.01
40	7.2	504	70	246 ± 42	25 ± 4	0.51 ± 0.05	0.98 ± 0.01

C. Fits to kinetics composed of a second and a first order phase

T[a] (°C)	[P][b] (μM)	[A][c] (μM)	$[A]/[P]$ (mol/mol)	k_1[d] (min^{-1})	k_2[e] ($l\ mol^{-1}min^{-1}$)	f[f]	R[g]
40	7.2	15.8	2.2	0.166 ± 0.059	1087 ± 307	0.36 ± 0.07	0.76 ± 0.01
40	7.2	31.7	4.4	0.164 ± 0.017	529 ± 48	0.47 ± 0.03	0.87 ± 0.004
40	7.2	63.3	8.8	0.138 ± 0.019	152 ± 39	0.65 ± 0.04	0.94 ± 0.01
40	7.2	189.4	26.3	0.119 ± 0.020	40 ± 10	0.59 ± 0.05	0.97 ± 0.01
40	7.2	252	35	0.111 ± 0.014	29 ± 5	0.60 ± 0.04	0.98 ± 0.01
40	7.2	315.4	43.8	0.097 ± 0.012	26 ± 6	0.63 ± 0.04	0.98 ± 0.01
40	7.2	504	70	0.124 ± 0.021	25 ± 4	0.51 ± 0.05	0.98 ± 0.01

Fits of the data shown in Figure 3.2B were performed to three different models, composed of either two parallel first-order phases (A), two parallel second-order phases (B) or two parallel phases of first and of second order (C). The rate constants of the two kinetic phases, the relative contribution of the fast phase, and the final folding yield were free fit parameters.

[a]temperature, [b]concentration of OmpA, [c]concentration of amphipol A8-35, [d]rate constant of the fast phase. [e]rate constant of the slow phase, [f]relative contribution of the fast phase, [g]final fraction of folded OmpA

3.4.3 Stoichiometry of folding of OmpA into A8-35

To determine the stoichiometry of folding of OmpA into A8-35, we plotted the yields of folded OmpA obtained at different A8-35 concentrations (Figure 3.2) as a function of the molar A8-35/OmpA ratio (Figure 3.3). For analysis, we fitted a simple mass action law for OmpA folding into A8-35 to the experimental data and obtained a stoichiometry of 0.75 ± 0.5 for the interaction of A8-35 with OmpA. The equilibrium constant was K = 0.28 ± 0.06 μM^{-1}, corresponding to a free energy of $\Delta G°$ = 32.6 ± 0.6 kJ/mol (7.8 kcal/mol) for OmpA folding into A8-35.

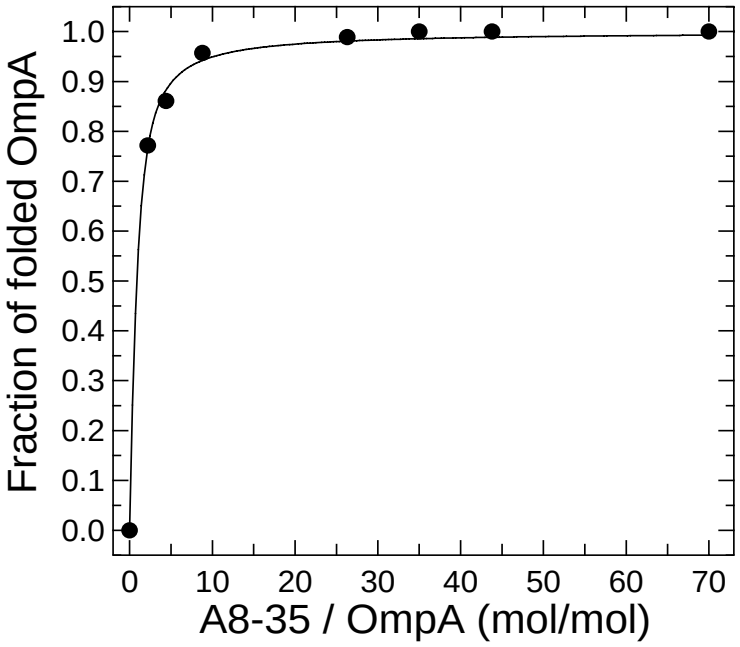

Figure 3.3 OmpA binding and folding into A8-35 as a function of the A8-35 concentration. Fractions of folded OmpA were determined after 1 day of incubation at different concentrations of A8-35 from the gels shown in Figure 2A by densitometry. The data were analyzed by fitting a mass action law for partitioning of OmpA into A8-35.

3.4.4 Temperature-dependence of OmpA folding into A8-35 by SDS-PAGE

In our experiments on the rate-law of OmpA folding into A8-35, we determined the folding kinetics at 40 °C at different A8-35 concentrations. To investigate the activation energies of the two OmpA folding phases into A8-35, we performed experiments at

different temperatures ranging from 10 to 50 °C. We first investigated the folding kinetics with the KTSE method.

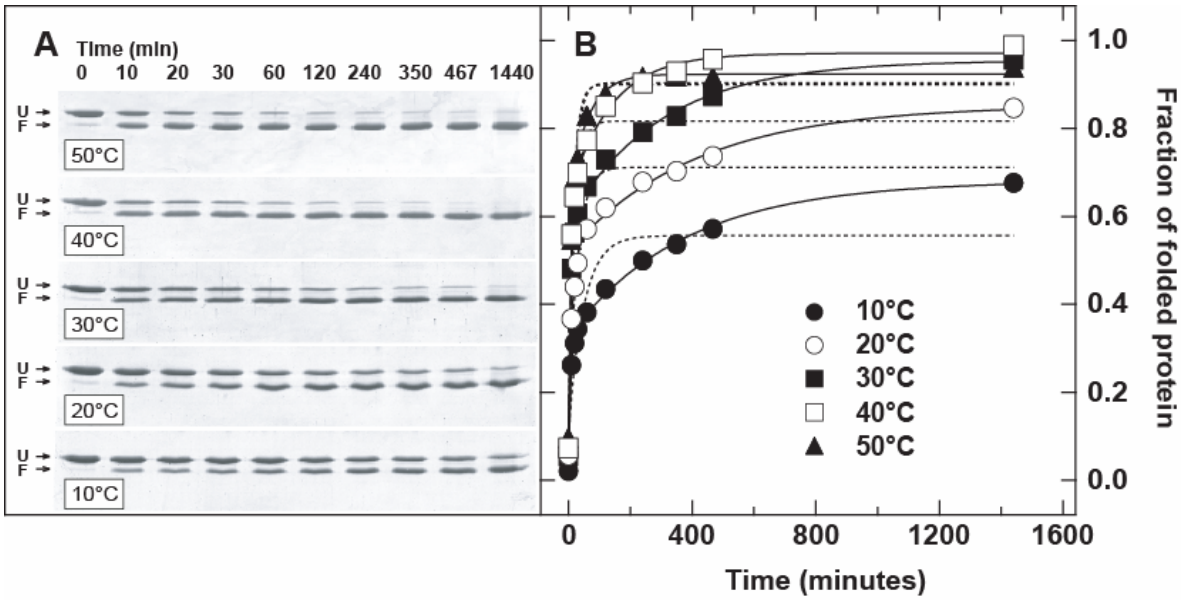

Figure 3.4 Kinetics of insertion and folding of OmpA into amphipol A8-35 determined at different temperatures. A Each SDS-Polyacrylmide gels shows the formation of the folded form of OmpA with increased incubation time. The OmpA folding reactions analyzed in these gels were performed at temperatures of 10, 20, 30, and at 40 °C (from gel at the bottom to gel on the top of panel A). The OmpA concentration was 15 µM and the A8-35/OmpA ratio was 35 mol/mol in all experiments. **B** The gels of panel A were analyzed by densitometry and the fraction of folded OmpA was plotted as a function of time at each temperature. The data were fitted to double-exponential functions (solid lines) and to single exponential functions (dotted lines).

The gels shown in Figure 3.4A indicated that kinetics were slower and yields of folded OmpA were smaller at lower temperatures. However, in contrast to previous OmpA folding experiments into lipid bilayers of dioleoyl phosphatidylcholine (Kleinschmidt and Tamm 1996), formation of the folded form of OmpA was still observed at 20 °C or below and even reached 50 % at 10 °C within 7 h. To determine the rate constants of the folding kinetics, the fraction of folded OmpA was again determined by densitometry and plotted as a function of time at each temperature (Figure 3.4B). Kinetics was fitted to two parallel first-order processes as observed before in the analysis of the concentration dependence of OmpA folding. The corresponding rate constants, relative contributions of the faster process and folding yields are shown in Table 3.2.

Table 3.2 Rate constants for folding of OmpA into amphipol A8-35 at different temperatures.

A. OmpA insertion and folding into A8-35 (KTSE)

T[a] (°C)	[P][b] (μM)	[A][c] (μM)	$[A]/[P]$ (mol/mol)	k_1[d] (min^{-1})	k_2[e] (min^{-1})	f[f]	Y[g]
10	15	525	35	0.141 ± 0.020	0.0027 ± 0.00031	0.33 ± 0.33	0.68 ± 0.01
20	15	525	35	0.107 ± 0.022	0.0026 ± 0.00083	0.51 ± 0.03	0.85 ± 0.04
30	15	525	35	0.152 ± 0.027	0.0034 ± 0.00078	0.59 ± 0.03	0.95 ± 0.03
40	15	525	35	0.177 ± 0.048	0.0076 ± 0.0028	0.64 ± 0.05	0.97 ± 0.03
50	15	525	35	0.163 ± 0.070	0.018 ± 0.011	0.61 ± 0.14	0.92 ± 0.02

B. OmpA insertion and folding into A8-35 (Fluorescence)

T[a] (°C)	[P][b] (μM)	[A][c] (μM)	$[A]/[P]$ (mol/mol)	k_1[d] (min^{-1})	k_2[e] (min^{-1})	f[f]	Y[g]
5	1.25	43.7	35	0.094 ± 0.080	277 ± 52	0.11	0.35
10	1.25	43.7	35	0.044 ± 0.009	113 ± 44	0.23	0.40
20	1.25	43.7	35	0.100 ± 0.017	252 ± 16	0.25	0.56
30	1.25	43.7	35	0.104 ± 0.030	314 ± 39	0.36	0.72
40	1.25	43.7	35	0.086 ± 0.014	295 ± 37	0.50	0.82
50	1.25	43.7	35	0.171 ± 0.991	1047 ± 1190	0.49	0.99

[a]temperature
[b]concentration of OmpA
[c]concentration of amphipol A8-35
[d]rate constante of the fast phase.
[e]rate constante of the slow phase
[f]relative contribution of the fast phase
[g]calculated folding yield
[h]percentage of fluorescence of the folded form of OmpA

The rate constant of the faster process showed little dependence on termperature, while the rate constant of the slower process increased about 6 to 7-fold from 10 to 50 °C. Folding yields increased with temperature from 68% at 10 °C to more than 95 % at 30 °C or higher, which is in agreement with a higher relative contribution of the fast folding process and with the increased rate constant of the slower process at higher temperatures. The temperature dependences of the rate constants were used to calculate the activation energies from Arrhenius plots (Figure 3.5). The activation energies were 6 ± 4 kJ/mol for the first process and 36 ± 9 kJ/mol for the second process, respectively.

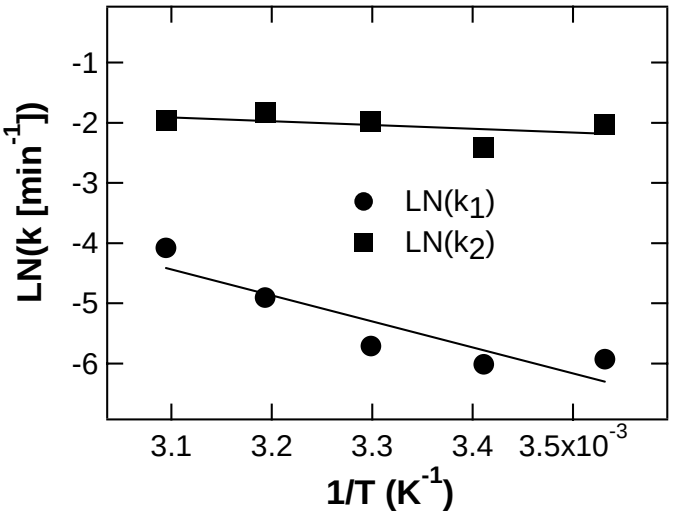

Figure 3.5 Determination of the activation energies of the folding of OmpA into A8-35. For an Arrhenius plot, the logarithms of the rate constants, determined from the double exponential fits shown in Figure 3.4B, were plotted against the reciprocal temperature.

3.4.5 Temperature-dependence of OmpA folding kinetics into A8-35 by fluorescence spectroscopy

While kinetics obtained from KTSE experiments report directly on the formation of folded OmpA, the initial binding of unfolded OmpA to A8-35 may be resolved by fluorescence spectroscopy, as demonstrated in previous studies on the folding of OmpA into lipid bilayers (Surrey and Jähnig 1992; Surrey and Jähnig 1995; Kleinschmidt and Tamm 1996; Kleinschmidt and Tamm 2002). Therefore we recorded fluorescence spectra of OmpA at different times after denaturant dilution in presence of A8-35 and monitored folding kinetics by the increase in fluorescence intensity at 330 nm. Figure 3.6 shows the time courses of folding monitored at temperatures ranging from 5 to 50 °C.

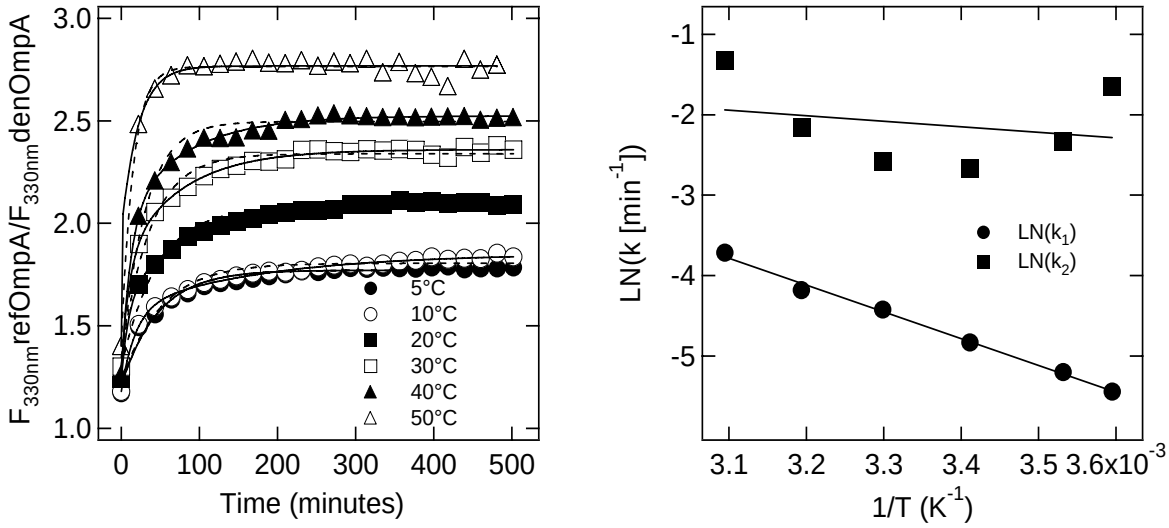

Figure 3.6 The fluorescence kinetics of the interaction of OmpA with amphipol A8-35 depend on temperature. Left Time-courses of A8-35 induced changes of the intrinsic Tryptophan fluorescence of OmpA after urea-dilution in presence of A8-35. The OmpA concentration was 1.25 μM and the molar ratio A8-35/OmpA was 35. Fluorescence kinetics were fitted to double exponential (solid lines) and monoexponential (dashed lines) functions. **Right** Arrhenius plots of the logarithm of the rate constants determined from the double exponential fits shown in panel A versus the reciprocal temperatures at which the reactions were performed. The activation energies for the two observed folding steps were determined from linear fits.

All fluorescence intensities of OmpA at 330 nm were divided by the fluorescence intensity of unfolded OmpA in 8 M urea at the same temperature to correct for the temperature dependence the fluorescence of unfolded OmpA. To correct for the fluorescence intensities of folded OmpA, we recorded fluorescence spectra of OmpA that was refolded into A8-35 at 40°C at temperatures from 5 to 50 °C and plotted fluorescence at 330 nm as a function of temperature. Linear fits had a slope of –8900 ± 380 cps/°C and an y-axis intercept of (1.12 ± 0.01) 10^6 cps. Fluorescence kinetics showed largest fluorescence changes at 50 °C and much smaller relative changes at 5 °C. OmpA folding kinetics exhibited an Arrhenius temperature dependence. The calculated activation energies were 5.7 kJ/mol for the fast step and 28 kJ/mol for the slower step, respectively. In comparison, the activation energy for the second step of OmpA folding into DOPC bilayers was determined previously to 46 kJ/mol (Kleinschmidt and Tamm 1996). These results showed that OmpA folded more readily into A8-35 than into DOPC bilayers.

3.4.6 Equilibrium unfolding

To compare the stabilities of OmpA in A8-35 and in LDAO, we performed equilibrium unfolding titrations with refolded OmpA either in LDAO (Figure 3.7A) or in A8-35 (Figure 3.7B) and monitored progress of unfolding as a function of the concentration of the denaturant urea by fluorescence spectroscopy.

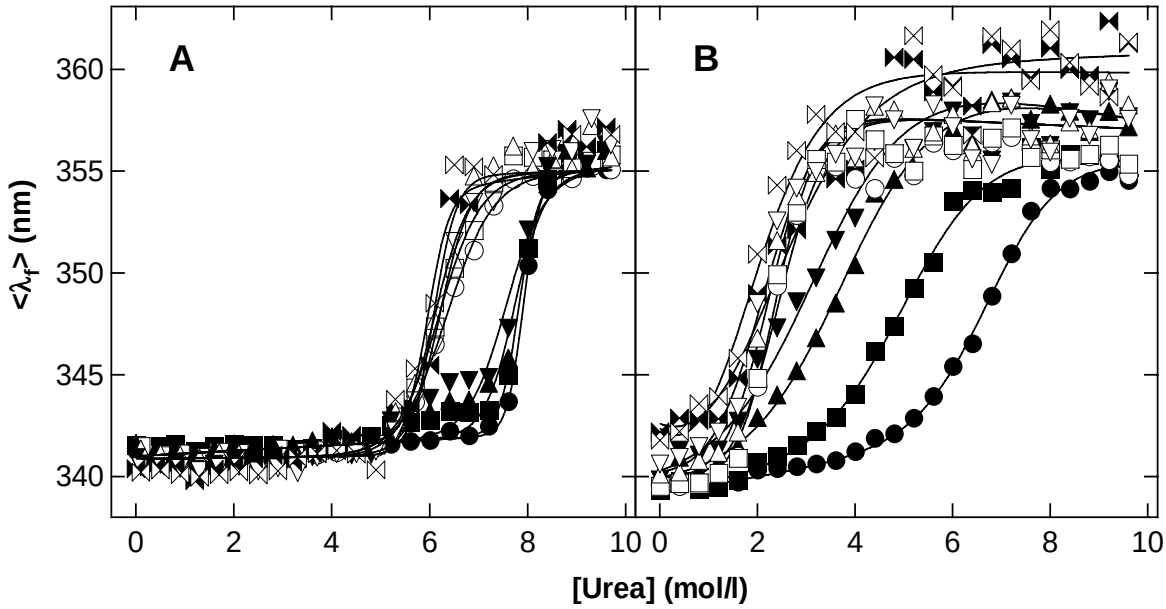

Figure 3.7 Unfolding (filled symbols) and refolding (open symbols) titrations of OmpA in LDAO (**A**) and in A8-35 (**B**) with urea determined by fluorescence spectroscopy. Samples of OmpA in LDAO were incubated for 3 (●), 7 (■), 10 (▲), 17 (▼), and 25 (⋈) days (panel **A**) and samples of OmpA in A8-35 for 3 (●), 10 (■), 24 (▲), 38 (▼), 52 (⋈) days (panel **B)** at 40 °C. The OmpA concentration was 1.25 μM in all experiments.

Since the kinetics of unfolding or folding strongly depend on the urea concentration and are therefore different for each sample, fluorescence spectra of each sample were recorded at different incubation times of up to 52 days. The intensity weighted average fluorescence emission maxima $\langle \lambda_F \rangle$ of fluorescence spectra of OmpA were calculated and plotted as a function of the urea concentration for each time period of equilibration. We also performed refolding titrations with denatured OmpA at selected denaturant concentrations in presence of either LDAO (Figure 3.7A) or A8-35 (Figure 3.7B). After 25 days (LDAO) and 52 days (A8-35) of incubation, the midpoints of the unfolding transition shifted from 8 to 6 M urea (LDAO) and from 7 to 2 M urea (A8-35). Unfolding and

refolding titrations superimposed after 25 days of sample incubation for OmpA in LDAO micelles (Figure 3.7A) and after 52 days of sample incubation of OmpA in A8-35 (Figure 3.7B). To determine $\Delta G°$, all titrations shown in Figure 3.7 were fitted to Eq. 1.6. The calculated energies of folding or unfolding were then plotted as a function of incubation time. Figure 3.8 shows that the energies for unfolding and for folding approached each other with time, indicating equilibration. Equilibration took 18-25 days in LDAO (Figure 3.8A) and 30 to 40 days in A8-35 (Figure 3.8B).

Once samples reached equilibrium, the thermodynamic stabilities of OmpA were calculated to $\Delta G°_{LDAO}$ = 60 kJ/mol in LDAO and to $\Delta G°_{A8\text{-}35}$ = 8 kJ/mol in A8-35.

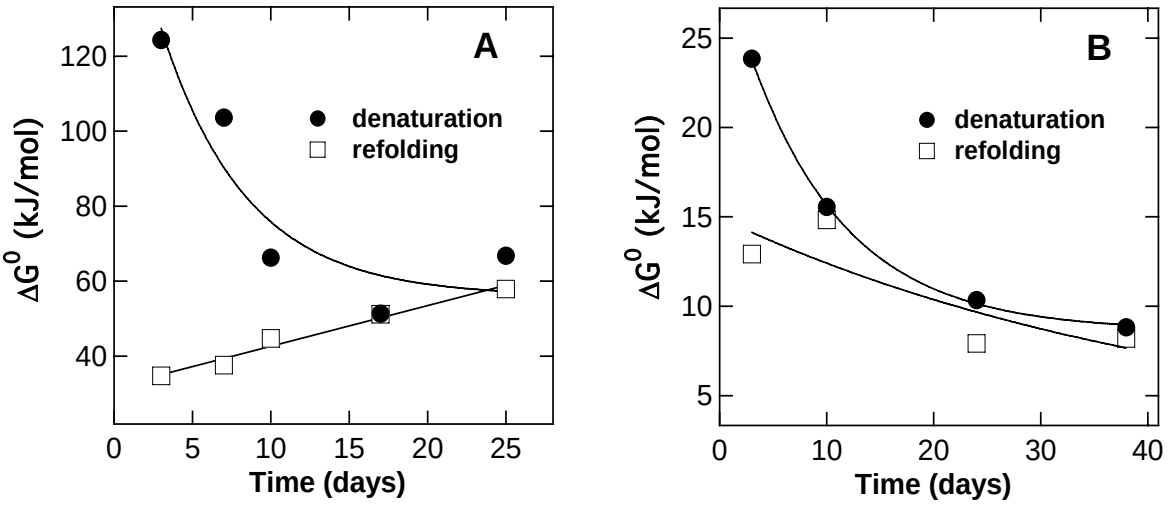

Figure 3.8 Energies of unfolding calculated by fitting the data of the Figure 3.7 to Eq. 3.6. Equilibrium was reached after 25 days for LDAO (**A**) and after 52 days for A8-35 (**B**), respectively. At equilibrium, free energies of unfolding were 60 kJ/mol for OmpA in LDAO micelles and 5 kJ/mol for OmpA in A8-35.

3.4.7 Concentration-dependence of the folding of OmpA into A8-35

To determine at which A8-35/OmpA molar ratio does OmpA quantitatively fold, we have investigated the insertion and folding of OmpA into A8-35 at different molar ratios (Figure 3.4). The amphipol/protein ratios were 2.2, 4.4, 8.8, 26.3, 35, 43.8 and 70 (mol/mol). The fraction of folded OmpA determined from the gels by densitometry was plotted as a function of time (Figure 3.4B). Folding was performed at 40°C, pH 10.0, and at a concentration of 7.2 µM OmpA. Quantitative folding of OmpA into A8-35 was observed at a A8-35/OmpA molar ratio of 8.8 or higher. Based on this result we decided to study the kinetics of folding of OmpA at A8-35/OmpA ratios of at least 8.8 mol/mol.

3.5 Discussion

3.5.1 Folding of OmpA into amphipol A8-35

Our results demonstrate by analysis of the shift in the electrophoretic mobility, by limited proteolysis, by fluorescence and CD spectroscopy and by single-channel conductance that OmpA can be quantitatively refolded into the amphipathic polymer A8-35 from a completely denatured state in 8 M urea and in absence of detergent micelles or lipid bilayers. The development of β-sheet secondary structure in presence of A8-35 is remarkable, because this amphipol is negatively charged and previous work had indicated that OmpA would not fold well into negatively charged detergents, such as SDS. In addition, amphipols are polymers and therefore much different from the previously used phospholipids and detergents. After refolding, OmpA migrates on SDS-PAGE at an apparent molecular weight of 30 kDa as previously obtained for the refolded OmpA in a range of detergent micelles and lipid bilayers, while denatured OmpA migrates at 35 kDa apparent molecular weight (Schweizer et al. 1978; Surrey and Jähnig 1992; Surrey and Jähnig 1995; Kleinschmidt et al. 1999; Kleinschmidt and Tamm 2002; Kleinschmidt 2003). Trypsin digestion of the folded OmpA into A8-35 leads to a 24 kDa protected fragment as similar reported for trypsin digested OmpA refolded into lipid bilayers (Surrey and Jähnig 1992), indicating that the OmpA transmembrane domain is protected by the amphipol. OmpA refolded into detergent micelles has been shown to form small (50-80 pS) and large (260-320 pS) channels by single-channel measurements using black lipid films (Arora et al. 2000). We have obtained similar conductance states for amphipol refolded OmpA using the same method. We also observed that there is a correlation of functional activity to the electrophoretic mobility shift like previously seen for the 30 kDa form of OmpA (Schweizer et al. 1978; Vogel and Jähnig 1986; Dornmair et al. 1990; Surrey and Jähnig 1992; Rodionova et al. 1995; Surrey and Jähnig 1995; Sugawara et al. 1996; Arora et al. 2000).

The insertion and folding of OmpA into A8-35 was investigated as a function of A8-35/OmpA molar ratio and it was determined that only at and above 8.8 mol/mol A8-35/OmpA ratio folding was quantitatively.

3.5.2 Kinetics of OmpA folding into amphipol A8-35

Our results indicated a strong temperature dependence of the folding of OmpA into amphipol A8-35 using two different methods, namely SDS-PAGE and fluorescence spectroscopy, respectively. The data from KTSE experiments and fluorescence kinetics could be best fitted to double-exponential functions. Our previous data on the folding kinetics of OmpA into phospholipid bilayers fitted well to single-step second-order or even pseudo first-order kinetics (Kleinschmidt and Tamm 2002). Reanalyzing the data we observed that it could be as well fitted to double-exponential fits (Pocanschi et al. 2005). The double-exponential kinetics would indicate two folding steps, and since we detect only two bands on SDS-PAGE, corresponding to folded and unfolded OmpA we concluded that there must be two parallel folding pathways for OmpA folding. Similar kinetics were recently obtained for FomA folding into lipid bilayers (see e.g. Pocanschi et al. 2005). The contribution of the fast folding step to the overall folding rate of OmpA increases with temperature, irrespective of the method employed, SDS-PAGE or fluorescence spectroscopy (see Tables 3.1 and 3.2).

3.5.3 Stability of OmpA in LDAO and in A8-35

The reduced stability of OmpA in A8-35 compared to LDAO in this experiment is not surprising, since at pH 10, both OmpA (pI = 5.7) and A8-35 are strongly negatively charged and charge-charge repulsions destabilize OmpA (Surrey and Jähnig 1995). It will be interesting to compare these results with stabilities of OmpA in neutral amphipols.

3.5.4 Parallel folding pathways

It is possible that after rapid dilution of the denaturant urea, two major populations of aqueous forms of OmpA formed that adsorbed, inserted and folded with different rates into A8-35. An explanation could be that immediately after urea dilution in presence of A8-35, a population of unfolded OmpA is present within a critical proximity to A8-35 for rapid binding and folding while another population of OmpA will form a hydrophobically collapsed state in solution, prior to interaction with A8-35. Conformational changes

required from a hydrophobically collapsed state would be larger, resulting in much slower insertion kinetics.

4 The major outer membrane protein of *Fusobacterium nucleatum* (FomA) folds and inserts into lipid bilayers via parallel folding pathways

4.1 Abstract

Membrane protein insertion and folding was studied with the major outer membrane protein FomA of *Fusobacterium nucleatum*. Previously, the outer membrane protein A of *E. coli* (OmpA) has been the only outer membrane protein for which quantitative refolding into lipid bilayers from a completely denatured state in 8 M urea could be observed. In contrast to the 8-stranded transmembrane β-barrel of OmpA, FomA forms a much larger transmembrane domain that is predicted to consist of 14 β-strands.

FomA, over-expressed in *E. coli* in form of inclusion bodies, was solubilized in 10 M urea in denatured form and shown to insert and fold into phospholipid bilayers. We demonstrate that folding is quantitative when performed with lipid bilayers of short-chain phospholipids at basic pH. Successful refolding is demonstrated by circular dichroism and fluorescence spectroscopy, by SDS-polyacrylamide gel-electrophoresis, and by single channel recordings. Refolded FomA had an average single channel conductance of 1.1 nS, in agreement with previous studies on FomA isolated from membranes in native form.

Insertion and folding was successful also with detergent micelles and with bilayers of dioleoyl phosphatidylcholine. The kinetics of bilayer insertion and folding of FomA were analyzed by electrophoresis and were faster for bilayers of the short-chain dicapryl phosphatidylcholine than for bilayers of dioleoyl phosphatidylcholine. In contrast to the previously described folding kinetics of OmpA into these lipids, the kinetics of FomA folding were slower and were well described only by double-exponential functions. The kinetics provided evidence for parallel folding pathways of FomA *in vitro*. For folding into each of the lipid bilayers, the two kinetic pathways were strongly temperature-dependent with estimated activation energies for the faster pathways of 19 kJ/mol (dicapryl phosphatidylcholine) and 70 kJ/mol (dioleoyl phosphatidylcholine).

4.2 Introduction

A central question for the assembly of biological membranes is how integral membrane proteins (IMPs) are folded and inserted into lipid bilayers, which separate the different the functional units of living cells. Since IMPs are hydrophobic and usually insoluble in water, investigations on the biophysical mechanism of membrane insertion and folding of IMPs are experimentally challenging and until today, insertion and folding have been studied for only few integral membrane proteins. Based on currently solved high resolution structures of membrane proteins, two different types of integral membrane proteins can be distinguished by their transmembrane secondary structures: β-barrel membrane proteins and α-helix bundle membrane proteins. Transmembrane β-barrels have so far been reported for the outer membranes of Gram-negative bacteria and for cell organelles with outer membranes. In the outer membranes of bacteria, there are currently no known integral proteins with transmembrane α-helices. While many, but not all β-barrel membrane proteins can be refolded into detergent micelles, the outer membrane protein A of *E. coli* (OmpA, 325 residues, M_r = 35 kDa) has been the only membrane protein that quantitatively inserts and folds into lipid bilayers from a completely denatured state in urea (Surrey and Jähnig 1992; Surrey and Jähnig 1995). Refolding into detergent micelles has been studied with several outer membrane proteins, for example with outer membrane proteins A (OmpA) (Dornmair et al. 1990; Kleinschmidt et al. 1999), F (OmpF) (Surrey et al. 1996), and G (OmpG) (Fajardo et al. 1998; Conlan et al. 2000; Conlan and Bayley 2003) with PhoE (Van Gelder et al. 1994; de Cock and Tommassen 1996; de Cock et al. 1999), with the *E. coli* auto-transporter adhesin involved in diffuse adherence (AIDA) (Mogensen et al. 2005) and others, for a review see (Buchanan 1999). Folding of outer membrane proteins into detergent micelles is often fast and yields of folded IMPs are usually much higher than folding yields into lipid bilayers because of the shorter chain lengths of typical detergents and because of the physical properties of the micelles (Surrey and Jähnig 1995; Kleinschmidt et al. 1999; Kleinschmidt and Tamm 2002). Micelles and bilayers both have a hydrophobic core and a polar surface, but they do not have much else in common. In contrast to micelles, lipid-bilayers contain a much larger number of molecules that are tightly packed. The lipid bilayers, which form the backbone of biological membranes, have been extensively studied in the past as models for biomembranes and today it is obvious

that the biophysical principles of insertion and folding of integral membrane proteins are best studied with lipid bilayers in well-defined *in vitro* model systems. Since OmpA, which has a 171 residue 8-stranded β-barrel transmembrane domain refolds quantitatively into phospholipid bilayers from a completely denatured state in urea, this IMP has been an extensively studied model in the past (Surrey and Jähnig 1992; Surrey and Jähnig 1995; Kleinschmidt and Tamm 1996; Kleinschmidt et al. 1999; Kleinschmidt and Tamm 1999; Kleinschmidt and Tamm 2002; Bulieris et al. 2003), for a review, see (Kleinschmidt 2003).

In the present study we aimed to investigate insertion and folding of a second outer membrane protein that should have a much larger transmembrane domain. We were interested to examine, whether there are common characteristic features of outer membrane protein insertion and folding, similar to those described for OmpA of *E. coli.* We chose FomA, the major outer membrane protein of *Fusobacterium nucleatum* for this study. The structure of FomA has not yet been solved, but circular dichroism spectroscopy and topology prediction methods suggested a 14-stranded β-barrel transmembrane domain (Puntervoll et al. 2002). For outer membrane protein topology analyses, these methods have proven to be quite successful. For example already in 1986, the transmembrane domain of OmpA was predicted by Vogel and Jähnig (Vogel and Jähnig 1986) to form an 8-stranded transmembrane β-barrel, i.e. long before Pautsch and Schulz solved the crystal structure, which confirmed this topology (Pautsch and Schulz 1998). FomA is assumed to be directly involved in the binding between fusobacteria and *Streptococcus sanguis* on the tooth-surface, and to *Porphyromonas gingivalis* in the periodontal pockets (Kinder and Holt 1993). These events are essential for colonisation, and thus a part of the etiology of periodontitis. The FomA binding functions depend directly on its structure and outer membrane topology.

We have studied insertion and folding of FomA (40 kDa, 371 residues), since like OmpA it is also present as a monomer in membranes. FomA forms voltage-dependent general diffusion channels (Kleivdal et al. 1995; Kleivdal et al. 1999; Puntervoll et al. 2002), which have a conductivity of 1.2 nS, i.e. much larger than the conductivity of 250-320 pS that has been reported for the large open state of OmpA (Arora et al. 2000). This is in agreement with a larger transmembrane domain of FomA. We were interested to determine the effect of the size of a transmembrane β-barrel (i.e. of the number of transmembrane β-strands) on the insertion and folding behaviour of outer membrane proteins. In the present study, we have addressed the following questions: Is it possible to refold FomA *in vitro* from a completely denatured state into either detergent micelles or

model membranes of phospholipids and is folding quantitative? How fast are the kinetics of FomA insertion and folding and which activation energy is required? How do the rates of insertion and folding of FomA compare to those of OmpA? Does FomA folding depend on the chain length of the phospholipids in the bilayer or on the size of the lipid vesicles?

4.3 Materials and methods

4.3.1 Materials

All phospholipids were from Avanti Polar Lipids (Alabaster, AL). Coomassie Brilliant Blue was from BIO-RAD (Hercules, CA, USA), LDAO and n-decane were from Fluka (Buchs, Switzerland), 2-mercaptoethanol and glycerol were from Merck (Darmstadt, Germany), acrylamide, bis-acrylamide and urea were from Serva (Heidelberg, Germany), IPTG was from BioVectra (Oxford, CT, USA), SDS and TEMED were from Roth (Karlsruhe, Germany), Borate, Bromphenol Blue, EDTA, MES, Tris, trypsin, trypsin inhibitor and all other chemicals were purchased from standard sources such as Sigma (Steinheim, Germany) and were of analytical grade.

4.3.2 Construction of plasmid

In order to express the FomA protein the form of cytoplasmic inclusion bodies, the *fomA* gene was cloned into the expression vector pET-11c (Stratagen) containing the strong viral T7 promoter. The *fomA* gene was amplified by the polymerase chain reaction (PCR) as described (Sambrook et al. 1989), using plasmid pHB14 (Jensen et al. 1996) as template, and the following primers: 5'-Acatatg<u>GAAGTTATGCCTGCACC</u>-3' (*Nde*I restriction site in lower case) and 5'-CCTTAGCagatctAGATTAGAAAGTAACTTTC-3' (*Bgl*II restriction site in lower case). The 5' primer was constructed to replace the first codon of the part of the gene encoding the mature protein with a start codon (underlined). A 7 min extension at T=72 °C was included at the end of the PCR reaction to ensure the presence of 3' A-overhangs. The 1073 bp PCR product was cloned into the pCR2.1-TOPO cloning vector (Invitrogen) as described by the manufacturer. Bacterial colonies harbouring the fomA gene were identified by PCR using the cloning primers. Subsequently, the DNA fragment containing the *fomA* gene was excised from the resulting plasmid by a

double digestion with the restriction endonucleases *Nde*I and *Bgl*II, and the pET-11c vector was linearised using enzymes *Nde*I and *Bam*HI as described (Sambrook et al. 1989). Both the 1058 bp *fomA* fragment and the 5639 bd vector fragment were purified by agarose gel electrophoresis and subsequent isolation with the JETSORB kit (Genomed). The two DNA molecules were ligated to each other and transformed into *E.coli* DH5α, and the resulting ampicillin resistant colonies were screen by PCR using the cloning primers. The successful construction of the plasmid, termed pET-10953, was confirmed by sequencing using the ABI PRISM BigDye Terminator Cycle Sequencing Ready Reaction Kit and the ABI PRISM 377 DNA Sequencer (Applied Biosystems).

4.3.3 Isolation of FomA from inclusion bodies

FomA was expressed in form of cytoplasmic inclusion bodies in *E. coli* B strain PC2889 harboring the plasmid pET-10953 carrying the *fomA* gene under control of a T7 promoter as previously described (Qi et al. 1994). In short: To induce FomA expression, 0.1 mol IPTG were added to 100 ml of a PC2889 culture at OD_{660} = 0.6. After 2-3 hours, cells were harvested at T=4 °C by 5 min centrifugation at 5000 g. Wet cells were weighed and the pellet was resuspended in TEN buffer (10 mM TrisHCl, 5 mM EDTA, 100 mM NaCl, pH 8.0), using 3 ml buffer / 1 g wet cells. 80 µl of a 10 mg/ml lysozyme solution and 4 mg of sodium deoxycholate were added per 1 g cells to disintegrate the cell wall at room temperature. Cells were subsequently disrupted using a French pressure cell, and the non-soluble FomA inclusion bodies were pelleted by centrifugation at 3000 g for 15 min at 4 °C. Inclusion bodies were resuspended in 10 ml Borax/NaOH buffer (10 mM Borax, 2 mM EDTA, 10 M urea, pH 10.0). Yields were 4 mg FomA per 100 ml *E. coli* culture. FomA concentrations of stock solutions were determined using the method of Lowry *et al.* (Lowry et al. 1951).

4.3.4 Preparation of small and large unilamellar vesicles

10 mg of phospholipid were dissolved in chloroform, dried under a stream of nitrogen on the bottom of a glass test tube, and desiccated under high vacuum for at least 3 h to remove residual solvent. The lipids were dispersed in 10 mM Borax/NaOH buffer, pH 10.0, containing 2 mM EDTA to a concentration of 10 mg/ml. Small unilamellar vesicles

(SUVs) were prepared by ultrasonication using the microtip of a Branson W450D ultrasonifier at 50% pulse cycle for 50 min under cooling with an ice/water bath. Titanium dust was removed by centrifugation. All SUVs were equilibrated overnight at 4 °C and used on the next day (Kleinschmidt and Tamm 1996). Vesicles were prepared by seven cycles of freeze-thawing the hydrated lipids in liquid nitrogen and in a water bath at 35 °C, respectively. To obtain LUVs, lipid dispersions were extruded 30-fold through a pair of polycarbonate membranes with a pore size of 100 nm (Nucleopore, Whatman, Clifton, NJ) using a mini-extruder (Avanti, Alabaster, AL) as described previously (Kleinschmidt and Tamm 2002).

4.3.5 Trypsin digestion experiments

For trypsin digestion experiments, 200 µl of FomA samples (0.6 mg/ml) were incubated with 12 µl trypsin solution (1 mg/ml) at 40 °C for 2 hours. Digestion was stopped by addition of 12 µl trypsin inhibitor (1 mg/ml), type I-S from soybean (Sigma).

4.3.6 SDS-polyacrylamide gel electrophoresis

SDS-polyacrylamide gel electrophoresis (SDS-PAGE) (10% acrylamide) was performed as described previously (Kleinschmidt and Tamm 1996; Kleinschmidt and Tamm 2002) using the method of Laemmli (Laemmli 1970) with the modifications described by Weber and Osborne (Weber and Osborne 1964), but without heat denaturation of the samples, if not otherwise specified.

4.3.7 Kinetics of tertiary structure formation detected by electrophoresis

The kinetics of tertiary structure formation were determined as described previously for OmpA (Kleinschmidt and Tamm 1996; Kleinschmidt and Tamm 2002; Bulieris et al. 2003; Kleinschmidt 2003). In short: FomA was completely denatured in 10 M urea. Folding of FomA was initiated by rapidly mixing 10 µl of denatured FomA (10 mg/ml) with 290 µl of Borax/NaOH buffer (10 mM, pH 10.0, with 2 mM EDTA) containing dicapryl phosphatidylcholine (*di*$C_{10:0}$PC) or dioleoyl phosphatidylcholine (*di*$C_{18:1}$PC) vesicles, respectively. Unless stated otherwise, the molar lipid/protein ratio was

1000. The final FomA concentration was 7 µM. Samples of the reaction mixture were taken at different times after the initiation of folding, at each temperature and an equal volume of 0.125 M Tris buffer, pH 6.8, containing 4% SDS, 20% glycerol, 10% 2-mercaptoethanol and 0.01% bromphenol blue was added. SDS binds to both folded and unfolded FomA and inhibits further folding, similarly as described previously for OmpA (Surrey and Jähnig 1995; Kleinschmidt and Tamm 1996). Time courses of folding were monitored over 24 hours.

4.3.8 Folding monitored by circular dichroism spectroscopy

Far UV circular dichroism (CD) spectra of 14 µM FomA were recorded on a Jasco 715 CD spectropolarimeter using a 0.1 mm cuvette. In short, 10 µl of denatured FomA (10 mg/ml) was mixed with 140 µl of Borax/NaOH buffer (10 mM, pH 10.0, with 2 mM EDTA) containing *di*$C_{10:0}$PC or *di*$C_{18:1}$PC SUVs, respectively, at lipid/protein ratio of 1000 mol/mol. Samples were incubated for 24 h at 40°C followed by dialysis at 10°C to remove urea. All samples were then dialyzed for 12 hrs against 2 l buffer (10 mM Borax, 2 mM EDTA, pH 10). Dialysis buffer was exchanged 3 times. FomA concentration after dialysis was 14 µM. Dialysis was performed to remove urea, which causes high noise levels in the CD spectral region below 205 nm. High noise levels were also observed with *di*$C_{18:1}$PC bilayers, but not with *di*$C_{10:0}$PC bilayers despite of dialysis. The same procedure was used for FomA refolding into LDAO detergent at 800 mol/mol and also for water collapsed FomA. Twelve scans, from 190 to 250 nm (205–250 nm in presence of 10 M urea) with a response time of 16 s, a bandwidth of 1 nm, and a scan speed of 20 nm/min were accumulated and averaged. Background spectra without FomA were subtracted for all samples. The recorded CD spectra were normalized to obtain the mean residue molar ellipticity [Θ](λ) according to

$$[\Theta](\lambda) = 100\frac{\Theta(\lambda)}{c \cdot n \cdot l} \qquad \text{(Eq. 4.1)}$$

where l is the path length of the cuvette, Θ(λ) is the recorded ellipticity at wavelength λ, c is the concentration and n the number of amino acid residues of FomA.

4.3.9 Fluorescence spectroscopy

16 µl denatured FomA (1.9 mg/ml) in 10 M urea buffer was rapidly mixed to 984 µl of 10 mM Borax, 2 mM EDTA, pH 10.0 containing sonicated lipid vesicles under concurrent 64-fold dilution of the denaturant urea. The final FomA concentration was 0.7 µM and the molar L/P ratio was 1000. Samples were then incubated for 24 hours in a water bath at 40 °C. Fluorescence spectra of FomA were recorded at room temperature as described previously (Bulieris et al. 2003) on a Spex Fluorolog-3 spectrofluorometer with double monochromators in the excitation and emission pathways. The excitation wavelength was 290 nm, and the bandwidths of the excitation monochromators were 2 nm. The bandwidths of the emission monochromators were 3.7 nm. The integration time was 0.05 s, and an increment of 0.5 nm was used to scan spectra in the range of 300–380 nm. Three scans were averaged for each spectrum.

4.3.10 Single-channel conductance experiments

Planar lipid bilayers were formed from a solution of 1% diphytanoylphosphatidyl-choline (*di*phPC) in *n*-decane using the method of Mueller *et al.* (Mueller et al. 1962) with the modifications described by Busath and Szabo (Busath and Szabo 1981). The lipid solution was painted on a 500-µm hole in a Teflon partition separating two 6-ml compartments, which were filled with MES buffer (10 mM MES, pH 6.0) containing 1 M KCl. The compartments were connected to the recording system through two AgCl-coated silver electrodes, one of which (the front, *cis* side) was grounded, whereas the other (the rear, *trans* side) was connected to a custom designed trans-impedance amplifier. The painted *di*phPC/n-decane bilayer membranes were tested for integrity by checking the reflectance optically and also by their resistance and capacitance. After the bilayers were formed, 10 µl refolded FomA (3 µg/ml) in LDAO micelles at detergent/FomA ratio of 800 mol/mol were added to the *cis* compartment. The final FomA concentration was 240 pM. 20 mV potential was applied to the *trans* compartment. The frequency bandwith was 100 Hz. Single-channel conductance events were recorded with the IGOR NIDAQ Tools extensions and analyzed using the software IGOR (Wavemetrics, Portland, OR). Formation of transmembrane channels of refolded FomA only was confirmed in two

control experiments: In a first control experiment**,** 10 µl denatured FomA (3 µg/ml) in 10 M urea were added to the *cis* compartment to a final concentration of 240 pM in absence of LDAO. In a second control experiment 26 µl LDAO (10 µg/ml) without FomA were added to the *cis* compartment.

4.4 Results

4.4.1 FomA inserts into preformed lipid bilayers and detergent micelles

To investigate whether FomA can insert and fold from a completely unfolded state in 10 M urea, we first tested whether a 30-fold urea dilution and incubation of FomA with preformed detergent micelles would lead to a change in the electrophoretic mobility of FomA in SDS-polyacrylamide gels, if the samples are not heat-denatured prior to SDS-PAGE (cold SDS-PAGE). Previously, it was observed for several natively isolated outer membrane proteins that two different electrophoretic mobilities in SDS polyacrylamide gels can be distinguished, when samples of the protein are either heat-denatured or not prior to SDS-PAGE. This property was first described for OmpA of *E. coli* and termed heat-modifiability (Schweizer et al. 1978). It has later been observed for other outer membrane proteins (OMPs), such as OmpG (Conlan and Bayley 2003) and FhuA (Locher and Rosenbusch 1997) of *E. coli*.

The unfolded form of FomA in 10 M urea migrated at 40 kDa in cold SDS-PAGE (Figure 4.1A, lane 1). When we incubated samples of unfolded FomA with micelles of LDAO-detergent or lysocapryl phosphatidylcholine under concurrent dilution of the denaturant for 24 hrs at 40 °C, FomA migrated at an apparent molecular weight of 37 kDa in cold SDS-PAGE (Figure 4.1A, lane 2 and 3). The same migration at 37 kDa was observed previously for natively isolated and not heat-denatured FomA from outer membranes (Bakken et al. 1989; Kleivdal et al. 1995).

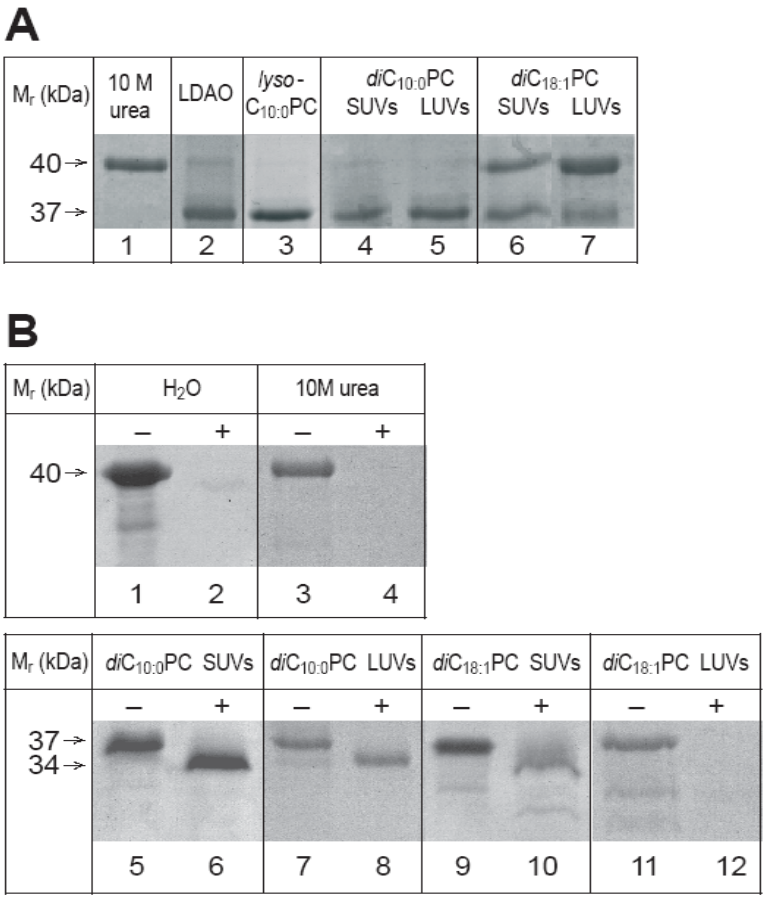

Figure 4.1 FomA inserts into LDAO detergent micelles and into lipid bilayers of *di*$C_{10:0}$PC and *di*$C_{18:1}$PC. A Urea-denatured FomA migrated at an apparent molecular weight of 40 kDa (lane 1), but formed a 37 kDa form after incubation with LDAO detergent micelles (lane 2) or lyso-capryl phosphatidylcholine (lane 3). FomA inserted quantitatively into *di*$C_{10:0}$PC, independent of the vesicles size with either SUVs (lane 4) or LUVs (lane 5). Similarly, FomA inserted into vesicles of *di*$C_{18:1}$PC, but with lower yields of the 37 kDa form, which were 50% in SUVs (lane 6) and 20% in LUVs (lane 7). All samples were incubated at 40 °C for 24 hrs. **B** While urea-denatured FomA and water-collapsed FomA (lanes 3 and 1) were completely digested by trypsin (lanes 4 and 2), the micelle and bilayer inserted 37 kDa forms of FomA (lanes 5, 7, 9, 11) remained largely protected against proteolysis leading to a 34 kDa fragment after trypsin digestion (lanes 6, 8, 10, 12).

While the presence of preformed micelles induced formation of a 37 kDa from, the dilution of the urea in absence of detergent (Figure 4.1B, lane 1) did not have any effect on the electrophoretic mobility, suggesting that FomA does not fold in absence of micelles. We then tested, whether FomA can also insert and fold into bilayers of phospholipids and whether insertion and folding depends on lipid properties or on the methods used to prepare the lipid vesicles. With preformed lipid bilayers of *di*$C_{10:0}$PC, the unfolded 40 kDa form of FomA was quantitatively converted to the 37 kDa form, independent of the size of the vesicles i.e. SUVs prepared by ultrasonication or LUVs, prepared by extrusion (Figure

4.1A, lane 4 and 5). In contrast, only about (~40-50%) of the 37 kDa form of FomA were formed with SUVs of *di*$C_{18:1}$PC and even lower amounts (~10%) were observed with LUVs of *di*$C_{18:1}$PC under otherwise identical conditions (Figure 4.1A, lane 6 and 7). This last experiment indicated that formation of the 37 kDa form depended on both, the chain length of the phospholipid and on the size of the lipid vesicles, similar to previous observations on the membrane insertion and folding of OmpA (Kleinschmidt and Tamm 1996; Kleinschmidt and Tamm 2002; Kleinschmidt 2003).

To determine whether the 37 kDa form is inserted into lipid bilayers or detergent micelles, we performed digestion experiments with trypsin, because micelle- or membrane-inserted parts of the polypeptide chain of FomA would be protected against degradation. Figure 4.1B, lanes 1 and 3 shows that both, water-collapsed and denatured FomA (5 µg) were completely digested by trypsin (lanes 2 and 4), since no band could be observed on SDS-PAGE after 2 hours of incubation of FomA with trypsin at 37 °C. In detergent micelles and lipid bilayers, most of the polypeptide chain of FomA was protected against trypsin digestion, which led to a 34 kDa fragment. The same fragment was obtained, independent of the composition and size of the lipid vesicles (Figure 4.1B, lanes 6, 8, and 10), although with *di*$C_{18:1}$PC, the bilayer protected fragment of FomA was more difficult to detect because of lower yields of the 37 kDa form in refolding attempts and because of dilution of the solutions upon addition of trypsin and trypsin inhibitor (lane 12).

4.4.2 Fluorescence spectroscopy

The polypeptide chain of FomA contains 8 fluorescent tryptophans. In integral membrane proteins, tryptophans and other aromatic residues typically are located in girdles close to the membrane-water interface in the hydrophobic core of the lipid bilayer (Wimley and White 1996; Yau et al. 1998).

Similarly, we expected an average location in the membrane-water interface also for the tryptophans of FomA. The fluorescence properties of tryptophan in polar aqueous environment and in hydrophobic environment are very different. Therefore, we recorded the fluorescence spectra of FomA in the urea-denatured form, in aqueous solution after denaturant dilution, and after incubation with preformed lipid bilayers that were composed either of *di*$C_{10:0}$PC or of *di*$C_{18:1}$PC by fluorescence spectroscopy to monitor changes in the Trp environment (Figure 4.2A).

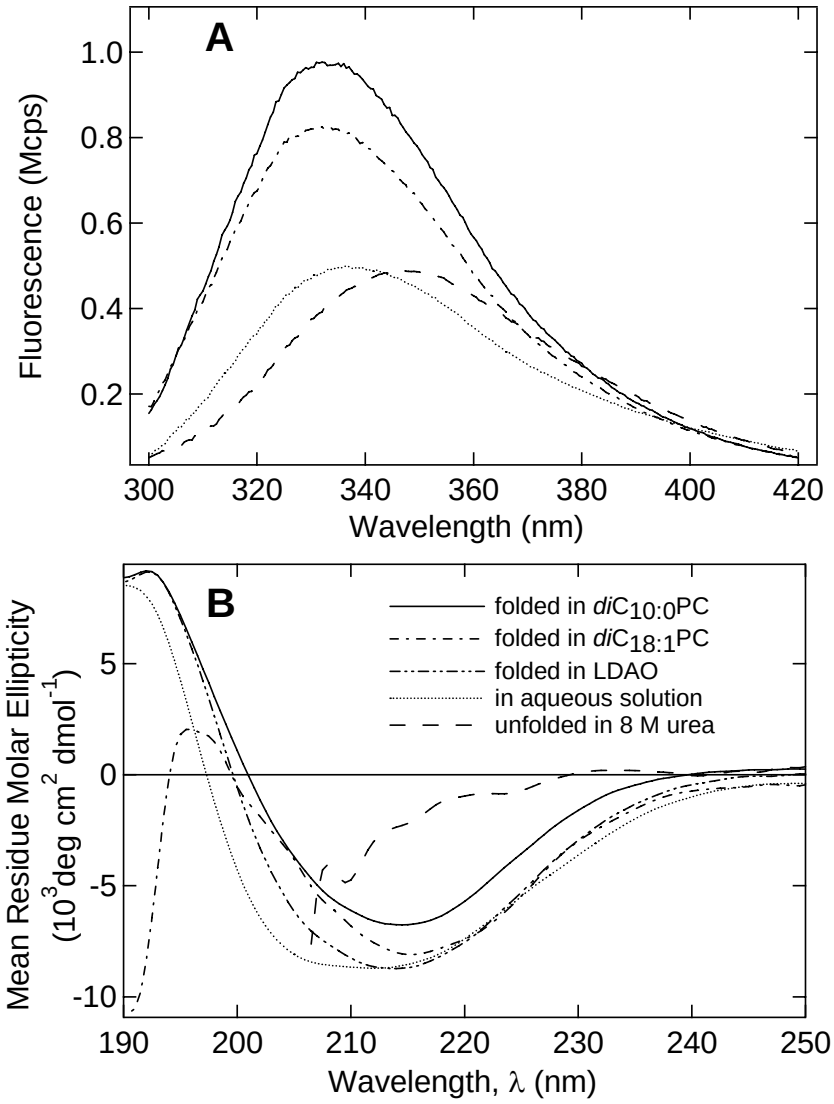

Figure 4.2 Fluorescence spectra (A) and Circular dichroism spectra (B) of FomA - in unfolded form in 8 M urea (dashed line, ---------), in aqeous solution after urea dilution (dotted, ……), after incubation with detergent micelles of LDAO (dash-dot-dot, —. .), after incubation with *di*$C_{10:0}$PC (solid line, —), and after incubation with *di*$C_{18:1}$PC (dash-dot, — .). Background spectra without FomA were subtracted. The FomA concentration was 0.7 µM in a volume of 1 ml (**A**) and 14 µM in a volume of 150 µl (**B**). Samples were incubated at 40 °C for 24 hrs prior to recording spectra. Spectra were recorded at room temperature in 10 mM Borax/NaOH, 2 mM EDTA, pH 10.0, in all CD and fluorescence experiments.

In the urea-unfolded state, spectra of FomA had fluorescence emission maxima at λ_{max}(U) = 347 nm. After urea dilution, the maximum fluorescence of FomA in aqueous solution was observed at λ_{max}(W) = 337 nm, while the fluorescence intensity was similar to the urea-unfolded state. Spectra of FomA after incubation with preformed lipid bilayers of *di*$C_{10:0}$PC or alternatively of *di*$C_{18:1}$PC were characterized by a fluorescence emission

maximum at λ_{max} (L) = 332 nm and by an intensity that was almost double the fluorescence intensity of the urea-unfolded and aqueous forms of FomA at the same concentration. These results indicated that the fluorescent Trp residues of folded FomA were located predominantly in more hydrophobic environment after incubation with lipid bilayers.

4.4.3 Unfolded FomA forms β-pleated sheet secondary structure in presence of lipid bilayers

To examine the changes in protein secondary structure in the micelle or membrane inserted forms of FomA we recorded circular dichroism (CD) spectra. The CD spectra of denatured, water collapsed and refolded FomA are shown in Figure 4.2B. The spectrum of denatured FomA was similar to that of denatured OmpA (Surrey and Jähnig 1995; Kleinschmidt et al. 1999) and relatively small mean residue molar ellipticities, [Θ], between 215 nm and 225 nm indicated that FomA is largely unstructured in urea. When the denaturant urea was diluted, FomA clearly developed secondary structure in aqueous solution even in absence of detergent or lipid bilayers. The spectrum of aqueous FomA was characterized by a large increase in amplitude and by broad minimum centered around ~211 nm and ranging from 205 to 215 nm. Noise levels below 205 nm were low for spectra of aqueous FomA, which had a maximum at 190 nm. This suggests the presence of some α-helical secondary structure. The overall shape of this spectrum indicated a mixture of random coil, β-sheet and α-helical secondary structure.

Spectra of FomA in LDAO micelles had a maximum at 192.5 nm and — in comparison to the aqueous form of FomA — a much narrower minimum centered at 215 nm, while FomA inserted into lipid bilayers of *di*$C_{10:0}$PC (LUVs) and *di*$C_{18:1}$PC (SUVs) had minima at 214.5 nm and at 215.5 nm, respectively. The line-shapes of lipid-inserted FomA had slightly reduced amplitudes in comparison to LDAO-micelle inserted FomA, but were characterized by a further reduced line-width of the minima around 214-215 nm. Clearly, all spectra of FomA either in detergent micelles or lipid bilayers indicated predominantly β-sheet secondary structure in FomA. Since trypsin digestion indicated insertion into the lipid bilayer, it is conceivable that FomA forms a transmembrane β-barrel.

4.4.4 Micelle-inserted FomA is functionally active

Single channel measurements were performed to test, whether the 37 kDa form of FomA that is developed upon incubation with LDAO detergent micelles is functionally active, i.e. whether our refolding attempts were successful (Figure 4.3A, trace c). Indeed, 10 µl FomA (3 µg/ml) pre-incubated with an 800-fold molar excess of LDAO for refolding, followed by reconstitution into black lipid membranes of diphytanoyl phosphatidylcholine led to formation of functional pore units as observed by stepwise increases of the current across the membrane (Figure 4.3A, trace c). All current increments were converted to the corresponding changes in the bilayer membrane conductance. The conductance of one pore-forming unit was in the range 0.1-2.1 nS with an average single-channel conductance of 1.1 nS for a total of 93 single-channel events (Figure 4.3B) This average conductance was similar to the previously observed average conductance of FomA isolated from membranes in the native form (Kleivdal et al. 1995). Addition of 10 µl denatured (40 kDa form) FomA in 10 M urea (3 µg/ml) and in absence of LDAO to the *cis*-side of the Teflon chamber with a freshly formed black lipid film did not result in any channel formation (Figure 4.3A, trace a). Similarly, no transmembrane conductance was observed when 26 µl LDAO (10 µg/ml) without FomA was added to the *cis*-compartment of the Teflon chamber (Figure 4.3A, trace b).

These results strongly suggest that our refolding attempts were successful and that the 37 kDa fragment detected by SDS-PAGE strictly corresponded to the properly folded, functionally active FomA, which is a transmembrane β-barrel. We conclude from the results shown in Figures 4.1, 4.2 and 4.3 that folding of FomA from a completely denatured state in 10 M urea is quantitative at pH 10 with detergent micelles and most importantly also with lipid bilayers of *di*$C_{10:0}$PC.

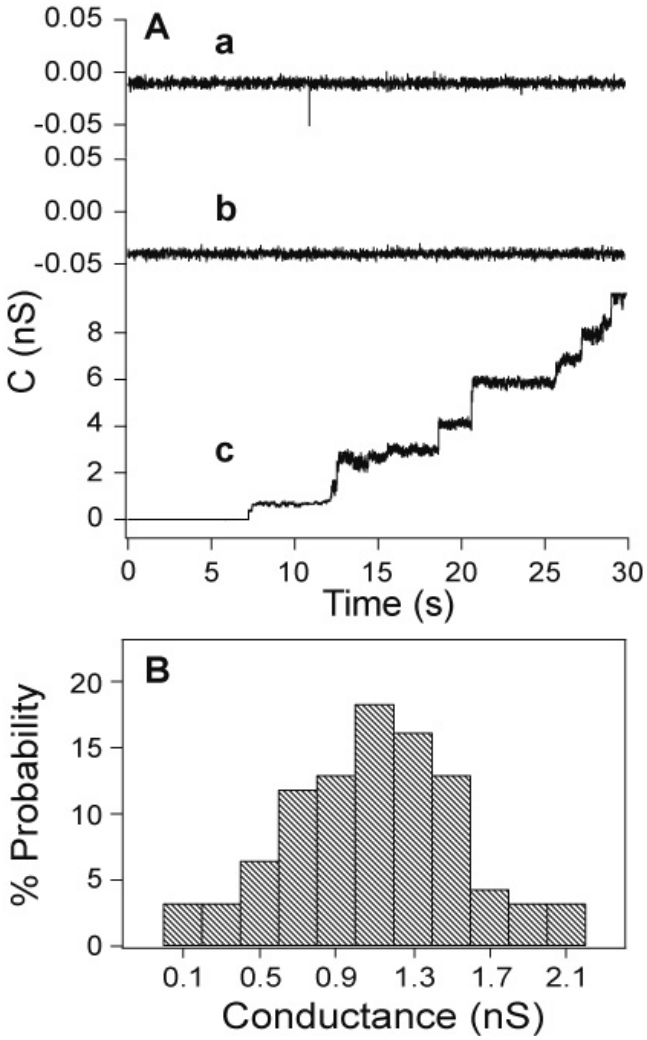

Figure 4.3 A Conductivity across black lipid bilayers of diphytanoyl phosphatidylcholine - after addition of: 10 µl of a stock solution of 3 µg/ml denatured FomA (trace **a)**; 26 µl LDAO detergent (from a stock solution of 10 µg/ml LDAO) in the absence of FomA (trace **b**); 10 µl FomA (3 µg/ml) that was incubated with LDAO micelles for refolding at a molar ratio LDAO/FomA of 800 mol/mol (trace **c**). Both, cis and trans compartments of the Teflon chamber were filled with 1 M KCl, 10 mM MES, pH 6.0. The protein concentration was always 10 ng/ml (240 pM). **B Histogram of the probability of conductivity** - A total of 93 events were recorded at room temperature. The conductance of one pore-forming unit of refolded FomA in black lipid films of diphytanoyl phosphatidylcholine was in the range 0.1 - 2.1 nS with a maximum probability of conductance at 1.1 nS.

4.4.5 Kinetics of insertion and folding of FomA into lipid bilayers

For a first characterization of the mechanism of membrane insertion and folding of FomA into membranes, we performed kinetic experiments, in which we used phospholipid

bilayers formed of dicapryl phosphatidylcholine (*di*$C_{10:0}$PC) (Kleinschmidt and Tamm 2002) or of dioleoylphosphatidylcholine (*di*$C_{18:1}$PC) as target membranes. These lipids were chosen for a comparison of FomA folding with previous work on the membrane insertion and folding of OmpA (Kleinschmidt and Tamm 1996; Kleinschmidt and Tamm 2002). Although in our initial experiments FomA folding into *di*C_{10}PC was quantitative with both LUVs and SUVs, folding yields of FomA in lipid bilayers of *di*$C_{18:1}$PC were higher, when SUVs were prepared by ultrasonication (Figure 4.1). For a better comparison we performed all our kinetic studies with SUVs.

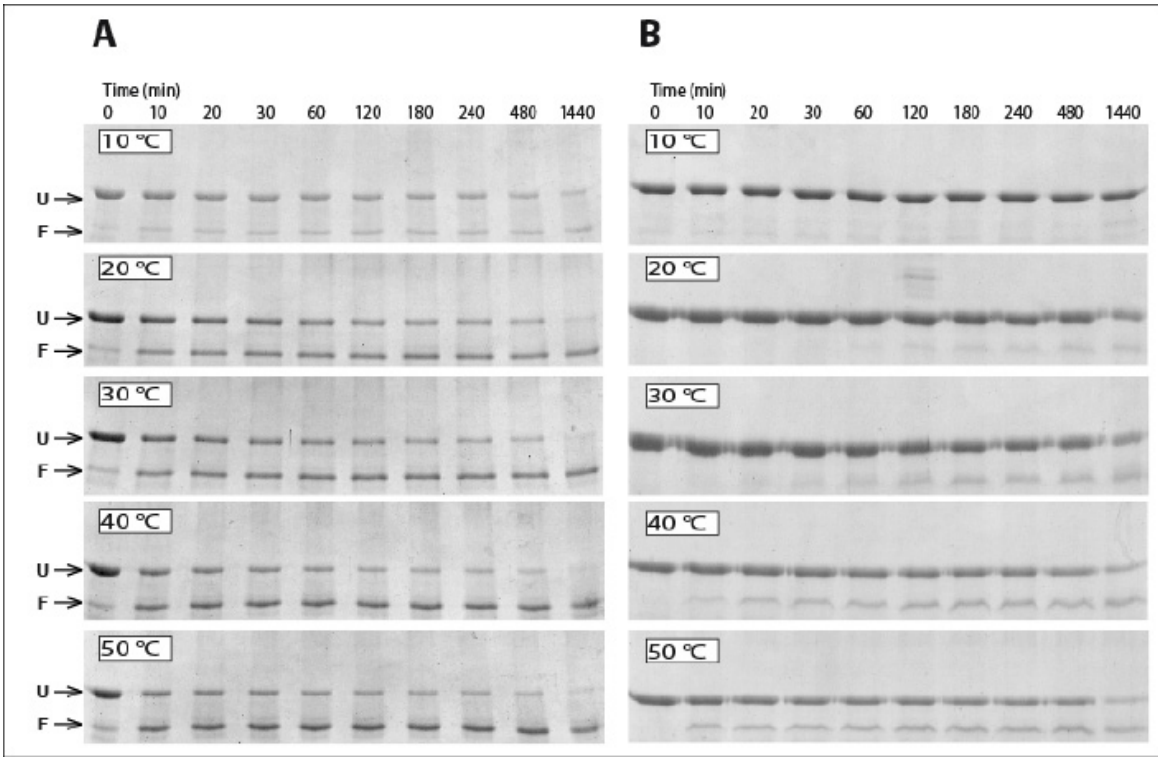

Figure 4.4 SDS-Polyacrylamide gels of the time courses of FomA insertion and folding into lipid bilayers (SUVs) of *di*$C_{10:0}$PC (A) and of *di*$C_{18:1}$PC (B) at temperatures of 10, 20, 30, 40, and 50 °C. The arrows indicate the electrophoretic migration of the folded (F) and unfolded (U) forms of FomA, which migrated at M_{app} (F) = 37 kDa and at M_{app} (U) = 40 kDa, respectively. The FomA concentration was 7 µM and the lipid/FomA ratio was 1000 mol/mol in 10 mM borate buffer (pH 10.0, containing 2 mM EDTA).

Figure 4.4A shows the SDS-polyacrylamide gels for the kinetics of FomA folding into *di*$C_{10:0}$PC, at different temperatures between 10 °C and 50 °C. Folding kinetics observed by the appearance of the 37 kDa band were generally slow and had to be monitored over a time course of 24 hrs (1440 min). At 10 °C, only about 50 % of FomA folded after 24 hrs, whereas at 50 °C, 50 % folding was obtained already after 10 min,

demonstrating the strong temperature dependence of FomA folding. The change from 10 °C to 20 °C had the largest effect on FomA folding and at 20 °C, yields of folded FomA reached 50% after 1 hr and were near quantitative after 24 hrs.

When insertion and folding of FomA was monitored with *di*$C_{18:1}$PC (Figure 4.4B), formation of the folded 37 kDa form of FomA took much longer and 50% folding were obtained only after 24 hrs at 50 °C. Again, FomA insertion and folding was slower at lower temperatures and almost no folding was observed at 10 °C.

4.4.6 Kinetics densitometric analysis and rates of FomA folding

To determine the rate constants of membrane insertion and folding of FomA in lipid bilayers as a function of temperature, the gels of Figure 4.4 were analyzed by densitometry (Figure 4.5) to first obtain the fractions of folded FomA as a function of time at each temperature. This analysis was performed for FomA folding into *di*$C_{10:0}$PC (gels of Figure 4A) and for FomA folding into *di*$C_{18:1}$PC (gels of Figure 4.4B) bilayers. The corresponding plots of the fractions of folded FomA at each temperature are shown in Figure 4.5A (*di*C_{10}PC) and B (*di*$C_{18:1}$PC).

In previous work (Kleinschmidt and Tamm 2002), the folding kinetics of OmpA into lipid bilayers of either *di*$C_{10:0}$PC, *di*$C_{11:0}$PC, or *di*$C_{12:0}$PC were also analyzed by densitometry performed on SDS-PA gels. These previous kinetic data were fitted to a single-step second-order kinetics, i.e. appearance of the folded form with time followed the integrated second-order rate-law (see ***e.g.*** Kleinschmidt and Tamm 2002 for details):

$$[\mathrm{P_F}](\mathrm{t}) = \frac{[\mathrm{P_U}]_0[\mathrm{L}]_0 \cdot \left(\exp\left\{\left([\mathrm{P_U}]_0 - [\mathrm{L}]_0\right)\cdot \mathrm{k_{2.ord}} \cdot \mathrm{t}\right\} - 1\right)}{[\mathrm{P_U}]_0 \cdot \exp\left\{\left([\mathrm{P_U}]_0 - [\mathrm{L}]_0\right)\cdot \mathrm{k_{2.ord}} \cdot \mathrm{t}\right\} - [\mathrm{L}]_0} \qquad \text{(Eq. 4.2)}$$

where $[P_F](t)$ and $[P_U](t)$ are, respectively, the concentrations of folded and unfolded protein at time *t*, $[L](t)$ is the concentration of the lipid at time *t* after initiation of the folding reaction. $k_{2.ord}$ is the second-order rate constant $[P_U]_0$, and $[L]_0$ are the initial concentrations of the lipid and unfolded protein.

At larger lipid concentrations (L/P > ~100 mol/mol), fits to a single-step pseudo first-order kinetics were sufficient to describe the folding kinetics of OmpA in this

previous work and mono-exponential fits gave good approximations to the folding kinetics of OmpA (Kleinschmidt and Tamm 2002). We therefore attempted to fit our kinetic data obtained for the folding of FomA to Eq. 4.2, but found that this kinetic model is unsatisfactory for describing our FomA folding kinetics.

None of the kinetics of FomA folding, neither with *di*$C_{10:0}$PC nor with *di*$C_{18:1}$PC could be well fitted to a single-step second order-kinetics (see dotted fit lines in Figure 4.5). Clearly, the FomA folding kinetics into lipid bilayers were more complex than those of OmpA. We could fit our kinetic data assuming a 2-step mechanism with two pseudo-first order components. The non-linear least-square fits to double-exponential functions (Eq. 4.3) are shown in Figure 4.5 (solid lines):

$$[P_F](t) = q \cdot \left[A_0 + A_{FR} \exp(k_F t) + A_{SR} \exp(k_S t) \right] \qquad \text{(Eq. 4.3)}$$

In Eq. 4.3 $[P_F](t)$ is the concentration of the folded protein at time t, k_F and k_S are the rate constants of the fast and the slow kinetic phases and the pre-exponential factors A_{FR} and A_{FS} their relative contributions to the folding kinetics.

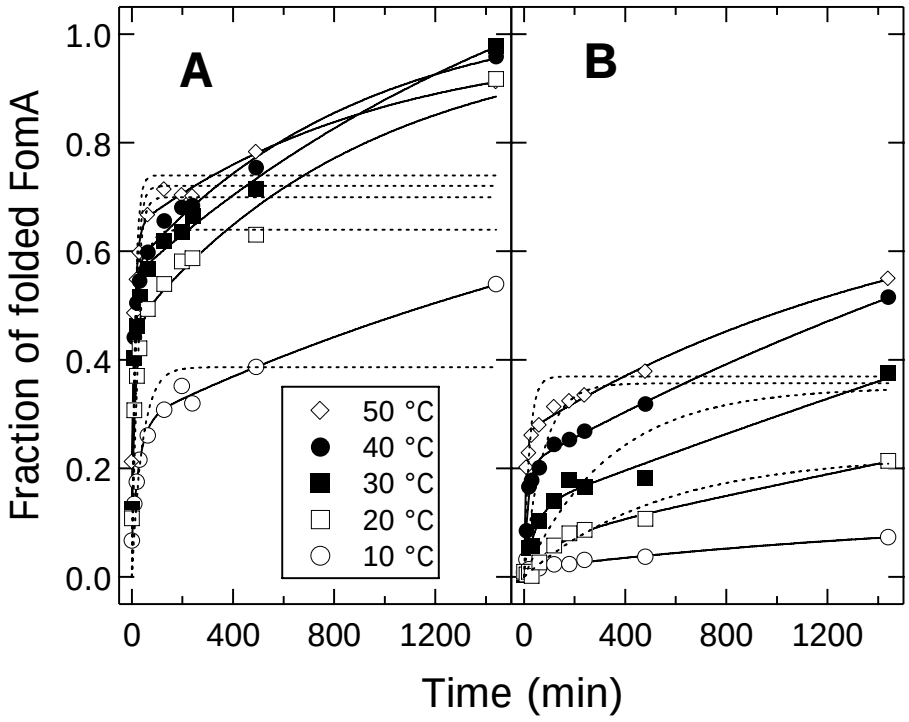

Figure 4.5 The fraction of folded FomA was determined at different times after initiation of folding by densitometry of the unfolded and folded FomA bands for each of the

polyacrylamide gels shown in Figure 4.4. The kinetics of FomA folding into lipid bilayers (SUVs) of *di*$C_{10:0}$PC (A) and *di*$C_{18:1}$PC (B) were determined at selected temperatures and fitted to double exponential functions. Alternatively, data for FomA insertion and folding into *di*$C_{18:1}$PC at 30 and at 40 °C were also fitted to a second-order rate law, assuming a single insertion and folding step (dotted lines) (Kleinschmidt and Tamm 2002).

In Table 4.1, the relative contributions and the calculated rate constants of the two observed kinetic phases of FomA insertion and folding are summarized for folding into *di*$C_{10:0}$PC (A) and for folding into *di*$C_{18:1}$PC (B). All rate constants increased with temperature. The kinetics of OmpA folding into *di*$C_{18:1}$PC (Figure 4.7) and the calculated rate constants are presented for comparison (Table 4.2).

Table 4.1 Rate constants for insertion and folding of FomA into *di*$C_{10:0}$PC and into *di*$C_{18:1}$PC

A. FomA insertion and folding into *di*$C_{10:0}$PC

T (°C)	[P] (μM)	[L] (mM)	A_{FR}[a]	k_F (*di*$C_{10:0}$PC) (min^{-1})	A_{SR}[a]	k_S (*di*$C_{10:0}$PC) (min^{-1})
50	7	7	0.55	0.082	0.45	0.00103
40	7	7	0.48	0.105	0.52	0.00113
30	7	7	0.34	0.086	0.66	0.00053
20	7	7	0.27	0.058	0.73	0.00038
10	7	7	0.26	0.032	0.74	0.00037

B. FomA insertion and folding into *di*$C_{18:1}$PC

T (°C)	[P] (μM)	L/P (mM)	A_{FR}	k_F (*di*$C_{18:1}$PC) (min^{-1})	A_{SR}	k_S (*di*$C_{18:1}$PC) (min^{-1})
50	7	7	0.35	0.118	0.65	0.00062
40	7	7	0.17	0.059	0.83	0.00027
30	7	7	0.06	0.022	0.94	0.00009

[a] A_{FR} and A_{SR} are the relative contributions of each of the two kinetic phases (obtained by division of each preexponential fit parameter by the sum of the two preexponential fit parameters).

For FomA folding into *di*$C_{10:0}$PC, the rate constant of the fast kinetic phase was about 100–fold greater than the rate constant of the slow kinetic phase. When folding of FomA was monitored at temperatures above 30 °C, both kinetic phases contributed to about the same extent to the formation of folded FomA. At 30 °C or below, the slow phase dominates. Both rate constants showed similar temperature dependences.

Table 4.2 Rate constants for insertion and folding of OmpA into *di*$C_{18:1}$PC

Double-exponential fit

T (°C)	[P] (μM)	[*L*] (mM)	A_{FR}	k_F (*di*$C_{18:1}$PC) (min^{-1})	A_{SR}	k_S (*di*$C_{18:1}$PC) (min^{-1})
40	9	3.6	0.46	0.152	0.54	0.038
30	9	3.6	0.52	0.056	0.48	0.0017

[a]A_{FR} and A_{SR} are the relative contributions of each of the two kinetic phases (obtained by division of each preexponential fit parameter by the sum of the two preexponential fit parameters).

For FomA folding into *di*$C_{18:1}$PC, the rate constant of the fast kinetic phase was about 200 –fold greater than the rate constant of the slow kinetic phase. The slow process dominated up to 50 °C. The rate constants of the slow process of FomA folding into *di*$C_{18:1}$PC were significantly smaller than the rate constants of the slow process of FomA folding into *di*C_{10}PC. The rate constants of the faster phases of the two folding reactions in *di*C_{10}PC and in *di*$C_{18:1}$PC were more similar above 30 °C. Rate constants for FomA insertion and folding into *di*$C_{18:1}$PC at 20 °C or below were not determined because folding yields were low.

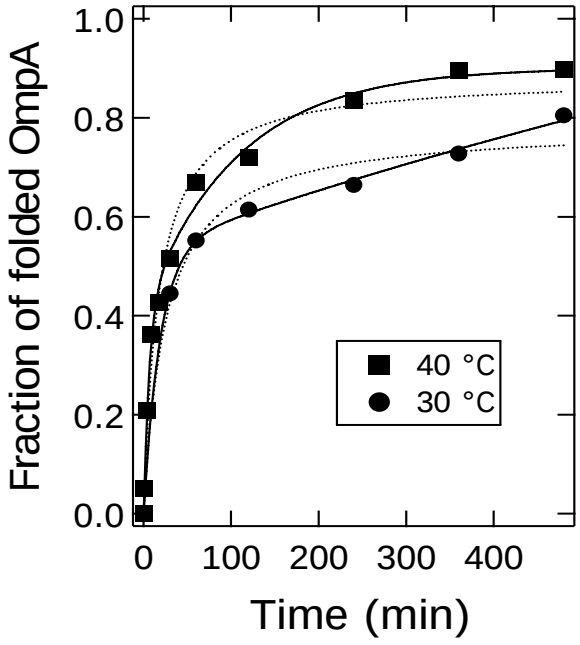

Figure 4.6 Folding of OmpA into di$C_{18:1}$PC The fraction of folded outer membrane protein A (OmpA) in *di*$C_{18:1}$PC is plotted at 30 and at 40 °C. The concentrations of OmpA and *di*$C_{18:1}$PC were 9 μM and 3.4 mM, respectively in a total volume of 11 μl. Data were taken from Kleinschmidt and Tamm (Kleinschmidt and Tamm 1996) and fitted to a double-exponential

function (solid line), Eq. 4.3, or to a single-step second order kinetics, Eq. 4.2 (dotted line), as described (Kleinschmidt and Tamm 2002).

4.4.7 Determination of activation energies

The temperature dependences of the rate constants of insertion and folding of FomA into lipid bilayers (SUV) of *di*$C_{10:0}$PC and of *di*$C_{18:1}$PC were used for estimating the activation energies of insertion and folding from Arrhenius plots (Figure 4.7).

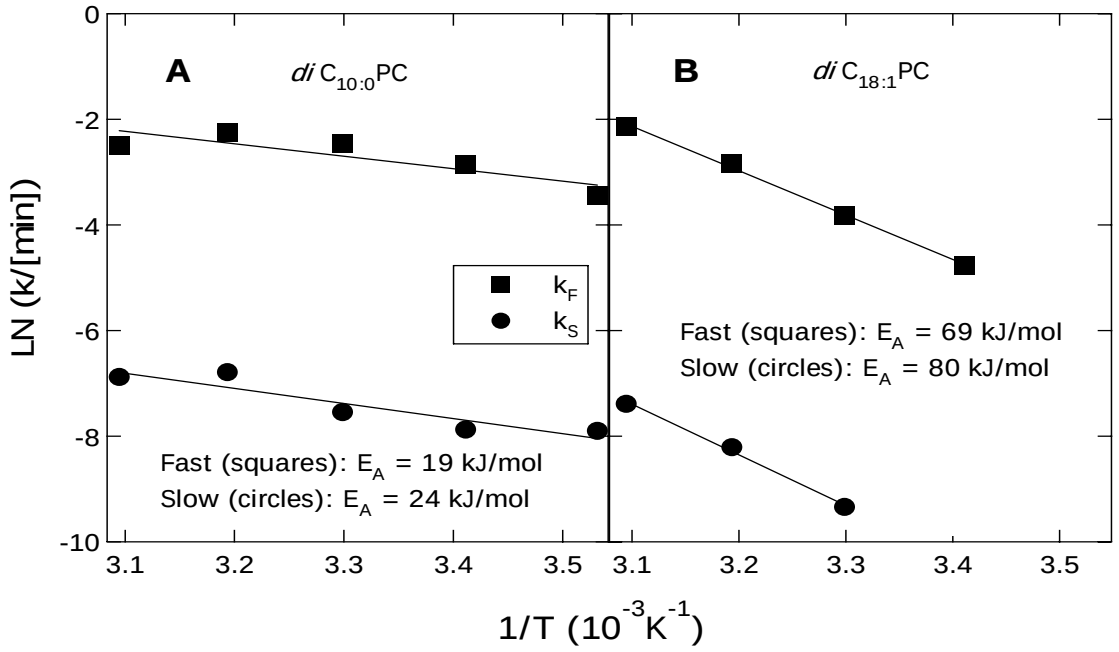

Figure 4.7 Arrhenius plots - of the rate constants of FomA folding into *di*$C_{10:0}$PC (A) and *di*$C_{18:1}$PC (B) determined from double exponential fits to the FomA folding kinetics shown Figure 4.5A and B.

Activation energies for FomA folding into *di*$C_{10:0}$PC were E_A(*di*$C_{10:0}$PC, F) ≈ 19 kJ/mol for the faster step and E_A(*di*$C_{10:0}$PC, S) ≈ 24 kJ/mol for the slower step, respectively. For FomA folding into *di*$C_{18:1}$PC, activation energies were E_A(*di*$C_{18:1}$PC, F) ≈ 69 kJ/mol for the fast step and E_A(*di*$C_{18:1}$PC, S) ≈ 80 kJ/mol for the slow step, respectively.

4.5 Discussion

4.5.1 Functional insertion and folding of FomA

In this study, we showed that the major outer membrane protein FomA of *F. nucleatum* spontaneously inserted and folded into phospholipid bilayers by analysis of the shift in the electrophoretic mobility, by limited proteolysis, by fluorescence and circular dichroism spectroscopy and by single channel recordings. The latter demonstrated that refolded FomA was functionally active and had an average single channel conductance of 1.1 nS as reported previously for FomA that was isolated from membranes in native form at much lower yields. The channel conductance of FomA strictly correlated with the presence of the 37 kDa form of FomA. Since it forms a much larger, membrane inserted monomeric channel than OmpA, FomA is an important new alternative model system to study the biophysical principles and mechanism of membrane insertion and folding of β-barrel OMPs. FomA will allow investigations on the effects of the size of the transmembrane domain on the principles of insertion and folding of β-barrel OMPs, for example in comparison with OmpA.

In our experiments, quantitative refolding of FomA was possible upon incubation with LDAO micelles, or alternatively with *di*$C_{10:0}$PC bilayers that were prepared either as LUVs or as SUVs. Refolding was also possible with *di*$C_{18:1}$PC (SUVs), but with only 50% yield. It was not possible to directly transfer refolded FomA from lipid bilayers of *di*$C_{10:0}$PC or *di*$C_{18:1}$PC into black lipid films of *di*phPC without the use of detergent, but comparison of electrophoretic mobility shifts, the proteolytic fragments and the circular dichroism spectra of FomA in *di*$C_{10:0}$PC and LDAO clearly indicated that the 37 kDa form that FomA developed in lipid bilayers is the same form as developed in LDAO micelles.

Our present observations of a strict correlation of functional activity to an electrophoretic mobility shift of the migration of FomA to 37 kDa after folding, reflect previous reports for OmpA of *E. coli*. In previous work, a wide range of experiments on OmpA structure and function had demonstrated a strict correlation between functional activity and the presence of the 30 kDa form of OmpA (Schweizer et al. 1978; Vogel and Jähnig 1986; Dornmair et al. 1990; Surrey and Jähnig 1992; Rodionova et al. 1995; Surrey and Jähnig 1995; Sugawara et al. 1996; Arora et al. 2000). Denatured OmpA migrated at

35 kDa and only the 30 kDa inserted and folded form of OmpA was functionally active and largely protected against protease digestion by the lipid bilayer. Proteolysis of membrane-inserted OmpA resulted in a 24 kDa N-terminal fragment that consisted of the 19 kDa transmembrane domain of OmpA and a fraction of the 154 residue periplasmic domain. A possible explanation, why only natively folded outer membrane proteins may exhibit a changed electrophoretic mobility could be that most folding intermediates of membrane proteins may not be stable enough to prevent unfolding in the presence of both, the denaturing detergent SDS and the electrical field that is applied to the membrane protein in electrophoresis.

Our experiments also demonstrated that folding of FomA did not require the presence of molecular chaperones or of translocon-like insertion machinery. However, *in vitro* experiments on FomA folding worked best at pH 10, above the pI of FomA (pI=8.9) and lower yields were obtained at pH 7 (data not shown). This has been observed previously for OmpA and is a consequence of the improved solubility of FomA, OmpA, and very likely other outer membrane proteins in negatively charged form (Surrey and Jähnig 1995; Kleinschmidt and Tamm 2002). *In vivo*, solubility of outer membrane proteins in the bacterial periplasm is conferred by complex formation with soluble periplasmic chaperones, such as Skp (Chen and Henning 1996; Bulieris et al. 2003). Proteinaceous cofactors such as Skp or SurA will also assist membrane insertion and folding of FomA in cells leading to a more rapid formation of native FomA structure, similarly as observed for OmpA (Lazar and Kolter 1996; Rouvière and Gross 1996; Rizzitello et al. 2001). Although like FomA, OmpA also quantitatively inserted and folded in absence of proteinaceous folding assistants, folding was greatly facilitated by the simultaneous presence of lipid bilayers, the seventeen-kilodalton-protein (Skp) and lipopolysaccharide (Bulieris et al. 2003). Preliminary results from our laboratory revealed that Skp also binds to unfolded FomA in aqueous solution (Qu & Kleinschmidt, in preparation) at neutral pH.

4.5.2 Chain length dependence of insertion and folding of FomA into lipid bilayers

The chain-length dependence for FomA insertion and folding is consistent with the hydrophobic thickness of most outer membrane proteins of known crystal structure, which

is in the range of 22 to 24 Å, see *ref.* (Lee 2003) for a review. The hydrophobic thickness of lipid bilayers of *di*$C_{12:0}$PC in the fluid phase was determined to 19.5 ± 1 Å (Lewis and Engelman 1983), suggesting that fluid bilayers of short-chain lipids would provide a better hydrophobic matching to outer membrane proteins than fluid *di*$C_{18:1}$PC, because the chains of *di*$C_{10:0}$PC may be stretched in the vicinity of IMPs with longer hydrophobic thickness (de Planque et al. 1998), for reviews see *refs.* Marsh 1990; Killian 1998. The energy requirement for bilayer thickening is small up to the limit of full extension of the acyl chains. The energy cost of a 33% increase in bilayer thickness, which corresponds to a ~25% reduction of the molecular surface area, is only about 2 kT per molecule (Parsegian et al. 1979; Lis et al. 1982). *Di*$C_{18:1}$PC, which has a hydrophobic thickness of 27 ± 1 Å, respectively (Lewis and Engelman 1983), would have to be compressed to match the hydrophobic thickness of FomA or other outer membrane proteins. Lewis and Engelman demonstrated in a previous study that BR with a hydrophobic thickness of ~30 Å (Pebay-Peyroula et al. 1997) remains well dispersed in bilayers with hydrophobic thicknesses ranging from 19.5 Å to 34 Å (Lewis and Engelman 1983). In their study, BR aggregation occurred in thick bilayers when the mismatch exceeded 6 Å. However, in thin bilayers a mismatch of up to 14 Å was tolerated. Membrane thinning may not occur as readily as membrane thickening, because even 2-3% surface area increases destabilize the bilayer structure and break membranes (Kwok and Evans 1981).

A similar dependence of outer membrane protein folding on lipid acyl chain length was observed previously for OmpA, which inserted and folded only into lipid bilayers composed of phospholipids with 12 or fewer carbons in their hydrophobic chains, when folding experiments were performed with large unilamellar lipid vesicles prepared by extrusion through 100 nm pores (Kleinschmidt and Tamm 2002). Folding into bilayers of lipids with longer acyl chains required the preparation of SUVs for OmpA folding (Surrey and Jähnig 1992; Surrey and Jähnig 1995; Kleinschmidt and Tamm 1996). It is somewhat surprising that unlike the 8-stranded OmpA, the larger FomA still folds into LUVs of *di*$C_{18:1}$PC, albeit with relatively small yields. Increased folding yields of FomA were obtained when small unilamellar vesicles of *di*$C_{18:1}$PC were prepared, what we expected from our previous experiments with OmpA (Kleinschmidt and Tamm 1996). Lipid bilayers of SUVs have a relatively high surface curvature, are under curvature stress, and are likely to also contain temporary local defects in the lipid surface. More hydrophobic surface is therefore exposed to FomA when it is adsorbed to a curved membrane surface, which may facilitate insertion and folding of FomA.

4.5.3 Kinetics of FomA folding into phospholipid bilayers indicate parallel folding pathways

Our investigation of the kinetics of FomA insertion and folding indicated a strong temperature-dependence of the folding rates for both, folding of FomA into bilayers of the short-chain phospholipid *di*$C_{10:0}$PC and into bilayers of the long-chain phospholipid *di*$C_{18:1}$PC. Interestingly, the data from KTSE experiments could neither be fitted to a single-step second-order rate law (Eq. 4.2) nor to a pseudo first-order rate law. Instead, the data were reasonably well fitted to double-exponential functions (Figure 4.5). This observation needs an explanation, since previous data on the folding kinetics of OmpA into bilayers of short-chain phospholipids fitted well to single-step second-order kinetics or even pseudo first-order kinetics (Kleinschmidt and Tamm 2002). Double-exponential kinetics as observed here for folding of FomA into bilayers of either *di*$C_{10:0}$PC or *di*$C_{18:1}$PC (Figure 4.5) would indicate two folding steps. However, in our electrophoretic mobility analysis on the folding of FomA, we observed only two bands, at 40 and at 37 kDa and no intermediate form could be distinguished by electrophoresis. Since there was a strict correlation between the presence of the 37 kDa form and functional activity of FomA, folding was measured by the relative increase of the 37 kDa form as a fraction of the entire protein. Therefore an intermediate migrating at an apparent molecular weight of 37 kDa cannot lead to the observation of two kinetic phases in our densitometric analysis. If an intermediate was formed that migrated at the same apparent molecular weight as unfolded FomA (40 kDa), three possibilities for FomA folding may be considered. The first possibility is that the intermediate was formed fast, prior to the formation of the 37 kDa form and that this intermediate was required for subsequent formation of the 37 kDa form, i.e. the two folding steps would be sequential with the slower step being the formation of the 37 kDa form. In this case, formation of the 37 kDa form would still be rate limiting and the fast formation of an intermediate would not be detectable in the kinetics of the formation of 37 kDa form of FomA. However, we observed a fast and a slow phase in our kinetic analysis. A second possibility would be that the two folding steps are sequential and that the formation of the intermediate at 40 kDa is slow compared to the formation of the 37 kDa form. In this case, the kinetics of formation of the 37 kDa form should have been sigmoidal, with a lag phase prior to formation of the 37 KDa form. However, this has

not been observed. This means that there are true parallel pathways of FomA folding. It is possible that after rapid dilution of the denaturant urea, two major populations of aqueous forms of FomA formed that adsorbed, inserted and folded with different rates into the lipid bilayer. These formations of the two different states possibly preceded insertion and folding because the biphasic folding kinetics were observed with two different phospholipid bilayer preparations into which FomA could insert and fold. Formation of two different forms of aqueous FomA prior to insertion and folding into the membrane is further supported by the similar temperature-dependencies of the two observed kinetic phases, for both, folding of FomA into *di*$C_{10:0}$PC and folding of FomA into *di*$C_{18:1}$PC (Figure 4.7).

Membrane protein folding of OmpA into lipid bilayers was lipid concentration dependent and followed a second-order rate-law, which could be approximated at high lipid/protein ratios by a pseudo first-order description (Kleinschmidt and Tamm 2002). For better comparison, we also calculated the 2nd order rate constants $k_{F,2.ord} = k_F/[L]$ that are independent of the lipid concentrations from fits to our kinetic data for both the fast and the slow folding steps of FomA (Table 4.1).

The rate constants are directly related to the half-lifes for formation of folded FomA, $\tau_{1/2}$ that are given by:

$$\tau_{1/2} = \frac{\ln(2)}{k_F} \qquad \text{(Eq. 4.4)}$$

for a pseudo first-order kinetics, if the concentration of the lipid [*L*] is large compared to the protein concentration (Atkins 1998). Therefore, half-lifes of FomA folding into *di*$C_{10:0}$PC range from ~22 min (at 10 °C) to ~7 min (at 40 to 50 °C) for the fast folding pathway and from ~1900 min (10 °) to ~700 min (50 °C) for the slow folding pathway. Similarly, folding of FomA into *di*$C_{18:1}$PC is characterized by half-lifes ranging from ~30 min (at 10 °C) to ~6 min (at 40 to 50 °C) for the fast folding pathway and from ~7800 min (10 °C) to ~1100 min (at 40 to 50 °C) for the slow pathway. Clearly, the slow phase is physiologically not relevant, since cells divide approx. every 20 min. The concentration of the outer membrane lipids in cells may actually be estimated to approximately 10 mM from the cell volume ($1.57 \cdot 10^{-18}$ m^3), the cell surface ($7.85 \cdot 10^{-12}$ m^2) and the lipid-headgroup area assumed to be ~65 $Å^2$, see *e. g.* (Marsh 1990), assuming that about half of the inner surface of the outer membrane is covered by lipid, while the other half is covered by integral membrane proteins (both leaflets of the bilayer must be taken into account to

compare with the lipid concentrations in membrane protein refolding into liposomes *in vitro*). The concentration of the lipids available for insertion and folding in cells is therefore ~2–fold higher, which should result in ~2–fold shorter half-lifes.

The rate for the fast folding pathway determined from this analysis is therefore a very reasonable rate for outer membrane protein insertion and folding. The discovery of two parallel kinetic phases for the folding of FomA led us to examine again our previous data on the folding of OmpA. We had analyzed our previous data on the folding of OmpA by fits to single-step kinetics. These fits described the folding of OmpA into short-chain phospholipids very well (Kleinschmidt and Tamm 2002) and we could not distinguish any significant improvements by fits to double-exponential kinetics. However, since OmpA folding was much slower with long-chain phospholipids (Kleinschmidt and Tamm 1996) we also reanalyzed previous data on the folding of OmpA into bilayers of the longer-chain phospholipid *di*$C_{18:1}$PC (Kleinschmidt and Tamm 1996) as examined by SDS-PAGE. Our fits to single-step second-order kinetics are shown together with fits to two-step kinetics in Figure 4.7. The assumption of a two-step kinetics for OmpA folding into these membranes describes the data somewhat better than the assumption of a single-phase kinetics, although the differences between the two fits are not as pronounced as for the folding of FomA and there may be also only statistical deviation of the experimental data from single-step second order kinetics.

It is further interesting to compare the relative contribution A_{FR} and A_{SR} of the slow and fast kinetic phases of FomA folding into the two bilayers composed of *di*$C_{10:0}$PC and *di*$C_{18:1}$PC (Table 4.1). The relative contribution of the fast folding process to the overall folding rate of FomA increases with temperature, for each of the lipids. At 50 °C, the rate constant for the fast process of FomA folding into *di*$C_{10:0}$PC is about the same as the rate constant for the fast FomA folding process into *di*$C_{18:1}$PC. However, the relative contribution of this process to the overall folding rate is less for *di*$C_{18:1}$PC than for *di*$C_{10:0}$PC indicating a dependence on lipid bilayer properties of the relative contribution of the fast folding route to the total rate of insertion and folding of FomA.

In the present work, we have demonstrated that FomA of *Fusobacterium nucleatum* is a useful model to study insertion and folding of outer membrane proteins into membranes. Next to OmpA, FomA is the only β-barrel membrane protein that currently has been shown to quantitatively insert and fold into lipid bilayers. The transmembrane β-barrel of FomA is almost twice as large as that of OmpA and comparisons between the two proteins in studies on outer membrane protein insertion and folding will be very useful to

clarify mechanistic principles of the folding process. Initial comparison with published work on OmpA demonstrates that *in vitro*, overall folding rates of the larger FomA are much slower than those of OmpA. However, our study also demonstrates that *in vitro* there are parallel folding pathways for FomA insertion and folding, but that only one of the pathways may be fast enough to be physiologically relevant. At 40 °C, the observed fast process is characterized by half-lifes in the range of a few minutes for both, FomA and OmpA. Although the half-lifes for the fast process are shorter for OmpA, they are still in a reasonable time range also for the larger FomA. It will be interesting to compare the effects of lipid bilayer composition, the periplasmic chaperone Skp, or possible other folding assistants on the relative contributions of the slow and fast phases of FomA folding in future studies. FomA will be a very useful model protein for such studies, since the relative contributions of efficient and non-efficient folding pathways seem well distinguishable with the relatively simple kinetic analysis used in this study.

5 The stability of membrane proteins in micelles and bilayers investigated with the ferrichrom receptor FhuA

5.1 Abstract

Detergent–micelle extraction of integral membrane proteins for structural and functional studies often leads to a strong loss in protein activity suggesting that the protein becomes thermodynamically less stable. To quantitatively assess the destabilization, we have performed unfolding studies using the integral membrane protein FhuA as an example. Unfolding was monitored by fluorescence spectroscopy and the stabilities of wt-FhuA and the mutant FhuAΔ5-160 were determined in lipid bilayers and in detergent micelles, respectively.

Wild-type (wt) FhuA consists of a 22-stranded β-barrel domain and an N-terminal cork domain (residues 1-160) inside the barrel. At 35 °C, the energy required for unfolding of FhuAΔ5–160 from a bilayer integrated state was about 21 kJ/mol (5.0 kcal/mol), i.e. 4 times larger than for FhuAΔ5–160 that was solubilized in micelles of the detergent LDAO ($\Delta E \approx 5$ kJ/mol). Urea-induced unfolding detergent-solubilized wt–FhuA and FhuAΔ5–160, indicated that the β-barrel domain of wt–FhuA is stabilized by interactions with the cork domain. When wt-FhuA was reconstituted into a phospholipid membrane, unfolding of the cork domain preceded unfolding of the β-barrel domain. These two steps could not be distinguished in the urea-induced unfolding of the detergent-micelle solubilized form of wt-FhuA. Our results indicate that the stability of membrane proteins is most strongly affected by the structure of the supramolecular assembly (micelle vs. bilayer) rather than by the chemical structure of monomeric amphiphiles.

5.2 Introduction

For structural and functional studies, membrane proteins are often extracted into detergent micelles, which solubilize the membrane proteins from their membrane environment and allow the separation of the membrane protein of interest. A negative side effect is that this extraction often leads to the deactivation of the membrane protein (cf. Lo Piero and Petrone 1994; Orlowski et al. 1998). In detergent micelles, integral membrane proteins are surrounded by amphiphiles with hydrophobic chains that are in contact with the hydrophobic transmembrane surface of the integral membrane protein. The amphiphiles in the protein-micelle complexes are in an equilibrium with monomeric amphiphiles in solution and the exchange between the micellar state and the monomeric state is rapid (le Maire et al. 2000; Garavito and Ferguson-Miller 2001). This frequent exchange at the interface of the membrane protein with the micelle is likely to contribute to the destabilization of integral membrane proteins in detergent micelles, which is one of the reasons why researchers are investigating alternatives to the classical detergent-micelle solubilization of membrane proteins (for examples, see Chaudier et al. 2002; Popot et al. 2003).

Protein stability, i.e. the free energy of unfolding, has been determined experimentally using either chaotropic denaturants such as urea and guanidinium chloride or using heat to induce protein unfolding (Aune and Tanford 1969; Pace and McGrath 1980; Johnson and Fersht 1995; Otzen and Fersht 1995; Martin et al. 2002). The major obstacle why there are only a few studies on the stability of integral membrane proteins is that these are usually very hydrophobic and insoluble in aqueous buffer. Exceptions are IMPs of the β-barrel class, such as outer membrane proteins (OMPs) of Gram-negative bacteria. OMPs are characterized by a relatively low average hydrophobicity, which is comparable to the average hydrophobicity of soluble proteins. OMPs can therefore be completely unfolded by urea to investigate their stability and folding. For example, outer membrane protein A (OmpA), which forms an 8-stranded β-barrel in the outer membrane of *E. coli*, is completely unfolded and soluble in 8 M urea in absence of any detergent or lipid. Unfolding is completely reversible and OmpA folds into micelles of a wide range of different detergents (Dornmair et al. 1990; Kleinschmidt et al. 1999) and also into lipid bilayers (Surrey and Jähnig 1992; Kleinschmidt and Tamm 1996; Kleinschmidt and Tamm

2002). In addition, denaturant unfolding and refolding of OMPs into detergent micelles has been a very successful strategy for outer membrane protein crystallization and structure determination (for a review see e.g. Buchanan 1999).

Many recent articles have shown that lipid-protein interactions are often crucial to membrane protein activity. In the past, the thermodynamic stability of membrane proteins and peptides in membrane environment has often been calculated solely based on theoretical considerations, not taking into account that specific interactions of membrane proteins with the bilayer of micelle that surrounds it may strongly impact membrane protein stability. For example, detegent micelles are metastable and detergent molecules of the micelles partition as monomers into solution, transiently exposing hydrophobic surface of the protein to the aqueous space. In contrast, lipid bilayers are more tightly packed and biological membrane composed of phospholipid bilayers are usually impermeable to solutes of the aqueous phase. Lipids that are tightly arranged around integral membrane proteins may have unique properties in stabilizing membrane proteins.

We have chosen the active iron transporter FhuA of the outer membrane of *E. coli* to study the impact of lipid membranes and detergent micelles on the stability of an integral membrane protein. FhuA (78 kDa) is a two domain protein composed of 714 amino acid residues. FhuA has an N-terminal 160 residue domain termed "cork domain" that fills the 554 residue transmembrane domain, which forms a 22-stranded β-barrel in the outer membrane of the bacterium. While the lipid exposed surface of FhuA is very hydrophobic, the pore structure, composed of amphipathic β-strands, explains that the average hydrophobicity of this and other similar outer membrane proteins is low. In initial experiments, the thermodynamic stabilities of FhuA and of a FhuA mutant (FhuAΔ5-160), in which almost the entire cork domain was deleted on the DNA level, where low enough to thoroughly investigate how the supramolecular environment affects protein stability.

In the present work, we therefore addressed several questions: How different are the stabilities of integral membrane proteins in lipid bilayers and in detergent micelles? Is the stability of the β-barrel domain affected by the presence of the N-terminal cork domain? Are the loss in secondary and tertiary structure coupled or separable processes? To which extent is the stability of integral membrane proteins affected by the pH of the solvent, by the hydrophobic thickness of the lipid bilayer and by the lipid headgroup charge?

5.3 Materials and methods

5.3.1 Isolation of wt-FhuA and FhuAΔ5-160

His_6-tagged wt-FhuA was purified from *E. coli* strain AW740 harboring the plasmid pHX405 (Moeck et al. 1996) as described (Ferguson et al. 1998). His_6-tagged FhuAΔ5-160 was isolated from *E. coli* strain BL21 (DE3) carrying plasmid pBk7H also as described (Ferguson et al. 1998), but with the following modifications to the protocol: FhuAΔ5-160, solubilized in LDAO detergent micelles, was dialyzed at 6.5 °C against 2 l of ammonium acetate buffer (50 mM, pH 8.0), containing 250 mM NaCl, 0.1% LDAO and 5 mM imidazole. FhuA was loaded onto a Ni^{2+}- NTA agarose (QIAGEN, Ontario, Canada) column coupled to an automated FPLC (Pharmacia LKB, Uppsala, Sweden). In the two purification procedures, each variant of FhuA (either wt-FhuA or FhuAΔ5-160) bound selectively to Ni^{2+}- NTA agarose and a single symmetrical peak containing purified FhuA eluted at around 200 mM imidazole, in a linear imidazole gradient from 5 to 500 mM. The fractions containing purified FhuA were pooled and concentrated by ultra filtration. Imidazole was removed by overnight dialysis against 2 l of sodium borate buffer (10 mM, pH 9.0) containing 2 mM EDTA and 0.1% LDAO detergent and at 6.5 °C. SDS-PAGE analyses of purified FhuA variants showed single bands at 78kDa (wt-FhuA) and at 62 kDa (FhuAΔ5-160).

5.3.2 Preparation of large unilamellar vesicles

20 mg of phospholipid were dissolved in chloroform, dried under a stream of nitrogen on the bottom of a glass test tube, and desiccated under high vacuum for at least 3 h to remove residual solvent. The lipids were dispersed in 10 mM borate buffer, pH 10.0, containing 2 mM EDTA to a concentration of 20 mg/ml. Large unilamellar vesicles (LUVs) were prepared by seven cycles of freeze-thawing the hydrated lipids in liquid nitrogen and in a water bath at 35°C, respectively. To obtain LUVs, lipid dispersions were extruded 42-fold through a pair of polycarbonate membranes with a pore size of 100 nm (Nucleopore,

Whatman, Clifton, NJ) using a mini-extruder (Avanti, Alabaster, AL) as described previously (Kleinschmidt and Tamm, 2002).

5.3.3 Reconstitution of wt-FhuA and FhuAΔ5-160 into phospholipids bilayers

Phospholipids (Avanti Polar Lipids, Alabaster, AL) were dissolved in chloroform and mixed at the desired ratios. Dry lipid films were prepared under a stream of nitrogen, followed by desiccation for at least 3 hours. Lipid films were dispersed in HEPES buffer (10 mM, pH 7.0, 2 mM EDTA) followed by addition of LDAO solubilized FhuA. Na cholate was added to a final concentration of 0.2%. The samples were incubated for 3 hours at room temperature. Cholate was subsequently removed by dialysis against 500 ml of HEPES buffer at 6.5 °C. The dialysis buffer was exchanged 3 times after every 3 hrs. Finally, the molar lipid/protein ratio was determined as described (Lowry et al. 1951; Rouser et al. 1970) and whenever necessary adjusted by lipid addition. At different pH, HEPES buffer was replaced either by citric acid (pH 3), sodium citrate (pH 4-6), Tris (pH 8.5), or by borax/sodium hydroxide (pH 10) buffer.

5.3.4 Unfolding experiments

Samples of wt-FhuA or FhuAΔ5-160, either solubilized in LDAO detergent micelles or reconstituted into lipid bilayers, were mixed with buffer containing 10 M urea to prepare samples at urea concentrations ranging from 0 to 10 M. After mixing, samples were incubated for equilibrium unfolding at a selected temperature for at least 24 hrs prior to recording fluorescence spectra to obtain the fraction of unfolded protein as a function of the urea concentration. To ensure that unfolding had reached a stationary state, the time dependence of unfolding was first determined by monitoring the fluorescence signal. All spectra were corrected by background subtraction using fluorescence spectra of samples without protein but with otherwise identical composition. To investigate the heat-induced unfolding of FhuA (either wt-FhuA or FhuAΔ5-160), an 800-fold molar excess of LDAO or an 800-fold molar excess of phospholipid bilayers was used at a FhuA concentration of 1.905 μM in a total volume of 1 ml buffer. All samples were equilibrated at 35 °C for 3 hrs and fluorescence spectra were recorded subsequently at temperatures between 35 and 100

°C with an increment of 2 °C. After each incremental temperature increase, samples were equilibrated for additional 20 min before a new spectrum was recorded.

5.3.5 Fluorescence spectroscopy

Fluorescence spectra were recorded on a SPEX- Fluorolog-322 spectrometer with double monochromators in the excitation and emission pathways. Tryptophan fluorescence was excited at a wavelength of 290 nm. The excitation and emission bandwidths were 2 and 3.7 nm, respectively. Spectra were scanned from 300 to 420 nm with an integration time of 0.05 s and an increment of 0.5 nm.

5.3.6 Unfolding monitored by CD spectroscopy

Far-UV CD measurements were performed at 30 ˚C on a Jasco 720 CD spectrometer using a thermostated 0.1 mm cuvette. Five scans were accumulated for each spectrum in the range of 190 to 250 nm with a response time of 8 s, a bandwidth of 1 nm, and a scan speed of 5 nm/min. The concentration of FhuA was 40 µM. The detergent/protein or phospholipid/protein molar ratio was 800. Background scans of samples without protein, but with otherwise identical compositions were subtracted.

5.3.7 Determination of $\Delta G°$

The unfolding of FhuA is a function of the urea concentration, or alternatively a function of temperature. Fluorescence emission spectra of FhuA (f_λ) depend on the degree of unfolding and are characterized by the spectral parameter $\langle\lambda_f\rangle$

$$\langle \lambda_F \rangle = \frac{\sum f_\lambda \cdot \lambda}{\sum f_\lambda} \qquad \text{(Eq. 5.1)}$$

f_λ are the fluorescence intensities at a given wavelength λ. $\langle\lambda_f\rangle$ depends on the entire spectrum and therefore better describes the contributions of the folded and unfolded states of the protein than the intensity at a selected individual wavelength. For an equilibrium

unfolding transition between two conformational states ($S_1 \rightarrow S_2$) of a protein, the mole fraction of state S_1 can be expressed using $\langle\lambda_f\rangle$ of the spectrum of the mixture (i.e. $\langle\lambda_m\rangle$) and $\langle\lambda_f\rangle$ of the spectra of the states S_1 and S_2 i.e. $\langle\lambda_1\rangle$ and $\langle\lambda_2\rangle$, respectively (cf. Mann et al. 1993; Roumestand et al. 2001). The spectrum F_λ at a selected urea concentration is a linear combination of the spectra of the states S_1 and S_2:

$$F_\lambda(S_1+S_2)\cdot c = \left[X\cdot f_\lambda(S_1)+(1-X)\cdot f_\lambda(S_2)\right]\cdot c \qquad \text{(Eq. 5.2)}$$

$f_\lambda(S_1)$ and $f_\lambda(S_2)$ are the fluorescence spectra of the states S_1 and S_2, respectively, X is the mole fraction of S_1, and c the concentration of the protein. With the parameters $\langle\lambda_M\rangle$, $\langle\lambda_1\rangle$, and $\langle\lambda_2\rangle$ for the fluorescence spectra of the mixture and the individual states S_1 and S_2, $\langle\lambda_M\rangle$ can be expressed as

$$\langle\lambda_M\rangle = \frac{\sum_\lambda \lambda\cdot F_\lambda(S_1+S_2)}{\sum_\lambda F_\lambda(S_1+S_2)} = \frac{X\cdot\sum_\lambda \lambda\cdot f_\lambda(S_1)+(1-X)\cdot\sum_\lambda \lambda\cdot f_\lambda(S_2)}{X\cdot\sum_\lambda f_\lambda(S_1)+(1-X)\cdot\sum_\lambda f_\lambda(S_2)} \qquad \text{(Eq. 5.3)}$$

This equation can be rewritten to obtain the mole fraction of the folded protein, X_1 and therefore the equilibrium constant K of the unfolding reaction:

$$X_1 = \left(\frac{\langle\lambda_M\rangle-\langle\lambda_1\rangle}{\langle\lambda_2\rangle-\langle\lambda_M\rangle}\cdot\frac{\sum_\lambda f_\lambda(S_1)}{\sum_\lambda f_\lambda(S_2)}+1\right)^{-1} \qquad K = \frac{\langle\lambda_1\rangle-\langle\lambda_M\rangle}{\langle\lambda_M\rangle-\langle\lambda_2\rangle}\cdot\frac{\sum_\lambda f_\lambda(S_1)}{\sum_\lambda f_\lambda(S_2)} \qquad \text{(Eq. 5.4)}$$

$\langle\lambda_M\rangle$ is therefore used to describe the fluorescence of a mixture of folded and unfolded protein as a function of the equilibrium constant K

$$\langle\lambda_M\rangle = \frac{\langle\lambda_1\rangle+\frac{1}{Q_R}K\langle\lambda_2\rangle}{\left(1+\frac{1}{Q_R}K\right)} \quad \text{with} \quad Q_R = \frac{\sum_\lambda f_\lambda(S_1)}{\sum_\lambda f_\lambda(S_2)} \qquad \text{(Eq. 5.5)}$$

Q_R is the ratio of the total fluorescence intensities of the folded over the unfolded state, respectively. The equilibrium constant and the energy of the unfolding transition are given by:

$$\Delta G^{\circ}_{1\to 2} = -RT\ln(K) = -RT\ln\left(\frac{1-X_1}{X_1}\right) \qquad \text{(Eq. 5.6)}$$

A prerequisite for deriving a free energy of unfolding ($\Delta G°$) is that the folding and unfolding reactions have reached equilibrium. Since for our model (FhuA) reversibility of folding could not be fully demonstrated i.e. we were unable to refold FhuA completely, we monitored the changes that occured in fluorescence intensities and in the $\langle\lambda_F\rangle$ parameter upon unfolding in urea as a function of time. We observed that after approximately 72 hours incubation there were no further changes in the above mentioned parameters

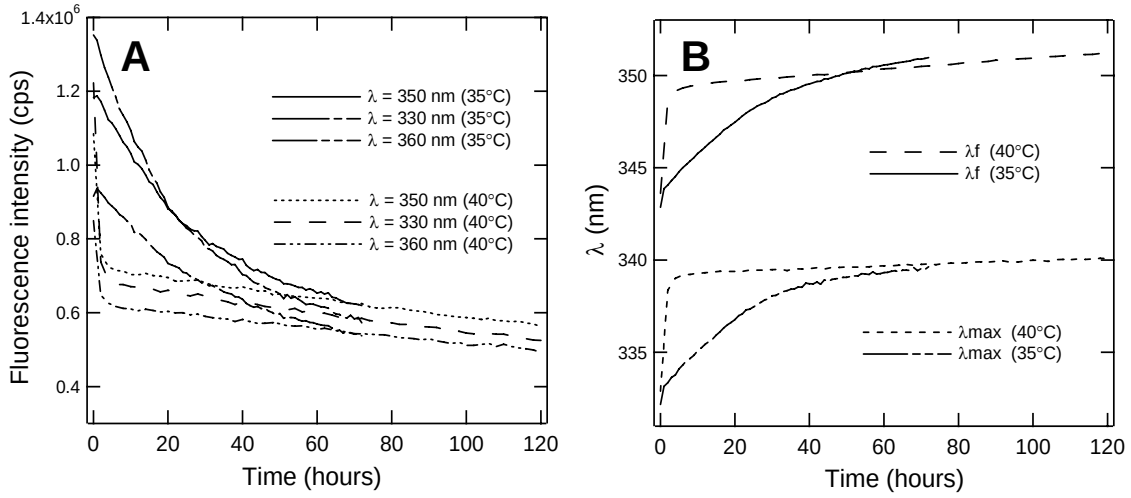

Figure 5.1 Changes in fluorescence intensities (A), and λ (B) of wt-FhuA in 5.5 M urea as a fuction of time at 35 and 40 °C, respectively Denaturation of 0.65 µM wt-FhuA in 5.5 M urea (10 mM Hepes, 2 mM EDTA, 0.1% LDAO, pH 7.0) was monitored by fluorescence spectroscopy as a function of time. 5.5 M urea was chosen because the midpoint of unfolding transition corresponds to this urea concentration, i.e. errors in the calculation of ΔE occur if sample is not in a near stationary state, i.e. with only minor changes in concentration of folded and unfolded FhuA in the transition region. The sample reaches a near stationary state after approximately 72 hours incubation independent of the temperature or of the parameter used to monitor unfolding of wt-FhuA.

indicating that samples reached a near stationary state in which the ratio of folded/unfolded protein remains approximately constant in time (Figure 5.1). We named the calculated energy of unfolding ΔE to distinguish it from $\Delta G°$ for a true equilibrium. The free energy of unfolding ($\Delta G°$) depends linearly on the concentration of the denaturant urea in the

transition region and can be obtained by extrapolation to 0 M urea (see e.g. Pace 1990; Pace et al. 1998):

$$\Delta G^{\circ}_{1\rightarrow 2} = \Delta G^{\circ}_{1\rightarrow 2}\left(\mathrm{H_2O}\right) - m \cdot c\left(\mathrm{urea}\right) \qquad \text{(Eq. 5.7)}$$

$\langle\lambda_1\rangle$ and $\langle\lambda_2\rangle$ were found to depend linearly on the denaturant concentration. Therefore we obtain:

$$\left\langle \lambda_M \right\rangle = \frac{\left(\left\langle \lambda_{1,0} \right\rangle + m_1 \cdot c_D\right) + \left(\left\langle \lambda_{2,0} \right\rangle + m_2 \cdot c_D\right)\frac{1}{Q_R}K}{\left(1 + \frac{1}{Q_R}K\right)} \qquad \text{(Eq. 5.8)}$$

Using relations (5.6), (5.7) and (5.8) leads to

$$\left\langle \lambda_M \right\rangle = \frac{\left(\left\langle \lambda_{1,0} \right\rangle + m_1 \cdot c_D\right) + \left(\left\langle \lambda_{2,0} \right\rangle + m_2 \cdot c_D\right)\frac{1}{Q_R}e^{-\frac{\Delta G^{\circ}(\mathrm{H_2O})}{RT} - m\frac{c_D}{RT}}}{\left(1 + \frac{1}{Q_R}e^{-\frac{\Delta G^{\circ}(\mathrm{H_2O})}{RT} - m\frac{c_D}{RT}}\right)} \qquad \text{(Eq. 5.9)}$$

Assuming that ΔE approximates $\Delta G°$ in our experiments, we used Eq. 5.9 in fits to all unfolding titrations monitored by fluorescence spectroscopy. The linear extrapolations from the pre- and post transition regions of the folded and unfolded states were therefore included in a direct fit of the unfolding titration obtained from the spectroscopic signal $\langle\lambda_M\rangle$ as a function of the denaturant concentration (c_D), where $\langle\lambda_{1,0}\rangle$, $\langle\lambda_{2,0}\rangle$, m_1, and m_2 are the intercepts ($\langle\lambda_{i,0}\rangle$) and slopes ($m_i$) of the pre- (index 1) and post- (index 2) transitional baselines, respectively. These parameters, the energy of the unfolding transition in absence of the denaturant, $\Delta G°(H_2O)$ and the slope m that describes the change in the energy of unfolding as a function of the denaturant concentration (c_D), are fit parameters. The ratio of the total fluorescence intensities is determined from the fluorescence spectra of the folded and unfolded form of the protein and used as a fixed fit parameter.

5.3.8 Temperature dependence of $\Delta G°$ and enthalpy of unfolding

The temperature dependence of $\Delta G°$ is described by a modified form of the Gibbs-Helmholtz equation (c.f. Pace and Scholtz 1997). $\Delta G°(T) = \Delta H° - T\Delta S°$ can be obtained from the unfolding transition at the protein melting temperature (i.e. at the midpoint of the thermal unfolding transition):

$$\Delta G(T) = \Delta H_M - T \cdot \Delta S_M + \int_{E_M}^{E(T)} dE = \left(1 - \frac{T}{T_M}\right)\Delta H_M + \int_{T_M}^{T} dH - \int_{T_M}^{T} TdS - \int_{T_M}^{T} SdT$$

This leads to:

$$\Delta G°(T) = \Delta H_M° \cdot \left(1 - \frac{T}{T_M}\right) - \Delta c_P \left[T_M - T + T \cdot \ln\left(\frac{T}{T_M}\right)\right] \qquad \text{(Eq. 5.10)}$$

In Eq. 5.10, $\Delta G°(T)$ is the free energy of unfolding and Δc_p is the change in heat capacity for the unfolding reaction. T_m is the melting temperature and $\Delta H_M°$ the enthalpy change at the melting temperature. The enthalpy change was then calculated from the temperature dependence of the equilibrium constant using the van't Hoff equation:

$$\frac{d\ln(K)}{d\,1/T} = -\frac{\Delta H°}{R} \qquad \text{(Eq. 5.11)}$$

Here, R is the universal gas constant, K the equilibrium constant, T the temperature and $\Delta H°$ the change in enthalpy. Since we assume that in our experiments the near stationary state approximates the equilibrium of unfolding, $\Delta E(T)$ corresponds to $\Delta G°(T)$ under this assumption.

5.3.9 Folding of wt-FhuA into phospholipid bilayers

CD spectroscopy

20 µl of denatured wt-FhuA (8.7 mg/ml) were mixed with 380 µl of borate buffer (10mM, pH 9.0, with 2 mM EDTA) containing LUVs of *di*$C_{10:0}$PC at a molar lipid/protein

ratio of 1000. Samples were incubated for 24 hrs at 40 °C followed by dialysis at 10 °C. Samples were dialyzed for 12 hrs against 5 l buffer (10 mM borate, 2 mM EDTA, pH 9.0). Dialysis buffer was exchanged 3 times. Dialysis was performed to remove urea, which causes high noise levels in the CD spectra below 205 nm. Far UV CD spectra of 5.5 µM wt-FhuA were recorded on a Jasco 715 CD spectropolarimeter using a 0.5 mm cuvette. Three scans were accumulated and averaged from 195 to 250 nm (209-250 nm in presence of 8 M urea) with a response time of 2 s, a bandwidth of 1 nm, a step resolution of 0.5 nm, a sensitivity of 50 mdeg, and a scan speed of 20 nm/min. Background spectra without wt-FhuA were subtracted for all samples. The recorded CD spectra were normalized to obtain the mean residue molar ellipticity $[\Theta](\lambda)$ according to Eq. 4.1.

Fluorescence spectroscopy

Refolded wt-FhuA: 115 µl refolded wt-FhuA (0.44 mg/ml) in *di*C_{10}PC lipid bilayers at L/P = 1000 mol/mol were mixed to 885 µl of borate buffer (10 mM sodium borate, 2 mM EDTA, pH 9.0).

Denatured wt-FhuA: 5.7 µl denatured wt-FhuA (8.7 mg/ml) in 8 M urea were mixed to 994.3 µl of borate buffer (10 mM sodium borate, 2 mM EDTA, pH 9.0) containing 8 M urea.

Native wt-FhuA: 1.2 µl native wt-FhuA (43.5 mg/ml) in 0.1% LDAO were mixed to 998.8 µl of borate buffer (10 mM sodium borate, 2 mM EDTA, pH 9.0) containing 0.1% LDAO.

Wt-FhuA concentration was 0.64 µM in a volume of 1 ml. Fluorescence spectra were recorded at room temperature on a Spex Fluorolog-3 spectrofluorometer with double monochromators in the excitation and emission pathways. The excitation wavelength was 290 nm, and the bandwidths of the excitation monochromators were 2 nm. The bandwidths of the emission monochromators were 3.7 nm. The integration time was 0.05 s, and an increment of 0.5 nm was used to scan spectra in the range of 300-380 nm. Three scans were averaged for each spectrum.

SDS-polyacrylamide gel electrophoresis

SDS-polyacrylamide gel electrophoresis (SDS-PAGE) (10% acrylamide) was performed as described previously (Kleinschmidt and Tamm 1996; Kleinschmidt and Tamm 2002) using the method of Laemmli (Laemmli 1970) with the modifications described by Weber and Osborne (Weber and Osborne 1964), but without heat

denaturation of the samples, if not specified otherwise. Refolding conditions were same as for CD spectroscopy. 10 µl wt-FhuA (0.43 mg/ml) were mixed with 5 µl treatment buffer before loading samples on SDS-PAGE.

5.4 Results

5.4.1 Fluorescence spectroscopy indicates urea-induced unfolding of detergent solubilized wt-FhuA and FhuAΔ5-160

To monitor unfolding of FhuA solubilized in LDAO-micelles, we first recorded fluorescence spectra of wt-FhuA and FhuAΔ5-160 as a function of the urea concentration.

Emission spectra of wt-FhuA (Figure 5.2A) and FhuAΔ5-160 (Figure 5.2B) taken at concentrations from 0 to 7.5 M urea, indicated a single unfolding transition for both membrane proteins. The transitions were characterized by a strong decrease of the fluorescence intensity and by a red-shift in the wavelength of the fluorescence emission maximum. The intensity weighted average fluorescence emission maxima $\langle\lambda_F\rangle$ (Figure 5.2C) indicated unfolding transitions with midpoints at 6 M urea for wt-FhuA (○) and correspondingly at 2.2 M urea for FhuAΔ5-160 (□). This large difference between the unfolding transitions of the two FhuA variants indicated that deletion of the cork domain has a strong destabilizing effect on FhuAΔ5-160 compared to wt-FhuA.

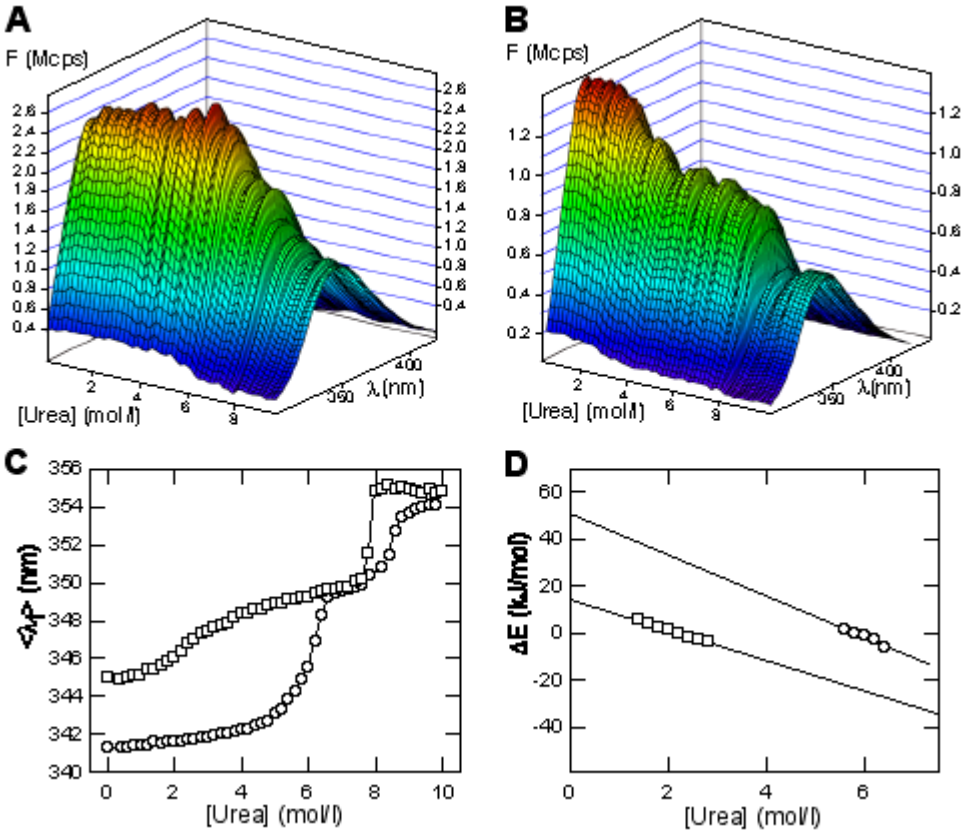

Figure 5.2 Fluorescence spectra of wt-FhuA (A) and FhuAΔ5-160 (B) at selected urea concentrations ranging from 0 to 10 M at 30 °C The intensity weighted average fluorescence emission maxima $\langle\lambda_f\rangle$ of wt-FhuA (○) and FhuAΔ5-160 (□) are shown in panel C. The intensity weighted average emission wavelength $\langle\lambda_1\rangle$ of folded wt-FhuA was 5 nm blue-shifted compared to FhuAΔ5-160, because Trp-21 is not present in FhuAΔ5-160. The unfolding titration was fit to Eq. 5.9 (solid lines). The energies of unfolding (ΔE) calculated for the transition region of unfolding of wt-FhuA and FhuAΔ5-160 depended linearly on the urea concentrations just like the free energy of unfolding ($\Delta G°$) in other studies (D). Both proteins were solubilized in detergent micelles in 10 mM Hepes Buffer at pH 7. The LDAO detergent concentration was 4.4 mM. The protein concentration was 0.64 µM.

5.4.2 CD spectroscopy demonstrates a two-state unfolding of detergent-micelle solubilized wt-FhuA and FhuAΔ5-160

We monitored the urea-induced unfolding of FhuA by circular dichroism to investigate the loss of secondary structure in wt-FhuA and FhuAΔ5-160. Similar to the fluorescence data, the circular dichroism spectra indicated simple two state transitions for both, wt-FhuA and FhuAΔ5-160. Spectra of the fully folded proteins exhibited minima at 218 nm, which are characteristic for β-sheet secondary structure. At high concentrations of urea, spectral lineshapes of wt-FhuA and FhuAΔ5-160 were characteristic for complete

random coil structure in both FhuA variants. The change of the circular dichroism signal at 218 nm was plotted as a function of the urea concentration in Figure 5.3A for wt-FhuA and in Figure 5.3B for FhuAΔ5-160. The midpoints of the two-state unfolding titrations were observed at 6.2 M urea (wt-FhuA) and 2.7 M urea (FhuAΔ5-160).

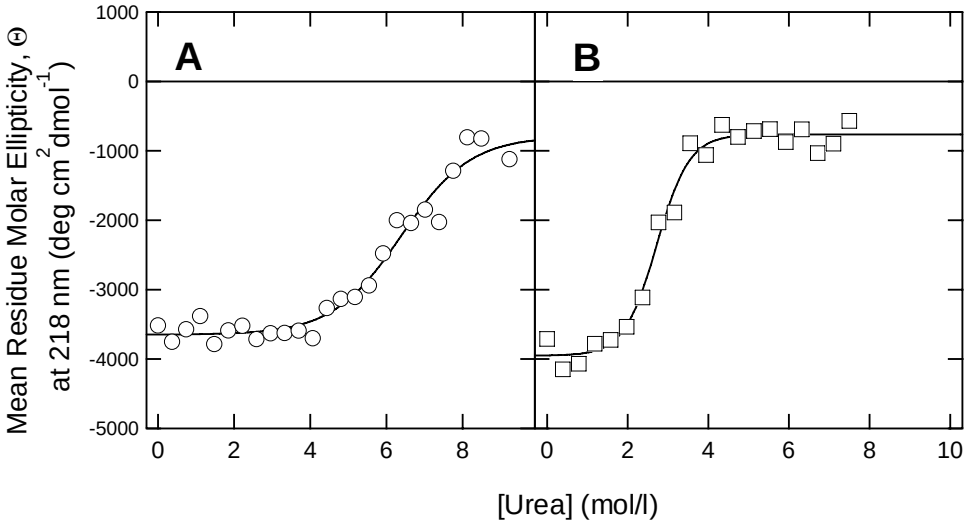

Figure 5.3 Urea-induced unfolding of the β-sheet secondary structure of solubilized wt-FhuA (A) and FhuAΔ5-160 (B) determined by circular dichroism spectroscopy The mean residue molar ellipticity of FhuA was monitored at 218 nm as a function of the urea concentration. The FhuA concentration was 40 μM at a molar LDAO/FhuA ratio of 800 in 10 mM HEPES buffer at pH 7 and at 30 °C, containing 2 mM EDTA.

These transitions correspond both to the first unfolding transitions observed by fluorescence spectroscopy, indicating a two-state unfolding process. This indicates that all protein structure is lost at the urea concentrations correponding to the first unfolding steps that were observed by fluorescence spectroscopy. Both fluorescence and circular dichroism spectroscopy clearly indicate that FhuAΔ5-160 is far less stable than wt-FhuA. Based on the observed two-state unfolding equilibrium, we calculated the energy of unfolding at each urea concentration from the fluorescence data of the first transitions and found a linear dependence on urea concentration (Figure 5.2D) for both wt-FhuA and FhuAΔ5-160. An estimate for the stability of wt-FhuA and FhuAΔ5-160 was calculated using Eq 5.9. The energies of unfolding obtained in this way were $\Delta E = 50 \pm 7$ kJ/mol for wt-FhuA and $\Delta E = 11.9 \pm 0.5$ kJ/mol for FhuAΔ5-160.

5.4.3 The stability of wt-FhuA and FhuAΔ5-160 is strongly temperature dependent

To determine, how the stability of FhuA changes with temperature we performed urea-induced unfolding at temperatures of 35, 40, 45, and 55 °C.

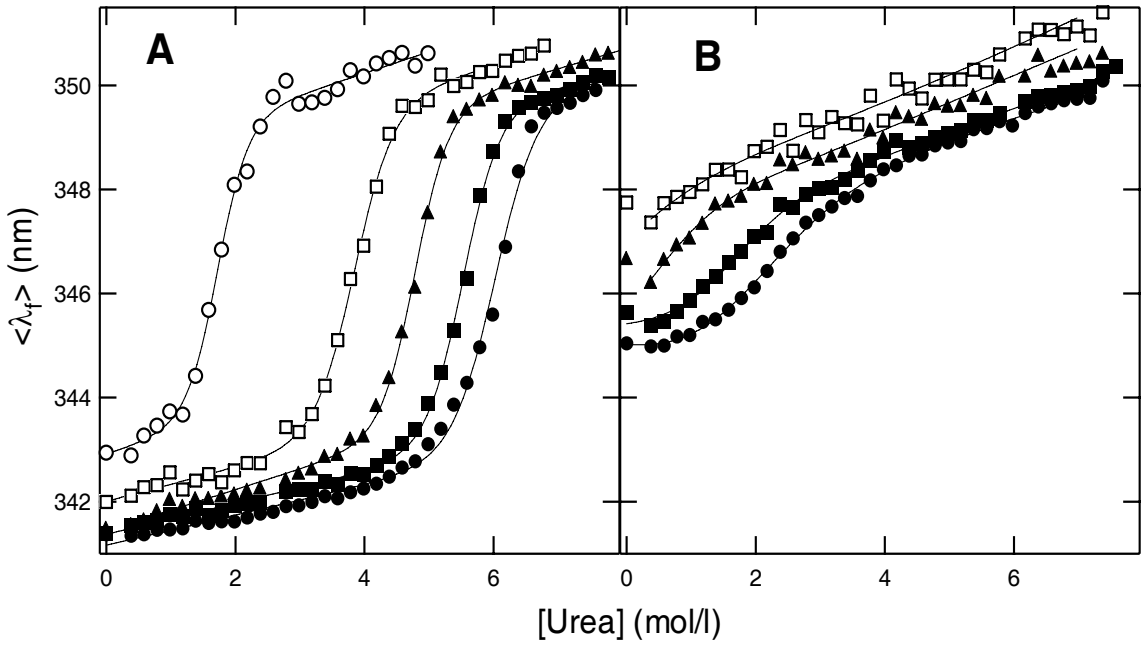

Figure 5.4 Urea-induced unfolding of wt-FhuA (A) and FhuAΔ5-160 (B) at 30 (●), 35 (■), 40 (▲), 45 (□), and 55 (○) °C To monitor unfolding, the intensity weighted average fluorescence emission maximum of each FhuA variant was plotted as a function of the urea concentration at a selected temperature. The data were fit to Eq. 5.11 (solid lines).

The estimated energies of unfolding for both wt-FhuA and FhuAΔ5-160 at different temperatures are presented in Table 5.1.

Table 5.1 Estimated energies of unfolding of wt-FhuA and FhuAΔ5-160 from LDAO micelles

A Wt-FhuA/LDAO		
Temperature (°C)	Δ*E* (kJ/mol)	*m*-value (kJ/mol)
30	45.5 ± 1.6	7.1 ± 0.6
35	44.6 ± 1.5	8.6 ± 0.5
40	44.7 ± 2.4	9.5 ± 0.5
45	34.8 ± 0.2	8.8 ± 0.7
55	18.7 ± 1.2	10.6 ± 1.7
B FhuAΔ5-160/LDAO		
Temperature (°C)	Δ*E* (kJ/mol)	*m*-value (kJ/mol)
30	5.6 ± 1.6	3.5 ± 0.4
35	4.8 ± 2.6	4.4 ± 0.8
C OmpA[a]		
Temperature (°C)	Δ*E* (kJ/mol)	*m*-value (kJ/mol)
30	108.6	
35	87.9	
35	107.9 ± 1.9	12.8 ± 2.2
40	80.0	
45	81.3	
45	80.4 ± 2.2	9.5 ± 0.3
55	59.8	
55	75.9 ± 10.4	9.3 ± 1.4
60	23.1	
60	25.2 ± 2.1	3.5 ± 0.3
65	12.5	
65	9.3 ± 1.4	3.9 ± 0.6

[a]Energies of unfolding of LDAO-solublized outer membrane protein A (OmpA) are listed. These were obtained from equilibrium unfolding experiments performed at the corresponding temperatures at pH 7

5.4.4 The lipid bilayer strongly stabilizes wt-FhuA and FhuAΔ5-160 against urea-induced unfolding

The major aim of our investigation was to compare the stability of an integral membrane protein in detergent micelles and in lipid bilayers. We therefore reconstituted wt-FhuA and FhuAΔ5-160 into bilayers of the lipids dioleoylphosphatidylcholine (DOPC) and dioleoylphosphatidylglycerol (DOPG) at a molar ratio of 6:4. Urea-induced unfolding was again monitored by fluorescence spectroscopy at temperatures of 35, 40, 45, and 55 °C (Figure 5.5).

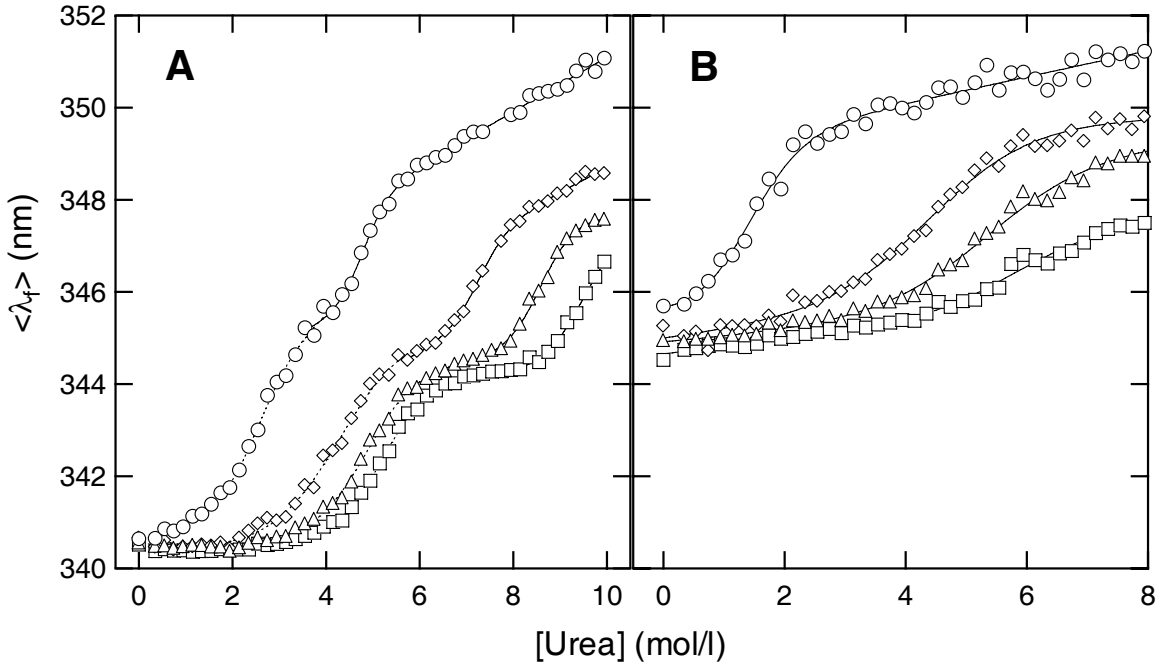

Figure 5.5 Urea unfolding of wt-FhuA (A) and FhuAΔ5-160 (B) after reconstitution into a phospholipid bilayer composed of 60%PG and 40% PC The intensity weighted average emission maxima of the fluorescence spectra were determined as a function of the urea concentration. Unfolding experiments were performed at 35 (□), 40 (Δ), 45 (◊), and 55 (○) °C. Unfolding curves were fit to Eq. 5.9 (solid lines). The lipid concentration was 64 µM. The protein concentration was 0.64 µM.

Unfolding of FhuAΔ5-160 indicated that the lipid bilayer stabilizes FhuAΔ5-160. Midpoints of the unfolding transitions were shifted towards higher urea concentrations of 5.8 M (35 °C), 5.1 M (40 °C), 4.3 M (45 °C), and 1.4 M (55 °C) urea. In comparison to the unfolding of detergent-micelle solubilized membrane protein, the lipid bilayer strongly stabilized FhuAΔ5-160. Further experiments with lipid bilayers of different DOPC/DOPG

composition indicated that this strong stabilizing effect was a lot greater than the dependence of the FhuAΔ5-160 stability on the DOPC/DOPG ratio (Table 5.2).

Table 5.2 Energies of unfolding of wt-FhuA and FhuAΔ5-160 after reconstitution into phospholipids bilayers (PC/PG 40:60)

A Wt-FhuA[a]

	Temperature (°C)	Δ*E* (kJ/mol)	*m*-value (kJ/mol)
(first transition)	35	25.2 ± 1.4	4.8 ± 0.3
	40	19.5 ± 0.6	4.3 ± 0.4
	45	12.9 ± 1.7	3.2 ± 0.6
	55	13.9 ± 4	6.0 ± 2
(second transition)	35	59.6 ± 12	6.3 ± 1.2
	40	57.0 ± 14	6.6 ± 1.7
	45	55.7 ± 13	7.7 ± 1.7
	55	41.0 ± 10	8.7 ± 1.9
B FhuAΔ5-160[a]			
	35	20.8 ± 6	3.9 ± 1.1
	40	14.4 ± 2.8	2.8 ± 0.6
	45	12.3 ± 3	3.8 ± 0.6
	55	6.8 ± 3.9	5.6 ± 1.3

[a]Estimates are based on non-linear least-square fits of the data presented in Figure 5.5 to Eq. 5.9. It should be noted that in some cases the experimental data presented in Figure 5.5 were difficult to fit. As a consequence, in these cases, the Δ*E* data of this table have relatively large errors as indicated.

A comparison of the urea-induced unfolding after solubilization of FhuAΔ5-160 in micelle forming *lyso*-laurylphosphatidylcholine or octadecanoyldimethylammonium-N-oxide confirmed that the hydrophobic chain length or headgroup structure of the lipid or detergent molecule has a smaller effect than the supramolecular organization of the enviroment of FhuAΔ5-160. The major stabilization of FhuAΔ5-160 arises from the bilayer structure.

In comparison to FhuAΔ5-160, wt-FhuA exhibited a two-stage unfolding transition, that was characterized by a first unfolding step with a change in $\langle\lambda_f\rangle$ from 340.5 to 344 nm and a second unfolding step from 344 to 347.6 nm at 40 °C (Figure 5.5A). At this temperature, the unfolding of FhuAΔ5-160 was characterized by a change in $\langle\lambda_f\rangle$ from 344 to 349 nm (Figure 5.5B), which correlated well with the second stage of wt-FhuA unfolding. (Once unfolded, the single Trp-21 that is present in the cork domain, has a

strongly reduced and red-shifted fluorescence intensity. Consequently, the contribution of the stronger fluorescent 8 Trps in the beta barrel domain dominate the fluorescence properties which are then similar to the fluorescence emission of folded FhuAΔ5-160). We therefore conclude that in contrast to detergent solubilized wt-FhuA, lipid membrane incorporated wt-FhuA allows the unfolding of the cork-domain without a concurrent denaturation of the barrel domain, in particular at temperatures below 45 °C.

5.4.5 The lipid bilayer strongly stabilizes FhuA and FhuAΔ5-160 against heat-induced unfolding

We next monitored the heat-induced unfolding of wt-FhuA and FhuAΔ5-160 to confirm our observations on the stability of FhuA in denaturant-unfolding experiments. Figure 5.6 shows the intensity weighted average fluorescence emission maxima of wt-FhuA (●, ○) and FhuAΔ5-160 (■, □) in LDAO micelles and in lipid bilayers. The heat-induced unfolding of FhuAΔ5-160 confirms that the lipid bilayer significantly stabilizes the β-barrel domain of FhuA. Unfortunately, unfolding of FhuA in lipid bilayers could not be monitored to completion because temperatures approached the boiling point of the sample. Therefore, we were only abled to calculate the energies of unfolding for LDAO-solublized wt-FhuA and FhuAΔ5-160. The midpoint of unfolding of detergent-micelle solubilized FhuAΔ5-160 at 52 °C was observed at least 20 °C below the midpoint of unfolding FhuAΔ5-160 after reconsitution into a lipid bilayer, indicating a strong stabilization by the lipid bilayer environment. The experiment also confirmed that the presence of the cork domain in wt-FhuA stabilizes the entire protein. When both variants were solublized in LDAO-micelles, the unfolding of wt-FhuA was characterized by a midpoint of the unfolding at 69 °C, 17 °C above the midpoint of the unfolding of FhuAΔ5-160.

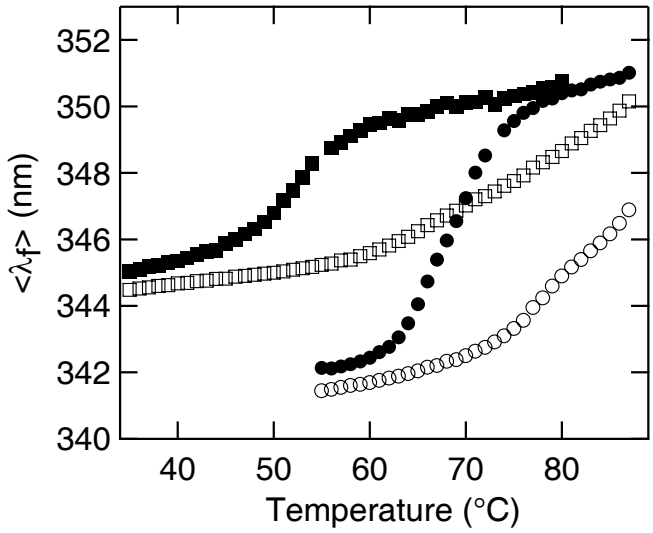

Figure 5.6 Intensity weighted average fluorescence emission of wt-FhuA (●, ○) and FhuAΔ5-160 (■, □) in LDAO micelles (filled symbols) and in lipid bilayers (open symbols) in 10 mM Hepes at pH 7 as a function of temperature The heat-induced unfolding curves of both FhuA variants were fit to Eq 5.9. (solid lines).

5.4.6 Temperature dependence of the energy of unfolding of wt-FhuA and FhuAΔ5-160

We calculated the energies of unfolding of the solubilized forms of wt-FhuA and FhuAΔ5-160 in LDAO micelles at pH 7 from our urea-unfolding experiments at the selected temperatures (Figure 5.4) and from our thermal unfolding experiments (Figure 5.6). The temperature dependence of the energy of unfolding is shown in Figure 5.7A.

Under the assumption that ΔE approximates the free energy of unfolding, $\Delta G°$, we also analyzed our data by plotting ln(K) vs 1/T. The van't Hoff plot of ln(K) vs 1/T was linear and we were therefore able to determine the enthalpy of unfolding with Eq 5.11. Enthalpies of $\Delta H° = 250$ kJ/mol for FhuAΔ5-160 and $\Delta H° = 640$ kJ/mol for wt-FhuA were calculated (Table 5.3).

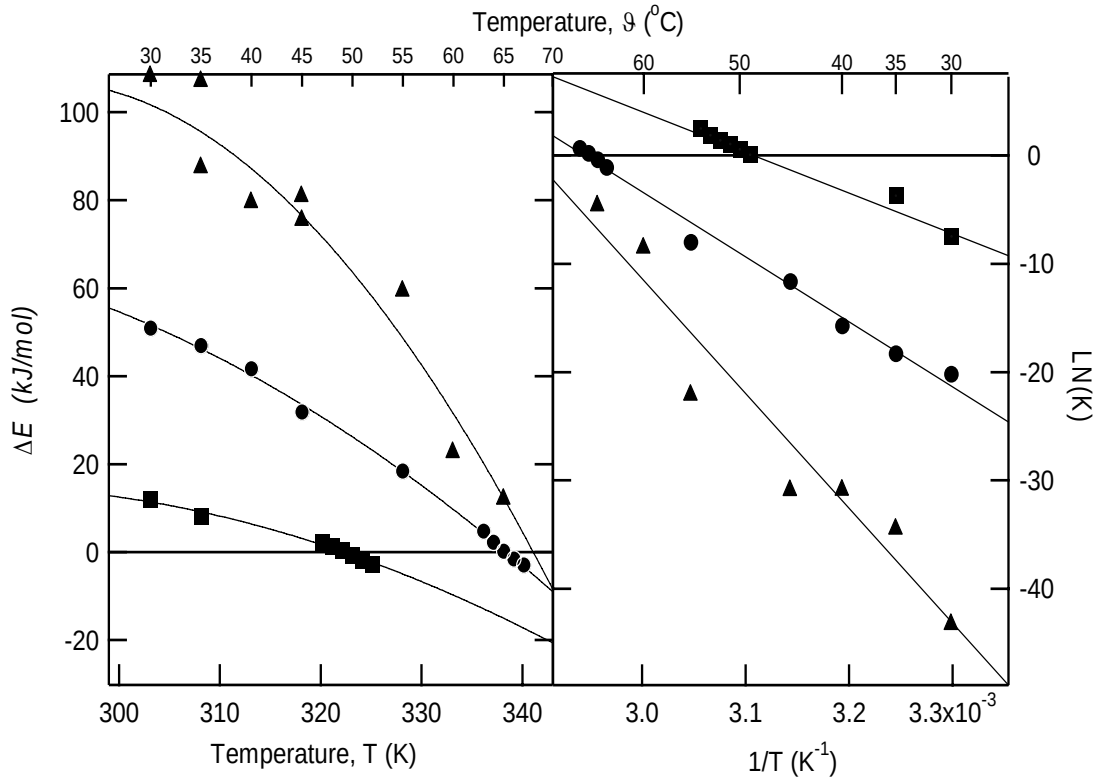

Figure 5.7 **A** The energy of unfolding of OmpA (▲), wt-FhuA (●) and FhuAΔ5-160 (■) solubilized in LDAO as a function of temperature. Δ*E* was calculated using Eq. 5.9 from the urea unfolding experiment presented in Figure 5.2 and from the heat denaturation experiment presented in Figure 5.5 using Eq. 5.3 and 5.4. The temperature depences of Δ*E* were fit to Eq. (5.11) (solid lines). **B** Van't Hoff plot of the data presented in panel **A.**

Table 5.3 Melting temperatures, enthalpies and entropies of unfolding of wt-FhuA, FhuAΔ5-160, and OmpA in LDAO micelles[a]

	T_M (°C)	ΔH_M°(kJ/mol)	ΔS_M° (kJ/mol)	Δc_p
wt-FhuA	65.3 ± 0.2	643 ± 28	9.9	8150 ± 2800
FhuAΔ5-160	49.1 ± 0.4	255 ± 40	0.8	6500 ± 4700
wt-OmpA	67.9 ± 2.5	1467 ± 380	4.3	28044 ± 21000

[a]Estimates are based on non-linear least-square fits of the data presented in Figure 5.7A to equation 5.10 assuming that Δ*E* corresponds to Δ*G*°.

5.4.7 The stability of FhuAΔ5-160 in lipid bilayers is dependent on pH

We were also interested to investigate the stability of FhuAΔ5-160 at selected pH and therefore monitored the urea-induced unfolding of this membrane protein at selected pH values between 3 and 10 (Figure 5.8). We found that the stability of FhuAΔ5-160 strongly depended on the selected pH of the bulk solution. The pH-dependence of the stability of the integral membrane protein was also affected by the composition of the lipid bilayer (Figure 5.9).

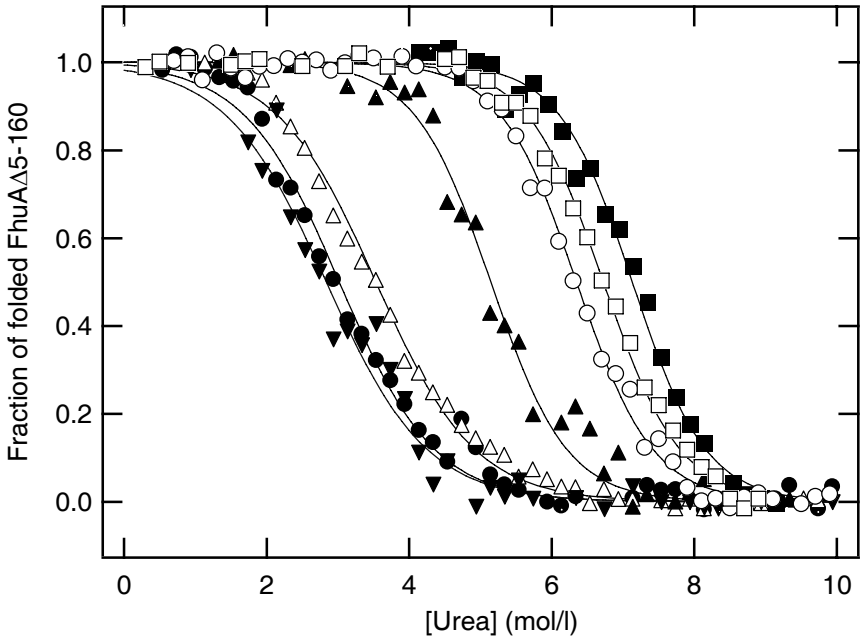

Figure 5.8 Urea-induced unfolding of FhuAΔ5-160 at 40 °C in lipid bilayers at pH 3 (●), pH 4 (○), pH 5 (■), pH 6 (□), pH 7 (▲), pH 8.5 (Δ), and pH 10 (▼) The fraction of folded FhuAΔ5-160 was calculated according to Eq. 5.5 and plotted as a function of the urea concentration. Unfolding curves were fit to a combination of Eqs. 5.6 and 5.7 (solid lines). The lipid bilayer was composed of DOPC and DOPG at a molar ratio of 2/3. The molar lipid/protein ratio was 100 at a protein concentration of 0.64 μM.

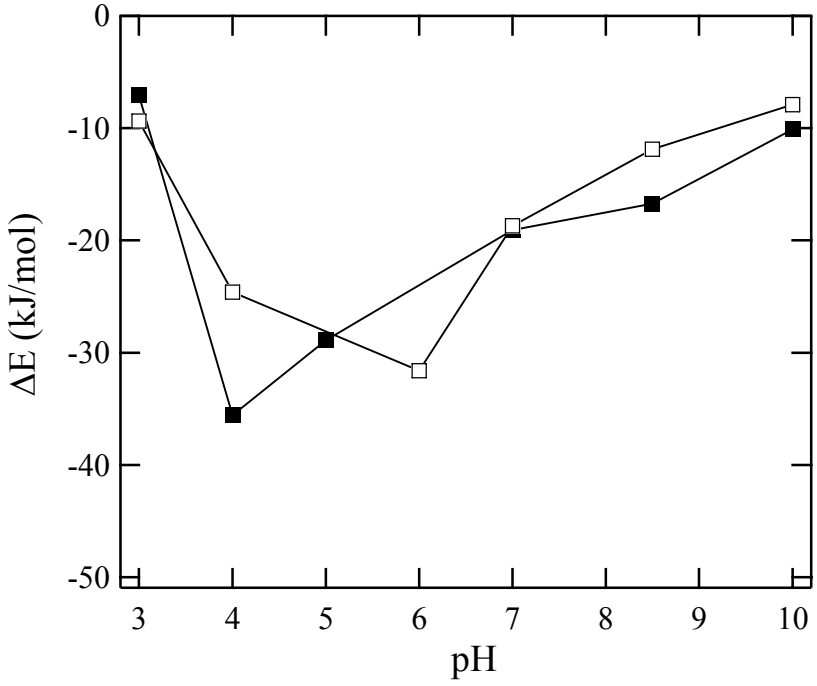

Figure 5.9 The energies of the urea-induced unfolding of FhuAΔ5-160 at 40 °C as a function of pH FhuAΔ5-160 was reconsituted into lipid bilayers composed of DOPC and DOPG at molar ratios of 4/6 (□) and 9/1 (■). The energies of unfolding were calculated according to Eqs. 5.5 and 5.6 from the unfolding titrations shown in Figure 5.8.

5.4.8 The stability of FhuAΔ5-160 is dependent on the chain length of the lipid bilayer

The urea-induced unfolding of FhuAΔ5-160 was monitored as a function of the hydrophobic thickness of the lipid bilayer and of the micelle-forming phospholipids, respectively. Figure 5.10 shows the intensity weighted average fluorescence emission maxima of FhuAΔ5-160 in lipid bilayers (A) and in micelles (B). The midpoints of the unfolding transitions were located between 3 M urea for FhuAΔ5-160 reconstituted into *di*$C_{10:0}$PC (Figure 5.10, A (●)) and 6 M urea for FhuAΔ5-160 reconstituted into *di*$C_{15:0}$PC (Figure 5.10, A (□)) lipid bilayers. Instead, the midpoints of the unfolding transitions of FhuAΔ5-160 reconstituted into *lyso*C_nPC (Figure 5.10 B) were only between 2 and 3 M urea suggesting a less stable FhuAΔ5-160 in phospholipids micelles.

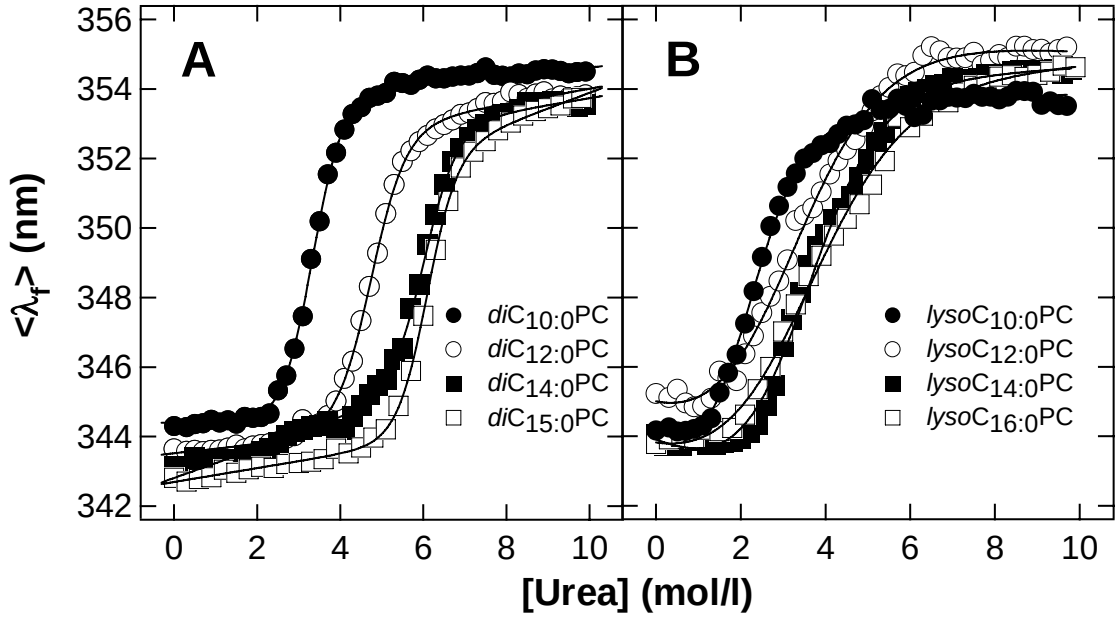

Figure 5.10 Urea-induced unfolding of FhuAΔ5-160 after reconstitution into phospholipid bilayers (A) and detergent micelles (B) of different hydrophobic thicknesses. Intensity weighted average fluorescence emission maxima $\langle\lambda_f\rangle$ were plotted as a function of urea concentration. Samples were measured after 72 hours incubation at 35 °C.

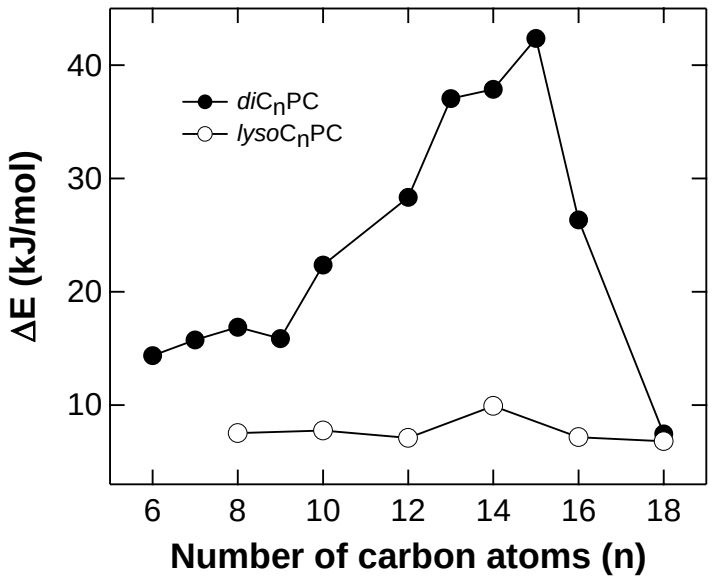

Figure 5.11 Energies of unfolding of FhuAΔ5-160 after reconstitution into phospholipid bilayers (●) and detergent micelles (○) of different hydrophobic thicknesses. Samples were measured after 72 hours incubation at 35 °C.

Equation 5.9 was used here to fit all unfolding titrations monitored by fluorescence spectroscopy and the calculated ΔE were plotted as a function of chain lengths (Figure

5.11). The stability of FhuAΔ5-160 in micelles of *lyso*C_nPC was very low (approximately 7 kJ/mol) and not dependent on the acyl chain length. The stability of FhuAΔ5-160 in lipid bilayers strongly depended on the length of the hydrophobic chains with a maximum at n = 15 (ΔE = 42.4 kJ/mol). The obtained ΔE values are presented in table 5.4.

Table 5.4 Estimated energies of unfolding of FhuAΔ5-160 from bilayers and micelles of different hydrophobic thicknesses.

A *di*C_nPC

n	L/P (mol/mol)	ΔE (kJ/mol)
6	23000	14.4 ± 1.8
7	14000	15.7 ± 2.5
8	10000	16.9 ± 1.5
9	6000	15.9 ± 1.3
10	1000	22.4 ± 0.7
12	100	28.3 ± 1.0
13	100	37.0 ± 1.9
14	100	37.9 ± 1.4
15	100	42.4 ± 1.1
16	100	26.3 ± 1.7
18	100	7.4 ± 2.0

B *lyso*C_nPC

n	L/P (mol/mol)	ΔE (kJ/mol)
8	40000	7.5 ± 1.1
10	40000	7.7 ± 0.9
12	20000	7.1 ± 0.5
14	1300	9.9 ± 0.6
16	1300	7.2 ± 0.6
18	1200	6.8 ± 0.9

5.4.9 The stability of FhuA is dependent on the lipid headgroup charge

We reconstituted wt-FhuA and FhuAΔ5-160 into bilayers of the lipids dioleoylphosphatidylcholine (DOPC) and dioleoylphosphatidylglycerol (DOPG) at different molar ratios ranging from 0 to 100 and a L/P of 100 mol/mol. Urea-induced unfolding was again monitored by fluorescence spectroscopy at 35 °C (Figure 5.12).

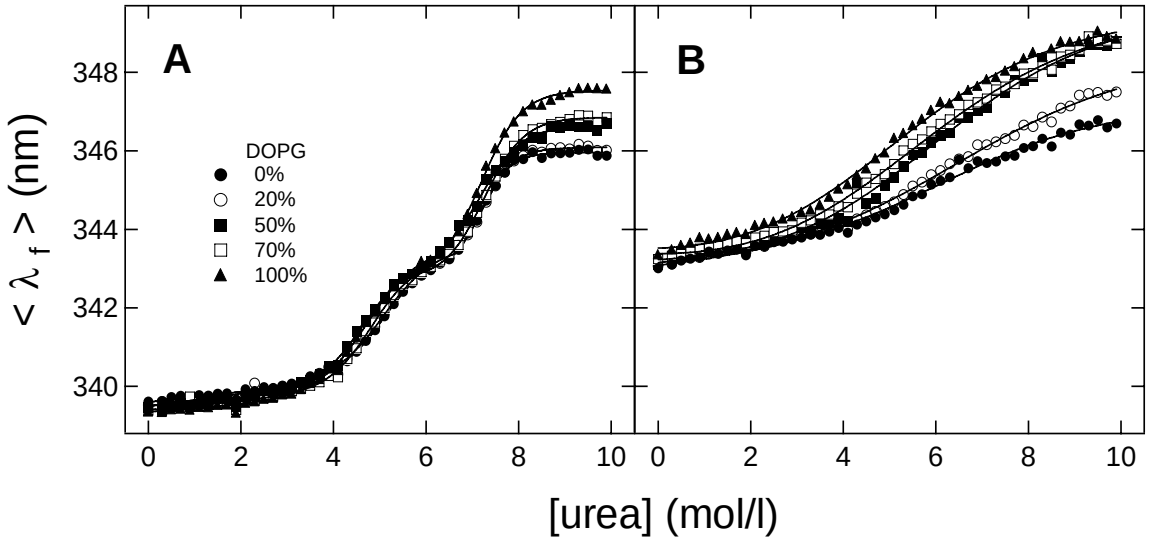

Figure 5.12 Urea unfolding of wt-FhuA (A) and FhuAΔ5-160 (B) after reconstitution into phospholipid bilayers composed of DOPG and DOPC at different molar ratios The intensity weighted average emission maxima of the fluorescence spectra were determined as a function of the urea concentration. Unfolding experiments were performed at 35 °C. Unfolding curves were fit to Eq. 5.9 (solid lines). The lipid concentration was 64 μM. The protein concentration was 0.64 μM.

Wt-FhuA unfolded in 2 steps, first with a midpoint at 4.5 M urea and the second at 7.5 M urea while FhuAΔ5-160 unfolded in a single step with midpoints around 5.5 M urea for lipid bilayers with low content of the negatively charged DOPG and around 4.5 M urea for lipid bilayers containing mostly DOPG, respectively.

Equation 5.9 was used here to fit all unfolding titrations showed in Figure 5.12 and the calculated ΔE were plotted as a function of DOPG content of the lipid bilayer (Figure 5.13).

The stabilities calculated from the second unfolding transition of wt-FhuA - which corresponded to the unfolding of the barrel domain - were strongly dependent on the lipid headgroup charge. Although not so pronounced for the unfolding of the cork domain of wt-FhuA or for the unfolding of FhuAΔ5-160, the general tendency was a decrease in the stability of these proteins with increasing the concentration of negatively charged DOPG and concomitant decrease in concentration of the zwitterionic DOPC. The obtained ΔE values are showed in Table 5.5.

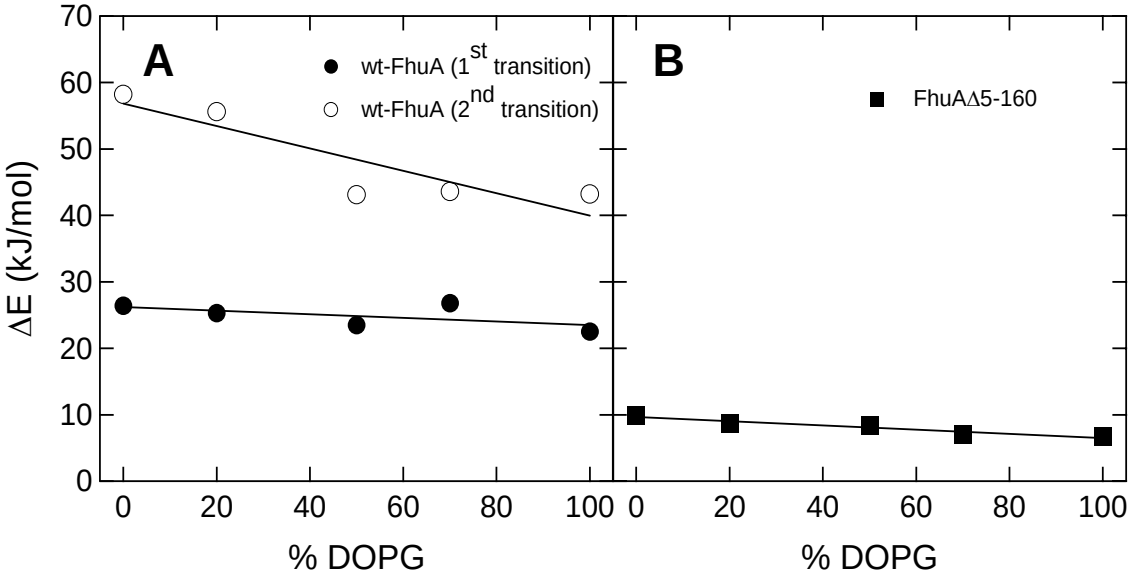

Figure 5.13 Energies of unfolding of wt-FhuA (A) and FhuAΔ5-160 (B) as a function of lipid headgroup charge The unfolding titrations shown in Figure 5.11 were fitted to Eq. 5.9 (solid lines). The energies of unfolding were calculated for the transition regions of unfolding of wt-FhuA and FhuAΔ5-160. The lipid concentration was 64 μM. The protein concentration was 0.64 μM.

Table 5.5 Estimated energies of unfolding of wt-FhuA and FhuAΔ5-160 from bilayers of different phospholipid composition.

A Wt-FhuA

DOPC/DOPG (mol/mol)	ΔE_1 (kJ/mol)	ΔE_2 (kJ/mol)
100/0	26.4 ± 1.2	58.2 ± 3.6
80/20	25.3 ± 2.1	55.6 ± 2.7
50/50	23.5 ± 1.6	43.1 ± 0.2
30/70	26.8 ± 2.0	43.6 ± 1.7
0/100	22.5 ± 1.4	43.2 ± 2.1

B FhuAΔ5-160

DOPC/DOPG (mol/mol)	ΔE (kJ/mol)
100/0	9.9 ± 1.9
80/20	8.7 ± 1.0
50/50	8.4 ± 1.0
30/70	7.0 ± 0.5
0/100	6.7 ± 0.4

5.4.10 Wt-FhuA folds into phospholipid bilayers

We discovered that wt-FhuA folds in lipid bilayers, when the denaturant urea is strongly diluted in presence of LUVs of *di*$C_{10:0}$PC. Evidence for folding was obtained with

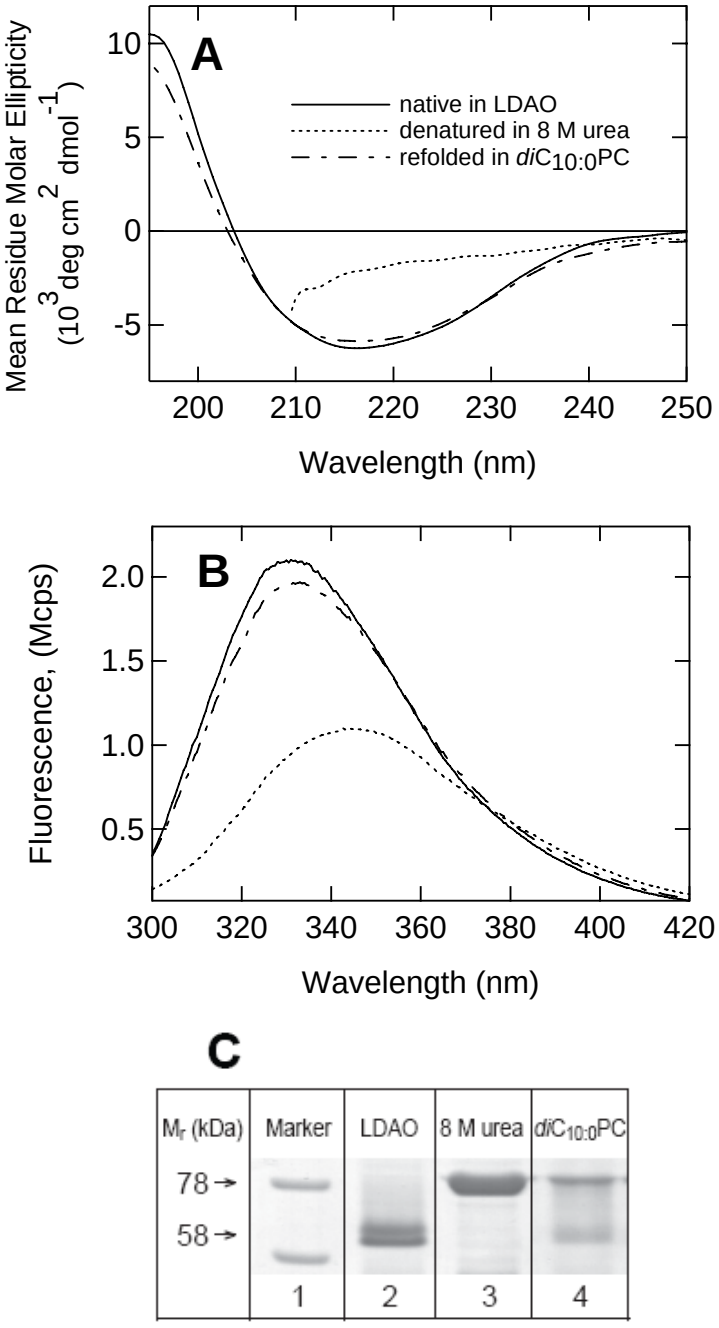

Figure 5.14 Circular dichroism, fluorescence spectra and SDS-PAGE indicate membrane insertion and β-sheet secondary structure formation in wt-FhuA A Circular dichroism and **B** Fluorescence spectra of wt-FhuA in unfolded form in 8 M urea (-------), in native form in 0.1%

LDAO (———), and after refolding in *di*$C_{10:0}$PC vesicles (—-—-—-). Background spectra without wt-FhuA were subtracted. **C** SDS-Polyacrylamide gels of wt-FhuA folding into *di*$C_{10:0}$PC lipid bilayers at 40 °C (lane 4). 40% folding yields were obtained as determined by densitometric analysis of the bands. The arrows indicate the electrophoretic migration of the native purified (lane 2) and unfolded (lane 3) forms of wt-FhuA. The wt-FhuA concentration was 5.5 µM in a volume of 400 µl (A) and 10 µl (C) and 0.64 µM in a volume of 1 ml (B), respectively. Samples were incubated at 40 °C for 24 hrs prior to recording of spectra. Spectra were recorded at room temperature in 10 mM borate, 2 mM EDTA, pH 9.0, in all CD and fluorescence experiments. Except for wt-FhuA samples in 8 M urea, residual urea was removed by dialysis.

a range of different methods. We first examined the secondary structure of wt-FhuA under different conditions and recorded circular dichroism spectra of native and unfolded form in 8 M urea and after dilution of urea in presence of LUVs of *di*$C_{10:0}$PC, (Figure 5.14A). The CD spectrum of denatured wt-FhuA in 8 M urea was typical for a random coil structure. The CD spectrum of the native form of wt-FhuA indicated predominantly β-sheet secondary structure. After reacting unfolded wt-FhuA with LDAO or with LUVs of *di*$C_{10:0}$PC, the CD spectra of wt-FhuA indicated a high content of β-sheet secondary structure and had the typical line-shape expected for β-barrel integral membrane proteins.

These spectra were nearly identical. A detailed analysis of the CD spectra was performed using DICHROWEB (Lobley et al. 2002; Whitmore and Wallace 2004), using different algorithms (Provencher and Glockner 1981; Compton and Johnson 1986; Manavalan and Johnson 1987; van Stokkum et al. 1990; Andrade et al. 1993; Sreerama and Woody 1993; Sreerama et al. 1999; Sreerama and Woody 2000) The results are summarized in Table 5.6.

Table 5.6 Analysis of CD spectra of FhuA using different methods

Environment coil	Method	α - helix (%)	β - strand (%)	turn (%)	β - sheet (%)	random (%)
LDAO (native)	Contin	8.1	40.8	16.6	-	34.5
	Selcon3	8	40.4	17.7	-	33.9
	CDSSTR	10.9	36.6	22.8	-	29.7
	K2D[1,2]	21	-	-	30	49
di$C_{10:0}$PC (refolded)	Contin	13.5	34.8	22.4	-	29.3
	Selcon3[2]	10.9	37.1	21.8	-	29.2
	CDSSTR	12	35	23	-	30
	K2D[1,2]	21	-	-	30	49

[1] K2D does not distinguish between β - strands and turns
[2] result not reliable

Fluorescence spectra of native, unfolded and refolded wt-FhuA were recorded at 35 °C (Figure 5.14B). Fluorescence spectra of native and refolded wt-FhuA in LUVs of *di*$C_{10:0}$PC had an intensity maximum at 328 nm, while the spectra of urea-unfolded wt-FhuA had a maximum at 347 nm.

Wt-FhuA folding into LUVs of *di*$C_{10:0}$PC was investigated by SDS-polyacrylamide gel electrophoresis (Figure 5.14C), without heat-denaturing the samples prior to electrophoresis. Denatured wt-FhuA migrated at 78 kDa (Lane 3) and native and refolded wt-FhuA in LUVs of *di*$C_{10:0}$PC migrated at 58 kDa.

5.5 Discussion

A requirement for calculating a free energy of unfolding ($\Delta G°$) is that the folding and unfolding reactions have reached equilibrium. Since for our model (FhuA) reversibility of folding could not be fully demonstrated i.e. we were unable to refold FhuA completely, we monitored FhuA unfolding in urea as a function of time by fluorescence spectroscopy. We observed that after approximately 72 hours incubation FhuA the unfolding transition did not shift to lower urea concentrations. This indicated that samples reached a near stationary state in which the ratio of folded/unfolded protein remained approximately constant in time. By fitting the unfolding titrations using Eq. 5.9 we were able to calculate the energy of unfolding on FhuA. We named the calculated energy of unfolding ΔE to distinguish it from $\Delta G°$ for a true equilibrium. Under the same assumption that ΔE approximates $\Delta G°$ we calculated $\Delta H°$ and Δc_p from our unfolding experiments.

In the present work, we have shown that the stability of two variants of the integral membrane protein FhuA is greatly reduced after extraction into detergent micelles. Our results also demonstrate that while the unfolding of wt-FhuA from the bilayer integrated state takes place in two steps, this protein unfolds in a single step from LDAO detergent micelles.

It is interesting to compare the stability of wt-FhuA in lipid bilayers and LDAO micelles with the stability of wt-FhuA in Triton-X-100 detergent investigated in an earlier study (Bonhivers et al. 2001). Bonhivers et al. found a two-state unfolding transition of wt-FhuA by differential scanning calorimetry (DSC). In DSC experiments on the unfolding of wt-FhuA solubilized in Triton-X-100, the two unfolding transitions overlapped partially and were characterized by maxima at 65 and at 75 °C. According to these earlier DSC data,

the unfolding of wt-FhuA in Triton-X-100 was completed at 80 °C. In our experiments, thermal unfolding of wt-FhuA depended strongly on the environment of the integral membrane protein. In LDAO-micelles, unfolding was completed at 78 °C, whereas the unfolding of bilayer integrated wt-FhuA did not complete until well above 90 °C (Figure 5.6). In comparison to our study with FhuAΔ5-160, the earlier study compared wt-FhuA with a mutant lacking residues 22-127 (Table 5.6).

FhuAΔ22-127 solubilized in Triton-X-100 showed a single unfolding transition in DSC, characterized by a maximum at 62 °C that was completed at 70 °C. In this study LDAO solubilized FhuAΔ5-160 completed unfolding at 60 °C, but bilayer inserted FhuAΔ5-160 remained completely folded at 60 °C and denatured only very slowly. Unfolding of bilayer inserted FhuAΔ5-160 did not complete until 90 °C. In summary, the comparison shows that Triton-X-100 is favorable over LDAO as a detergent for keeping FhuA stable in solution. However, extraction of FhuA into Triton-X-100 still destabilizes the protein in comparison to a lipid bilayer environment.

Table 5.7 Enthalpies and heat capacities obtained in this study compared to previous results

This study	
in LDAO	
wt-FhuA	$\Delta H°$ = 640 KJ/mol (single transition, in LDAO) van't Hoff
FhuA Δ5-160	$\Delta H°$ = 250 KJ/mol (single transition in LDAO) van't Hoff
wt-FhuA	$\Delta H_M°$ = 644 ± 28 KJ/mol (single transition, in LDAO) direct
	Δc_p =8.1 ± 1.7 kJ/mol/K
FhuAΔ5-160	$\Delta H_M°$= 255 ± 40 KJ/mol (single transition in LDAO) direct
	Δc_p = 6.5 ± 5 kJ/mol/K
in DOPC/DOPG 60:40	
wt-FhuA	$\Delta H°$ = 355 kJ/mol (cork) ; $\Delta H°$ = 632 kJ/mol (barrel) van't Hoff
	sum = 987 kJ/mol
FhuAΔ5-160	$\Delta H°$ = 342 kJ/mol (single transition) van't Hoff
(Bonhivers et al. 2001)	
wt-FhuA	$\Delta H°$ = 598 KJ/mol (transition 1) and 670 kJ/mol (transition 2)
	(Triton)
FhuAΔ22-127	$\Delta H°$ = 836 kJ/mol (Triton)

Initial studies to investigate outer membrane protein stability were performed with the 22-stranded iron siderophor receptors FepA (Klug et al. 1995; Klug and Feix 1998) and FhuA(Bonhivers et al. 2001; Plancon et al. 2002). Feix and coworkers investigated the stability of spin-labeled single site cysteine mutants of FepA in Triton-X 100 detergent micelles by monitoring urea and guanidinium chloride induced unfolding. They determined a free energy for FepA unfolding to about 6.2 kcal/mol (26.5 kJ/mol) at 22°C and pH 7.2 with an equilibrium transition midpoint at 5.5 M urea. Bonhivers et al. (Bonhivers et al. 2001) investigated the thermal stability of FhuA in LDAO micelles in absence and in presence of ferrichrom iron by differential scanning calorimetry and circular dichroism spectroscopy. They also investigated the thermal denaturation of a FhuA variant (FhuAΔ21-128), in which 108 residues of the 160 residue N-terminal cork domain were removed and found. The stability of FhuA in micelles increased upon ligand binding. Thermal unfolding of wt-FhuA by calorimetry was characterized by two transitions centered at 65 and 74.4 °C with enthalpies of 598 and 670 kJ/mol, while FhuAΔ21-128 displayed a single transition at 61.6 °C with an enthalpy of 836 kJ/mol. Circular dichroism spectroscopy indicated that most secondary structure of wt-FhuA was lost at temperatures above 72 °C, corresponding to the second transition observed in calorimetry.

Our results on the stability of FhuA in lipid bilayers of different composition of the headgroup suggest an increase in the stability of FhuA in bilayers containing the zwitterionic PC and a destabilization in presence of the negatively charged PG. Recently, the same effect was obtained on the example of OmpA (Hong and Tamm 2004) indicating that this might be a characteristic feature of β-barrel membrane proteins.

6 Association of spin-labelled lipids with β-barrel proteins from the outer membrane of *Escherichia coli*

6.1 Abstract

The interaction of spin-labelled lipids with β-barrel transmembrane proteins has been studied by electron spin resonance (ESR) methods developed for α-helical integral proteins. The outer membrane protein OmpA and the ferrichrome-iron receptor FhuA from the outer membrane of *Escherichia coli* were reconstituted in bilayers of dimyristoyl phosphatidylglycerol. The ESR spectra from phosphatidylglycerol spin-labelled on the 14-C atom of the *sn*-2 chain contain a second component from motionally restricted lipids contacting the intramembranous surface of the β-barrel, in addition to that from the fluid bilayer lipids. The stoichiometry of motionally restricted lipids, 11 and 32 lipids/monomer for OmpA and FhuA, respectively, is constant irrespective of lipid/protein ratio. It is proportional to the number of transmembrane β-strands, eight for OmpA and 22 for FhuA, and correlates well with the intramembranous perimeter of the protein. Spin-labelled lipids with different polar headgroups display a differential selectivity of interaction with the two proteins. The more pronounced pattern of lipid selectivity for FhuA than for OmpA correlates with the preponderance of positively charged residues facing the lipids in the extensions of the β-sheet and shorter interconnecting loops, on the extracellular side.

6.2 Introduction

Because of the favourable timescale of electron spin resonance (ESR) spectroscopy, ESR spectra of spin-labelled lipids have proved a particularly useful means for studying lipid interactions with transmembrane proteins (see e.g. ref. Marsh 1989). Spectra are resolved from the lipids interacting directly with the intramembranous surface of the protein. This allows determination of the stoichiometry and selectivity of the lipid-protein

interaction, and also the rate of exchange at the lipid-protein interface (Marsh and Horváth 1989). Lipid-protein interactions with a large range of integral proteins have been studied in this way, but so far these studies have been confined to α-helical proteins (Marsh and Horváth 1998; Marsh and Páli 2004). The sole exceptions are the β-sheet configurations of certain transmembrane peptides (Wolfs et al. 1989; Horváth et al. 1995; Horváth et al. 1997). So far, no such studies have been undertaken with the β-barrel proteins that are characteristic for the outer membranes of Gram-negative bacteria and of mitochondria. There are grounds to expect that lipid interactions with β-barrel proteins might differ from those with α-helical proteins. A β-barrel protein presents a rather different pattern of hydrophobic side chains to the lipids than do polytopic α-helical proteins. Also, the hydrophobic span of β-barrel outer membrane proteins is considerably shorter than those typical of α-helical proteins (Lee 2003).

In the present work, we describe spin-label ESR studies of lipid interactions with two β-barrel proteins from the outer membrane of *E. coli* that are reconstituted in bilayer membranes of the anionic lipid dimyristoyl phosphatidylglycerol. One of the proteins studied is the outer membrane protein OmpA, which is an eight-stranded β-barrel (Pautsch and Schulz 2000), and the other is the ferrichrome-iron receptor FhuA, which is a much larger 22-stranded β-barrel (Ferguson et al. 1998). Both proteins are monomeric and therefore the whole of the external surface of the barrel is expected to contact lipid. Lipid-protein interactions with the β-barrel proteins are detected by suitably spin-labelled lipids and are found to have stoichiometries and selectivities that correlate well with the 3-D structures of the two proteins.

6.3 Materials and methods

6.3.1 Materials

E. coli strain P.400, expressing wild-type OmpA was a generous gift from Dr. Ulf Henning, Tübingen. Wild-type OmpA was isolated and purified from the *E. coli* outer membrane in the unfolded form in 8 M urea, as previously described (Surrey and Jähnig 1992). *E. coli* strain BL21(AW740) carrying plasmid pHx405 and expressing wild-type FhuA was a generous gift from Dr. Wolfram Welte, Konstanz. His6-tagged wild-type

FhuA was extracted from *E. coli* outer membranes, and isolated and purified in *N*-lauroyl-*N*,*N*-dimethylammonium-*N*-oxide (LDAO) detergent micelles, without unfolding, as described (Ferguson et al. 1998). Phospholipids, dimyristoyl phosphatidylglycerol (DMPG) and dimyristoyl phosphatidylcholine (DMPC), were obtained from Avanti Polar Lipids (Alabaster, AL). Spin-labelled stearic acid, 14-SASL, was synthesized according to Hubbell and McConnell (Hubbell and McConnell 1971). Spin-labelled phosphatidylcholine, 14-PCSL, was synthesized by acylation of lysophosphatidylcholine with 14-SASL, as described in Marsh and Watts (Marsh and Watts 1982). Other spin-labelled phospholipids, 14-PGSL, 14-PSSL, 14-PESL and 14-PASL, were prepared from 14-PCSL by headgroup exchange mediated by phospholipase D (Marsh and Watts 1982). Spin-labelled phosphatidylinositol, 14-PISL, was prepared according to ref. (Somerharju and Wirtz 1982) as described in ref. (Mantipragada et al. 2003). All other chemicals were from Sigma Chemical Co. (St. Louis, MO).

Unfolded OmpA was refolded into detergent micelles as described (Kleinschmidt et al. 1999). Briefly, 500 µl of a 42 mg/ml solution of unfolded OmpA in 10 mM borate, 2 mM EDTA, pH 10 buffer that contained 8 M urea was diluted 20-fold with the borate buffer and mixed with an 800-fold molar excess of LDAO detergent. The mixture was incubated overnight at 40^{o}C to ensure complete refolding of the protein. Refolding was carried out at pH 10 because a yield of close to 100% was achieved at this pH-value (Kleinschmidt et al. 1999). Sample purity and folding were monitored by SDS polyacrylamide gel electrophoresis according to the method of Laemmli et al. (Laemmli 1970).

6.3.2 Reconstitution into membranes

Phospholipid solutions containing 1 mol% of the desired spin-labelled lipid were prepared in $CHCl_3$ and dried under a stream of dry nitrogen gas. The resulting lipid film was desiccated overnight under vacuum and then covered with argon. The dry lipid film was hydrated with 10 mM Hepes, 2 mM EDTA buffer, pH 7.0, and frozen (in liquid nitrogen) and thawed (in a water bath at ~5^{o} above the transition temperature of the phospholipid) seven times, to obtain uniform lipid vesicles. The reconstitution was carried out by mixing 1 mg of the above lipid vesicles with protein to the desired lipid-protein ratio, and then 10% sodium cholate solution was added to give a final concentration of

0.2% sodium cholate, in a total volume of 500 µl. The sample was mixed well and incubated at room temperature for 1 hour, vortexing from time to time. After 1 hour incubation, the protein was precipitated with 52.5% ammonium sulfate solution that was added to achieve 35% final concentration. The pellet containing the reconstituted protein was then centrifuged for 30 minutes at 35000 rpm in a Beckman 50TI rotor.

Initial lipid/protein ratios were determined after ammonium-sulfate precipitation by using the methods (Rouser et al. 1970) and (Lowry et al. 1951), for lipid and protein, respectively. After this, the samples were adjusted to the required lipid/protein ratio by adding appropriate quantities of solubilised lipid vesicles. The pellet was dissolved and vortexed in 500 µl 10 mM Hepes buffer pH 7.0, containing 2 mM EDTA and 250 mM NaCl. Detergent removal was achieved by extensive dialysis at 8°C against 10 mM Hepes buffer pH 7.0 containing 2 mM EDTA and 250 mM NaCl, using 10-kDa cut-off dialysis membranes. Final lipid/protein ratios were determined after ESR spectroscopy.

6.3.3 Electron spin resonance spectroscopy

ESR spectra were recorded on a 9-GHz Bruker EMX EPR spectrometer, with model ER 041 XK-D microwave bridge. Samples were placed in 50 µl glass capillaries and flame sealed. The capillaries were placed in a standard 4-mm quartz sample tube containing light silicone oil for thermal stability. The temperature of the sample was maintained constant by blowing thermostatted nitrogen gas through a quartz dewar. Spectra were recorded using the following instrumental settings: sweep width, 100 G; resolution, 1024 points; time constant, 20.48 ms; sweep time, 41.9 s; modulation frequency, 100 kHz; modulation amplitude, 1.0 G; incident power, 5 mW. Spectral subtraction and integration was performed as described in Marsh (Marsh 1982). Spectral reference libraries for the fluid and motionally restricted components were obtained from 14-PCSL in egg phosphatidylcholine dispersions and in sonicated DMPC small unilamellar vesicles, respectively, at various temperatures.

6.4 Results

6.4.1 OmpA reconstituted in DMPG

Figure 6.1 shows the ESR spectra of spin-labelled phosphatidylglycerol, 14-PGSL, in reconstituted membranes of dimyristoyl phosphatidylglycerol (DMPG) containing OmpA at different lipid/protein ratios. The spectra are recorded at 30°C, which is above the chain-melting transition of DMPG bilayers.

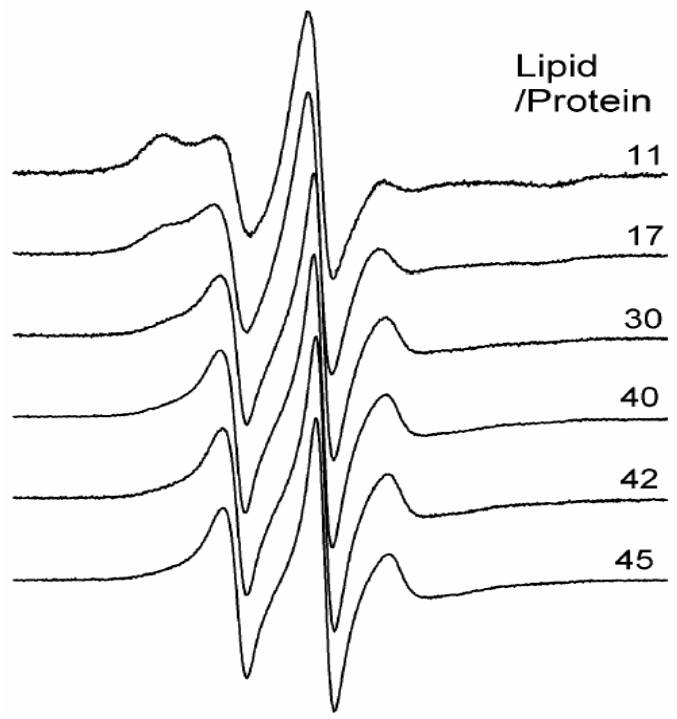

Figure 6.1 ESR spectra of phosphatidylglycerol spin labelled on the 14-C atom of the *sn*-2 chain (14-PGSL) in dimyristoyl phosphatidylglycerol membranes containing OmpA at the lipid/protein mole ratios indicated in the figure. T = 30 °C; total scan width = 100 gauss.

Figure 6.2 shows the transition curves for a sample with lipid/protein ratio 30:1 mol/mol, as registered by the central peak in the ESR spectra. This confirms that the OmpA/DMPG membranes are in the fluid phase at 30 °C.

The spin label is positioned at the 14-C atom of the *sn*-2 chain and gives rise to relatively sharp three-line spectra in fluid bilayer membranes because of the rather large angular amplitude of segmental motion towards the terminal methyl end of the chain (see,

e.g. Marsh 1981). This is responsible for the line narrowing in the fluid phase that is found in Figure 6.2. It is seen from Figure 6.1 that the spin-label spectra from DMPG membranes that contain OmpA consist of two components. In addition to the three-line spectrum, a second component with larger hyperfine splitting is resolved in the outer wings of the spectrum.

The proportion of this second component increases with the protein content of the membrane. A wide range of studies with α-helical transmembrane proteins (Marsh and Horváth 1998) indicate that this motionally restricted spectral component represents the population of spin-labelled lipids whose chains contact the intramembranous surface of the protein directly.

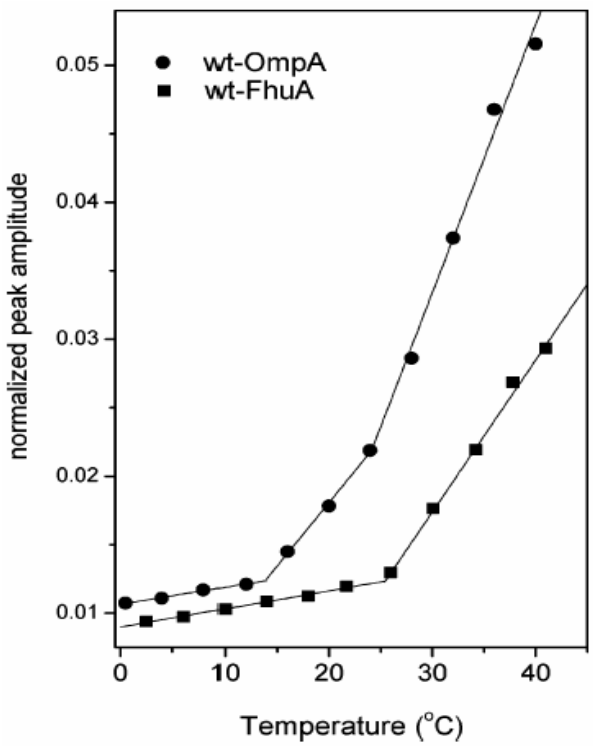

Figure 6.2 Temperature dependence of the central lineheight in the ESR spectra of the 14-PGSL spin label in dimyristoylphosphatidylglycerol membranes containing either OmpA (circles) or FhuA (squares) at lipid/protein ratios of 30 mol/mol and 58 mol/mol, respectively. The spectral lineheight is normalised to the double integral of the first-derivative spectra, in each case.

Figure 6.3 illustrates the two-component nature of the ESR spectra from OmpA/DMPG complexes (Figure 6.3A), by means of difference spectroscopy. The fluid component in Figure 6.3A is matched by a spectrum from fluid egg phosphatidylcholine bilayers at 8 °C (dotted line in Figure 6.3C). Subtraction of (1 - *f*) = 25% of the normalised intensity of the latter from the spectrum in Figure 6.3A yields the solid-line difference

spectrum given in Figure 6.3B. The latter motionally restricted component is reasonably well matched by the gel-phase spectrum from sonicated, small unilamellar DMPC vesicles at 9 °C (dotted line in Figure 6.3B).

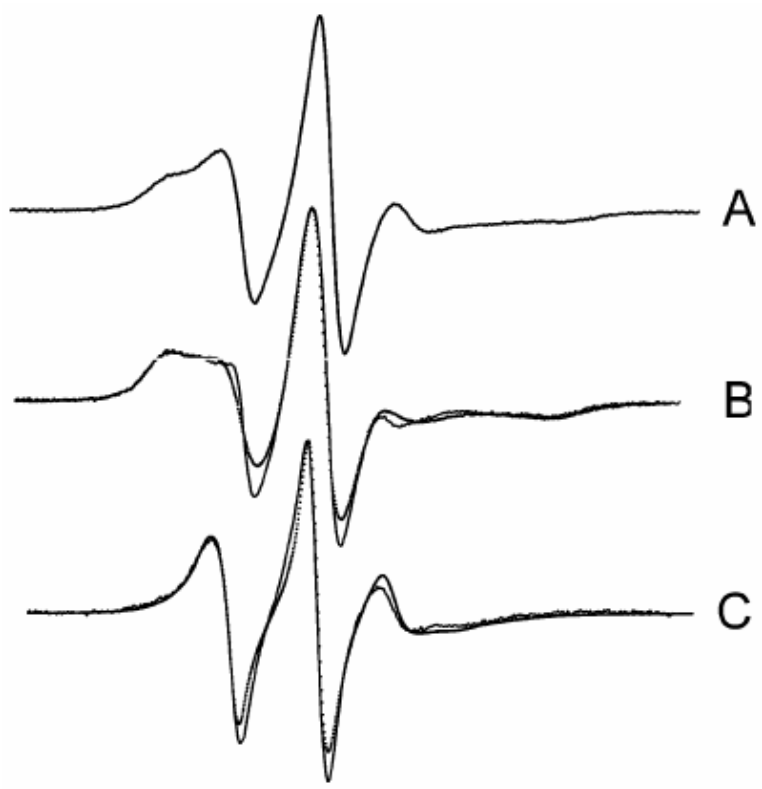

Figure 6.3 Spectral subtractions to quantitate the relative proportions of the fluid [fraction, (1 - *f*)] and motionally restricted (fraction, *f*) components from the ESR spectra of 14-PGSL in OmpA/DMPG membranes. A experimental spectrum from OmpA/DMPG 17:1 mol/mol membranes at 30 °C. **B** *Solid line*: difference spectrum obtained by subtracting 1 - *f* = 25% of dotted line spectrum in C. *Dotted line*: motionally restricted comparison spectrum (sonicated DMPC vesicles at 9 °C). **C** *Solid line*: difference spectrum obtained by subtracting *f* = 78% of dotted-line spectrum in B. *Dotted line*: fluid comparison spectrum (egg phosphatidylcholine dispersion at 8 °C).

The complementary difference spectrum, which is given by the solid line in Figure 6.3C, is obtained by subtracting *f* = 78% of the normalised intensity of the gel-phase sonicated DMPC spectrum (i.e., the dotted line in Figure 6.3B) from Figure 6.3A, and corresponds reasonably well with fluid component used for subtraction (viz., the dotted line in Figure 6.3C). The relative proportions of fluid and motionally restricted spin-labelled lipid were determined by spectral subtraction and integration (Marsh 1982), as described in Figure 6.3.

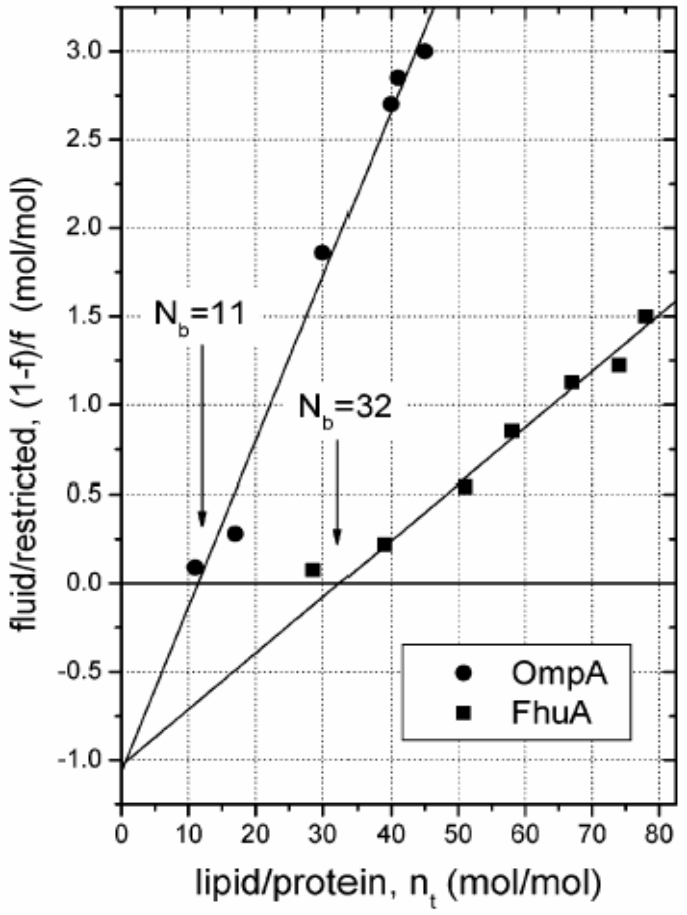

Figure 6.4 Dependence of the ratio of fluid to motionally restricted populations, (1 - *f*)/*f*, of 14-PGSL spin label on lipid/protein ratio, n_t, in dimyristoylphosphatidylglycerol membranes containing either OmpA (circles) or FhuA (squares).

Figure 6.4 gives the ratio, (1 - *f*)/*f*, of the fluid to motionally restricted populations of 14-PGSL as a function of the total lipid/protein ratio, n_t, in the sample. The data is plotted according to the equation for equilibrium lipid-protein exchange that has proved appropriate for analysis of the association of spin-labelled lipids with α-helical transmembrane proteins (Brotherus et al. 1981; Marsh 1985):

$$(1-f)/f = (n_t/N_b - 1)/K_r \qquad \text{(Eq. 6.1)}$$

where N_b is the number of lipid association sites at the perimeter of the β-barrel and K_r is the association constant of the spin-labelled lipid relative to that of the unlabelled host lipid (i.e., DMPG). The linearity of the plot according to Eq. 6.1 indicates that the number of association sites, $N_b \approx 11$ lipids/protein, remains constant, irrespective of the total lipid/protein ratio, just as for α-helical transmembrane proteins (Marsh and Horváth 1998).

Also, the relative association constant, $K_r \approx 1$, obtained from the *y*-intercept in Figure 6.4, indicates that there is relatively little selectivity between the spin-labelled and unlabelled phosphatidylglycerol for the interaction with OmpA.

Figure 6.5 shows the ESR spectra of different lipids spin-labelled on the 14-C atom of the lipid chain in reconstituted OmpA/DMPG membranes of fixed lipid/protein ratio. A selectivity between the different lipids for interaction with OmpA is evident from the different proportions of the two components attributable to fluid and motionally restricted lipids in Figure 6.5.

From Eq. 6.1, the ratio of the relative association constant, K_r, of a given lipid to that, K_r^{PG}, of phosphatidylglycerol is given by:

$$K_r / K_r^{PG} = (1/ f_{PG} - 1)/(1/ f - 1) \qquad \text{(Eq. 6.2)}$$

where f_{PG} is the fraction of motionally restricted spin-labelled phosphatidylglycerol and f that of the spin-labelled lipid in question. Values for the selectivity, K_r/K_r^{PG}, deduced in this way by using difference spectra derived from Figure 6.5 are given in Table 6.1.

Only phosphatidic acid displays an enhanced selectivity, relative to phosphatidylglycerol, for interaction with OmpA. All other negatively charged lipids and zwitterionic lipids have a lower affinity for association with OmpA than does phosphatidylglycerol.

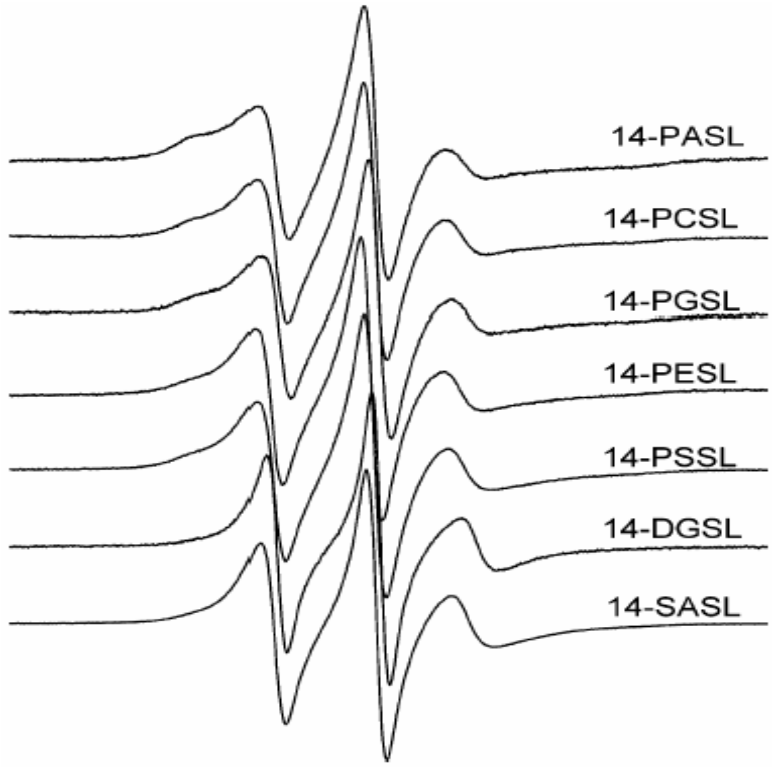

Figure 6.5 ESR spectra of spin-labelled phospholipids (14-PXSL) with different polar headgroups, and of the corresponding spin-labelled diacylglycerol (14-DGSL) and stearic acid (14-SASL), in dimyristoylphosphatidylglycerol membranes containing OmpA at fixed lipid/protein ratio of 24 mol/mol. T = 30 °C; total scan width = 100 gauss.

Table 6.1 Relative Association Constants, K_r, of 14-PXSL, 14-DGSL, and 14-SASL Spin-Labeled Lipids for Interaction with OmpA or FhuA in Dimyristoylphosphatidyl-glycerol Membranes[a]

lipid	K_r/K_r^{PG}	$\Delta G - \Delta G^{PG}$ (kJ/mol)[b]	lipid	K_r/K_r^{PG}	$\Delta G - \Delta G^{PG}$ (kJ/mol)[b]
OmpA			FhuA		
14-PASL	2.5	−2.3	14-PASL	1.5	−1.0
14-PCSL	0.6	+1.1	14-PCSL	1.1	−0.3
14-PESL	0.5	+1.7	14-PESL	0.6	+1.2
14-PSSL	0.55	+1.6	14-PSSL	1.4	−0.8
14-DGSL	∼0.1	∼+5.8	14-DGSL	0.4	+2.5
14-SASL	∼0.2	∼+4.1	14-SASL	3.0	−2.8

[a] Relative association constants, K_r, are normalized to the value for 14-PGSL either in OmpA/DMPG membranes of lipid/protein ratio 24 mol/mol or in FhuA/DMPG membranes of lipid/protein ratio 53 mol/mol. Measurements for OmpA are at 30 °C and for FhuA at 34 °C. [b] Free energy of association, relative to 14-PGSL: $\Delta G - \Delta G^{PG} = -RT \ln(K_r/K_r^{PG})$.

6.4.2 FhuA reconstituted in DMPG

Figure 6.6 shows the ESR spectra of 14-PGSL in reconstituted membranes of DMPG that contain FhuA. Spectra are recorded in the fluid phase of the lipid-protein membranes (cf. transition curve in Figure 6.2). As for membranes containing OmpA, the spectra consist of two components, and the proportion of the motionally restricted component increases with increasing protein content in the membrane.

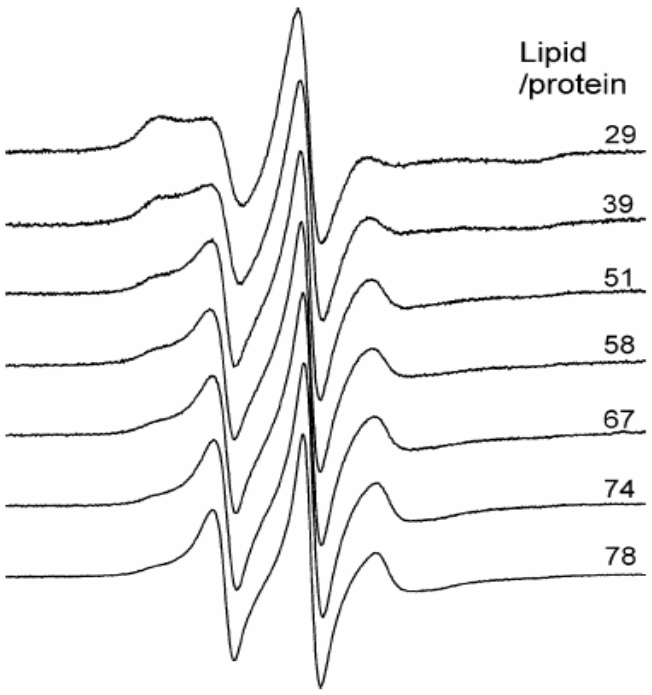

Figure 6.6 ESR spectra of phosphatidylglycerol spin labelled on the 14-C atom of the *sn*-2 chain (14-PGSL) in dimyristoyl phosphatidylglycerol membranes containing FhuA at the lipid/protein mole ratios indicated in the figure. T = 34 °C; total scan width = 100 gauss.

Figure 6.4 gives the dependence on lipid/protein ratio of the ratio of fluid to motionally restricted spin-labelled lipid associated with FhuA. The stoichiometry, N_b, of lipid-protein interaction $N_b \approx 32$ mol/mol is considerably larger than that for the smaller β-barrel protein OmpA. Again, the association constant for spin-labelled phosphatidylglycerol is $K_r \approx 1$, relative to that for the unlabelled DMPG.

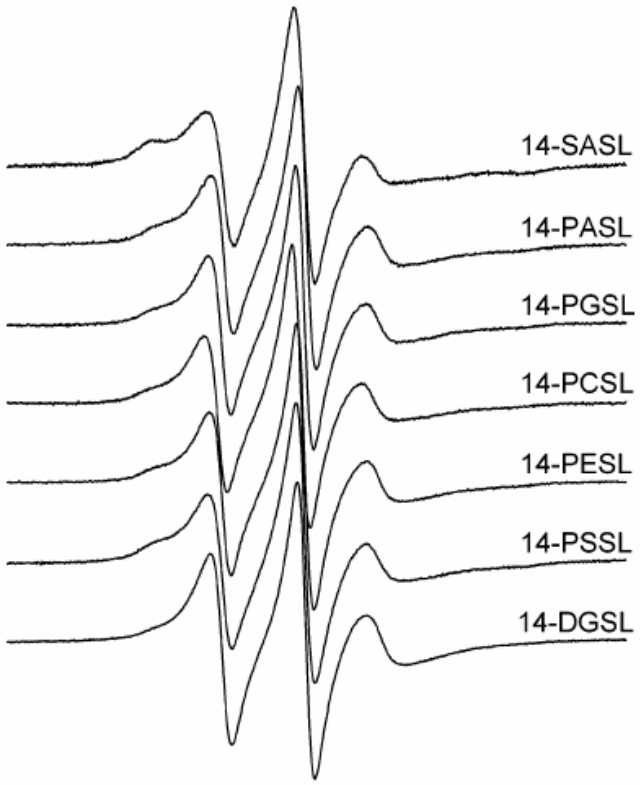

Figure 6.7 ESR spectra of spin-labelled phospholipids (14-PXSL) with different polar headgroups, and of the corresponding spin-labelled diacylglycerol (14-DGSL) and stearic acid (14-SASL), in dimyristoyl phosphatidylglycerol membranes containing FhuA at fixed lipid/protein ratio of 53 mol/mol. T = 34°C; total scan width = 100 gauss.

Figure 6.7 shows the ESR spectra of the different spin-labelled lipids in reconstituted FhuA/DMPG membranes of fixed lipid/protein ratio. Again, as for OmpA, a selectivity of interaction with FhuA is evident from the different proportions of the fluid and motionally restricted components in the spectra of the various spin-labelled lipids.

Table 6.1 lists the selectivity of FhuA for the different spin-labelled lipids, in terms of the association constants, K_r/K_r^{PG}, relative to that for spin-labelled phosphatidylglycerol. The pattern of selectivity differs from that for OmpA. In particular, a higher selectivity (relative to phosphatidylglycerol) is found for phosphatidylserine and phosphatidylinositol.

6.5 Discussion

6.5.1 Stoichiometry of the lipid interaction

The number of diacyl lipids that can be accommodated at one intramembranous surface of a β-sheet with n_β strands is (Marsh 1997):

$$N_b = n_\beta D_\beta / \left(d_{ch} \cos\theta_\beta \right) \qquad \text{(Eq. 6.3)}$$

where θ_β is the strand tilt within the sheet, D_β = 0.47 nm (Fraser and Mac Rae 1973) is the interstrand separation, and d_{ch} = 0.48 nm is the width of a lipid chain. For OmpA (n_β = 8), the mean strand tilt is θ_β = 43.1° deduced from the crystal structure (Páli and Marsh 2001) and θ_β = 46°±1° deduced from infrared dichroism in lipid bilayers (Ramakrishnan et al. 2005). Both predict a lipid stoichiometry for OmpA of N_b = 11 lipids per monomer. For FhuA (n_β = 22), the strand tilt is θ_β = 38.3° from x-ray (Páli and Marsh 2001) and θ_β = 44.5° ± 1° from infrared dichroism (Ramakrishnan et al. 2005). This gives lipid stoichiometries for FhuA of N_b = 27 mol/mol from the crystal structure and N_b = 30 mol/mol in bilayers. Estimates of the stoichiometries for both proteins therefore correspond rather closely with the experimental determinations of the number of motionally restricted lipids interacting with the two β-sheet proteins.

Equation 6.3 applies to a continuous planar sheet and could be modified by the curvature of a β-barrel. For a barrel of approximately elliptical cross section, the number of lipids that can be accommodated at the perimeter is:

$$N_b \approx \pi \left[\frac{3}{2}(a+b) - \sqrt{ab} \right] \Big/ d_{ch} \qquad \text{(Eq. 6.4)}$$

where a and b are the semi-axes of the ellipse. For OmpA, the cross-section is only slightly elliptical: $a \approx b \approx 1.2$ nm (Pautsch and Schulz 2000) and thus $N_b \approx 16$ mol/mol. This value is significantly larger than the estimate for a planar sheet and somewhat larger than the population of motionally restricted lipid that is found experimentally. For FhuA, $a \approx 2.3$

nm and $b \approx 1.9$ nm (Ferguson et al. 1998), and Eq. 6.4 yields a value of $N_b \approx 28$ mol/mol. This is close to the estimate from Eq. 6.3, because the FhuA barrel is relatively large in size, and curvature of the β-sheet is therefore less than for OmpA. Both estimates therefore correspond reasonably well with the number of motionally restricted lipids that are associated with FhuA, as determined by ESR spectroscopy.

6.5.2 Selectivity of the lipid-protein interaction

On the periplasmic side, the eight transmembrane β-strands of OmpA are connected by short turns, the charged residues of which are preponderantly acidic (Pautsch and Schulz 1998). Because there is only one basic residue (as opposed to four acidic residues), there is little basis for a selectivity for negatively charged lipids in the periplasmic leaflet. On the extracellular side, the loops connecting the β-strands of OmpA are larger and the strands themselves extend beyond the intramembranous segments of the protein. There are no charged residues immediately adjacent to the transmembrane segments but two basic side chains are located four residues away in extensions of the β-strand (Pautsch and Schulz 1998). These two positively-charged residues are therefore situated ca. 1 nm above the hydrophobic core of the membrane, facing the lipid headgroups. Thus they could account for the selectivity of the negatively charged lipids, phosphatidic acid and phosphatidylglycerol, over the zwitterionic lipids, phosphatidylcholine and phosphatidylethanolamine, but not for the low selectivity for phosphatidylserine and phosphatidylinositol. The relative paucity of charged residues close to the lipid headgroups in OmpA is illustrated by the electrostatic surface of the protein that is shown in the upper panel of Figure 6.8. Under these circumstances, uncharged residues in the aromatic girdles, which are located at the polar-apolar interfaces (Pautsch and Schulz 1998; Pautsch and Schulz 2000), may modulate the selectivity of lipid-protein interaction.

A limited lipid selectivity of this type has been found recently for the interfacial tryptophan residues of gramicidin A channels reconstituted in DMPC (Kóta et al. 2004). At pH 7.0, the fatty acid spin label (14-SASL) is expected to be protonated in negatively charged DMPG bilayers (Sankaram et al. 1990). The low selectivity for diacylglycerol and protonated fatty acid is accounted for by the low polarity of these latter two lipids, which causes them to locate more deeply in the bilayer than do the phospholipids (Rama Krishna and Marsh 1990; Schorn and Marsh 1996). FhuA has 22 transmembrane strands and

considerably more charged residues that are located close to the region of the phospholipid headgroups than does OmpA. This is clear from comparison of the electrostatic surfaces of the two proteins that are given in Figure 6.8.

The periplasmic turns of FhuA contain thirteen acidic residues and four basic residues (Locher et al. 1998). Although still bearing a net negative charge, the ratio of basic to acidic residues is somewhat higher than in the periplasmic turns of OmpA. In the extracellular extensions of the FhuA β-strands, six basic residues and two acidic residues are located two residues away from the hydrophobic-polar interface, i.e., they face the lipid headgroups. A further six basic residues and one acidic residue are located four residues away from this surface. Additionally, two basic and two acidic residues are located in cytoplasmic loops, close to the hydrophobic transmembrane sector. There is thus a strong preponderance of positively charged residues at the extracellular surface that accounts for the marked selectivity of FhuA, relative to OmpA, for anionic lipids (see lower panel of Figure 6.8). The pattern of lipid selectivity with FhuA conforms more closely with that found for α-helical integral proteins. In the latter case, there is little selectivity between phosphatidylglycerol and phosphatidylcholine, but a preferential selectivity for other negatively charged lipids (Marsh and Horváth 1998).

In further connection with the selectivity of FhuA for certain negatively charged phospholipids, it is interesting to note the cluster of basic residues that is concentrated at the binding site of the single lipopolysaccharide (LPS) molecule which is resolved in the crystal structure of OmpA (PDB code 2FCP; Ferguson et al. 1998). Arginines 382 and 384 and lysines 351, 439, and 441 are all located in the region of the phosphorylated glucosamines or of the acyl chain carboxyl groups of LPS. This part of the LPS molecule corresponds to the expected location of the phospholipid headgroups in a lipid bilayer.

As for OmpA, the selectivity of FhuA for apolar diacylglycerol is low. The selectivity of FhuA for stearic acid (14-SASL), however, is much higher than that of OmpA. The association constant of 14-SASL with FhuA is in the range that might be expected for the negatively charged, ionized form of the fatty acid (see, e.g., Marsh and Horváth 1998). Presumably, the negative surface potential of DMPG bilayers is neutralized locally in the regions of high positive charge on FhuA (see Figure 6.8) and results in ionization of the fatty acid at these association sites on the protein. Currently, relatively little is known about the effects of specific lipids on the function of outer membrane proteins. Negatively charged lipopolysaccharide is, however, known to be involved in activation of the *E. coli* outer membrane protease OmpT (Kramer et al. 2002).

Furthermore, negatively charged lipids are found to be important for the folding and membrane insertion of outer membrane proteins, such as the *E. coli* phosphate transporter PhoE (de Cock et al. 1999; de Cock et al. 2001) and including also OmpA (Bulieris et al. 2003).

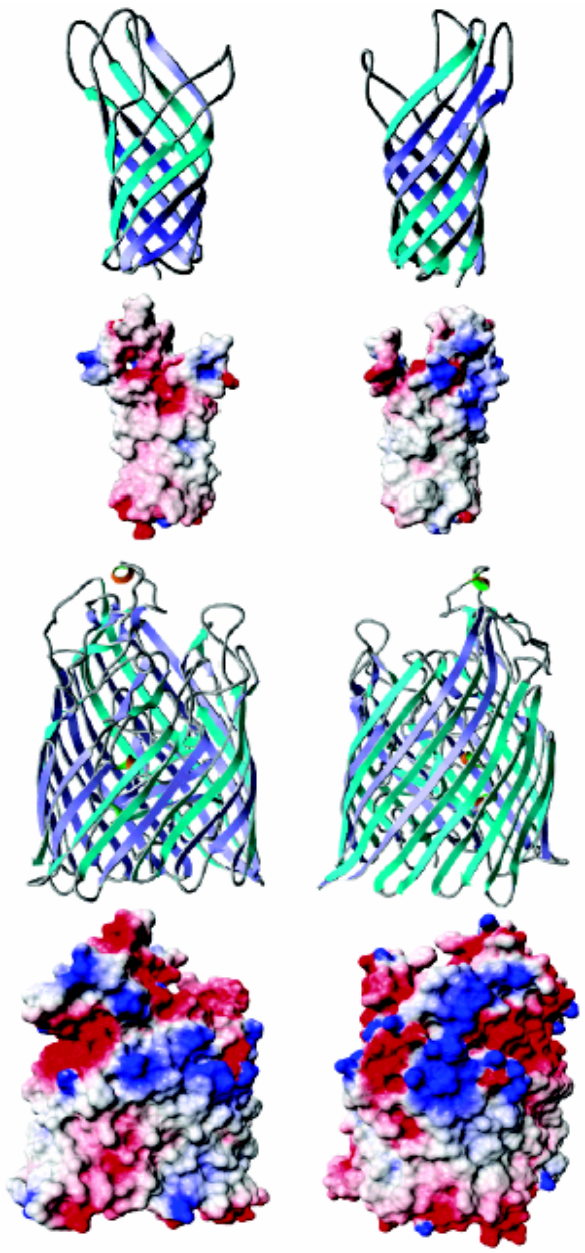

Figure 6.8 Ribbon diagrams and electrostatic surfaces of OmpA 1-171 (upper panel; PDB:1QJP; Pautsch and Schulz 2000) and of FhuA (lower panel; PDB:2FCP; Ferguson et al. 1998). Ribbon diagrams are prepared with DeepView (Guex and Peitsch 1997) and electrostatic surfaces with MolMol (Koradi et al. 1996). In the electrostatic colouring: blue is positive, red is negative and white is apolar. For each protein, a back and a front view is shown.

7 Orientation of β-barrel proteins OmpA and FhuA in lipid membranes. Chainlength dependence from infrared dichroism

7.1 Abstract

The outer membrane proteins OmpA and FhuA of *E. coli* are monomeric β-barrels of widely differing size. Polarised attenuated total reflection infrared spectroscopy has been used to determine the orientation of the β-barrels in phosphatidylcholine host matrices of different lipid chainlengths. The linear dichroism of the amide I band from OmpA and FhuA in hydrated membranes generally increases with increasing chainlength from *di*$C_{12:0}$ to *di*$C_{17:0}$ phosphatidylcholine, in both the fluid and gel phases. Measurements of the amide I and amide II dichroism from dry samples are used to deduce the strand tilt ($\beta = 46°$ for OmpA, and $\beta = 44.5°$ for FhuA). These values are then used to deduce the order parameters, $\langle P_2(\cos\alpha)\rangle$, of the β-barrels from the amide I dichroic ratios of the hydrated membranes. The orientational ordering of the β-barrels, and their assembly in the membrane, are discussed in terms of hydrophobic matching with the lipid chains.

7.2 Introduction

The integral proteins of the outer membrane of Gram-negative bacteria perform a variety of functions, including those of receptors, lipases, passive diffusion pores, sugar transport pores, and ligand-gated transport systems. In spite of the diversity in function, the outer-membrane proteins are mainly, if not exclusively, of the β-barrel type: the second structural paradigm, in addition to the α-helix, for transmembrane proteins. The size of the β-barrel ranges from eight to 22 strands, the shear number of the barrel ranges from eight to 24, and the degree of oligomerisation varies from monomer to trimer (for a review, see ref. Schulz 2002). The β-strands are tilted, relative to the barrel axis by 36° to 42° (Páli and

Marsh 2001). This structural information is obtained mostly from x-ray diffraction of crystals produced from purified proteins in detergent (Cowan et al. 1992; Weiss and Schulz 1992; Kreusch et al. 1994; Schirmer et al. 1995; Meyer et al. 1997; Ferguson et al. 1998; Forst et al. 1998; Buchanan et al. 1999; Dutzler et al. 1999; Snijder et al. 1999; Vogt and Schulz 1999; Pautsch and Schulz 2000), and to a much lesser extent from solution-state NMR of proteins in detergent micelles (Arora et al. 2001; Fernandez et al. 2001; Fernandez et al. 2002; Hwang et al. 2002). These environments approximate those of the lipid bilayer in biological membranes, but do not provide information on the orientation of the β-barrel proteins in the membrane. The latter feature not only determines the way in which the protein is integrated into the membrane, but also might be responsible at least partly for the functional differentiation between the various β-barrel proteins.

In principle, the dichroism of the amide bands in the infrared spectra from aligned membranes can be used to determine both the β-strand tilt and the orientation of the β-sheet plane or β-barrel axis (Marsh 1997; Marsh 1998). Combination of the dichroism from amide I and amide II bands allows determination of both orientational parameters. If the strand tilt is known from x-ray diffraction, only one dichroic ratio is required to determine the orientation of the β-sheet or β-barrel. Several previous analyses of infrared dichroism from β-barrel membrane proteins have not exploited this possibility (Nabedryk et al. 1988; Goormaghtigh et al. 1990; Rodionova et al. 1995). Recently, this method of analysis has been applied successfully to ATR-FTIR studies on two isoforms of the VDAC voltage-dependent anion-selective channel from the outer membrane of mitochondria (Abrecht et al. 2000). In the present work, we investigate the dependence on lipid chainlength of the orientational tilt of two β-barrel transmembrane proteins with very different sizes. One of these outer membrane proteins from *E. coli* is OmpA, which has eight β-strands; the other is the β-barrel domain of the ferrichrome-iron receptor FhuA mutant without the cork domain, which has 22 β-strands. Both proteins are monomers and therefore are those most likely to respond to the lipid environment. The β-barrel orientation displays a characteristic dependence on the lipid chainlength that is determined by the hydrophobic span of the outer membrane proteins and correlates well with the lipid requirement for spontaneous membrane insertion of OmpA (Kleinschmidt and Tamm 2002).

7.3 Theoretical background

The order parameter, $\langle P_2(\cos\alpha)\rangle$, for the axis of a β-barrel protein with circular cross-section is related to the amide band dichroic ratio, $R(\Theta)$, by (Tamm and Tatulian 1997; Marsh 1998):

$$\left\langle P_2(\cos\alpha)\right\rangle = \frac{E_x^2/E_y^2 - R(\Theta) + E_z^2/E_y^2}{P_2(\cos\Theta)\left[E_x^2/E_y^2 - R(\Theta) - 2E_z^2/E_y^2\right]} \qquad \text{(Eq. 7.1)}$$

where E_x, E_y, E_z are the components of the electric field vector in the sample, normalised to those of the incident infrared beam. The *z*-axis is normal to the ATR plate; the *x*-axis lies in the plane of incidence, and the *y*-axis is orthogonal to the latter. The order parameter is defined in terms of the Legendre polynomial: $\left\langle P_2(\cos\alpha)\right\rangle = \frac{1}{2}\left(3\left\langle\cos^2\alpha\right\rangle - 1\right)$, where angular brackets indicate an ensemble average over all amides. The orientation of the amide transition moment, relative to the β-strand axis, is given by $\Theta = 90°-\beta$ for the amide I band, and by $\Theta = \beta$ for the amide II band, where β is the tilt angle of the strands to the barrel axis (see left-hand panel of Figure 7.1). The angle α is the inclination of the barrel axis to the normal to the orienting substrate (i.e., the ATR crystal), and the order parameter is determined by the distribution in α. In the case of partial disorder in alignment of the sample on the substrate, the order parameter, $\langle P_2(\cos\alpha)\rangle$, is the product of the order parameter, $\langle P_2(\cos\alpha)\rangle_o$, of the barrel axis relative to the membrane normal, and an order parameter, $S_{disorder}$, that characterises the misalignment of the membrane. For a model in which a fraction (1-*f*) of the sample is totally disordered, and the remainder is perfectly ordered: $\langle P_2(\cos\alpha)\rangle = f\langle P_2(\cos\alpha)\rangle_o$ (Fraser 1953).

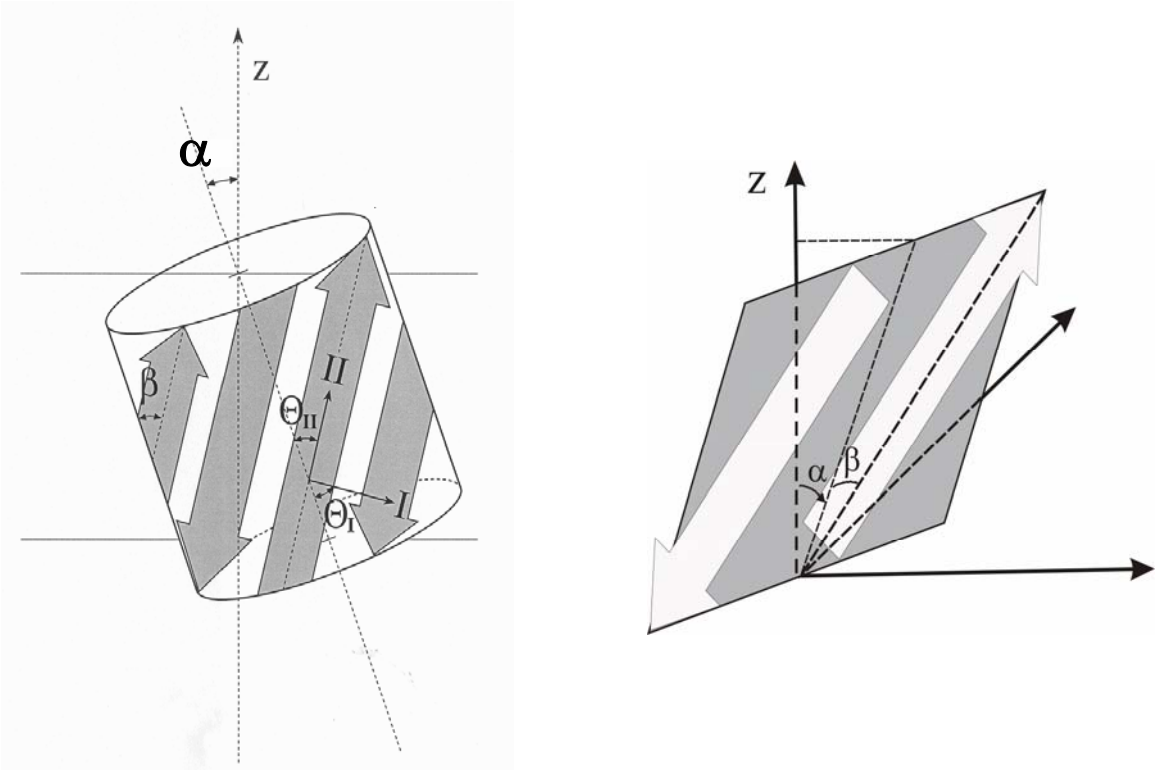

Figure 7.1 Orientation of transition moments, Θ_M, in β-sheets (right) and β-barrels (left) The β-strand tilt is β; the tilt of the barrel or sheet axis, relative to the membrane normal (*z*), is α. For the amide I band: $\Theta_I = 90°-\beta$, and for the amide II band: $\Theta_{II} = \beta$.

The dichroism of a flattened β-barrel, or of β-strands extending beyond the barrel domain, may be depicted better in terms of a planar β-sheet. For the latter, the dichroic ratio of the amide I band is given by (Marsh 1997):

$$R_I = \frac{E_x^2}{E_y^2} + \frac{2\langle\cos^2\alpha\rangle\langle\sin^2\beta\rangle}{1-\langle\cos^2\alpha\rangle\langle\sin^2\beta\rangle}\frac{E_z^2}{E_y^2} \qquad \text{(Eq. 7.2)}$$

and that of the amide II band by:

$$R_{II} = \frac{E_x^2}{E_y^2} + \frac{2\langle\cos^2\alpha\rangle\langle\cos^2\beta\rangle}{1-\langle\cos^2\alpha\rangle\langle\cos^2\beta\rangle}\frac{E_z^2}{E_y^2} \qquad \text{(Eq. 7.3)}$$

where α is the inclination of the β-sheet to the normal to the orienting substrate, and β is the tilt of the β-strands within the β-sheet (see right-hand panel of Figure 7.1). For a partially oriented sample:

$$\left\langle \cos^2 \alpha \right\rangle = f \left\langle \cos^2 \alpha \right\rangle_o + (1 - f)/3 \qquad \text{(Eq. 7.4)}$$

where (1-*f*) is the fraction unoriented, and $\langle \cos^2 \alpha \rangle_o$ is referred to the membrane normal, just as for the β-barrel case.

7.4 Materials and methods

7.4.1 Materials

E. coli strain P.400, expressing wild-type OmpA was a generous gift from Dr. Ulf Henning, Tübingen. Wild-type OmpA was isolated and purified from the *E. coli* outer membrane in the unfolded form in 8 M urea, as described in ref. (Surrey and Jähnig 1992). *E. coli* strain BL21(DE3) carrying plasmid pBk7H and expressing FhuAΔ5-160 was a generous gift from Drs. Helmut Killmann and Volker Braun, Tübingen (Braun et al. 1999). The His_6-tagged barrel domain of FhuA, without the cork domain, was extracted from *E. coli* outer membranes, and isolated in *N*-lauroyl-*N*,*N*-dimethylammonium-*N*-oxide (LDAO) detergent micelles, without any unfolding, essentially as described in ref. (Ferguson et al. 1998), except that minimal medium was used. In addition to ampicillin, the minimal medium contained also kanamycin but not tetracycline. Symmetrical, disaturated phosphatidylcholines with odd and even chainlengths from $C_{12:0}$ to $C_{17:0}$ were obtained from Avanti Polar Lipids (Alabaster, AL) and all other chemicals were from Sigma Chemical Co. (St. Louis, MO).

Unfolded OmpA was folded into detergent micelles as described in ref. (Kleinschmidt et al. 1999). Briefly, 500 μL of a 42 mg/ml solution of unfolded OmpA in 10 mM borate, 2 mM EDTA, pH 10 buffer that contained 8 M urea was diluted 20-fold with the borate buffer and mixed with an 800-fold molar excess of LDAO detergent. The mixture was incubated overnight at 40°C to ensure complete refolding of the protein. Refolding was carried out at pH 10 because a yield of close to 100% is achieved at this pH-

value (Kleinschmidt et al. 1999). Sample purity and folding were monitored by SDS polyacrylamide gel electrophoresis according to the method in (Laemmli 1970), except that samples were not boiled prior to electrophoresis.

The gene encoding the transmembrane domain of OmpA (amino acid residues 0-176) was amplified *via* PCR from pET1113 (Kleinschmidt et al. 1999), kindly provided by Dr. Tanneke den Blaauwen, University of Amsterdam. The upstream primer 5'-CGGCAT-ATGGCTCCGAAAGATAACACCTG-3', was used to introduce a start codon (underlined) to replace the signal sequence of *proOmpA* and the downstream primer 5'-CTGCTC-GAGTCAAGCTGCTTCGCCCTGACCGA-3' converted the codon for proline 177 to a stop codon (underlined). TCA in the downstream primer corresponds to the reversed complement, TGA, in the *proompA* gene, which is a stop-codon. The gene of OmpA (0-176) was then ligated into pET22b (Novagen) using the *NdeI* and *XhoI* restriction enzyme cut sites to yield the plasmid pET22bB1. The plasmid was transformed into *E. coli* strain BL21(DE3) ΔlamB ΔompF::Tn5 ΔompA ΔompC ΔfhuA (Prilipov et al. 1998) using the protocol "One-step preparation and transformation of competent cells" (Ausubel et al. 1999). OmpA (0-176) was subsequently purified as described in refs. (Surrey and Jähnig 1992) and (Pautsch et al. 1999).

For refolding of the transmembrane domain of OmpA, 12 mg of denatured OmpA(0-176) were diluted into 20 mL 25 mM LDAO in 10 mM borate buffer containing 2 mM EDTA (pH 10). The proteins were incubated at 40 °C for 12 hours. The yield of refolding was 100% as confirmed by SDS-PAGE and CD spectroscopy. In SDS-PAGE, OmpA0-176 displayed the typical band-shift from 19 kDa (unfolded) to 23 kDa (folded form) as observed previously (Pautsch et al. 1999), if samples were not boiled prior to electrophoresis. The full-length wt-OmpA similarly displayed a band-shift from 35 kDa to 30 kDa in SDS-PAGE as described previously (Surrey and Jähnig 1992), if samples were not heat-denatured prior to electrophoresis. Folding was quantitative, because the bands for the unfolded proteins disappeared after refolding, but appeared again, when samples were boiled (heat-denatured) in SDS prior to electrophoresis. After refolding, OmpA was concentrated 20-fold in an Amicon ultrafiltration chamber using Amicon YM-10 membranes.

7.4.2 Reconstitution into membranes

Lipid stock solutions were prepared in $CHCl_3$ and dried under a stream of dry nitrogen gas. The resulting lipid film was desiccated overnight under vacuum and then covered with argon. The dry lipid film was hydrated with 10 mM Hepes, 2 mM EDTA buffer, pH 7.0, and frozen (in liquid nitrogen) and thawed (in a water bath at ~5^{o}C above the transition temperature of the phospholipid) seven times, to obtain uniform lipid vesicles.

The reconstitution was carried out by mixing 1 mg of the above lipid vesicles with protein to the desired lipid-protein ratio, and then 10% sodium cholate solution was added to give a final concentration of 0.2% sodium cholate, in a total volume of 500 μL. The sample was mixed well and incubated at room temperature for 1 hour, vortexing from time to time. After 1 hour incubation, the protein was precipitated with 52.5% ammonium sulfate solution that was added to 35% final concentration. The pellet containing the reconstituted protein was then centrifuged for 30 minutes at 35000 rpm in a 50TI rotor. The pellet contains the reconstituted sample and, because the outer membrane proteins have a low density, the reconstituted membrane pellets tend to float when centrifuged. This decreases the protein and lipid content and invariably changes the lipid-protein (L/P) ratios from the expected range. L/P ratios were therefore determined after ammonium-sulfate precipitation (Lowry et al. 1951; Rouser et al. 1970), and then the samples were adjusted to achieve a L/P ratio close to 50 mol/mol by adding solubilised lipid vesicles. The pellet was dissolved and vortexed in 500 μL 10 mM Hepes buffer pH 7.0, containing 2 mM EDTA and 250 mM NaCl. Detergent removal was achieved by extensive dialysis at 8°C against 10 mM Hepes buffer pH 7.0 containing 2 mM EDTA and 250 mM NaCl, using 10-kDa cut-off dialysis membranes. Four or five changes of 2 L buffer were made every 7-8 h, with the last dialysis step overnight.

7.4.3 ATR spectroscopy

OmpA was purified and reconstituted as described above. The reconstituted sample was layered on a clean ZnSe ATR crystal. Initially, the sample was dried with dry nitrogen purge and then desiccated overnight with a vacuum pump. The dry lipid film was incubated in a Bruker IFS 25 FTIR spectrometer by purging with dry nitrogen at 1.5

kp/cm^2 flow rate. ATR spectra were recorded at a nominal resolution of 2 cm^{-1} with parallel and perpendicular polarisation of the incident beam. Then the sample was hydrated with 10 mM Hepes pH 7.0 buffer containing 2 mM EDTA and 250 mM NaCl prepared in D_2O, and washed (using a pipette) again with the same buffer in order to remove noninserted lipid and protein (Rodionova et al. 1995). Meanwhile, ATR spectra were recorded at both polarisations for every wash. The sample holder was temperature controlled using a recirculating water bath and the spectra were recorded in the gel phase (~10^o below the lipid chain-melting temperature) and in the fluid phase (~10^o above the lipid chain-melting temperature) of the membranes. Further details of the ATR spectroscopy are given in ref. (Kóta et al. 2004).

To determine the dichroic ratio each spectrum was analysed using OPUS-Version 3.02 software from Bruker (Karlsruhe, Germany). If necessary, spectra were smoothed with 11-point Savitsky-Golay smoothing to remove the noise from the residual water vapour. A local baseline was established and curve fitting using the Levenberg- Marquardt algorithm was carried out from 1500 to 1708 cm^{-1} and from 1600 to 1700 cm^{-1}, for dry and hydrated samples, respectively. The intensity ratios of parallel and perpendicular polarisation were taken as ATR dichroic ratio (R) from the intensities obtained at 1630 cm^{-1} and 1530 cm^{-1} from the curve fitting analysis, for the amide I and amide II bands, respectively. The dichroic ratio changes with the first two to three washes and then becomes stable, which is taken to correspond to the respective hydrated samples. To calculate molecular orientations from dichroic ratios, intensities of the infrared electric field components were obtained from the thick film approximation: E_x^2 / E_y^2 = 0.450 and E_z^2 / E_y^2 = 1.550 for a ZnSe ATR crystal (see e.g. ref. Marsh 1999).

7.5 Results

7.5.1 Outer-membrane protein OmpA

Figure 7.2 shows the amide region from the polarised ATR spectra of OmpA in aligned membranes of ditridecanoyl phosphatidylcholine (*di*$C_{13:0}$PC). In the dry state (Figures 7.2A,B), both the amide I and amide II bands are visible, whereas in membranes hydrated with D_2O (Figures 7.2C,D), the amide II band is shifted to much lower

frequencies where it overlaps with bands from the lipid. Qualitatively, the band shapes resemble those of other β-barrel outer membrane proteins in the dry (Nabedryk et al. 1988) and hydrated (Rodionova et al. 1995) states.

Band fitting shown in Figure 7.2 demonstrates the predominant β-sheet content of the protein, with the major band at ca. 1630 cm^{-1} in the amide I region ($\nu_{\perp}(\pi,0)$ mode), and at ca. 1530-1550 cm^{-1} in the amide II region ($\nu_{//}(0,\pi)$ mode). The minor band at ca. 1675 cm^{-1} in the amide I region ($\nu_{//}(0,\pi)$ mode) from hydrated membranes is characteristic of antiparallel β-sheets (Miyazawa 1960).

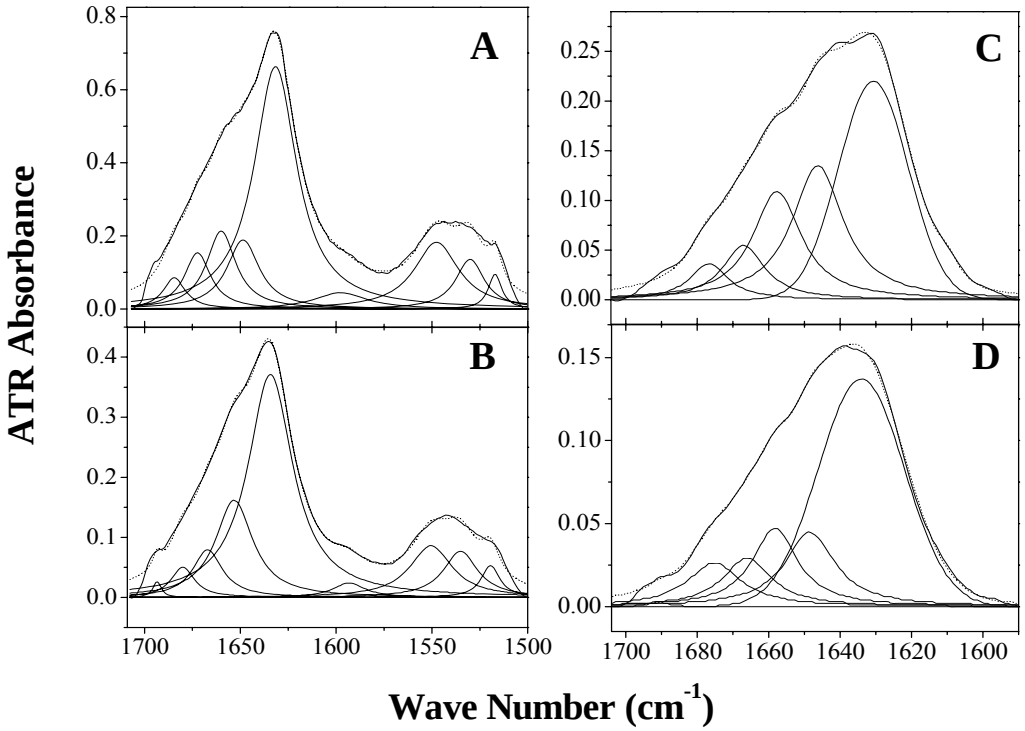

Figure 7.2 Polarised ATR-FTIR spectra of OmpA reconstituted with ditridecanoyl phosphatidylcholine lipid Spectra A and B are obtained in the dry state, whereas spectra C and D are obtained in the hydrated fluid phase. The spectra in the upper panels (A, C) correspond to parallel polarisation and in the lower panels (B, D) correspond to perpendicular polarisation of the incident radiation. Note the different ordinate scales. The dotted lines correspond to the theoretical fit with the bands obtained from the band fitting analysis shown below the experimental spectrum.

Table 7.1 gives the results of band fitting for the amide I region from OmpA in disaturated phosphatidylcholines of different chain lengths. Fitting data are given for hydrated membranes in the gel and fluid phases, recorded at temperatures 10° C below and 10° C above the respective chain-melting transitions. Transition temperatures for *di*$C_{12:0}$,

di$C_{13:0}$, *di*$C_{14:0}$, *di*$C_{15:0}$ and *di*$C_{17:0}$PCs are: -2, 14, 23, 34 and 48 °C, respectively (Marsh 1990).

Table 7.1 Band fitting of the polarised ATR spectra from the amide I band of OmpA in hydrated disaturated phosphatidylcholines of different chainlengths, C(*n*:0), in the gel and fluid phases

C(*n*:0)	Gel		Fluid	
	position (cm^{-1})	normalised area (%)[a]	position (cm^{-1})	normalised area (%)[a]
C(12:0)			1631	41
			1645	36
			1653	16
			1663	5
			1674	2
C(13:0)	1631	42	1633	49
	1646	30	1645	18
	1657	18	1658	17
	1667	7	1666	9
	1676	3	1676	7
C(14:0)	1631	58	1632	59
	1647	19	1645	10
	1657	14	1653	18
	1665	7	1663	10
	1673	2	1672	3
C(15:0)	1632	56	1633	58
	1645	10	1646	14
	1653	19	1655	15
	1663	11	1663	10
	1673	4	1672	3
C(17:0)	1633	63	1633	56
	1645	7	1652	28
	1655	15	1663	10
	1664	11	1672	5
	1673	4	1682	1

[a]Relative band intensities are obtained by combining integrated absorbances, $A_{//}$ and $A_{\perp}$, with radiation polarised parallel and perpendicular, respectively, to the plane of the incident beam. The appropriate combination that reflects the full intensity is $A_{//} + \left(2E_z^2 / E_y^2 - E_x^2 / E_y^2\right)A_{\perp}$ (Marsh 1999).

To obtain the true absorbed intensity that reflects relative populations in aligned samples, it is necessary to combine absorbances, $A_{//}$ and $A_{\perp}$, for parallel and perpendicular

polarised radiation (Marsh 1999). The appropriate admixture with $A_{\perp}$ in the present geometry is $A_{//} + \left(2E_z^2 / E_y^2 - E_x^2 / E_y^2\right)A_{\perp}$. This is used to calculate the percentage populations that are presented in Table 7.1. Generally speaking, the populations are rather similar in the different lipid hosts and in the fluid and gel phases. There is, however, a tendency to a decrease in β-sheet population at shorter chain lengths, with a corresponding increase in the 1645 cm^{-1} band corresponding to disordered structures. With the exception of *di*$C_{12:0}$PC, the mean β-sheet population of OmpA in the different lipid hosts is 59 ± 6%, from Table 7.1 for hydrated membranes. For comparison, the β-sheet content of OmpA truncated to residues 22-192 is 63% from the crystal structure (Pautsch and Schulz 2000); PDB:1QJB). This is similar to the values obtained in the longer lipid hosts. The full-length protein has 325 residues. Therefore an appreciable part (ca. 55%) of the sizeable periplasmic domain must also be β-sheet. For comparison, the resolved 127 residues from the homologous C-terminal domain of RmpM (which shares 35% sequence identity with the periplasmic C-terminal domain of OmpA) contains 25% β-strands and 25% β-turns (Grizot and Buchanan 2004).

From the dichroic ratios of the amide I and amide II bands of the dry sample, it is possible to determine the tilt, β, of the β-strands within the β-sheet. From Eqs. 7.2 and 7.3 for a β-sheet one obtains a consistent mean value of β = 46.2 ± 0.8° (N = 5) from measurements in disaturated phosphatidylcholines of different chainlengths from C12 to C17. Analysis according to Eq. 7.1 for axially symmetric barrels yields a similar value for the strand tilt: β = 48° ± 5°, averaged over membranes with host lipids of different chainlengths. For the barrel domain alone of OmpA, a somewhat smaller value of β = 43.9 ± 0.9° (N = 5) is obtained for the mean strand tilt.

The upper panel of Figure 7.3 shows the dichroic ratios of the amide I band from OmpA in bilayer membranes hydrated in D_2O, as a function of chain length of the disaturated phosphatidylcholine. Values are given for membranes in the gel phase and for those in the fluid phase, above the lipid chain-melting temperature.

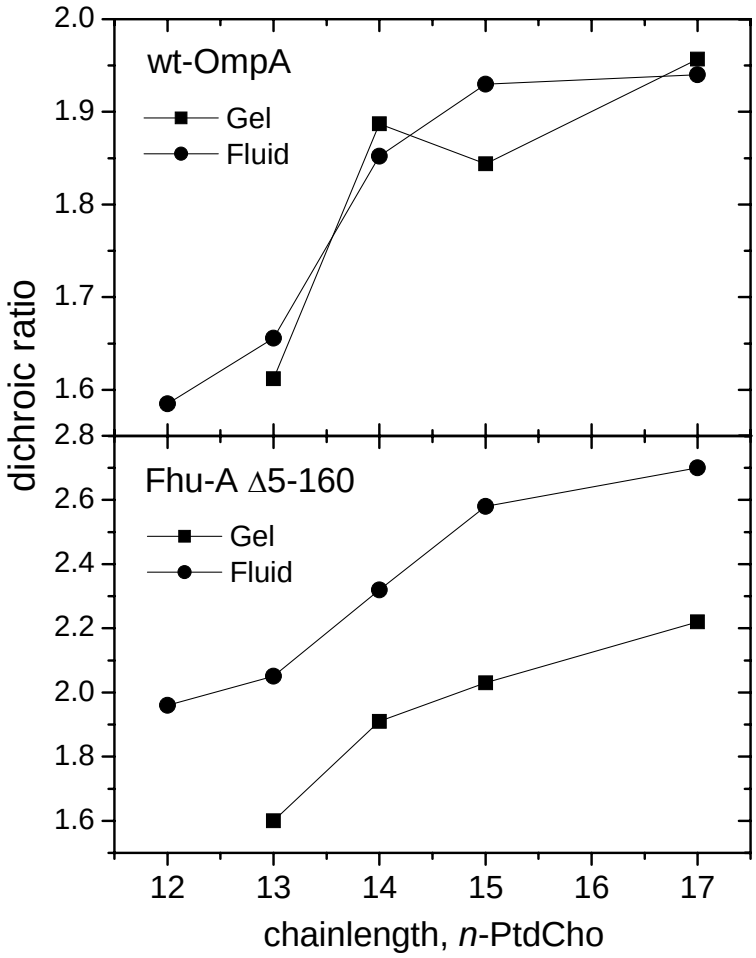

Figure 7.3 Dependence of the dichroic ratios from the amide I band of OmpA (upper panel) and of FhuA barrel domain (lower panel) on chainlength, *n*, of the disaturated phosphatidylcholine membrane in which the protein is incorporated. Dichroic ratios are given for samples in the gel phase (squares) and in the fluid phase (circles). Membranes are hydrated in D_2O buffer.

The general trend is an increase in amide I dichroic ratio with increasing lipid chain length. Use of Eq. 7.2, together with the mean value of the strand tilt, β, deduced from the dichroic ratio of the dry sample, yields the values for the order parameter, $\langle P_2(\cos\alpha)\rangle$, and mean tilt, α, of the β-sheets that are given in Table 7.2. The trend is similar to that of the dichroic ratios: the order parameters increase, and the tilt angles decrease, with increasing lipid chainlength. The differences in order parameters between gel- and fluid-state membranes are not large.

Previous ATR measurements on full-length OmpA in single supported bilayers of *di*$C_{14:0}$PC at room temperature (Rodionova et al. 1995) yield comparable degrees of order when analysed by the present methods ($\langle P_2(\cos\alpha)\rangle$ = 0.35-0.38). Also measurements on

di$C_{16:0}$PC from the same work, are consistent with the present observed trends with chainlength for phosphatidylcholines in the gel phase.

Table 7.2 Order parameters, $\langle P_2(\cos\alpha)\rangle$, and mean effective inclinations, α, of the β-sheets of OmpA reconstituted in disaturated phosphatidylcholines, *di*C(*n*:0)PC, with different chainlengths, *n*, in the gel and fluid phases

C(*n*:0)	Gel		Fluid	
	$\langle P_2(\cos\alpha)\rangle$	α (°)	$\langle P_2(\cos\alpha)\rangle$	α (°)
C(12:0)	-	-	0.26 (0.25)[b]	45 (45)[b]
C(13:0)	0.32 (0.35)[b]	42 (41)[b]	0.34 (0.30)[b]	42 (43)[b]
C(14:0)[a]	0.40 (0.52)[b]	39 (35)[b]	0.39 (0.53)[b]	40 (34)[b]
C(15:0)	0.39 (0.51)[b]	40 (35)[b]	0.42 (0.57)[b]	38 (32)[b]
C(17:0)	0.43 (0.62)[b]	38 (30)[b]	0.42 (0.61)[b]	38 (30)[b]

[a]For full-length OmpA, data obtained with 10% dimyristoylphosphatidylglycerol in dimyristoylphosphatidylcholine host matrix.
[b]Values in parentheses are obtained with the barrel domain of OmpA (residues 0-176).

Similar conclusions to those drawn from Table 7.2 can also be deduced by analysing the dichroic ratios according to Eq. 7.1 for cylindrical β-barrels. The net values for the tilt, α, of the barrel are considerably larger, however, than those given in Table 7.2. Note that these values include the tilt of the β-strands in the periplasmic domains, in addition to that of the transmembrane β-barrel.

Experiments were also performed with a truncated form of OmpA, consisting of residues 0-176, that corresponds essentially to the transmembrane barrel domain. Order parameters and effective values for the tilt of the barrel axis are given by the values in parentheses in Table 7.2. The order parameters are higher (and the tilt angles corresponding are lower) for the barrel domain of OmpA than for the full-length protein, at least in the lipids of longer chainlengths. The effective tilt angles, θ, of the lipid chains, relative to the substrate normal, are given in Table 7.3.

Table 7.3 Effective tilt, θ (degrees), of lipid chains in aligned membranes of disaturated phosphatidylcholines, *di*C(*n*:0)PC, containing either OmpA or FhuA

C(*n*:0)	θ_s (2851 cm^{-1})[a]		θ_{as} (2921 cm^{-1})[b]	
	Gel	Fluid	Gel	Fluid
OmpA:				
C(12:0)	-	41 (37)[c]	-	41 (38)[c]
C(13:0)	27 (33)[c]	40 (33)[c]	29 (32)[c]	42 (35)[c]
C(14:0)	23 (32)[c]	28 (36)[c]	28 (34)[c]	32 (40)[c]
C(15:0)	41 (31)[c]	38 (37)[c]	41 (33)[c]	40 (38)[c]
C(17:0)	31 (33)[c]	30 (42)[c]	33 (35)[c]	32 (44)[c]
FhuA:				
C(12:0)	-	43	-	44
C(13:0)	28	43	26	42
C(14:0)	22	24	26	27
C(15:0)	30	41	33	43
C(17:0)	27	45	30	46

[a]Deduced from the dichroism of the CH_2 symmetric stretch band at 2851 cm^{-1}.
[b]Deduced from the dichroism of the CH_2 antisymmetric stretch band at 2921 cm^{-1}.
[c]Values in parentheses are for the reconstituted barrel domain of OmpA.

These values are derived from the dichroic ratios of the CH_2 symmetric and antisymmetric stretch bands at 2851 cm^{-1} and 2921 cm^{-1}, respectively. Eq. 7.1 is used for the order parameter of the lipid chains (with $\theta \equiv \alpha$), where the orientation of the transition moment for the CH_2 stretch vibrations is $\Theta = 90°$. Essentially consistent values for θ are obtained from the symmetric and antisymmetric stretch bands.

In the gel phase, the values of θ represent the tilt of the long axis of the nearly all-*trans* chains. (In the fluid phase, θ is an effective value that corresponds to the mean order parameter of the individual chain segments that are undergoing rotational isomerism.) For comparison, the tilt of the chains of disaturated phosphatidylcholines in gel-phase bilayers that is determined from x-ray diffraction, lies in the range $\theta = 30\text{-}35°$ (Marsh 1990). The

values of θ that are found for the gel-phase membranes in Table 7.3 are of a similar size and therefore suggest that the OmpA-containing membranes are reasonably well aligned.

7.5.2 Outer-membrane iron siderophore receptor FhuA

Figure 7.4 shows the polarised ATR spectra of the FhuA barrel domain in aligned membranes of dipentadecanoyl phosphatidylcholine. The amide I bands are particularly sharp in the dry state. The low-intensity $\nu_{//}(0,\pi)$ mode of the antiparallel β-sheet at ca. 1695 cm^{-1} is readily visible, in addition to the high intensity $\nu_{\perp}(\pi,0)$ mode at ca. 1630 cm^{-1}. Intermediate bands correspond to β-turns and unordered loops. Considerably broader amide I bands are obtained for the hydrated membranes, even in the gel phase. This corresponds to an increase in the protein dynamics, compared with the dry state. The overall band frequencies and secondary structure are, however, conserved.

Table 7.4 gives the results of band fitting for the amide I region from FhuA in hydrated membranes of disaturated phosphatidylcholines with different chain lengths. The β-sheet population displays a pattern similar to that found with OmpA in the same lipids, with a small decrease at shorter chain lengths. The effective β-sheet population is slightly less than that of OmpA. With the exception of *di*$C_{12:0}$PC, the mean β-sheet population deduced for the β-barrel domain of FhuA in the different lipids of Table 7.3 is 55 ± 3%. For comparison, the β-sheet content for residues 161-723 that is deduced from the crystal structure of FhuA is 63% (Ferguson et al. 2000); PDB:1QFG). The lower panel of Figure 7.3 shows the dependence on lipid chainlength of the amide I dichroic ratios for the β-barrel domain of FhuA.

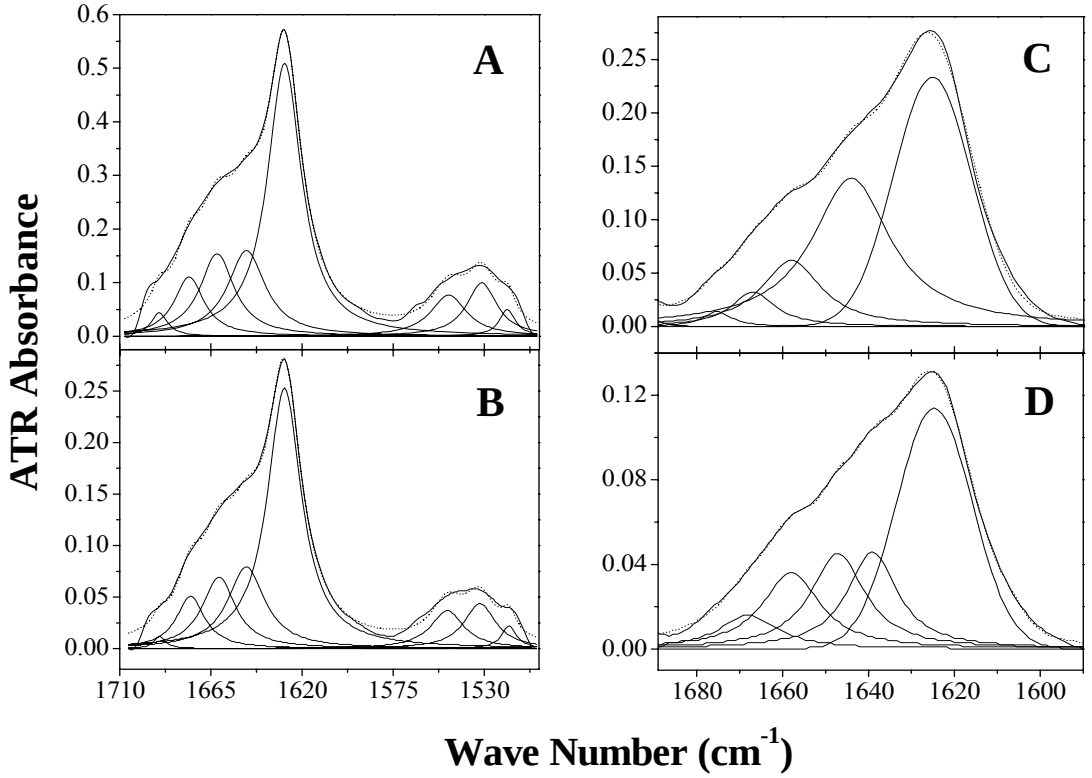

Figure 7.4 Polarised ATR-FTIR spectra of the β-barrel domain of FhuA reconstituted with dipentadecanoyl phosphatidylcholine lipid Spectra A and B are obtained in the dry state, whereas spectra C and D are obtained in the hydrated gel phase. The spectra in the upper panels (A, C) correspond to parallel polarisation, and in the lower panels (B, D) correspond to perpendicular polarisation of the incident radiation. Note the different ordinate scales. The dotted lines correspond to the theoretical fit with the bands obtained from the band fitting analysis shown below the experimental spectrum.

The dichroic ratios increase progressively with increasing chainlength of the reconstituting disaturated phosphatidylcholine phospholipid. From the amide I and amide II dichroic ratios of the dry samples, a consistent mean tilt of $\beta = 44.5° \pm 0.7°$ ($N = 5$) can be deduced from measurements in phosphatidylcholines of chainlengths from C(12:0) to C(17:0), by using Eqs. 7.2 and 7.3. Together with this value, the order parameters and mean tilts of the β-sheets of FhuA that are obtained from the amide I dichroic ratios, by using Eq. 7.2, are given in Table 7.5.

Table 7.4 Band fitting of the polarised ATR spectra from the amide I band of FhuA in hydrated disaturated phosphatidylcholines of different chainlengths, C(*n*:0), in the gel and fluid phases

C(*n*:0)	Gel		Fluid	
	position (cm^{-1})	normalised area (%)[a]	position (cm^{-1})	normalised area (%)[a]
C(12:0)	-	-	1625	40
			1641	29
			1652	21
			1662	8
			1671	2
C(13:0)	1624	48	1626	48
	1640	22	1641	12
	1649	16	1652	19
	1657	9	1662	14
	1666	5	1671	7
C(14:0)	1624	52	1625	52
	1639	12	1642	23
	1647	16	1653	19
	1655	13	1663	4
	1665	7	1669	2
C(15:0)	1625	52	1626	51
	1641	12	1641	11
	1648	18	1648	20
	1658	13	1658	12
	1667	5	1667	6
C(17:0)	1625	48	1626	46
	1640	17	1643	27
	1647	16	1651	14
	1656	12	1660	9
	1665	7	1668	4

[a]Relative band intensities are obtained by combining integrated absorbances, $A_{//}$ and $A_{\perp}$, with radiation polarised parallel and perpendicular, respectively, to the plane of the incident beam. The appropriate combination that reflects the full intensity is $A_{//} + \left(2E_z^2 / E_y^2 - E_x^2 / E_y^2\right)A_{\perp}$ (Marsh 1999).

Similar to the situation with OmpA, the orientation of FhuA improves progressively with increasing chainlength of the reconstituting lipid. However, the degree of orientation of FhuA is considerably greater in the fluid phase than in the gel phase, unlike for OmpA. Also, the order parameters for FhuA are greater than those for OmpA in

the same lipid system, in both fluid and gel phases. Again, analysis of the amide dichroism according to Eq. 7.1 for axially symmetric barrels leads to similar conclusions.

The mean strand tilt in the different host lipids is β = 42° ± 4°, similar to that obtained with the β-sheet formalism, but the order parameters for the barrel axis are considerably lower. Table 7.5 gives the effective tilt angles of the lipid chains for the various phosphatidylcholine membranes containing FhuA. As for membranes containing OmpA, the effective chain tilts in the gel phase are similar to those in gel-phase phosphatidylcholine bilayers. This suggests that the membranes containing FhuA are also reasonably well oriented.

Table 7.5 Order parameters, $\langle P_2(\cos\alpha)\rangle$, and mean effective inclinations, α, of the β-sheets of FhuA reconstituted in disaturated phosphatidylcholines, *di*C(*n*:0)PC, with different chainlengths, *n*, in the gel and fluid phases

C(*n*:0)	Gel		Fluid	
	$\langle P_2(\cos\alpha)\rangle$	α (°)	$\langle P_2(\cos\alpha)\rangle$	α (°)
C(12:0)	-	-	0.48	36
C(13:0)	0.31	43	0.51	35
C(14:0)	0.48	36	0.65	29
C(15:0)	0.57	33	0.79	22
C(17:0)	0.63	30	0.80	21

7.6 Discussion

Measurements from the amide infrared dichroism yield consistent values for the β-strand tilt in the different phosphatidylcholine lipid hosts. A somewhat larger value of the strand tilt (β ≈ 46 ± 1°) was obtained for OmpA than for FhuA (β ≈ 44.5 ± 1°). For comparison, the mean value of the strand tilt derived from the value of $\langle \cos^2\beta\rangle$ calculated using the crystal structure of OmpA (PDB: 1QJP) is β = 43.1° (Páli and Marsh 2001). This latter value includes only residues 1-171 of native mature OmpA (Pautsch and Schulz 2000), without the comparably large periplasmic domain that constitutes residues 172-325, and is closer to the value of β = 44 ± 1° obtained here for OmpA also truncated to residues

0-176. In the case of FhuA, a mean value of β = 38.3° (Páli and Marsh 2001) was obtained from the crystal structure (PDB:2FCP) for the β-barrel domain comprising residues 161-723 (Ferguson et al. 1998). This is significantly smaller than the value of the strand tilt obtained for FhuA truncated to the barrel domain from infrared dichroism. To the extent that the truncated barrel domain represents the whole protein, the somewhat larger tilt obtained in membranes may represent a slight relaxation of the FhuA barrel structure, relative to packing of the whole protein in the crystal. Correspondingly, from the change in bandwidths in Figures 7.2 and 7.4, a greater flexibility of the protein structure is evidenced in the hydrated membrane than in the dry membrane. Unfortunately, it is not possible to measure the dichroic ratio of the amide II band reliably in the hydrated state. Therefore, we used the strand tilt determined from the dry samples to deduce the order parameter of the protein in hydrated membranes. The above considerations suggest that this might introduce some uncertainty into the values obtained for the order parameter. However, this is less likely to affect the dependence of the protein order parameter on lipid chainlength. (Note that the strand tilt determined in the dry state is independent of chainlength.)

The values obtained for the strand tilt, β, from the polarised ATR measurements can be used to obtain estimates of the sheet twist, θ, and the strand coiling, ε, by using the expressions derived for idealised β-barrels (Marsh 2000):

$$\theta = \frac{\theta_o + \frac{2\pi}{n}\left[\left(\frac{h}{d}\right)^2 \frac{\cos\beta}{\tan\beta} + \sin\beta\right]}{\left(\frac{h}{d}\right)^2 \frac{1}{\tan^2\beta} + \frac{1}{\cos^2\beta}} \qquad \text{(Eq. 7.5)}$$

and

$$\varepsilon = \left(\frac{h}{d}\right)\left(\frac{2\pi}{n} - \frac{\theta}{\sin\beta}\right)\cos\beta \qquad \text{(Eq. 7.6)}$$

where the number of strands is n = 8 and 22 for OmpA and FhuA, respectively. Optimised values for the twist in an unstrained sheet of long strands, and for the characteristic dimensions of a β-sheet in this model are: θ_o = -3.4° and h/d = 0.719, respectively (Páli and Marsh 2001). This yields values for the twist of θ = 18° and for the coiling of ε = 10°, from

the IR dichroism of OmpA in lipid membranes. For comparison, the twist and coiling angles obtained from the x-ray coordinates of crystalline OmpA are: θ = 18.1° and ε = 12.0° (see ref. (Páli and Marsh 2001)). For the FhuA barrel domain, θ = 6° and ε = 4° from IR dichroism, as compared with θ = 6.8° and ε = 3.5° deduced from the x-ray coordinates (Páli and Marsh 2001). The barrel geometry is therefore similar in the two environments.

The crystal structure (Pautsch and Schulz 1998) or hydropathy analysis (Vogel and Jähnig 1986) of the OmpA transmembrane barrel shows that the hydrophobic belt and aromatic girdles comprise an average of five outward-facing residues in each of the eight strands of the β-barrel. With a mean strand tilt of 44±1°, the transmembrane thickness of this hydrophobic stretch is therefore predicted to be $10\times h\cos\beta = 2.5\pm0.05$ nm, where h = 0.345 nm (Arnott et al. 1967) is the rise per residue in an antiparallel β-sheet. This agrees well with recent estimates for a range of β-barrel proteins from the *E. coli* outer membrane (Lee 2003). Whereas there is little systematic change in lipid order with lipid chainlength (see Table 7.3), progressive changes are found in the protein orientation (see Tables 7.2 and 7.4). The increasing orientational order, or decreasing tilt, of the β-barrels with increasing chainlength of the host phosphatidylcholine lipid therefore arises undoubtedly from hydrophobic matching (or mismatching) between the protein and lipid. The tilt of the barrel will be reduced when the hydrophobic span of the lipid bilayer increases relative to that of the protein, and will increase when the lipid bilayer thickness decreases. The greater orientational freedom of OmpA in *di*$C_{12:0}$PC than in phosphatidylcholines with longer chains correlates well with the optimal folding and insertion of OmpA into large unilamellar vesicles composed of this lipid (Kleinschmidt and Tamm 2002). The membrane ordering of FhuA is greater than that of OmpA, in the fluid phase of any particular lipid host. This presumably is the result of the difference in barrel size. FhuA has cross-sectional dimensions 3.9 nm × 4.6 nm (Ferguson et al. 1998) that considerably exceed the membrane thickness, whereas OmpA has an outer diameter of ca. 2.4 nm (Pautsch and Schulz 1998). In the gel phase, however, the order of FhuA is more comparable to that of OmpA, most probably because the protein ordering is dominated in both cases by that of the close-packed all-*trans* lipid chains.

For the trimeric β-barrel porin OmpF from *E. coli*, the lipid binding constants of di *cis*-monounsaturated phosphatidylcholines have been measured as a function of lipid chainlength by competition experiments with brominated dioleoyl phosphatidylcholine (O'Keeffe et al. 2000). A maximum in affinity was found for *di*$C_{14:1}$PC, with a progressive

decrease for longer chainlengths. In the latter regime, the lipid hydrophobic thickness is expected to exceed that of the protein, which is consistent with the increasing order of OmpA and FhuA with increasing chainlength. Note that a maximum in ordering of the protein is not expected under conditions of hydrophobic matching. In a single-component lipid system, the protein order will either increase or remain constant as the hydrophobic length of the lipid exceeds that of the protein.

The bilayer thickness for a diunsaturated lipid is less than that for a disaturated lipid of equal chainlength (Lewis and Engelman 1983). Consequently, that of *di*$C_{14:1}$PC is comparable to that of *di*$C_{12:0}$PC for the disaturated lipids used in this study. Extrapolation of the optimised data given in ref. (Nagle and Tristram-Nagle 2000) for *di*$C_{14:0}$PC, *di*$C_{16:0}$PC and *di*$C_{18:1}$PC predicts a hydrophobic thickness of $2D_c$ = 2.4 nm for *di*$C_{12:0}$PC and $2D_c$ = 2.3 nm for *di*$C_{14:1}$PC. Thus the monotonic increase in ordering of OmpA and FhuA with lipid chainlength (Tables 7.2 and 7.5) is consistent with the chainlength dependence of the lipid affinities for OmpF. Highest affinity, i.e., best matching, is found for a bilayer hydrophobic thickness of 2.3 nm, which corresponds to *di*$C_{12:0}$PC in the saturated phosphatidylcholine series. From the crystal structures, it has been deduced that the hydrophobic thicknesses of OmpA, OmpF and FhuA are each ca. 2.4 nm (Lee 2003). This presumably corresponds to the hydrophobic thickness of the *E. coli* outer membrane that is reasonably well mimicked by *di*$C_{12:0}$PC or *di*$C_{14:1}$PC, according to the data in ref. (Nagle and Tristram-Nagle 2000). It is worth noting, however, that extrapolation of the x-ray scattering data of ref. (Lewis and Engelman 1983) yields estimates of 2.15 nm and 1.95 nm for the hydrophobic thicknesses of *di*$C_{14:1}$PC and *di*$C_{12:0}$PC bilayer membranes, respectively. Until now, this latter more extensive data set has been used routinely in the discussion of hydrophobic matching. These lower values would imply that *di*$C_{14:1}$PC and *di*$C_{12:0}$PC bilayers are appreciably shorter than the hydrophobic thickness of the *E. coli* outer membrane. According to ref. (Lewis and Engelman 1983), the hydrophobic thickness of *di*$C_{14:0}$PC is 2.3 nm. This would correlate better with the chainlength dependence of the infrared order parameters that is given in Tables 7.2 and 7.5. The onset of maximum ordering, which presumably corresponds to achieving hydrophobic matching, occurs for phosphatidylcholine chainlengths C(14:0)-C(15:0). Significantly, the lipopolysaccharide component of the outer membrane is characterised by relatively short chains, both C12 and C14 (Harwood and Russell 1984).

It is significant to note that recent simulations of OmpA and OmpT in dimyristoyl phosphatidylcholine bilayers by means of molecular dynamics have revealed a dynamic tilt

of the β-barrel axis, relative to the membrane normal (Bond et al. 2002; Baaden and Sansom 2004). A tilt of ca. 5-10° was detected for OmpA and of ca. 20° for OmpT, although the duration of the simulation was probably insufficient to ensure a true thermodynamic average for this cooperative motion of the lipids plus protein. Because this represents a rigid body motion, off-axis rotations of finite amplitude are likely to be a general feature of small transmembrane proteins, including α-helical bundles. In the latter case, infrared dichroism cannot distinguish off-axis motion from the static tilt of individual helices, relative to the protein symmetry axis (Marsh 1998). This dynamic feature of protein incorporation into fluid lipid membranes may have functional significance. Our results with FhuA indicate that such effects will be less important for larger transmembrane proteins.

Summary

Life, in the form we know it, could not be imagined without the existence of biomembranes. They are a prerequisite for the formation and functioning of cells and different organelles within the cell. Biomembranes contain phospholipids and proteins in approximately equal amounts. Although intensively studied, many questions about their organization and function remained unanswered. During their biosynthesis, many secretory and plasma membrane proteins are transported across the endoplasmic reticulum (ER) membrane in eukaryotes or across the cytoplasmic membrane in prokaryotes. How do membrane proteins insert and fold for example into the outer membrane of bacteria after translocation is largely unknown.

Both classes namely α-helical and β-barrel integral membrane proteins (IMPs) require either detergent micelles or lipid bilayers for folding. This thesis is focused on the folding mechanism of outer membrane proteins (OMPs) of Gram-negative bacteria that form transmembrane β-barrels. Currently there are several studies on the folding of OMPs into detergent micelles while only the outer membrane protein A (OmpA) from *Escherichia coli* has been shown to quantitatively fold into lipid bilayers and has been successfully used as a model for studying the mechanism of folding of OMPs into phospholipids bilayers. The fatty core of a phospholipid bilayer requires hydrophobic amino acid residues at the interface of the integral membrane protein to the fatty acyl chains of the phospholipids. Polar amide groups of transmembrane proteins that are located in the fatty region of the membrane must form hydrogen bonds with a carbonyl oxygene of a peptide bond in close vicinity to allow the stable assembly of a protein segment in the hydrophobic region of the lipid bilayer.

This thesis describes several important advancements in the study of membrane protein folding of OMPs that will be summarized in separate paragraphs below. In the first project a new technology for isolating large amounts of β-barrel membrane proteins was established using amphipathic polymers (amphipols). To characterize similarities and differences to OmpA folding into lipid bilayers the kinetics of OmpA folding into

amphipols were studied in a second investigation. In a third study the folding kinetics of the major non-specific porin FomA of *Fusobacterium nucleatum* into lipid bilayers were characterized. It is shown that FomA can serve as a second, alternative model to study the folding of outer membrane proteins. Thermodynamics of folding are linked to energetics of unfolding. In a fourth investigation unfolding experiments were carried out in order to calculate the energy of folding. The ferrichrome-iron receptor FhuA from *E. coli* was used as an example. In the last two studies, lipid-protein interactions, that may be critical for the folding process were studied on the examples of OmpA and FhuA.

In view of their biotechnological importance and of relatively few available structures, I have explored in this thesis novel strategies to isolate large amounts of functionally active membrane proteins. I developed a completely new technology to refold overexpressed, but functionally inactive membrane proteins into an amphipathic polymer, a synthetic non-detergent surfactant. In contrast to detergent micelles, amphipols have a non-dissociating structure in aqueous solution and therefore better preserve the integrity and activity of OMPs. I found that the presence of a non-denaturing amphipathic environment — shielding the transmembrane region from water — suffices to allow OMPs to fold to their native structure. Folding was studied using the outer membrane proteins OmpA, FomA and the human voltage-dependent anion channel hVDAC1 (also known as mitochondrial porin). Neither natural biological compounds nor detergents were required for folding. I demonstrated that these novel tools in membrane protein research can be instrumental for the large-scale functional refolding of integral membrane proteins.

Since I was interested in the mechanism of membrane protein folding and since folding of OmpA into amphipol A8-35 may by quite different from the folding of OmpA into lipid bilayers, I investigated the folding kinetics of OmpA into amphipol A8-35 as functions of temperature and amphipol concentration. OmpA folding into amphipols revealed a two-phase refolding mechanism indicating two-parallel folding pathways. At 40 °C, folding kinetics could be fitted by a first order rate law while below 40 °C, folding kinetics were more complex and two folding phases were observed. The folding kinetics were fitted by double-exponential functions and the two rate constants were calculated at each temperature. Activation energies were ~5-6 kJ/mol for the fast phase and ~27-35 kJ/mol for the slower phase independent of the experimental method. Equilibrium

unfolding revealed that OmpA folding/unfolding into A8-35 was fully reversible and that amphipol-refolded OmpA was thermodynamically stable at room temperature.

The lipid bilayers, which form the backbone of biological membranes, have been extensively studied in the past as models for biomembranes. The biophysical principles of insertion and folding of integral membrane proteins are best studied with lipid bilayers in well-defined *in vitro* model systems. Previously, OmpA has been the only outer membrane protein for which quantitative refolding into lipid bilayers from a completely denatured state in 8 M urea could be observed. Since OmpA, which has a 171 residue 8-stranded β-barrel transmembrane domain refolds into phospholipid bilayers, this OMP has been an extensively studied model. In the current work, I have showed that FomA may serve as an alternative model to OmpA to study the membrane protein insertion and folding. Initial trials to fold the much bigger FhuA failed. In contrast to the 8-stranded transmembrane β-barrel of OmpA, FomA forms a much larger transmembrane domain that is predicted to consist of 14 β-strands. FomA, over-expressed in *E. coli* in form of inclusion bodies, was solubilized in 10 M urea in denatured form and shown to insert and fold into phospholipid bilayers. I demonstrate that folding is quantitative when performed with lipid bilayers of short-chain phospholipids at basic pH. Successful refolding is demonstrated by circular dichroism and fluorescence spectroscopy, by SDS-polyacrylamide gel-electrophoresis, and by single channel recordings. Refolded FomA had an average single channel conductance of 1.1 nS, in agreement with previous studies on FomA isolated from membranes in native form.

Insertion and folding was also successful with detergent micelles for example of LDAO and with bilayers of dioleoyl phosphatidylcholine. The kinetics of bilayer insertion and folding of FomA were analyzed by electrophoresis and were faster for bilayers of the short-chain dicapryl phosphatidylcholine than for bilayers of dioleoyl phosphatidylcholine. In contrast to the previously described folding kinetics of OmpA into these lipids, the kinetics of FomA folding were slower and were well described only by double-exponential functions. The kinetics provided evidence for parallel folding pathways of FomA *in vitro*. For folding into each of the lipid bilayers, the two kinetic pathways were strongly temperature-dependent with estimated activation energies of 19 kJ/mol (dicapryl phosphatidylcholine) and 70 kJ/mol (dioleoyl phosphatidylcholine) for the faster pathways. Both OmpA folding into amphipol A8-35 and FomA folding into lipid bilayers indicated

parallel folding pathways. A more detailed study is needed in order to examine whether they are related or entirely different.

The thermodynamics of folding can be investigated in unfolding experiments. To obtain the energy gain upon folding, unfolding experiments were carried out and the energy of unfolding was determined. Detergent–micelle extraction of IMPs for structural and functional studies often leads to a strong loss in protein activity suggesting that the protein becomes thermodynamically less stable. To quantitatively assess the destabilization, I have performed unfolding studies using the FhuA as an example. Unfolding was monitored by fluorescence spectroscopy and the stabilities of wt-FhuA and the mutant FhuAΔ5-160 were determined in lipid bilayers and in detergent micelles, respectively.

Wild-type (wt) FhuA consists of a 22-stranded β-barrel domain and an N-terminal cork domain (residues 1-160) inside the barrel. At 35 °C, the energy required for unfolding of FhuAΔ5–160 from a bilayer integrated state was about 21 kJ/mol, i.e. 4 times larger than for FhuAΔ5–160 that was solubilized in micelles of the detergent LDAO ($\Delta E \approx 5$ kJ/mol). Urea-induced unfolding of detergent-solubilized wt–FhuA and FhuAΔ5–160, indicated that the β-barrel domain of wt–FhuA is stabilized by interactions with the cork domain. When wt-FhuA was reconstituted into a phospholipid membrane, unfolding of the cork domain preceded unfolding of the β-barrel domain. These two steps could not be distinguished in the urea-induced unfolding of the detergent-micelle solubilized form of wt-FhuA. Our results indicate that the stability of membrane proteins is most strongly affected by the structure of the supramolecular assembly (micelle vs. bilayer) rather than by the chemical structure of monomeric amphiphiles. I found that FhuA is strongly stabilized by the cork domain, by the lipid bilayer and by the bilayer thickness.

The stoichiometry and selectivity of β-barrel OMPs for lipids are very important for the study of OMPs folding. These were studied using spin-labelled lipids and electron spin resonance (ESR) as previously used for α-helical integral proteins. OmpA and FhuA were reconstituted in bilayers of dimyristoyl phosphatidylglycerol. The ESR spectra from phosphatidylglycerol spin-labelled on the 14-C atom of the *sn*-2 chain contain a second component from motionally restricted lipids contacting the intramembranous surface of the β-barrel, in addition to that from the fluid bilayer lipids. The stoichiometry of motionally restricted lipids, 11 and 32 lipids/monomer for OmpA and FhuA, respectively, is constant

irrespective of lipid/protein ratio. It is proportional to the number of transmembrane β-strands, 8 for OmpA and 22 for FhuA, and correlates well with the intramembranous perimeter of the protein. Spin-labelled lipids with different polar headgroups display a differential selectivity of interaction with the two proteins. The more pronounced pattern of lipid selectivity for FhuA than for OmpA correlates with the preponderance of positively charged residues facing the lipids in the extensions of the β-sheet and shorter interconnecting loops, on the extracellular side.

In the last chapter of my thesis, polarised attenuated total internal reflection Fourier-transform infrared spectroscopy (ATR-FTIR) has been used to determine the orientation of the β-barrels in phosphatidylcholine host matrices of different lipid chainlengths. The linear dichroism of the amide I band from OmpA and FhuA in hydrated membranes generally increases with increasing chainlength from *di*$C_{12:0}$PC to *di*$C_{17:0}$PC phosphatidylcholine, in both the fluid and gel phases. Measurements of the amide I and amide II dichroism from dry samples are used to deduce the strand tilt ($\beta = 46°$ for OmpA, and $\beta = 44.5°$ for FhuA). These values are then used to deduce the order parameters, $\langle P_2(\cos\alpha)\rangle$, of the β-barrels from the amide I dichroic ratios of the hydrated membranes. The orientational ordering of the β-barrels, and their assembly in the membrane, are discussed in terms of hydrophobic matching with the lipid chains.

Zusammenfassung

Das Leben, wie wir es kennen, ist ohne die Existenz von Biomembranen nicht vorstellbar. Biologische Membranen sind eine Voraussetzung für die Bildung und das Funktionieren von Zellen und der verschiedenen Organellen inerhalb der Zelle. Die Biomembranen enthalten Phospholipide und Proteine in etwa gleiche Masse. Während ihrer Biosynthese werden viele sekretorische und Plasmamembranproteine durch die Membran des endoplasmatischen Retikulums (ER) von Eukaryoten oder durch die cytoplasmatische Membran von Prokaryoten transportiert. Über den Einbauprozess von integralen Membranproteinen in biologische Membranen ist nur wenig bekannt. So ist beispielsweise nicht geklärt, wie Aussenmembranproteine der Zellwand Gram-negativer Bakterien nach ihrer Translokation durch die Cytoplasmamembran in die äussere Membran einbauen und falten.

Beide Klassen integraler Membranproteine (IMPs), nämlich α-helikale und β-Fass Membranproteine erfordern für die Faltung entweder Detergenzmicellen oder Lipiddoppelschichten. Der Schwerpunkt dieser Dissertation ist das Studium der Faltung von Aussermembranproteinen (OMPs) Gram-negativer Bakterien, die β-Fass-Transmembranstrukturen ausbilden. Eine Reihe von Untersuchungen über die Faltung von OMPs wurden in Detergenzmicellen durchgeführt. Das einzige äussere Membranprotein, das bislang quantitativ in Lipiddoppelschichten faltet und erfolgreich als Modell für das Studium des Faltungsmechanismus von OMPs in Phospholipiddoppelschichten benutzt wurde, ist OmpA von *Escherichia coli*. Die hydrophobe Region einer Phospholipiddoppelschicht erfordert hydrophobe Aminosäurereste an der Oberfläche des integralen Membranenproteins zu den apolaren Acylketten der Phospholipide. Die polaren Amidgruppen der Transmembranproteine müssen Wasserstoffbindungen mit einem Carbonylsauerstoffatom einer Peptidbindung bilden, um den stabilen Einbau eines Proteinsegments in die hydrophobe Region der Lipiddoppelschicht zu ermöglichen.

Diese Dissertation beschreibt mehrere wichtige Fortschritte für das Studium der Membranproteinfaltung von OMPs die unten in separaten Abschnitten zusammengefasst

werden. Im ersten Projekt, wurde eine neue Tehnologie für die Isolierung von grösseren Mengen von β-Fass Membranproteinen mit Hilfe von amphipathischen Polymeren (Amphipolen) entwickelt. Die Unterschiede und die Ähnlichkeiten zwischen der OmpA Faltung in Lipiddoppelschichten bzw. in Amphipolen wurden in eine zweite Untersuchung studiert. In einer dritten Studie wurden die Faltungskinetiken des unspezifischen Porins FomA von *Fusobacterium nucleatum* in Lipiddoppelschichten untersucht. Es wird gezeigt, daß FomA als zweites alternatives Modell für die Faltung der äußeren Membranenproteinen, zusätzlich zu OmpA dienen kann. Die Thermodynamik der Faltung kann durch das Studium der Entfaltung beschrieben werden. In einem vierten Projekt wurden die Energieumsätze bei der Faltung eines Membranproteins untersucht. Der Ferrichromtransporter FhuA von *E. coli* wurde als Beispiel benutzt. In den letzten zwei Studien wurden Lipid/Protein Wechselwirkungen, die für den Faltungsprozess kritisch sein können, am Beispiel von OmpA und von FhuA studiert.

Zunächst habe ich angesichts der biotechnologischen Bedeutung und von verhältnismäßig wenigen bekannten hochaufgelösten Strukturen, neue Strategien erprobt, größere Mengen funktionell aktiver Membranenproteine zu isolieren. Ich habe eine vollständig neue Technik für die Reaktivierung von überexprimierten, aber inaktiven Membranproteinen entwickelt. Dazu wurde ein synthetisches polymeres Tensid, ein amphypathisches Polymer (Amphipol) benutzt. Im Gegensatz zu Detergenzmicellen haben Amphipole eine nichtdissoziierende Struktur in wässeriger Lösung und erhalten die Integrität und die Funktion von OMPs über einen längeren Zeitraum als Detergenzmicelles. Ich zeige mit Hilfe des Amphipols A8-35, dass das Vorhandensein eines nicht-denaturierenden amphipathischen Milieus genügt, um die Transmembranregion des OMPs vom Wasser abzuschirmen und die OMPs korrekt falten zu lassen. Die Faltung wurde am Beispiel des äußeren Membranproteins OmpA, FomA und des menschlichen Spannung-abhängigen Anionenkanal hVDAC1 (auch bekannt als mitochondrisches Porin) studiert. Weder natürliche biologische Verbindungen noch Detergenz waren für die Faltung notwendig. Diese Studie zeigt, dass Amphipole in der Membranproteinforschung für die funktionelle Rückfaltung integraler Membranproteine in großen Mengen sehr gut einsetzbar sind.

Da der Mechanismus der Membranproteinfaltung von grundlegenden Interesse ist und weil die OmpA Faltung in Amphipol A8-35 möglicherweise unterschiedlich zu der

Faltung von OmpA in Lipiddoppelschichten ablaufen kann, habe ich die Kinetik der OmpA Faltung in Amphipol A8-35 als Funktion der Temperatur- und der Amphipolkonzentration erforscht. Die OmpA Faltung in Amphipol A8-35 zeigt mindestens zwei parallele Faltungswege, im Unterschied zu früheren Arbeiten über die Faltung von OmpA in Lipiddoppelschichten. Bei 40 °C konnte die Kinetik der Faltung jedoch auch durch einen einzigen Faltungsweg erklärt werden. Unterhalb von 40 °C waren die Kinetiken der Faltung komplizierter und zwei Faltungsphasen wurden beobachtet. Um die Kinetiken der Faltung anzupassen, wurden doppelt-exponentielle Funktionen benutzt. Die Geschwindigkeitskonstanten wurden bei jeder Temperatur errechnet. Die Aktivierungsenergien waren ~5-6 kJ/mol für den schnellen Weg und ~27-35 kJ/mol für den langsamen Weg, unabhängig von der experimentellen Methode. Gleichgewichtsentfaltungsstudien zeigten, dass die OmpA Faltung/Entfaltung in A8-35 völlig reversibel ist und dass Amphipol-rückgefaltetes OmpA bei Raumtemperatur thermodynamisch stabil ist.

Die Lipiddoppelschichten, die das Rückgrat der biologischen Membranen bilden, werden als Modelle für Biomembranen eingehend studiert. Die biophysikalischen Grundregeln der Faltung und des Einbaus integraler Membranproteine in Lipiddoppelschichten wurden bislang jedoch wenig untersucht. OmpA ist bisher das einzige äußere Membranprotein, für das die quantitative Rückfaltung in Lipiddoppelschichten aus einem vollständig denaturierten Zustand im 8 M Harnstoff beobachtet werden konnte. Deswegen ist dieses OMP ein intensiv studiertes Modell für das Studium der Faltung von β-Fass Membranproteinen. In der gegenwärtigen Arbeit habe ich gezeigt, dass FomA als ein alternatives Modell für die Untersuchung des Membranenproteineinbaus und der Faltung dienen kann. Erste Versuche zur Faltung des viel grösseren FhuA waren hingegen nicht erfolgreich. Im Gegensatz zu dem 8-strängigen β-Fass von OmpA, bildet FomA eine viel größere Transmembrandomäne aus, für die vorhergesagt wird, dass sie aus 14 β-Strängen besteht. FomA, das in *E. coli* in Form von Einschlusskörpern überexprimiert wurde, kann in 10 M Harnstoff in entfalteter Form solubilisiert und danach durch Harnstoffverdünung in Phospholipiddoppelschichten gefaltet werden. Ich habe gezeigt, dass die Faltung quantitativ war, wenn sie mit Lipiddoppelschichten kurzgekettiger Phospholipide bei basischem pH durchgeführt wurde. Die erfolgreiche Rückfaltung wurde mittels CD- und Fluoreszenz-Spektroskopie, SDS-Polyacrylamid-Gelelektrophorese und durch Einzelkanalmessungen bestätigt.

Rückgefaltetes FomA hatte eine durchschnittliche Einzelkanalleitfähigkeit von 1,1 nS, in Übereinstimmung mit früheren Untersuchungen an FomA, das ohne Entfaltung aus Membranen isoliert wurde.
Der Einbau und die Faltung von FomA in aktiven Zustand waren mit Detergenzmicellen und auch mit Doppelschichtmembranen des Dioleoylphosphatidylcholins erfolgreich. Die Kinetiken des Doppelschichteinbaus und der Faltung des FomA wurden mittels Elektrophorese analysiert. Die Kinetiken waren für die Doppelschichten des kurzgekettigen Dicaprylphosphatidylcholins schneller als für die Doppelschichten des Dioleoylphosphatidylcholins. Im Gegensatz zur früher beschriebenen Kinetik der OmpA-Faltung in diese Lipide waren die Kinetiken der FomA Faltung langsamer und konnten nur durch doppelt-exponentielle Funktionen gut beschrieben werden. Die Kinetiken zeigten parallele Faltungswege von FomA *in vitro*. Für die Faltung in jede der Lipiddoppelschichten, waren die beiden kinetischen Faltungswege stark temperaturabhängig, mit Aktivierungsenergien von 19 kJ/mol (Dicaprylphosphatidylcholin) und von 70 kJ/mol (Dioleoylphosphatidylcholin) für die schnelleren Faltungswege. Sowohl die Kinetiken der OmpA Faltung in Amphipol A8-35 als auch die Kinetiken der FomA Faltung in Lipiddoppelschichten zeigen parallele Faltungswege an. Eine ausführlichere Studie ist erforderlich, um zu überprüfen, ob diese Faltungswege in Bezug zu einander stehen oder ob sie völlig unterschiedlich sind.

Die Thermodynamik der Faltung kann in Entfaltungsexperimenten untersucht werden. Um den Energiegewinn durch die Faltung zu bestimmen, wurden Entfaltungsexperimente durchgeführt und die zur Entfaltung notwendige Energie wurde ermittelt. Entfaltung wurde mittels Fluoreszenzspektroskopie erforscht und die Stabilitäten des Wildtyp-FhuA (wt-FhuA) und einer Mutante (FhuAΔ5-160), wurden in den Lipiddoppelschichten und in Detergenzmicellen ermittelt. Die Extraktion von IMPs in Detergenzmicellen für strukturelle und funktionelle Studien führt häufig zu einen starken Verlust an Proteinaktivität. Dies zeigt, dass das Protein thermodynamisch weniger stabil ist. Um diese Destabilisierung quantitativ zu ermitteln, habe ich Entfaltungsstudien mit dem integralen Membranenprotein FhuA als Beispiel in Doppelschichten und in Micellen durchgeführt.

Wt-FhuA besteht aus einem 22-strändigen β-Fass und aus einer N-terminalen Korkdomäne (Aminosäurereste 1-160) innerhalb des Fasses. Bei 35 °C war die Entfaltungsenergie von FhuAΔ5-160 in Lipiddoppelschichten ca. 21 kJ/mol, d.h. etwa 4

mal größer als für FhuAΔ5-160, in LDAO Detergenzmicellen (ΔE ≈ 5 kJ/mol). Die Harnstoff-induzierte Entfaltung von in Detergenz gelöstem wt-FhuA oder FhuAΔ5-160 zeigten, dass das β-Fass des wt-FhuA durch die Korkdomäne stabilisiert wird. Nach Rekonstitution von wt-FhuA in Phospholipiddoppelschichten, entfaltete die Korkdomäne des FhuA vor der β-Fassdomäne. Diese zwei Schritte konnten bei der Entfaltung aus in Detergenzmicellen gelöstem wt-FhuA nicht unterschieden werden. Unsere Ergebnisse zeigten, dass die Stabilität der Membranproteine durch die supramolekulare Struktur (Micelle oder Doppelschicht) sehr stark beeinflusst wird. Ich haben gefunden, dass FhuA stark durch die Korkdomäne, durch die Lipiddoppelschichten und durch die Doppelschichtdicke stabilisiert wird.

Die Stöchiometrie und Selektivität der β-Fass OMPs OmpA und FhuA für Lipide ist mit Hilfe von Spin Markierungen und Elektronenspinresonanz - (ESR) - spektroskopischen Methoden studiert worden, die sich für α-helicale Membranproteine bewährt haben. OmpA und FhuA wurden dazu in Dimyristoylphosphatidylglycerol-doppelschichten rekonstituiert. Die ESR-Spektren von Phosphatidylglycerol, das an Atom C-14 der *sn-2* Kette spin-markiert war, enthielten eine zweite Komponente von immobilisierten Lipiden in Kontakt mit der Intramembranoberfläche des β-Fasses, zusätzlich zum Spektrum der Spin-Label in der flüssigen Doppelschicht. Die Stöchiometrie beweglich eingeschränkter Lipide ist ungeachtet des Lipid/Proteinverhältnisses konstant, und zwar 11 bzw. 32 Lipide/Monomer für OmpA und FhuA. Sie ist zur Zahl der β-Stränge, 8 in OmpA und 22 in FhuA, proportional und in guter Übereinstimmung mit dem Umfang des Proteins in der Membran. Spin-markierte Lipide mit unterschiedlich polaren Kopfgruppen zeigen eine differentielle Selektivität für beide Proteine. Die Lipidselektivität ist für FhuA ausgeprägter als für OmpA und steht in Bezug zu überwiegend positiv geladenen Aminosäureresten, die mit den Lipiden in Kontakt sind.

Im letzten Kapitel meiner Dissertation, ist „polarized attenuated total internal reflection – Fourier transform infrared spectroscopy“ (ATR-FTIR) ist verwendet worden, um die Orientierung der β-Fässer in Phosphatidylcholindoppelschichten unterschiedlicher Lipidkettenlänge festzustellen. Der lineare Dichroismus der Amid I Bande von OmpA und von FhuA in hydratisierten Membranen nahm im allgemeinen mit Zunahme der Kettenlänge des Phosphatidylcholins von *di*$C_{12:0}$PC bis *di*$C_{17:0}$PC zu, sowohl in der flüssigen als auch in der Gelphase. Die Messungen des Lineardichroismus der Amid I und

der Amid II Bande trockener Proben wurden verwendet, um die Neigung der β-Stränge zu bestimmen (β = 46° für OmpA und β = 44.5° für FhuA). Diese Werte wurden dann verwendet, um die Ordnungsparameter, $\langle P_2(\cos\alpha)\rangle$, der β-Fässer aus den dichroitischen Verhältnissen der Amid I Bande zu bestimmen. Die Orientierung der β-Fässer und ihr Einbau in die Membran, wurden hinsichtlich der Übereinstimmung der hydrophoben Schichtdicke der Membran mit der Länge der hydrophoben Transmembranregion der Proteine diskutiert.

List of publications

Pocanschi, C.L., Dahmane, T., Apell, H.J., Gohon, Y., Kleinschmidt, J.H. and Popot, J.L. (2005) Amphipathic polymers: tools to fold integral membrane proteins to their active form. (*submitted*)

Pocanschi, C.L., Popot, J.L. and Kleinschmidt, J.H. (2005) Folding kinetics of the outer membrane protein OmpA of *E. coli* into the amphipathic polymer A8-35. (*submitted*)

Pocanschi, C.L., Apell, H.J., Puntervoll, P., Høgh, B., Jensen, H.B., Welte, W. and Kleinschmidt, J.H. (2005) The major outer membrane protein of *Fusobacterium nucleatum* (FomA) folds and inserts into lipid bilayers via parallel folding pathways. (*J Mol Biol*, *in press*)

Pocanschi, C.L. and Kleinschmidt, J.H. (2005) Folding, chain-length and lipid headgroup dependence of the stability of the iron-siderophore receptor FhuA in lyso-lipid micelles and lipid bilayers. (*in preparation*)

Pocanschi, C.L. and Kleinschmidt, J.H. (2005) The iron-siderophore receptor FhuA of *E.coli* is strongly stabilized by the cork domain and by the lipid bilayer. (*in preparation*)

Ramakrishnan, M., **Pocanschi, C.L.**, Kleinschmidt, J.H. and Marsh, D. (2004) Association of spin-labeled lipids with β-barrel proteins from the outer membrane of *Escherichia coli*. *Biochemistry* **43**(37), 11630-6

Ramakrishnan, M., Qu, J., **Pocanschi, C.L.**, Kleinschmidt, J.H. and Marsh, D. (2005) Orientation of β-barrel proteins OmpA and FhuA in lipid membranes. Chain length dependence from infrared dichroism. *Biochemistry* **44**(9), 3515-23

References

Abrecht, H., E. Goormaghtigh, et al. (2000). "Structure and orientation of two voltage-dependent anion-selective channel isoforms. An attenuated total reflection fourier-transform infrared spectroscopy study." J Biol Chem **275**(52): 40992-9.

Adams, V., L. Griffin, et al. (1991). "Porin interaction with hexokinase and glycerol kinase: metabolic microcompartmentation at the outer mitochondrial membrane." Biochem Med Metab Biol **45**(3): 271-91.

Adler, A. J., N. J. Greenfield, et al. (1973). "Circular dichroism and optical rotatory dispersion of proteins and polypeptides." Methods Enzymol **27**: 675-735.

Ahn, V. E., E. I. Lo, et al. (2004). "A hydrocarbon ruler measures palmitate in the enzymatic acylation of endotoxin." EMBO J **23**(15): 2931-41.

Andrade, M. A., P. Chacon, et al. (1993). "Evaluation of secondary structure of proteins from UV circular dichroism spectra using an unsupervised learning neural network." Protein Eng **6**(4): 383-90.

Anfinsen, C. B. (1973). "Principles that govern the folding of protein chains." Science **181**(96): 223-30.

Arnott, S., S. D. Dover, et al. (1967). "Structure of β-poly-L-alanine: refined atomic co-ordinates for an anti-parallel β-pleated sheet." J Mol Biol **30**(1): 201-8.

Arora, A., F. Abildgaard, et al. (2001). "Structure of outer membrane protein A transmembrane domain by NMR spectroscopy." Nat. Struct. Biol. **8**(4): 334-8.

Arora, A., D. Rinehart, et al. (2000). "Refolded outer membrane protein A of *Escherichia coli* forms ion channels with two conductance states in planar lipid bilayers." J. Biol. Chem. **275**(3): 1594-600.

Atkins, P. W. (1994). Physical chemistry. Oxford, Oxford University Press.

Aune, K. C. and C. Tanford (1969). "Thermodynamics of the denaturation of lysozyme by guanidine hydrochloride. I. Depdendence on pH at 25 degrees." Biochemistry **8**(11): 4579-85.

Ausubel, F. M., R. Brent, et al. (1999). Short Protocols in Molecular Biology. New York, John Wiley & Sons Inc.

Baaden, M. and M. S. Sansom (2004). "OmpT: molecular dynamics simulations of an outer membrane enzyme." Biophys J **87**(5): 2942-53.

Bakken, V., S. Aaro, et al. (1989). "Purification and partial characterization of a major outer-membrane protein of *Fusobacterium nucleatum*." J Gen Microbiol **135**(12): 3253-62.

Beher, M. G., C. A. Schnaitman, et al. (1980). "Major heat-modifiable outer membrane protein in gram-negative bacteria: comparison with the ompA protein of *Escherichia coli*." J Bacteriol **143**(2): 906-13.

Behlau, M., D. J. Mills, et al. (2001). "Projection structure of the monomeric porin OmpG at 6 Å resolution." J. Mol. Biol. **305**(1): 71-7.

Behrens, S., R. Maier, et al. (2001). "The SurA periplasmic PPIase lacking its parvulin domains functions *in vivo* and has chaperone activity." EMBO J. **20**(1-2): 285-94.

Benz, R. (1994). "Permeation of hydrophilic solutes through mitochondrial outer membranes: review on mitochondrial porins." Biochim Biophys Acta **1197**(2): 167-96.

Benz, R. and K. Bauer (1988). "Permeation of hydrophilic molecules through the outer membrane of gram-negative bacteria. Review on bacterial porins." Eur J Biochem **176**(1): 1-19.

Benz, R., K. Janko, et al. (1978). "Formation of large, ion-permeable membrane channels by the matrix protein (porin) of *Escherichia coli*." Biochim Biophys Acta **511**(3): 305-19.

Berven, F. S., K. Flikka, et al. (2004). "BOMP: a program to predict integral β-barrel outer membrane proteins encoded within genomes of Gram-negative bacteria." Nucleic Acids Res **32**(Web Server issue): W394-9.

Blackshear, P. J. (1984). "Systems for polyacrylamide gel electrophoresis." Methods Enzymol **104**: 237-55.

Bolla, J. M., C. Lazdunski, et al. (1988). "The assembly of the major outer membrane protein OmpF of *Escherichia coli* depends on lipid synthesis." EMBO J **7**(11): 3595-9.

Bond, P. J., J. D. Faraldo-Gomez, et al. (2002). "OmpA: a pore or not a pore? Simulation and modeling studies." Biophys J **83**(2): 763-75.

Bonhivers, M., M. Desmadril, et al. (2001). "Stability studies of FhuA, a two-domain outer membrane protein from *Escherichia coli*." Biochemistry **40**(8): 2606-13.

Booth, P. J. and A. R. Curran (1999). "Membrane protein folding." Curr Opin Struct Biol **9**(1): 115-21.

Booth, P. J. and S. High (2004). "Polytopic membrane protein folding and assembly in vitro and in vivo." Mol Membr Biol **21**(3): 163-70.

Bothmann, H. and A. Plückthun (1998). "Selection for a periplasmic factor improving phage display and functional periplasmic expression." Nat. Biotechnol. **16**(4): 376-80.

Bothmann, H. and A. Plückthun (2000). "The periplasmic *Escherichia coli* peptidylprolyl cis,trans-isomerase FkpA. I. Increased functional expression of antibody fragments with and without cis-prolines." J. Biol. Chem. **275**(22): 17100-5.

Boyd, D., C. Schierle, et al. (1998). "How many membrane proteins are there?" Protein Sci **7**(1): 201-5.

Braun, M., H. Killmann, et al. (1999). "The β-barrel domain of FhuAΔ5-160 is sufficient for TonB-dependent FhuA activities of *Escherichia coli*." Mol Microbiol **33**(5): 1037-49.

Braun, V. (1998). "Pumping iron through cell membranes." Science **282**(5397): 2202-3.

Brotherus, J. R., O. H. Griffith, et al. (1981). "Lipid-protein multiple binding equilibria in membranes." Biochemistry **20**(18): 5261-7.

Buchanan, S. K. (1999). "β-barrel proteins from bacterial outer membranes: structure, function and refolding." Curr Opin Struct Biol **9**(4): 455-61.

Buchanan, S. K., B. S. Smith, et al. (1999). "Crystal structure of the outer membrane active transporter FepA from *Escherichia coli*." Nat. Struct. Biol. **6**(1): 56-63.

Bulieris, P. V., S. Behrens, et al. (2003). "Folding and insertion of the outer membrane protein OmpA is assisted by the chaperone Skp and by lipopolysaccharide." J Biol Chem **278**(11): 9092-9.

Busath, D. and G. Szabo (1981). "Gramicidin forms multi-state rectifying channels." Nature **294**(5839): 371-3.

Casadio, R., I. Jacoboni, et al. (2002). "A 3D model of the voltage-dependent anion channel (VDAC)." FEBS Lett **520**(1-3): 1-7.

Champeil, P., T. Menguy, et al. (2000). "Interaction of amphipols with sarcoplasmic reticulum Ca^{2+}-ATPase." J Biol Chem **275**(25): 18623-37.

Chattopadhyay, A. and E. London (1987). "Parallax method for direct measurement of membrane penetration depth utilizing fluorescence quenching by spin-labeled phospholipids." Biochemistry **26**(1): 39-45.

Chaudier, Y., F. Zito, et al. (2002). "Synthesis and preliminary biochemical assessment of ethyl-terminated perfluoroalkylamine oxide surfactants." Bioorg Med Chem Lett **12**(12): 1587-90.

Chen, R. and U. Henning (1996). "A periplasmic protein (Skp) of *Escherichia coli* selectively binds a class of outer membrane proteins." Molecular Microbiology **19**(6): 1287-94.

Chimento, D. P., A. K. Mohanty, et al. (2003). "Crystallization and initial X-ray diffraction of BtuB, the integral membrane cobalamin transporter of *Escherichia coli*." Acta Crystallogr D Biol Crystallogr **59**(Pt 3): 509-11.

Colombini, M. (1989). "Voltage gating in the mitochondrial channel, VDAC." J Membr Biol **111**(2): 103-11.

Colombini, M., E. Blachly-Dyson, et al. (1996). "VDAC, a channel in the outer mitochondrial membrane." Ion Channels **4**: 169-202.

Compton, L. A. and W. C. Johnson, Jr. (1986). "Analysis of protein circular dichroism spectra for secondary structure using a simple matrix multiplication." Anal Biochem **155**(1): 155-67.

Conlan, S. and H. Bayley (2003). "Folding of a monomeric porin, OmpG, in detergent solution." Biochemistry **42**(31): 9453-65.

Conlan, S., Y. Zhang, et al. (2000). "Biochemical and biophysical characterization of OmpG: A monomeric porin." Biochemistry **39**(39): 11845-54.

Coulton, J. W., P. Mason, et al. (1986). "Protein fusions of β-galactosidase to the ferrichrome-iron receptor of *Escherichia coli* K-12." J Bacteriol **165**(1): 181-92.

Cowan, S. W., R. M. Garavito, et al. (1995). "The structure of OmpF porin in a tetragonal crystal form." Structure **3**(10): 1041-50.

Cowan, S. W., T. Schirmer, et al. (1992). "Crystal structures explain functional properties of two *E. coli* porins." Nature **358**(6389): 727-33.

Curran, A. R., R. H. Templer, et al. (1999). "Modulation of folding and assembly of the membrane protein bacteriorhodopsin by intermolecular forces within the lipid bilayer." Biochemistry **38**(29): 9328-36.

Danese, P. N. and T. J. Silhavy (1998). "Targeting and assembly of periplasmic and outer-membrane proteins in *Escherichia coli*." Annu. Rev. Genet. **32**: 59-94.

de Cock, H., K. Brandenburg, et al. (1999). "Non-lamellar structure and negative charges of lipopolysaccharides required for efficient folding of outer membrane protein PhoE of *Escherichia coli*." J Biol Chem **274**(8): 5114-9.

de Cock, H., M. Pasveer, et al. (2001). "Identification of phospholipids as new components that assist in the in vitro trimerization of a bacterial pore protein." Eur J Biochem **268**(3): 865-75.

de Cock, H., U. Schäfer, et al. (1999). "Affinity of the periplasmic chaperone Skp of *Escherichia coli* for phospholipids, lipopolysaccharides and non-native outer membrane proteins. Role of Skp in the biogenesis of outer membrane protein." Eur. J. Biochem. **259**(1-2): 96-103.

de Cock, H. and J. Tommassen (1996). "Lipopolysaccharides and divalent cations are involved in the formation of an assembly-competent intermediate of outer-membrane protein PhoE of E.coli." EMBO J **15**(20): 5567-73.

de Cock, H., S. van Blokland, et al. (1996). "In vitro insertion and assembly of outer membrane protein PhoE of *Escherichia coli* K-12 into the outer membrane. Role of Triton X-100." J Biol Chem **271**(22): 12885-90.

de Planque, M. R., D. V. Greathouse, et al. (1998). "Influence of lipid/peptide hydrophobic mismatch on the thickness of diacylphosphatidylcholine bilayers. A ^{2}H-NMR and ESR study using designed transmembrane α-helical peptides and gramicidin A." Biochemistry **37**(26): 9333-45.

Dekker, N., K. Merck, et al. (1995). "In vitro folding of *Escherichia coli* outer-membrane phospholipase A." Eur. J. Biochem. **232**(1): 214-9.

Dicker, I. B. and S. Seetharam (1991). "Cloning and nucleotide sequence of the *firA* gene and the firA200(Ts) allele from *Escherichia coli*." J. Bacteriol. **173**(1): 334-44.

Dornmair, K., H. Kiefer, et al. (1990). "Refolding of an integral membrane protein. OmpA of *Escherichia coli*." J Biol Chem **265**(31): 18907-11.

Dutzler, R., G. Rummel, et al. (1999). "Crystal structure and functional characterization of OmpK36, the osmoporin of Klebsiella pneumoniae." Structure Fold Des **7**(4): 425-34.

Dutzler, R., Y. F. Wang, et al. (1996). "Crystal structures of various maltooligosaccharides bound to maltoporin reveal a specific sugar translocation pathway." Structure **4**(2): 127-34.

Engelman, D. M. and T. A. Steitz (1981). "The spontaneous insertion of proteins into and across membranes: the helical hairpin hypothesis." Cell **23**(2): 411-22.

Faham, S., G. L. Boulting, et al. (2005). "Crystallization of bacteriorhodopsin from bicelle formulations at room temperature." Protein Sci **14**(3): 836-40.

Fajardo, D. A., J. Cheung, et al. (1998). "Biochemistry and regulation of a novel *Escherichia coli* K-12 porin protein, OmpG, which produces unusually large channels." J Bacteriol **180**(17): 4452-9.

Ferguson, A. D., J. Breed, et al. (1998). "An internal affinity-tag for purification and crystallization of the siderophore receptor FhuA, integral outer membrane protein from *Escherichia coli* K-12." Protein Sci **7**(7): 1636-8.

Ferguson, A. D., E. Hofmann, et al. (1998). "Siderophore-mediated iron transport: crystal structure of FhuA with bound lipopolysaccharide." Science **282**(5397): 2215-20.

Ferguson, A. D., W. Welte, et al. (2000). "A conserved structural motif for lipopolysaccharide recognition by procaryotic and eucaryotic proteins." Structure Fold Des **8**(6): 585-92.

Fernandez, C., K. Adeishvili, et al. (2001). "Transverse relaxation-optimized NMR spectroscopy with the outer membrane protein OmpX in dihexanoyl phosphatidylcholine micelles." Proc Natl Acad Sci U S A **98**(5): 2358-63.

Fernandez, C., C. Hilty, et al. (2001). "Solution NMR studies of the integral membrane proteins OmpX and OmpA from *Escherichia coli*." FEBS Lett **504**(3): 173-8.

Fernandez, C., C. Hilty, et al. (2002). "Lipid-protein interactions in DHPC micelles containing the integral membrane protein OmpX investigated by NMR spectroscopy." Proc Natl Acad Sci U S A **99**(21): 13533-7.

Forst, D., W. Welte, et al. (1998). "Structure of the sucrose-specific porin ScrY from *Salmonella typhimurium* and its complex with sucrose." Nat Struct Biol **5**(1): 37-46.

Foulds, J. and T. J. Chai (1978). "Defeat of colicin tolerance in *Escherichia coli* ompA mutants: evidence for interaction between colicin L-JF246 and the cytoplasmic membrane." J Bacteriol **133**(1): 158-64.

Fraser, R. D. B. (1953). "The interpretation of infrared dichroism in fibrous protein structures." J Chem Phys **21**: 1511-1515.

Fraser, R. D. B. and T. P. Mac Rae (1973). Conformation in Fibrous Proteins and Related Synthetic Peptides. New York, Academic Press.

Freudl, R., H. Schwarz, et al. (1986). "An outer membrane protein (OmpA) of *Escherichia coli* K-12 undergoes a conformational change during export." J. Biol. Chem. **261**(24): 11355-61.

Garavito, R. M. and S. Ferguson-Miller (2001). "Detergents as tools in membrane biochemistry." J Biol Chem **276**(35): 32403-6.

Gohon, Y., F. Giusti, et al. (2005). "Well-defined nanoparticles formed by hydrophobic assembly of a short and polydisperse random terpolymer, amphipol A8-35." Langmuir, in press.

Goormaghtigh, E., V. Cabiaux, et al. (1990). "Secondary structure and dosage of soluble and membrane proteins by attenuated total reflection Fourier-transform infrared spectroscopy on hydrated films." Eur J Biochem **193**(2): 409-20.

Greenfield, N. and G. D. Fasman (1969). "Computed circular dichroism spectra for the evaluation of protein conformation." Biochemistry **8**(10): 4108-16.

Grizot, S. and S. K. Buchanan (2004). "Structure of the OmpA-like domain of RmpM from Neisseria meningitidis." Mol Microbiol **51**(4): 1027-37.

Guex, N. and M. C. Peitsch (1997). "SWISS-MODEL and the Swiss-PdbViewer: an environment for comparative protein modeling." Electrophoresis **18**(15): 2714-23.

Hancock, R. E. W. (1987). Model membrane studies of porin function. New York, Wiley-Interscience.

Harms, N., G. Koningstein, et al. (2001). "The early interaction of the outer membrane protein Phoe with the periplasmic chaperone Skp occurs at the cytoplasmic membrane." J. Biol. Chem. **276**(22): 18804-11.

Harwood, J. L. and N. J. Russell (1984). Lipids in Plants and Microbes. London, George Allen and Unwin.

Heins, L., H. Mentzel, et al. (1994). "Biochemical, molecular, and functional characterization of porin isoforms from potato mitochondria." J. Biol. Chem. **269**(42): 26402-10.

Hilty, C., G. Wider, et al. (2004). "Membrane protein-lipid interactions in mixed micelles studied by NMR spectroscopy with the use of paramagnetic reagents." Chembiochem **5**(4): 467-73.

Hong, H. and L. K. Tamm (2004). "Elastic coupling of integral membrane protein stability to lipid bilayer forces." Proc Natl Acad Sci U S A **101**(12): 4065-70.

Horváth, L. I., T. Heimburg, et al. (1995). "Integration of a K+ channel-associated peptide in a lipid bilayer: conformation, lipid-protein interactions, and rotational diffusion." Biochemistry **34**(12): 3893-8.

Horváth, L. I., P. F. Knowles, et al. (1997). "A single-residue deletion alters the lipid selectivity of a K+ channel-associated peptide in the β-conformation: spin label electron spin resonance studies." Biophys J **73**(5): 2588-94.

Huang, K. S., H. Bayley, et al. (1981). "Refolding of an integral membrane protein. Denaturation, renaturation, and reconstitution of intact bacteriorhodopsin and two proteolytic fragments." J Biol Chem **256**(8): 3802-9.

Hubbell, W. L. and H. M. McConnell (1971). "Molecular motion in spin-labeled phospholipids and membranes." J Am Chem Soc **93**(2): 314-26.

Hwang, P. M., W. Y. Choy, et al. (2002). "Solution structure and dynamics of the outer membrane enzyme PagP by NMR." Proc Natl Acad Sci U S A **99**(21): 13560-5.

Jansen, C., M. Heutink, et al. (2000). "The assembly pathway of outer membrane protein PhoE of *Escherichia coli*." Eur J Biochem **267**(12): 3792-800.

Jensen, H. B., J. Skeidsvoll, et al. (1996). "Cloning of the fomA gene, encoding the major outer membrane porin of *Fusobacterium nucleatum* ATCC10953." Microb Pathog **21**(5): 331-42.

Johnson, C. M. and A. R. Fersht (1995). "Protein stability as a function of denaturant concentration: ther thermal stability of barnase in the presence of urea." Biochemistry **34**(20): 6795-804.

Kahn, T. W. and D. M. Engelman (1992). "Bacteriorhodopsin can be refolded from two independently stable transmembrane helices and the complementary five-helix fragment." Biochemistry **31**(26): 6144-51.

Kiefer, H. (2003). "*In vitro* folding of α-helical membrane proteins." Biochim Biophys Acta **1610**(1): 57-62.

Killian, J. A. (1998). "Hydrophobic mismatch between proteins and lipids in membranes." Biochim Biophys Acta **1376**(3): 401-15.

Kinder, S. A. and S. C. Holt (1993). "Localization of the *Fusobacterium nucleatum* T18 adhesin activity mediating coaggregation with *Porphyromonas gingivalis* T22." J Bacteriol **175**(3): 840-50.

Kleinschmidt, J. H. (2003). "Membrane protein folding on the example of outer membrane protein A of *Escherichia coli*." Cell Mol Life Sci **60**(8): 1547-58.

Kleinschmidt, J. H. (2005). Folding and stability of monomeric β-barrel membrane proteins. Protein-lipid interactions: From membrane domains to cellular networks. L. K. Tamm. Weinheim, Wiley-VCH**:** 27-56.

Kleinschmidt, J. H., T. den Blaauwen, et al. (1999). "Outer membrane protein A of *Escherichia coli* inserts and folds into lipid bilayers by a concerted mechanism." Biochemistry **38**(16): 5006-16.

Kleinschmidt, J. H. and L. K. Tamm (1996). "Folding intermediates of a β-barrel membrane protein. Kinetic evidence for a multi-step membrane insertion mechanism." Biochemistry **35**(40): 12993-3000.

Kleinschmidt, J. H. and L. K. Tamm (1999). "Time-resolved distance determination by tryptophan fluorescence quenching: probing intermediates in membrane protein folding." Biochemistry **38**(16): 4996-5005.

Kleinschmidt, J. H. and L. K. Tamm (2002). "Secondary and tertiary structure formation of the β-barrel membrane protein OmpA is synchronized and depends on membrane thickness." J Mol Biol **324**(2): 319-30.

Kleinschmidt, J. H. and L. K. Tamm (2002). "Structural Transitions in Short-Chain Lipid Assemblies Studied by ^{31}P-NMR Spectroscopy." Biophys. J. **83**: 994-1003.

Kleinschmidt, J. H., M. C. Wiener, et al. (1999). "Outer membrane protein A of *E. coli* folds into detergent micelles, but not in the presence of monomeric detergent." Protein Sci **8**(10): 2065-71.

Kleivdal, H., R. Benz, et al. (1995). "The *Fusobacterium nucleatum* major outer-membrane protein (FomA) forms trimeric, water-filled channels in lipid bilayer membranes." Eur J Biochem **233**(1): 310-6.

Kleivdal, H., R. Benz, et al. (1999). "Identification of positively charged residues of FomA porin of *Fusobacterium nucleatum* which are important for pore function." Eur J Biochem **260**(3): 818-24.

Kleivdal, H., P. Puntervoll, et al. (2001). "Topological investigations of the FomA porin from *Fusobacterium nucleatum* and identification of the constriction loop L6." Microbiology **147**(Pt 4): 1059-67.

Klug, C. S. and J. B. Feix (1998). "Guanidine hydrochloride unfolding of a transmembrane β-strand in FepA using site-directed spin labeling." Protein Sci **7**(6): 1469-76.

Klug, C. S., W. Su, et al. (1995). "Denaturant unfolding of the ferric enterobactin receptor and ligand-induced stabilization studied by site-directed spin labeling." Biochemistry **34**(43): 14230-6.

Koebnik, R. (1996). "*In vivo* membrane assembly of split variants of the *E.coli* outer membrane protein OmpA." EMBO J. **15**(14): 3529-37.

Koebnik, R. (1999). "Membrane assembly of the *Escherichia coli* outer membrane protein OmpA: exploring sequence constraints on transmembrane β-strands." J. Mol. Biol. **285**(4): 1801-10.

Koebnik, R. and L. Krämer (1995). "Membrane assembly of circularly permuted variants of the *E. coli* outer membrane protein OmpA." J. Mol. Biol. **250**(5): 617-26.

Koebnik, R., K. P. Locher, et al. (2000). "Structure and function of bacterial outer membrane proteins: barrels in a nutshell." Mol Microbiol **37**(2): 239-53.

Koradi, R., M. Billeter, et al. (1996). "MOLMOL: a program for display and analysis of macromolecular structures." J Mol Graph **14**(1): 51-5, 29-32.

Koronakis, V., A. Sharff, et al. (2000). "Crystal structure of the bacterial membrane protein TolC central to multidrug efflux and protein export." Nature **405**(6789): 914-9.

Kóta, Z., T. Páli, et al. (2004). "Orientation and lipid-peptide interactions of gramicidin A in lipid membranes: polarized attenuated total reflection infrared spectroscopy and spin-label electron spin resonance." Biophys J **86**(3): 1521-31.

Kramer, R. A., K. Brandenburg, et al. (2002). "Lipopolysaccharide regions involved in the activation of *Escherichia coli* outer membrane protease OmpT." Eur J Biochem **269**(6): 1746-52.

Kramer, R. A., D. Zandwijken, et al. (2000). "*In vitro* folding, purification and characterization of *Escherichia coli* outer membrane protease OmpT." Eur J Biochem **267**(3): 885-93.

Kreusch, A., A. Neubuser, et al. (1994). "Structure of the membrane channel porin from *Rhodopseudomonas blastica* at 2.0 Å resolution." Protein Sci **3**(1): 58-63.

Kurisu, G., S. D. Zakharov, et al. (2003). "The structure of BtuB with bound colicin E3 R-domain implies a translocon." Nat Struct Biol **10**(11): 948-54.

Kwok, R. and E. Evans (1981). "Thermoelasticity of large lecithin bilayer vesicles." Biophysical Journal **35**(3): 637-52.

Ladavière, C., M. Toustou, et al. (2001). "Slow Reorganization of Small Phosphatidylcholine Vesicles upon Adsorption of Amphiphilic Polymers." J Colloid Interface Sci **241**(1): 178-187.

Ladokhin, A. S. (1999). "Analysis of protein and peptide penetration into membranes by depth-dependent fluorescence quenching: theoretical considerations." Biophys J **76**(2): 946-55.

Ladokhin, A. S. and P. W. Holloway (1995). "Fluorescence of membrane-bound tryptophan octyl ester: a model for studying intrinsic fluorescence of protein-membrane interactions." Biophys. J. **69**(2): 506-17.

Laemmli, U. K. (1970). "Cleavage of structural proteins during the assembly of the head of bacteriophage T4." Nature **227**(5259): 680-5.

Lazar, S. W. and R. Kolter (1996). "SurA assists the folding of *Escherichia coli* outer membrane proteins." J. Bacteriol. **178**(6): 1770-3.

le Maire, M., P. Champeil, et al. (2000). "Interaction of membrane proteins and lipids with solubilizing detergents." Biochim Biophys Acta **1508**(1-2): 86-111.

Lee, A. G. (2003). "Lipid-protein interactions in biological membranes: a structural perspective." Biochim Biophys Acta **1612**(1): 1-40.

Lewis, B. A. and D. M. Engelman (1983). "Bacteriorhodopsin remains dispersed in fluid phospholipid bilayers over a wide range of bilayer thicknesses." J. Mol. Biol. **166**(2): 203-10.

Lewis, B. A. and D. M. Engelman (1983). "Lipid bilayer thickness varies linearly with acyl chain length in fluid phosphatidylcholine vesicles." J Mol Biol **166**(2): 211-7.

Linke, D., J. Frank, et al. (2004). "Folding kinetics and structure of OEP16." Biophys J **86**(3): 1479-87.

Lis, L. J., M. McAlister, et al. (1982). "Measurement of the lateral compressibility of several phospholipid bilayers." Biophys J **37**(3): 667-72.

Liu, J. and C. T. Walsh (1990). "Peptidyl-prolyl cis-trans-isomerase from *Escherichia coli*: a periplasmic homolog of cyclophilin that is not inhibited by cyclosporin A." Proc. Natl. Acad. Sci. U.S.A. **87**(11): 4028-32.

Liu, Y., D. M. Engelman, et al. (2002). "Genomic analysis of membrane protein families: abundance and conserved motifs." Genome Biol **3**(10): research0054.

Lo Piero, A. R. and G. Petrone (1994). "Effect of detergents on the chicken liver F1-ATPase: functional and structural aspects." Biochem Mol Biol Int **32**(1): 181-8.

Lobley, A., et al. (2002). "DICHROWEB: an interactive website for the analysis of protein secondary structure from circular dichroism spectra." Bioinformatics **18**(1): 211-2.

Locher, K. P., B. Rees, et al. (1998). "Transmembrane signaling across the ligand-gated FhuA receptor: crystal structures of free and ferrichrome-bound states reveal allosteric changes." Cell **95**(6): 771-8.

Locher, K. P. and J. P. Rosenbusch (1997). "Oligomeric states and siderophore binding of the ligand-gated FhuA protein that forms channels across *Escherichia coli* outer membranes." Eur. J. Biochem. **247**(3): 770-5.

Lodish, H. B., A. Zipursky, et al. (2000). Molecular Cell Biology. New York, W. H. Freeman and Company.

Lowry, O. H., N. J. Rosebrough, et al. (1951). "Protein measurement with the Folin phenol reagent." J Biol Chem **193**(1): 265-75.

Luecke, H., B. Schobert, et al. (1999). "Structure of bacteriorhodopsin at 1.55 Å resolution." J. Mol. Biol. **291**(4): 899-911.

Lugtenberg, B. and L. Van Alphen (1983). "Molecular architecture and functioning of the outer membrane of *Escherichia coli* and other Gram-negative bacteria." Biochim Biophys Acta **737**(1): 51-115.

Manavalan, P. and W. C. Johnson, Jr. (1987). "Variable selection method improves the prediction of protein secondary structure from circular dichroism spectra." Anal Biochem **167**(1): 76-85.

Mann, C. J. and C. R. Matthews (1993). "Structure and stability of an early folding intermediate of *Escherichia coli* trp aporepressor measured by far-UV stopped-flow circular dichroism and 8-anilino-1-naphthalene sulfonate binding." Biochemistry **32**(20): 5282-90.

Mann, C. J., C. A. Royer, et al. (1993). "Tryptophan replacements in the trp aporepressor from *Escherichia coli*: probing the equilibrium and kinetic folding models." Protein Sci **2**(11): 1853-61.

Manning, D. S., D. K. Reschke, et al. (1998). "Omp85 proteins of *Neisseria gonorrhoeae* and *Neisseria meningitidis* are similar to *Haemophilus influenzae* D-15-Ag and *Pasteurella multocida* Oma87." Microb Pathog **25**(1): 11-21.

Manting, E. H. and A. J. Driessen (2000). "*Escherichia coli* translocase: the unravelling of a molecular machine." Mol. Microbiol. **37**(2): 226-38.

Mantipragada, S. B., L. I. Horváth, et al. (2003). "Lipid-protein interactions and effect of local anesthetics in acetylcholine receptor-rich membranes from *Torpedo marmorata* electric organ." Biochemistry **42**(30): 9167-75.

Marsh, D. (1981). Electron spin resonance: spin labels. Berlin, Heidelberg and New York, Springer-Verlag.

Marsh, D. (1982). Electron spin resonance: spin label probes. Amsterdam, Elsevier.

Marsh, D. (1985). ESR spin label studies of lipid-protein interactions. Amsterdam, Elsevier.

Marsh, D. (1989). Experimental methods in spin-label spectral analysis. New York, Plenum Publishing Group.

Marsh, D. (1990). CRC Handbook of Phospholipid Bilayers. Boca Raton, CRC Press.

Marsh, D. (1990). Handbook of Lipid Bilayers. Boca Raton, FL, CRC Press.

Marsh, D. (1990). "Lipid-protein interactions in membranes." FEBS Letters **268**(2): 371-5.

Marsh, D. (1997). "Dichroic ratios in polarized Fourier transform infrared for nonaxial symmetry of β-sheet structures." Biophys J **72**(6): 2710-8.

Marsh, D. (1997). "Stoichiometry of lipid-protein interaction and integral membrane protein structure." Eur Biophys J **26**: 203-208.

Marsh, D. (1998). "Nonaxiality in infrared dichroic ratios of polytopic transmembrane proteins." Biophys J **75**(1): 354-8.

Marsh, D. (1999). "Quantitation of secondary structure in ATR infrared spectroscopy." Biophys J **77**(5): 2630-7.

Marsh, D. (1999). "Spin-label electron spin resonance and Fourier transform infrared spectroscopy for structural/dynamic measurements on ion channels." Methods Enzymol **294**: 59-92.

Marsh, D. (2000). "Infrared dichroism of twisted β-sheet barrels. The structure of *E. coli* outer membrane proteins." J Mol Biol **297**(3): 803-8.

Marsh, D. and L. I. Horváth (1989). Spin-label studies of the structure and dynamics of lipids and proteins in membranes. Amsterdam, Elsevier.

Marsh, D. and L. I. Horváth (1998). "Structure, dynamics and composition of the lipid-protein interface. Perspectives from spin-labelling." Biochim Biophys Acta **1376**(3): 267-96.

Marsh, D. and T. Páli (2001). "Infrared dichroism from the X-ray structure of bacteriorhodopsin." Biophys J **80**(1): 305-12.

Marsh, D. and T. Páli (2004). "The protein-lipid interface: perspectives from magnetic resonance and crystal structures." Biochim Biophys Acta **1666**(1-2): 118-41.

Marsh, D. and A. Watts (1982). Spin-labeling and lipid-protein interactions in membranes. New York, Wiley-Interscience.

Martin, A., I. Kather, et al. (2002). "Origins of the high stability of an in vitro-selected cold-shock protein." J Mol Biol **318**(5): 1341-9.

McCabe, E. R. (1994). "Microcompartmentation of energy metabolism at the outer mitochondrial membrane: role in diabetes mellitus and other diseases." J Bioenerg Biomembr **26**(3): 317-25.

McIntosh, T. J. and P. W. Holloway (1987). "Determination of the depth of bromine atoms in bilayers formed from bromolipid probes." Biochemistry **26**(6): 1783-8.

Meyer, J. E., M. Hofnung, et al. (1997). "Structure of maltoporin from *Salmonella typhimurium* ligated with a nitrophenyl-maltotrioside." J Mol Biol **266**(4): 761-75.

Missiakas, D., J. M. Betton, et al. (1996). "New components of protein folding in extracytoplasmic compartments of *Escherichia coli* SurA, FkpA and Skp/OmpH." Mol. Microbiol. **21**(4): 871-84.

Miyazawa, T. (1960). "Perturbation treatment of the characteristic vibrations of polypeptide chains in various configurations." J Chem Phys **32**: 1647-1652.

Moeck, G. S., P. Tawa, et al. (1996). "Ligand-induced conformational change in the ferrichrome-iron receptor of *Escherichia coli* K-12." Mol Microbiol **22**(3): 459-71.

Mogensen, J. E., D. Tapadar, et al. (2005). "Barriers to folding of the transmembrane domain of the *Escherichia coli* autotransporter adhesin involved in diffuse adherence." Biochemistry **44**(11): 4533-45.

Morona, R., C. Kramer, et al. (1985). "Bacteriophage receptor area of outer membrane protein OmpA of *Escherichia coli* K-12." J Bacteriol **164**(2): 539-43.

Mueller, P., D. O. Rudin, et al. (1962). "Reconstitution of cell membrane structure *in vitro* and its transformation into an excitable system." Nature **194**: 979-80.

Nabedryk, E., R. M. Garavito, et al. (1988). "The orientation of β-sheets in porin. A polarized Fourier transform infrared spectroscopic investigation." Biophys J **53**(5): 671-6.

Nagle, J. F. and S. Tristram-Nagle (2000). "Structure of lipid bilayers." Biochim Biophys Acta **1469**(3): 159-95.

Nilsson, J., B. Persson, et al. (2002). "Prediction of partial membrane protein topologies using a consensus approach." Protein Sci **11**(12): 2974-80.

O'Keeffe, A. H., J. M. East, et al. (2000). "Selectivity in lipid binding to the bacterial outer membrane protein OmpF." Biophys J **79**(4): 2066-74.

Oomen, C. J., P. Van Ulsen, et al. (2004). "Structure of the translocator domain of a bacterial autotransporter." EMBO J **23**(6): 1257-66.

Orlowski, S., M. A. Selosse, et al. (1998). "Effects of detergents on P-glycoprotein atpase activity: differences in perturbations of basal and verapamil-dependent activities." Cancer Biochem Biophys **16**(1-2): 85-110.

Otzen, D. E. and A. R. Fersht (1995). "Side-chain determinants of β-sheet stability." Biochemistry **34**(17): 5718-24.

Pace, C. N. (1990). "Measuring and increasing protein stability." Trends Biotechnol **8**(4): 93-8.

Pace, C. N., E. J. Hebert, et al. (1998). "Conformational stability and thermodynamics of folding of ribonucleases Sa, Sa2 and Sa3." J Mol Biol **279**(1): 271-86.

Pace, C. N. and T. McGrath (1980). "Substrate stabilization of lysozyme to thermal and guanidine hydrochloride denaturation." J Biol Chem **255**(9): 3862-5.

Pace, C. N. and J. M. Scholtz (1997). Measuring the conformational stability of a protein. Protein Structure. T. E. Creighton. Oxford, Oxford University Press. **174:** 299-321.

Páli, T. and D. Marsh (2001). "Tilt, twist, and coiling in β-barrel membrane proteins: relation to infrared dichroism." Biophys J **80**(6): 2789-97.

Parsegian, V. A., N. Fuller, et al. (1979). "Measured work of deformation and repulsion of lecithin bilayers." Proc. Natl. Acad. Sci. U.S.A. **76**(6): 2750-4.

Pautsch, A. and G. E. Schulz (1998). "Structure of the outer membrane protein A transmembrane domain." Nat Struct Biol **5**(11): 1013-7.

Pautsch, A. and G. E. Schulz (2000). "High-resolution structure of the OmpA membrane domain." J Mol Biol **298**(2): 273-82.

Pautsch, A., J. Vogt, et al. (1999). "Strategy for membrane protein crystallization exemplified with OmpA and OmpX." Proteins **34**(2): 167-72.

Pebay-Peyroula, E., G. Rummel, et al. (1997). "X-ray structure of bacteriorhodopsin at 2.5 angstroms from microcrystals grown in lipidic cubic phases." Science **277**(5332): 1676-81.

Plancon, L., C. Janmot, et al. (2002). "Characterization of a high-affinity complex between the bacterial outer membrane protein FhuA and the phage T5 protein pb5." J Mol Biol **318**(2): 557-69.

Pocanschi, C. L., H. J. Apell, et al. (2005). "The major outer membrane protein of *Fusobacterium nucleatum* (FomA) folds and inserts into lipid bilayers via parallel folding pathways." Submitted.

Pocanschi, C. L., T. Dahmane, et al. (2005). "Amphipathic polymers: tools to fold integral membrane proteins to their native form." Submitted.

Pocanschi, C. L. and J. H. Kleinschmidt (2005). "Folding, chain-length and lipid headgroup dependence of the stability of the iron-siderophore receptor FhuA in lyso-lipid micelles and lipid bilayers." In preparation.

Pocanschi, C. L. and J. H. Kleinschmidt (2005). "The iron-siderophore receptor FhuA of *E.coli* is strongly stabilized by the cork domain and by the lipid bilayers." In preparation.

Pocanschi, C. L., J. L. Popot, et al. (2005). "Folding kinetics of the outer membrane protein OmpA into the amphipathic polymer A8-35." Submitted.

Popot, J. L., E. A. Berry, et al. (2003). "Amphipols: polymeric surfactants for membrane biology research." Cell Mol Life Sci **60**(8): 1559-74.

Popot, J. L. and D. M. Engelman (2000). "Helical membrane protein folding, stability, and evolution." Annu. Rev. Biochem. **69**: 881-922.

Popot, J. L., S. E. Gerchman, et al. (1987). "Refolding of bacteriorhodopsin in lipid bilayers. A thermodynamically controlled two-stage process." J Mol Biol **198**(4): 655-76.

Prilipov, A., P. S. Phale, et al. (1998). "Coupling site-directed mutagenesis with high-level expression: large scale production of mutant porins from *E. coli*." FEMS Microbiol Lett **163**(1): 65-72.

Prince, S. M., M. Achtman, et al. (2002). "Crystal structure of the OpcA integral membrane adhesin from *Neisseria meningitidis*." Proc Natl Acad Sci U S A **99**(6): 3417-21.

Provencher, S. W. and J. Glockner (1981). "Estimation of globular protein secondary structure from circular dichroism." Biochemistry **20**(1): 33-7.

Puntervoll, P., M. Ruud, et al. (2002). "Structural characterization of the fusobacterial non-specific porin FomA suggests a 14-stranded topology, unlike the classical porins." Microbiology **148**(Pt 11): 3395-403.

Qi, S. Y., Y. Li, et al. (1994). "The region around residue 115 of human bactericidal/permeability-increasing protein is not involved in lipopolysaccharide binding or bactericidal activity. Chemical synthesis and expression of a gene coding for the active domain and characterization of recombinant proteins." Biochem J **298 Pt 3**: 711-8.

Rama Krishna, Y. V. and D. Marsh (1990). "Spin label ESR and 31P-NMR studies of the cubic and inverted hexagonal phases of dimyristoylphosphatidylcholine/myristic acid (1:2, mol/mol) mixtures." Biochim Biophys Acta **1024**(1): 89-94.

Ramakrishnan, M., C. L. Pocanschi, et al. (2004). "Association of spin-labeled lipids with β-barrel proteins from the outer membrane of *Escherichia coli*." Biochemistry **43**(37): 11630-6.

Ramakrishnan, M., J. Qu, et al. (2005). "Orientation of β-barrel proteins OmpA and FhuA in lipid membranes. Chain length dependence from infrared dichroism." Biochemistry **44**(9): 3515-23.

Ramm, K. and A. Plückthun (2000). "The periplasmic *Escherichia coli* peptidylprolyl cis,trans-isomerase FkpA. II. Isomerase-independent chaperone activity *in vitro*." J. Biol. Chem. **275**(22): 17106-13.

Ramm, K. and A. Plückthun (2001). "High enzymatic activity and chaperone function are mechanistically related features of the dimeric *E. coli* peptidyl-prolyl-isomerase FkpA." J. Mol. Biol. **310**(2): 485-98.

Ried, G. and U. Henning (1987). "A unique amino acid substitution in the outer membrane protein OmpA causes conjugation deficiency in *Escherichia coli* K-12." FEBS Lett **223**(2): 387-90.

Ried, G., I. Hindennach, et al. (1990). "Role of lipopolysaccharide in assembly of *Escherichia coli* outer membrane proteins OmpA, OmpC, and OmpF." Journal of Bacteriology **172**(10): 6048-53.

Ried, G., S. MacIntyre, et al. (1990). "Export of altered forms of an *Escherichia coli* K-12 outer membrane protein (OmpA) can inhibit synthesis of unrelated outer membrane proteins." Journal of Molecular Biology **216**(1): 39-47.

Rizzitello, A. E., J. R. Harper, et al. (2001). "Genetic Evidence for Parallel Pathways of Chaperone Activity in the Periplasm of *Escherichia coli*." J. Bacteriol. **183**(23): 6794-800.

Rodionova, N. A., S. A. Tatulian, et al. (1995). "Characterization of two membrane-bound forms of OmpA." Biochemistry **34**(6): 1921-9.

Roumestand, C., M. Boyer, et al. (2001). "Characterization of the folding and unfolding reactions of a small β-barrel protein of novel topology, the MTCP1 oncogene product P13." J Mol Biol **312**(1): 247-59.

Rouser, G., S. Fleischer, et al. (1970). "Two dimensional then layer chromatographic separation of polar lipids and determination of phospholipids by phosphorus analysis of spots." Lipids **5**(5): 494-6.

Rouvière, P. E. and C. A. Gross (1996). "SurA, a periplasmic protein with peptidyl-prolyl isomerase activity, participates in the assembly of outer membrane porins." Genes Dev. **10**(24): 3170-82.

Roy, A. M. and J. Coleman (1994). "Mutations in firA, encoding the second acyltransferase in lipopolysaccharide biosynthesis, affect multiple steps in lipopolysaccharide biosynthesis." J. Bacteriol. **176**(6): 1639-46.

Saint, N., C. El Hamel, et al. (2000). "Ion channel formation by N-terminal domain: a common feature of OprFs of *Pseudomonas* and OmpA of *Escherichia coli*." FEMS Microbiol Lett **190**(2): 261-5.

Sambrook, J., E. F. Fritsch, et al. (1989). Molecular cloning: a laboratory manual. Cold Spring Harbor. New York, Cold Spring Harbor Laboratory Press.

Sankaram, M. B., P. J. Brophy, et al. (1990). "Fatty acid pH titration and the selectivity of interaction with extrinsic proteins in dimyristoylphosphatidylglycerol dispersions. Spin label ESR studies." Biochim Biophys Acta **1021**: 63-69.

Schäfer, U., K. Beck, et al. (1999). "Skp, a molecular chaperone of gram-negative bacteria, is required for the formation of soluble periplasmic intermediates of outer membrane proteins." J. Biol. Chem. **274**(35): 24567-74.

Schirmer, T., T. A. Keller, et al. (1995). "Structural basis for sugar translocation through maltoporin channels at 3.1 Å resolution." Science **267**(5197): 512-4.

Schorn, K. and D. Marsh (1996). "Lipid chain dynamics and molecular location of diacylglycerol in hydrated binary mixtures with phosphatidylcholine: spin label ESR studies." Biochemistry **35**(12): 3831-6.

Schulz, G. E. (2002). "The structure of bacterial outer membrane proteins." Biochim Biophys Acta **1565**(2): 308-17.

Schulz, G. E. (2003). "Transmembrane β-barrel proteins." Adv Protein Chem **63**: 47-70.

Schweizer, M., I. Hindennach, et al. (1978). "Major proteins of the *Escherichia coli* outer cell envelope membrane. Interaction of protein II with lipopolysaccharide." Eur. J. Biochem. **82**(1): 211-7.

Sreerama, N., S. Y. Venyaminov, et al. (1999). "Estimation of the number of α-helical and β-strand segments in proteins using circular dichroism spectroscopy." Protein Sci **8**(2): 370-80.

Sreerama, N. and R. W. Woody (1993). "A self-consistent method for the analysis of protein secondary structure from circular dichroism." Anal Biochem **209**(1): 32-44.

Sreerama, N. and R. W. Woody (2000). "Estimation of protein secondary structure from circular dichroism spectra: comparison of CONTIN, SELCON, and CDSSTR methods with an expanded reference set." Anal Biochem **287**(2): 252-60.

Sen, K. and H. Nikaido (1991). "Lipopolysaccharide structure required for *in vitro* trimerization of *Escherichia coli* OmpF porin." Journal of Bacteriology **173**(2): 926-8.

Singer, S. J. and G. L. Nicolson (1972). "The fluid mosaic model of the structure of cell membranes." Science **175**(23): 720-31.

Snijder, H. J., I. Ubarretxena-Belandia, et al. (1999). "Structural evidence for dimerization-regulated activation of an integral membrane phospholipase." Nature **401**(6754): 717-21.

Somerharju, P. and K. W. Wirtz (1982). "Semisynthesis and properties of a fluorescent phosphatidylinositol analog containing a *cis*-parinaroyl moiety." Chem Phys Lipids **30**: 81-91.

Song, J., C. Midson, et al. (1998). "The topology of VDAC as probed by biotin modification." J Biol Chem **273**(38): 24406-13.

Sonntag, I., H. Schwarz, et al. (1978). "Cell envelope and shape of *Escherichia coli*: multiple mutants missing the outer membrane lipoprotein and other major outer membrane proteins." J Bacteriol **136**(1): 280-5.

Sorgato, M. C. and O. Moran (1993). "Channels in mitochondrial membranes: knowns, unknowns, and prospects for the future." Crit Rev Biochem Mol Biol **28**(2): 127-71.

Steeghs, L., H. de Cock, et al. (2001). "Outer membrane composition of a lipopolysaccharide-deficient Neisseria meningitidis mutant." EMBO J **20**(24): 6937-45.

Stuart, B. H. (2004). Infrared spectroscopy: fundamentals and applications. Chichester, John Wiley & Sons Ltd.

Subramaniam, S. and R. Henderson (2000). "Molecular mechanism of vectorial proton translocation by bacteriorhodopsin." Nature **406**(6796): 653-7.

Sugawara, E., M. Steiert, et al. (1996). "Secondary structure of the outer membrane proteins OmpA of *Escherichia coli* and OprF of *Pseudomonas aeruginosa*." J Bacteriol **178**(20): 6067-9.

Surrey, T. and F. Jähnig (1992). "Refolding and oriented insertion of a membrane protein into a lipid bilayer." Proc Natl Acad Sci U S A **89**(16): 7457-61.

Surrey, T. and F. Jähnig (1995). "Kinetics of folding and membrane insertion of a β-barrel membrane protein." J Biol Chem **270**(47): 28199-203.

Surrey, T., A. Schmid, et al. (1996). "Folding and membrane insertion of the trimeric β-barrel protein OmpF." Biochemistry **35**(7): 2283-8.

Tamm, L. K., F. Abildgaard, et al. (2003). "Structure, dynamics and function of the outer membrane protein A (OmpA) and influenza hemagglutinin fusion domain in detergent micelles by solution NMR." FEBS Lett **555**(1): 139-43.

Tamm, L. K., H. Hong, et al. (2004). "Folding and assembly of β-barrel membrane proteins." Biochim Biophys Acta **1666**(1-2): 250-63.

Tamm, L. K. and S. A. Tatulian (1997). "Infrared spectroscopy of proteins and peptides in lipid bilayers." Q Rev Biophys **30**(4): 365-429.

Thome, B. M., H. K. Hoffschulte, et al. (1990). "A protein with sequence identity to Skp (FirA) supports protein translocation into plasma membrane vesicles of *Escherichia coli*." FEBS Lett. **269**(1): 113-6.

Tribet, C., R. Audebert, et al. (1996). "Amphipols: polymers that keep membrane proteins soluble in aqueous solutions." Proc Natl Acad Sci U S A **93**(26): 15047-50.

van den Berg, B., P. N. Black, et al. (2004). "Crystal structure of the long-chain fatty acid transporter FadL." Science **304**(5676): 1506-9.

Van Gelder, P., H. De Cock, et al. (1994). "Detergent-induced folding of the outer-membrane protein PhoE, a pore protein induced by phosphate limitation." Eur J Biochem **226**(3): 783-7.

Vandeputte-Rutten, L., M. P. Bos, et al. (2003). "Crystal structure of Neisserial surface protein A (NspA), a conserved outer membrane protein with vaccine potential." J Biol Chem **278**(27): 24825-30.

Vandeputte-Rutten, L., R. A. Kramer, et al. (2001). "Crystal structure of the outer membrane protease OmpT from *Escherichia coli* suggests a novel catalytic site." EMBO J. **20**(18): 5033-9.

van Stokkum, I. H., H. J. Spoelder, et al. (1990). "Estimation of protein secondary structure and error analysis from circular dichroism spectra." Anal Biochem **191**(1): 110-8.

Vogel, H. and F. Jähnig (1986). "Models for the structure of outer-membrane proteins of Escherichia coli derived from raman spectroscopy and prediction methods." J Mol Biol **190**(2): 191-9.

Vogt, J. and G. E. Schulz (1999). "The structure of the outer membrane protein OmpX from *Escherichia coli* reveals possible mechanisms of virulence." Structure Fold. Des. **7**(10): 1301-9.

Voulhoux, R., M. P. Bos, et al. (2003). "Role of a highly conserved bacterial protein in outer membrane protein assembly." Science **299**(5604): 262-5.

Wallin, E. and G. von Heijne (1998). "Genome-wide analysis of integral membrane proteins from eubacterial, archaean, and eukaryotic organisms." Protein Sci **7**(4): 1029-38.

Wang, Y. (2002). "The function of OmpA in *Escherichia coli*." Biochem Biophys Res Commun **292**(2): 396-401.

Watts, A., S. K. Straus, et al. (2004). "Membrane protein structure determination using solid-state NMR." Methods Mol Biol **278**: 403-73.

Weber, K. and M. Osborne (1964). "The reliability of molecular weight determinations by dodecyl sulfate-polyacrylamide gel electrophoresis." J. Biol. Chem. **244**: 4406–4412.

Weiss, M. S., A. Kreusch, et al. (1991). "The structure of porin from *Rhodobacter capsulatus* at 1.8 Å resolution." FEBS Lett **280**(2): 379-82.

Weiss, M. S. and G. E. Schulz (1992). "Structure of porin refined at 1.8 Å resolution." J Mol Biol **227**(2): 493-509.

Whitmore, L. and B. A. Wallace (2004). "DICHROWEB, an online server for protein secondary structure analyses from circular dichroism spectroscopic data." Nucleic Acids Res **32**(Web Server issue): W668-73.

Whittaker, A. G., A. R. Mount, et al. (2000). Physical chemistry. New York, BIOS Scientific Publishers Ltd.

Wiener, M. C. and S. H. White (1991). "Transbilayer distribution of bromine in fluid bilayers containing a specifically brominated analogue of dioleoylphosphatidylcholine." Biochemistry **30**(28): 6997-7008.

Wimley, W. C. and S. H. White (1996). "Experimentally determined hydrophobicity scale for proteins at membrane interfaces." Nat Struc Biol **3**: 842-848.

Wolfs, J. A., L. I. Horváth, et al. (1989). "Spin-label ESR of bacteriophage M13 coat protein in mixed lipid bilayers. Characterization of molecular selectivity of charged phospholipids for the bacteriophage M13 coat protein in lipid bilayers." Biochemistry **28**(26): 9995-10001.

Yau, W. M., W. C. Wimley, et al. (1998). "The preference of tryptophan for membrane interfaces." Biochemistry **37**(42): 14713-8.

Zakharian, E. and R. N. Reusch (2003). "Outer membrane protein A of *Escherichia coli* forms temperature-sensitive channels in planar lipid bilayers." FEBS Lett **555**(2): 229-35.

Zakharian, E. and R. N. Reusch (2005). "Kinetics of folding of *Escherichia coli* OmpA from narrow to large pore conformation in a planar bilayer." Biochemistry **44**(17): 6701-7.

Zeth, K., K. Diederichs, et al. (2000). "Crystal structure of Omp32, the anion-selective porin from *Comamonas acidovorans*, in complex with a periplasmic peptide at 2.1 Å resolution." Structure Fold Des **8**(9): 981-92.

Zoonens, M., L. J. Catoire, et al. (2005). "NMR study of a membrane protein in detergent-free aqueous solution." Proc Natl Acad Sci U S A **102**(25): 8893-8.

Acknowledgements

I would like to thank PD Dr. Jörg H. Kleinschmidt for his great guidance and support during my entire doctoral study. I am also grateful to him for the opportunity to participate at the Biophysical Society Meeting in Long Beach, CA, USA in 2004.

Many thanks to Prof. Dr. Jean-Luc Popot, Prof. Dr. Derek Marsh, Dr. Muthu Ramakrishnan, Prof. Dr. Harald B. Jensen, Prof. Dr. Wolfram Welte and Prof. Dr. Hans-Jürgen Apell for fruitful collaborations.

I am very thankful to my aunt, Prof. Dr. Rodica Bozac, my father Dipl. Ing. Mircea Pocanschi and my uncle PD Dr. Adrian Pocanschi for their continuous encouragements. I want to thank my family, my mother and my wife who supported me all this time.

Last but not least I would like to thank my colleagues and friends from M9, M12 and elsewere for providing a very pleasant work environment.